Design and Synthesis of Macrocycles, Peptides and Coiled Coils with Sugar Connections

By

Sinclair Sweeney

A Thesis presented to
The National University of Ireland
For the degree of
Doctor of Philosophy.

Based on the research carried out in the
School of Chemistry,
National University of Ireland,
Galway.

Under the supervision and direction of
Prof. Paul V. Murphy
National University of Ireland,
Galway.

10/05/2016

Date

Declaration

This thesis has not been submitted before, in whole or in part, to this or any other university for any degree, and is, except where otherwise stated, the original work of the author.

Sinclair Sweeney

Acknowledgments

I would like to thank many people for their help, time and effort throughout the course of my Ph.D. First and foremost I would like to thank and extend my deepest gratitude to my supervisor Prof. Paul V. Murphy for his knowledge, guidance and encouragement throughout my Ph.D. I would also like to thank all of my group members for been fantastic and great fun. Thank you to Dr. Shane O'Sullivan for his insightful comments and suggestions and for laughing at my puns. And to the trio, Anthony Mc Donagh, Louise Kerins and Dr. Stephen Barron, a warm heartfelt thank you goes to you for constantly keeping the sprits high inside and outside of the laboratory.

I would like to thank all the technical staff of the School of Chemistry, N.U.I. Galway. In particular Dr. Róisín Doohan for her help with NMR and Marian Vignoles for MS support. I also would like to thank the Irish Research Council for their financial support. Without their research scholarship, none of this work would have been possible.

A big thank you to my family in lovely Leitrim, to my parents Raymond and Margaret Sweeney. Your support and patience was a prerequisite during this time. And to my siblings, Achuisle, Jude, Roland, Lenore, Launcelot, Salome, Trevor and Sinbad, thank you for all your advice and words of wisdom. Each and everyone of you has helped me to arrive to this point in my life.

And finally, I would like to thank my one and true love, Dr. Róise Mc Govern. Your enthusiasm and grá for science was an inspiration to me. Thank you for making these past years so special and I am eagerly looking forward to our next adventure.|

Abstract

Migrastatin is a secondary metabolite that is formed from the bacterium *Streptomyces platensis*. This compound has shown promising anti-metastatic activity by inhibiting tumour cell migration. Published derivatives of this bioactive molecule in the past have shown that the omission of a glutarimide side chain enhanced the IC_{50} *in vitro* by ~1000 fold. The work carried out as part of this thesis focused on synthesising analogues that centred around the core ring structure of migrastatin. Derivatives of migrastatin's congener, Dorrigocin A, in which there is a change in one of the olefin's geometry, have also been successfully synthesised. Some of these analogues have been biologically evaluated and show comparable results to potent analogues published in literature. A second batch of compounds is currently being screened over a wider range of tumour cell lines.

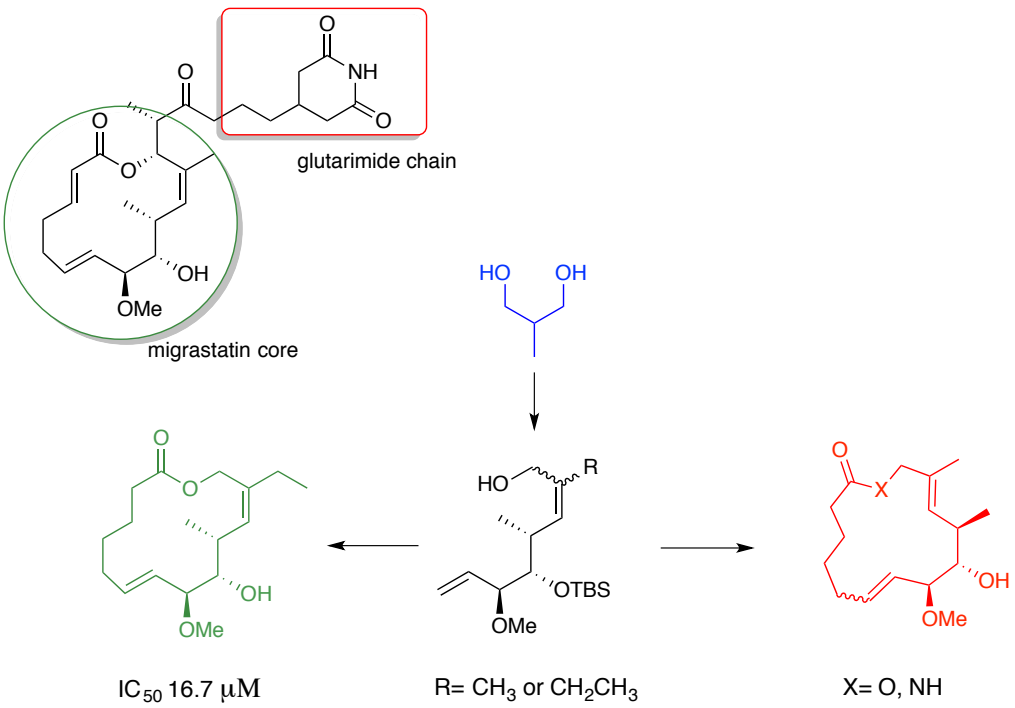

The second chapter of this thesis describes the synthesis of peptide scaffolds for displaying sugar moieties. Scaffolds are an important element of bioactive molecules for displaying pharmacophores with a defined distance and spatial orientation. Such parameters are required for effective receptor-ligand binding. Previous work within the Murphy group has explored diverse scaffolds with various ligands, length of linker ligand and valency of

ligands. To add to the diversity of such scaffolds, *de novo* peptides have now been designed to self-assemble into trimeric coiled coils when exposed to aqueous media. Lactose ligands were grafted onto the side of these coiled coils generating glycoclusters. These glycoclusters are currently under biological evaluation to ascertain their lectin inhibitory potential. This work has been published in Tetrahedron Letters (Sweeney, S. M. *et al*., *Tet. Lett.* **2016,** *57* (13), 1414-1417.)

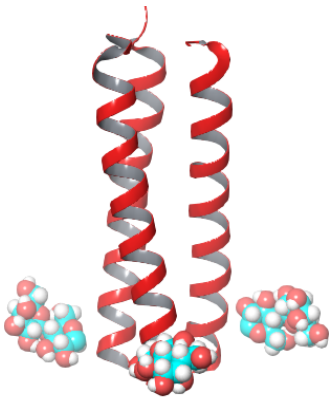

The final chapter describes the synthesis of peptidomimetic analogues of an endogenous endocrine hormone, somatostatin. Acromegaly is a disease that arises from the overexpression of natural growth hormone, which subsequently leads to the formation of enlarged hands and feet. Typically this disease originates from a tumour growth located on the hormone producing pituitary gland. Somatostatin opposes the action of growth hormone by inhibiting its secretion, however, somatostatin has a short half-life. Peptidomimetic analogues were designed to include a *N*-Acetylglucosamine to help stabilise a β-turn that is a structural feature present in somatostatin's pharmacophoric region. These peptides have shown activity in the μM region.

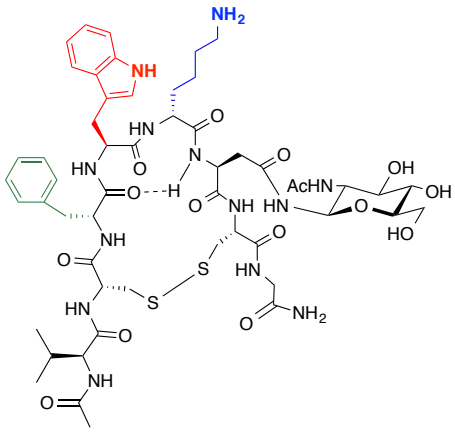

Contents

Symbols and Abbreviations

α	Alpha
AcOH	Acetic acid
ADMET	Acyclic diene metathesis
Ala	Alanine
apt	Apparent (spectral)
AUC	Analytical ultracentrifugation
β	Beta
BAIB	Diacetoxyiodobenzene
Boc	*tert*-butoxycarbonyl
BOP	(Benzotriazol-1-yloxy)tris(dimethylamino)phosphonium hexafluorophosphate
cAMP	Cyclic adenosine monophosphate
CD	Circular dichroism
CDK	Cyclin-dependent kinases
CH_3Cl	Chloroform
CM	Cross Coupling Metathesis
COSY	Correlated Spectroscopy
CPL	Circularly polarised light
CRD	Carbohydrate recognition domain
CSA	Camphorsulfonic acid
δ	Chemical shift in ppm downfield from TMS
d	Doublet (spectral)
DBU	1,8-Diazabicycloundec-7-ene
DCM	Dichloromethane
dd	Doublet of Doublets (spectral)
ddd	Doublet of Doublets of doublets (spectral)
DEAD	Diethyl azodicarboxylate
DEPT	Distortionless Enhancement by Polarisation Transfer
DIAD	Diisopropyl carboxylate
DIBAL	Diisobutylaluminium hydride
DIPEA	Diisopropylethylamine
d.r.	Diastereomeric ratio

DMAP	4-Dimethylaminopyridine
DMP	Dess Martin Periodinane
DMSO	Dimethylsulfoxide
(D2R)	Dopamine receptor
DPPA	Diphenylphosphoryl azide
dt	Doublet of triplets (spectral)
EDC.HCl	N-(3-Dimethylaminopropyl)-N'-ethylcarbodiimide hydrochloride
EDT	1,2-ethanedithiol
EMT	Epithelial–Mesenchymal Transition
e.e.	Enantiomeric excess
EnyneM	Enyne Metathesis
ES-HRMS	High-Resolution Mass Spectrometry – Electrospray Ionization
EtOAc	Ethyl acetate
Fmoc	Fluorenylmethyloxycarbonyl
FRAP	Fluorescence Recovery After Photobleaching
FTIR	Fourier transform infrared (spectroscopy)
g	Gram
Gln	Glutamine
Glu	Glutamate
Gly	Glycine
h	Hour(s)
HCTU	*O*-(6-Chlorobenzotriazol-1-yl)-*N*,*N*,*N*′,*N*′-tetramethyluronium hexafluorophosphate
HF	Hydrofluoric acid
HMBC	Heteronuclear Multiple Bond Correlation
HPLC	High pressure liquid chromatography
HSQC	Heteronuclear Single Quantum Correlation
HWE	Horner Wadsworth Emmons
Hz	Hertz
Ile	Isoleucine
IR	Infrared (spectroscopy)
J	Coupling constant (NMR), in Hz
LACDAC	Lewis acid-catalysed diene aldehyde cyclocondensation

Leu	Leucine
Lys	Lysine
M	Molar
M^+, M^-	Mass of the molecular ion (mass spectrometry)
MBHA	Rink amide 4-methylbenzhydrylamine
MeOH	Methanol
MET	Mesenchymal-Epithelial Transition
MHz	Megahertz
min	Minute(s)
mL, μL	Milliliter, microliter
mol, mmol	Mole, millimole
MTT	(3-(4,5-dimethylthiazol-2-yl)-2,5-diphenyltetrazolium bromide)
NMR	Nuclear Magnetic Resonance
NOESY	Nuclear Overhauser Effect Spectroscopy
PPI	Protein-Protein Interaction
Ph.	Phenyl
PyBOP	(Benzotriazol-1-yloxy)tripyrrolidinophosphonium hexafluorophosphate
q	Quartet (spectral)
RCM	Ring Closing Metathesis
ROESY	Rotating-frame Overhauser Effect Spectroscopy
ROM	Ring Opening Metathesis
rpm	Revolutions per minute
$[\alpha]_D$	Specific rotation
s	Singlet (spectral)
sec-BuLi	*sec*-Butyllithium
SPPS	Solid Phase Peptide Synthesis
SPS	Solution Peptide Synthesis
SSTR	Somatostatin receptor
t	Triplet (spectral)
TBAF	*tert*-butyl ammonium fluoride
TBDPS	*tert*-butyldiphenylsilyl
TBSOTf	*tert*-butyldimethylsilyl triflate

td	Triplet of doublets (spectral)
TEA	Triethylamine
TEMPO	2,2,6,6-Tetramethylpiperidinyloxy
TESCl	Triethylsilyl chloride
TFA	Trifluoroacetic acid
THF	Tetrahydrofuran
TLC	Thin Layer Chromatography
TMSCl	Trimethylsilyl chloride
TOCSY	Total Correlated Spectroscopy
Trp	Tryptophan

Contents

Chapter 1: Synthesis of migrastatin and dorrigocin A analogues

1.1 Introduction

The body is made up of trillions of cells, each cell being part of a specific tissue type giving rise to an ordered structure that must be highly regulated. During a daily lifecycle cells within the body undergo pre-programmed cell division called mitosis. The new cells that are formed replace old damaged or worn out cells for example in the case of tissue repair. Cell signalling and cell programmed death, apoptosis, are crucial processes for healthy tissue and normal function. Abnormal cells may occur however where this regulation has been disrupted. Old or damaged cells that should be removed from the body undergo cellular division leading to rogue cells capable of dividing uncontrollably. When apoptosis does not occur, these abnormal cells may eventually form a neoplasm.

Neoplasms, commonly referred to as tumours, can either be malignant or benign. Benign tumours are non-cancerous, are usually localised and do not invade or spread to other regions of the body. The majority of benign tumours respond well to therapeutic treatments. In certain circumstances however, if left untreated, some benign tumours may grow to a size that impacts on a surrounding organ, for example compression within the brain could lead to fatal circumstances. Malignant tumours are in fact cancerous growths. These tumours are capable of invading surrounding tissue and metastasise to form secondary tumours located in another region of the body. Typical treatment of malignant tumours include, (i) surgery to physically remove the tumour, (ii) radiation disrupting the DNA in quickly dividing cells and thus stopping cell division and (iii) chemotherapy therapy whereby genes are disrupted at cell division or during the copying process preceding splitting. These treatments can be long and non-specific such that the treatments also kill healthy quickly dividing tissue including skin, hair follicles and digestive tract lining. Another approach to target cancer is stopping the secondary tumour from forming in the first place and only treat the primary tumour. Usually the primary tumour is smaller than the secondary tumour and this would suggest it is more of a viable target for known therapies. Tumour cell migration inhibition is an alternative method that prevents the formation of the secondary tumour. An astonishing 90 % of cancer-related deaths occur from secondary tumours.[1] This anti-metastatic therapeutic approach may have potential as a combination therapy whereby the treatments previously mentioned could only be employed to eradicate the primary tumour.

1.2 Cell mobility and migration

The process of cell migration has been widely studied and encompasses many signalling pathways, which are still under constant research. Cell migration can be observed quite clearly when looking at an amoeba that is a single cell organism. This organism projects pseudopods in order to move in the direction of food and away from threatening environments. In multi-cellular organisms, for example humans, this phenomenon of cell migration spans all the way from gastrulation[2] and embryonic development to tissue repair and immune system proficiency.[3] Cell migration can be divided into two groups, collective migration or single cell migration. Collective cell migration is required for building and managing tissue structures e.g. tissue repair. Single cell migration on the other hand can cover small localised distances or long distances featured in the immune system. For example, leukocytes can spread to any part of the body in search of foreign objects and aid in its removal. The migration mechanism can be considered cyclic in nature.[4] When the cell is exposed to a migration-promoting agent, protrusions are created on one side of the cell and dissembled on the opposite side. These protrusions, either broad lamellipodia or spike-like filopodia, are synthesised in the direction of the migration-promoting agent.

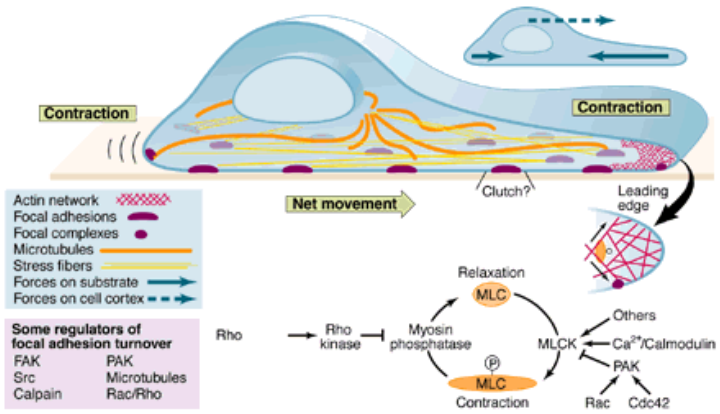

Figure 1.1 Representation of cellular movement. Adapted from reference 6 with copyright permission. Copyright © (1999) The American Association for the Advancement of Science.

The lamellipodia are broad finger like projections composed of actin filaments branched in scaffold manner whereas the filopodia have ordered structures of parallel bundles of actin filaments.[5] These filaments change the morphology of cytoskeleton by acting as traction points that the cell can crawl over, thereby resulting in cell movement. The cell develops this essential intrinsic polarized state as different molecular processes are occurring at

either point of the cell or indeed at either side of the cell sheet in relation to collective cell migration. The assembling and disassembling of these actin filaments is produced from complex signalling pathways detected by the leading edges of the lamellipodia and filopodia in the extra cellular material.[6] This process gives the cell an overall net forward movement, much like the way the Egyptians transported heavy goods to build their pyramids by rolling the desired object over rollers, bringing each used roller from the back to the front. As previously mentioned, cell migration is a prerequisite for embryonic development and life, however cell migration can also be pathological in dysregulated cells leading to tumour metastasis.

1.3 Cell Metastasis

Metastasis is a multi-step cascade that involves abnormal cells breaking away from a primary tumour and circulating through the body to form a secondary tumour. Typically the secondary tumour will occur at organs downstream from the primary tumour based on anatomical processes, governed by the position of organs along the circulatory system.[7] Primary tumour cells may also travel to areas far away from the original site, giving rise to seemingly "random" metastatic cells. This may be rationalised by a theory that conceptualises cells as plant seeds needing the right environment to grow. Stephen Paget wrote – *"The seeds of a plant are carried in all directions; but they can only live and grow if they fall on congenial soil"*.[8] Paget's theory could help the understanding of why disseminate metastatic breast cells can be found in bone, lung, liver and the brain for example.[9]

Tumour cell metastasis typically comprises of the following steps; (i) local invasion, cells invade surrounding normal tissue, (ii) intravasation, cells move through the walls of nearby lymph vessels or blood vessels, (iii) circulation, cells are carried through the bloodstream and the lymphatic system to other regions of the body, (iv) extravasation, the cells lodge in capillaries and migrate into the surrounding tissue, (v) proliferation, the cells divide and multiply to form small tumours known as micrometastases and (vi) angiogenesis, blood vessels grow around the newly formed micrometastases and bring oxygen and nutrients for tumour growth. Other forms of metastasis do not have to go through all these steps. Leukaemia, a disorder in incorrect blood cell formation, is already in the circulatory system and therefore does not have to breakthrough into the vascular system.

Reported observations suggest that an endogenous process called epithelial–mesenchymal transition (EMT), which is required for cell differentiation and embryonic development, also plays a role in tumour cell dissemination.[10,11] EMT is controlled by five separate pathways, the Hedgehog family, Wnt, TGF-β family, Notch pathway and receptor tyrosine kinases (RTK).[12] Metastatic epithelial cells however go through an EMT-like transformation. This is characterised by loss in epithelial properties, such as cell shape, a down regulation of transmembrane proteins involved in cell adhesion (this will be discussed later in this chapter) and loss of apico-basal polarity (top to bottom). Instead the emerging mesenchymal cells have front to back polarity allowing the cell to migrate in three dimensions and increase its motility.[13] EMT to mesenchymal-epithelial transition (MET) is reversible and this may be the reason why secondary tumours show biomarkers from primary tumour tissue.[14] It should also be noted that there are some arguments against the theory that EMT is required for metastasis.[15,16]

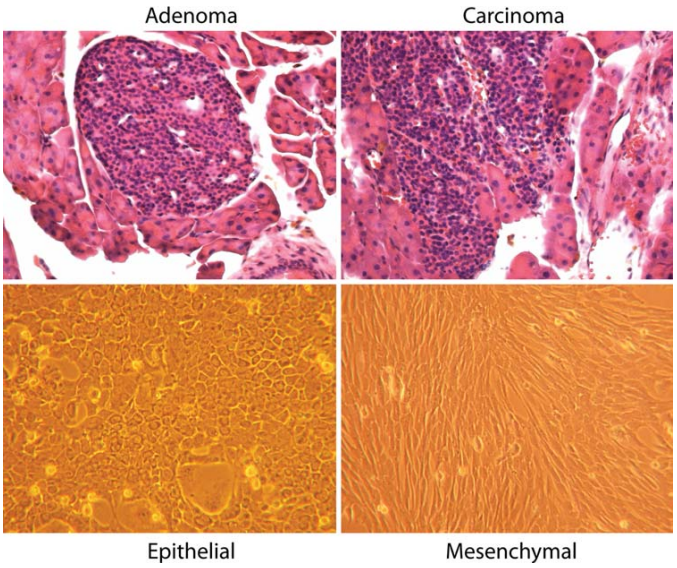

Figure 1.2 The upper panels show epithelial adenoma (left) transform into an invasive carcionoma (right) from histological sections. The lower panels show the transition from an epithelial cell (left) to mesenchymal sate (right) through the EMT process. Adapted from reference 10 with permission. Copyright © 2007 Springer.

Inhibition of the first migration step in metastasis stops the cascade and is therefore of medicinal interest. Controlling the migration and indeed inhibiting it could pave the way forward in reducing cancer related deaths. A natural occurring product, migrastatin, has

shown anti-metastatic properties by tumour cell migration inhibition. Synthetic analogues have shown increases in activity of the order of three orders of magnitude when compared to the parent compound.[17] The bioactive parent compound is a typical example of therapeutics potentially arising from natural sources.

1.4 Natural products and their uses

When comprehending natural products and their discoveries, it is always worth thinking that – Mother Nature is the source of many diseases and thus may also hold the solutions to these diseases.

Natural product sources encompass plant, marine and microorganisms, which all exhibit a diverse range of molecules. These molecules are generally composed of "*primary metabolites"* and "*secondary metabolites*". Both types of metabolites are biosynthesised and are broken down from proteins, lipids, nucleic acids and complex carbohydrates. Primary metabolites are essential for all living organisms, for example growth and reproduction. Secondary metabolites on the other hand are typically synthesised uniquely to a specific organism and are not involved in fundamental process such as growth. These metabolites form part of the organism's survival package within its surrounding environment.[18] Such compounds have been and still are of pharmaceutical interest as both animals and humans need compounds like these in order to combat diseases.

It has been estimated that 40 % of medicines are natural products or their derivatives.[19] As these compounds have been around for millennia, natural sources have produced a plethora of biologically validated bioactive molecules. Natural products have been of the highest importance for both past and modern therapeutics, not only as therapeutics themselves, but often as starting points in which lead compounds can be derived and synthesised. Secondary metabolites typically have great structural complexity embedded into these molecules. This complexity is likely due to the biosynthetic route or for the transport and removal of the compound of interest from its source. The obvious statement has to be mentioned that these compounds were not produced naturally with human therapy in mind! A term referred to as diverted total synthesis, introduced by Danishefsky, can generate molecules that are more interesting than the parent molecule itself with regard to activity and patient safety. In this way, synthesis of complicated natural products becomes more achievable by omitting certain parts of the parent molecule and this will be seen further on in this chapter.

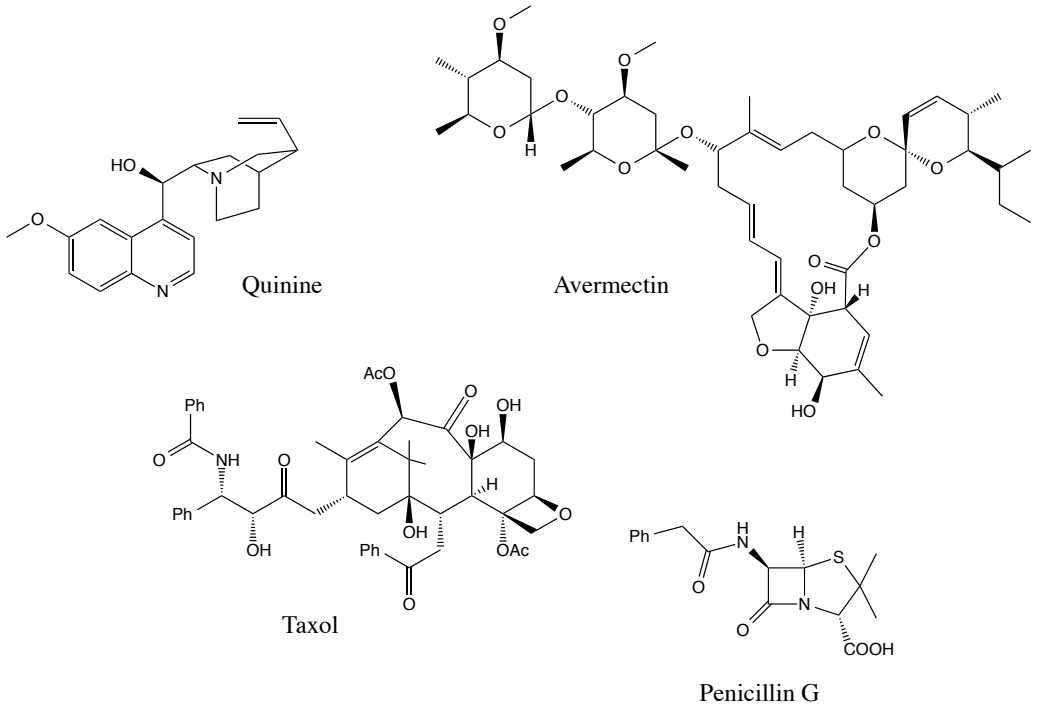

Figure 1.3 Known examples of natural products that are used as approved therapeutics.

The discovery of penicillin by Alexander Fleming in 1928 from *Penicillium notatum*, found in house mould, has led to the harvesting of antibacterial agents. The work performed by Howard Florey and Ernst Chain in 1938 on penicillin showed its therapeutic application when they scaled-up production in their academic laboratory and administered a course of antibiotics to patients with life threatening bacterial infections.

The knowledge of nature however, plants in particular, holding such key bioactive compounds has been known for generations. In the early 1600's, indigenous people from the Amazon region used the bark of the *Cinchona* plants for anti-fever remedies. In 1820, two French pharmacists, Caventou and Pelletier, isolated and identified the active ingredient, quinine, from *Cinchona* bark.[20] Since then, new analogues of quinine have been produced for the treatment of malaria. Another anti-malaria drug, isolated from the plant *Artemisia annua*, has shown high potency against malaria. This has led to Youyou Tu receiving half of the Nobel Prize in Physiology or Medicine in 2015 for her discovery in using this as a novel therapy in combating malaria.

Another example of natural product discovery lies within the blockbuster drug Taxol. This was isolated from the Pacific Yew tree, *Taxus brevifolia*, which further demonstrated the importance of screening natural compounds. This antimitotic agent stabilises microtubules in the cytoskeleton and disrupts their depolymerisation, which is required for mitosis.[21] The marine environment has also shown to be another source of chemotherapeutics. Ziconotide is an N-type calcium channel blocker derivative that comes from a cone snail, *Conus magus*. This compound is administered intrathecally as N-type calcium channels are densely populated in an area of the spinal cord called the dorsal horn.[22] Mass production of this active compound is synthetically carried out. Marine products have not been exploited yet to their full potential as logistically they are difficult to reach and typically the harvest is low. Fifty years after Fleming, Florey and Chain were awarded the Nobel Prize in Physiology or Medicine, Dr. William C. Cambell, an Irish parasitologist, and Satoshi Ōmura, were jointly awarded half the 2015 Nobel Prize in Physiology or Medicine "*for their discoveries concerning a novel therapy against infections caused by roundworm parasites*". Dr. Campbell played an important role in discovering the human therapeutical application of the natural product derivative, 8arbine8yl, in the treatment against river blindness. Ivermectin is a semi-synthetic derivative of the natural occurring 8arbine8yl that was obtained from a soil sample in Japan. The source of this compound was determined to come from the bacterial phylum *Streptomyces.* Due to toxicity problems of 8arbine8yl, the selectively hydrogenated derivative, 8arbine8yl, was produced which was subsequently introduced into agricultural livestock and then later into human clinical trials.[23] This lactone based bioactive agent is a refined compound, alluding to the earlier statement that natural products can serve as lead molecules or templates. Ivermectin, an endectocide due to activity both internally and externally, has been subsequently used in the treatment of the endemic river blindness by targeting the parasitic worm, *Onchocerca volvulus* and saving the sight and lives of thousands of people.

1.5 Isomigrastatin, migrastatin, dorrigocin A and dorrigocin B

Another promising *Streptomyces* derived lactone based compound, which has been briefly mentioned, has shown anti-metastatic potential. Migrastatin **1** has a fourteen membered lactone ring, connected to a glutarimide side chain shown in Figure 1.4. Researchers analysing soil samples in Japan, during the search of natural product therapeutics, first discovered this active metabolite. A bacterial strain, now named *Streptomyces* sp. MK929-43F1, showed promising results as a source for anti-metastatic agents.[24,25] From this and

over the last fifteen years since the first publishing of this discovery, migrastatin has seen continuous attention in relation to its total synthesis, diverted total synthesis, analogue synthesis and mode of action studies.[17,26,27,28,29]

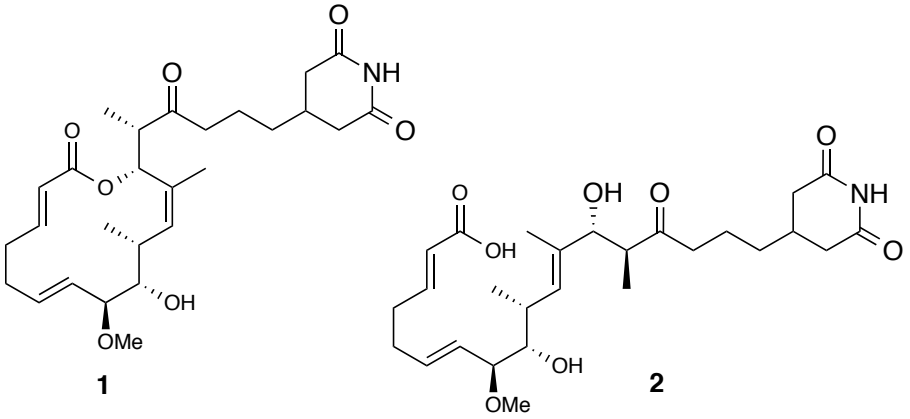

Figure 1.4 Migrastatin **1** and dorrigocin A **2** structures.

A documented bacteria, *Streptomyces platensis,* comes from the same phylum as the migrastatin producing bacteria, *Streptomyces*. It is well established as a known producer of dorrigocins that are acyclic migrastatin congeners. This species was believed to only produce dorrigocins however further studies exposed more compounds that were isolated and characterised. These additional compounds included isomigrastatin, which is a cyclic dorrigocin type, and **1**.[30] The dorrigocins are acyclic congeners and include dorrigocin A **2** and dorrigocin B and 13-*epi*-dorrigocin. They were subjected to various assays to determine their bioactive properties including anti-tumour and antifungal assays.[31] Cell lines including murine leukemia P388 and human lung sarcoma A549 were tested using a colorimetric assay to test for proliferation and cytotoxicity.[32] The IC_{50} (50 % inhibition concentration) results were not encouraging and showed low activity against tumour cell lines. It should be noted that the assay only tested for cell viability and cytotoxicity. Migration inhibition tests were not published. Dorrigocins were also checked for their applications as inhibitors of small signalling proteins called K-*ras*. Ras proteins are small GTPase proteins that are involved with cell proliferation, growth and signal transduction.[33] A study was performed on NIH/3T3 mouse fibroblasts where a mutated *K-ras* plasmid was added. The expression of the *K-ras* mutated plasmid resulted in a more rounded morphology of the transformed NIH/3T3 cell when compared to a normal non mutated cell which was flatter. The addition of test compounds **2** and dorrigocin B resulted in a reverse in morphology from round transformed cells back to flat ones. A further study showed that the dorrigocins fully inhibited carboxyl-methyltransferase from methylating *ras* proteins

by inhibiting their adherence to the cell membrane and therefore their function. The dorrigocins were also shown to be *ras* specific, depending on the size of the protein.[34] This specificity could have important potential in interfering with mutated *ras* oncogenes and thus disrupt cellular signalling of tumour cells resulting in tumour cell death.

As previously mentioned, isomigrastatin was discovered in the broth milieu of fermented bacteria. Isomigrastatin is the cyclic lactone version of dorrigocin B. It is a 12-membered lactone ring where the double bond has shifted to the side chain whilst retaining the *E* geometry, which is similar to the acyclic dorrigocin congeners. Isomigrastatin, like migrastatin, also shows tumour cell migration inhibition activity. Ju *et al.* proposed a biosynthetic route shown in Figure 1.5 for the hydrolysis of isomigrastatin into its representative metabolites.[35] This research outlines that **1**, **2**, dorrigocin B and 13-*epi*-dorrigocin A are all shunt metabolites of isomigrastatin. These shunt metabolites are biotransformation pathways resulting in a decrease of the parent compound's concentration. Compounds **1**, **2**, dorrigocin B **3**, iso-migrastatin **4**, and 13-*epi*-dorrigocin A **5**, will be further discussed. To determine the hypothesis that **1**, **2**, **3** and **5** were shunt metabolites from **4**, all isolated compounds excluding **4** were placed into chloroform (CH_3Cl), dimethylsulfoxide (DMSO), methanol (MeOH) and MeOH-H_2O separately at 25 °C for 90 days. After analysis, all compounds remained unchanged. Compound **4** was subjected to the same conditions and it was found that it was stable in anhydrous solvents but not in MeOH-H_2O. Subsequently, **4** was added to DMSO-H_2O and was incubated. It was observed that **4** underwent rapid hydrolysis and the isolated compounds were characterised as being **1**, **2**, **3** and **5**. To confirm their findings, **4** was subjected to aqueous conditions in $H_2{}^{18}O$-DMSO (9:1). The resulting compounds **1**, **2**, **3** and **5** were analysed by HPLC-ESI-MS. Hydrolysis of the lactone in **4** to **3** was observed by the incorporation of one and two ^{18}O (of less than 10 % intensity) atoms represented by path *f*, *h*, or *i* illustrated in Figure 1.5. In the case of compounds **2** and **5**, this occurs by attack of a water molecule at C-13 at a *Si* or *Re* side in an S_N2' (bimolecular nucleophilic substitution) manner and the incorporation of one and two ^{18}O atoms confirms this mechanism, path *a* and *b*. As **1** is a single diastereomer, the reaction must proceed in a *Re* face-specific concerted mechanism. MS analysis showed that both ^{16}O and one ^{18}O were found. The incorporation of one ^{18}O proceeds via path *d*. The incorporation of no ^{18}O can be observed in path *e*. Both pathways are possible due to the tetrahedral intermediate and the fact that either ^{16}O or ^{18}O can be eliminated during the breakdown of this intermediate.

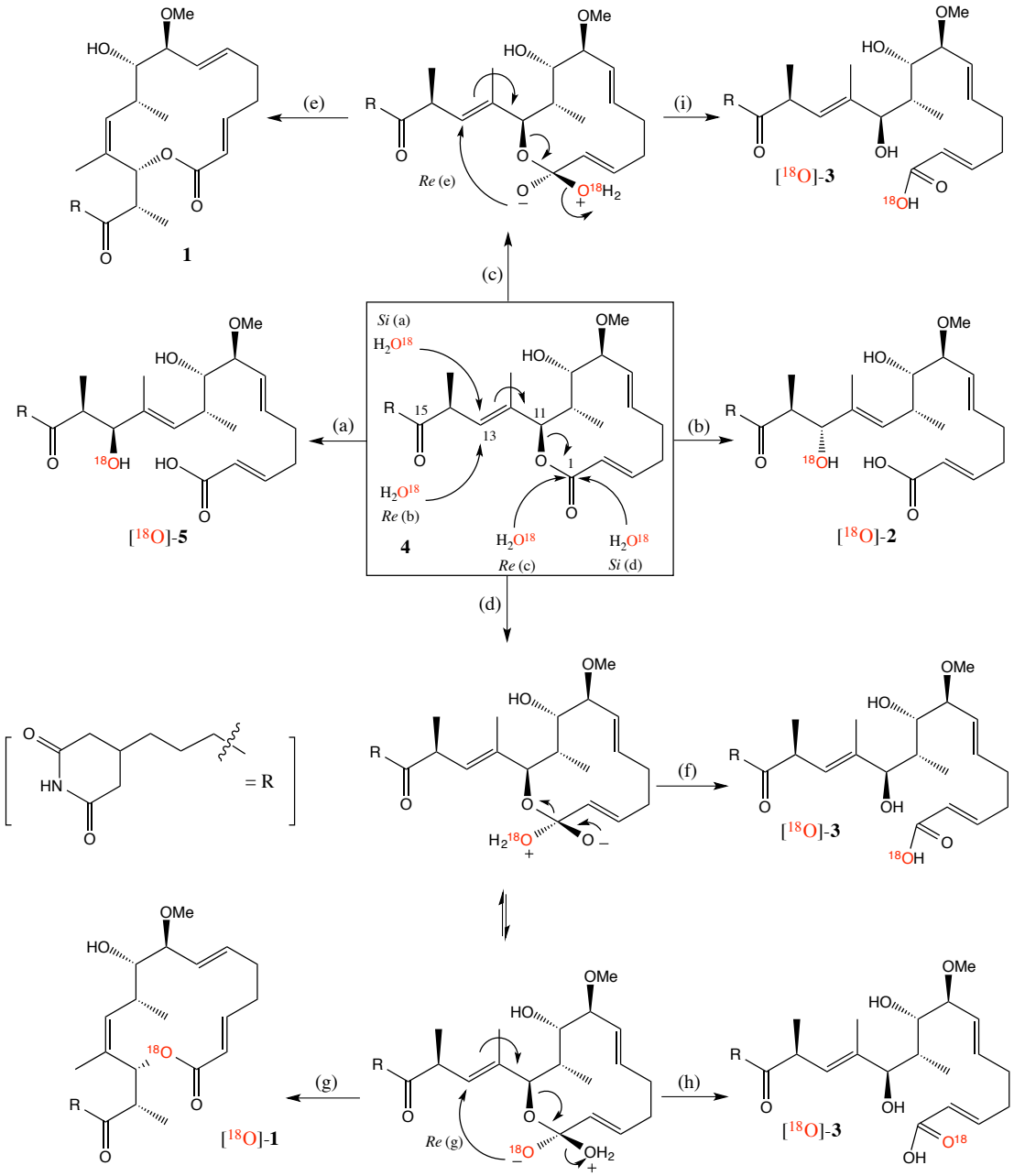

Figure 1.5 Proposed mechanism by Ju *et al*. for the H_2O-mediated rearrangement of **4** to **1**, **2**, **3** and **5** supported by the incorporation of ^{18}O from $H_2{}^{18}O$. Adapted with permission from reference 35. Copyright © (2005) American Chemical Society.

1.5.1 Total synthesis of Migrastatin

The anti-metastatic potential migrastatin encouraged the development of different total syntheses. These syntheses were challenging due to fact that five separate stereocenters were present in addition to three olefins and a glutarimide side chain that had to be encompassed. These synthetic routes by different research labs are examined.

1.5.1.1 Danishefsky and co-workers

After the isolation and identification of migrastatin in 2000, Danishefsky and co-workers reported the synthesis of the macrolide core in 2002.[36] This procedure was updated in 2004 to incorporate a vinyl aldehyde with predetermined stereochemistry on the carbon positioned alpha to the aldehyde. Their new modification to the synthetic route reduced the overall number of steps in their synthesis. To make aldehyde **9**, commercially available dimethyl 2,3-*O*-isopropylidene-L-tartrate was treated with 12arbine12ylaluminium hydride (DIBAL) to yield the corresponding dialdehyde intermediate and was subsequently reduced in tandem using divinylzinc to afford carbinol **7**. Dimethylation of **7** was followed by the removal of the acetonide group using acidic conditions to reveal the 1,2 diol **8**. This diol subsequently underwent oxidation using Criegee oxidation to furnish the desired aldehyde with defined stereochemistry as shown in Scheme 1.1.

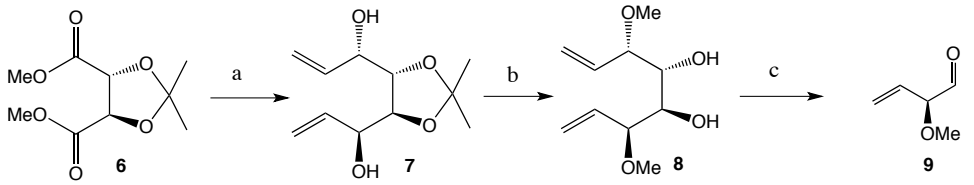

Reagents and conditions: (a) DIBALH, then $ZnCl_2$, H_2C=CHMgBr, toluene, -78 ^oC to room temp., 75 % (ds > 90%); (b) (i) MeI, NaH, DMF, room temp., (ii) 2 M HCl, MeOH, reflux, 80 %; (c) $Pb(OAc)_4$, Na_2CO_3, CH_2Cl_2, 0 ^oC to room temp.

Scheme 1.1 Synthesis of key aldehyde **9** by Gaul *et al*. Adapted with permission from reference 17. Copyright © (2004) American Chemical Society.

Next, the aldehyde was reacted with a dienophile to yield dihydropyrone lewis acid-catalysed diene aldehyde cyclocondensation (LACDAC). The ketone functional group was reduced with $LiBH_4$ to yield **11**. The resulting alcohol underwent a Ferrier rearrangement with the treatment of camphorsulfonic acid (CSA) in refluxing anhydrous tetrahydrofuran (THF) to yield the lactol with the desired *Z* olefin to form **12**. This lactol was reductively opened using $LiBH_4$. Both primary and secondary alcohols were protected with *tert*-butyldimethylsilyl triflate (TBSOTf) and the primary was subsequently deprotected under mild acid conditions. The primary alcohol was oxidised to the corresponding aldehyde **15**. This was then coupled with propionyl oxazolidinone in the presence of $MgCl_2$, triethylamine (TEA), and trimethylsilyl chloride (TMSCl), followed by trifluoroacetic acid (TFA) to afford two chiral centers with desired stereochemistry as a single diastereomer. The formed secondary alcohol was protected with triethylsilyl chloride (TESCl) furnishing **16**. After removal of the chiral auxiliary with $LiBH_4$, the resulting alcohol was oxidised

with Dess-Martin periodinane (DMP) to the aldehyde, coupled with dimethyl methylphosphonate and the newly formed alcohol was once again oxidised using DMP to form the *β*-ketophosphonate **18.**

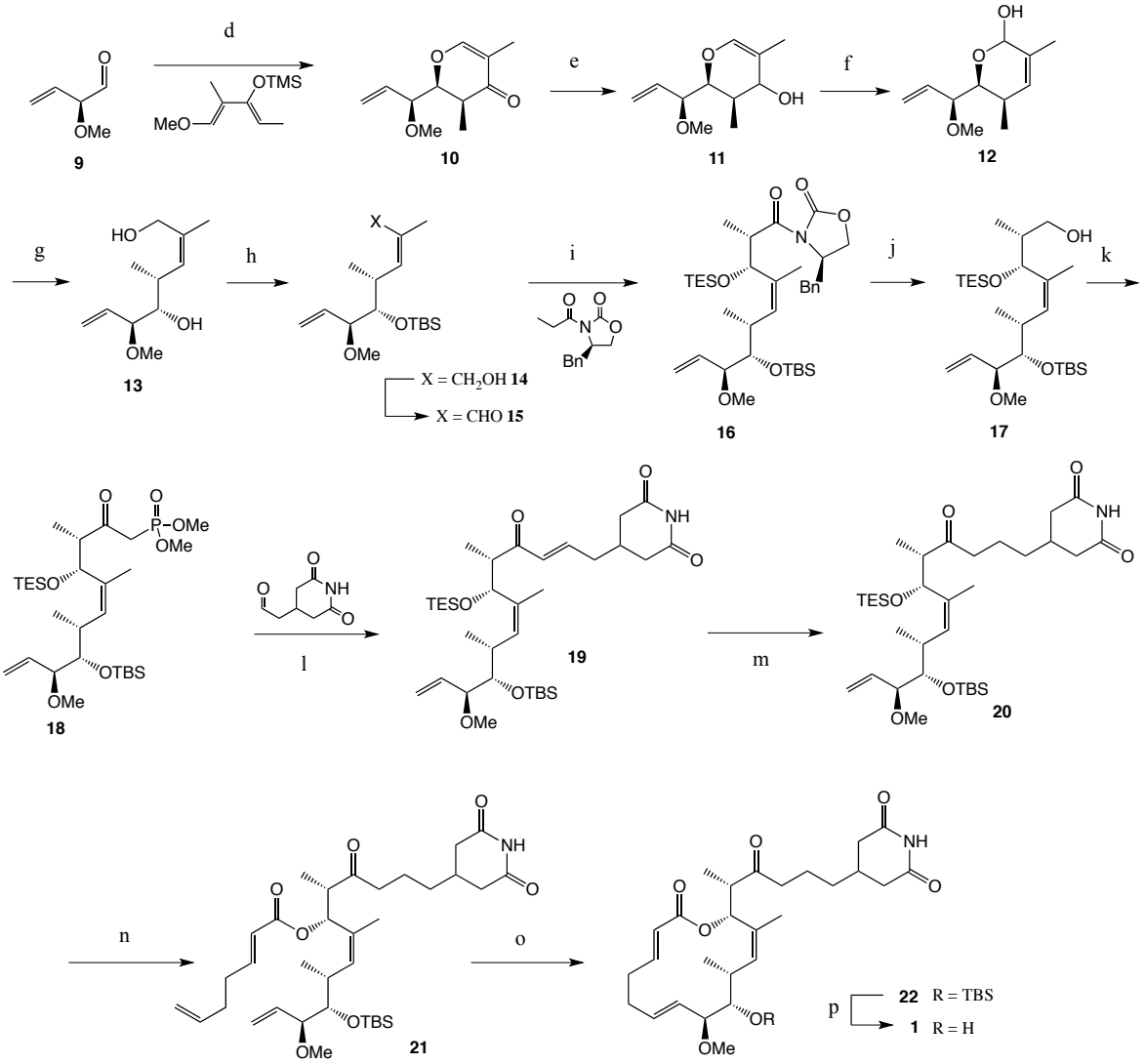

Reagents and conditions: (d) (i) $TiCl_4$, CH_2Cl_2, -78 °C, (ii) TFA, CH_2Cl_2, room temp., (e) $LiBH_4$, MeOH, THF, -10 °C. (f) CSA, H_2O, THF, reflux (g) $LiBH_4$, H_2O, THF, room temp., (h) (i) TBSOTf, 2,6-lutidine, CH_2Cl_2, room temperature, (ii) HOAc, H_2O, THF (3:1:1), room temp. (iii) Dess-Martin periodinane, CH_2Cl_2, room temp., (i) (i) $MgCl_2$, Et_3N, TMSCl, EtOAc, room temp., (ii) TFA, MeOH, room temp., (j) TESCl, imidazole, CH_2Cl_2, room temp., (ii) $LiBH_4$, MeOH, THF, room temp., (k) (i) Dess-Martin periodinane, CH_2Cl_2, room temp., (ii) dimethyl methylphosphonate, BuLi, THF, -78 to 0 °C, (iii) Dess-Martin periodinane, CH_2Cl_2, room temp., (l) LiCl, DBU, MeCN, room temp., (m) (i) $[(Ph_3P)CuH]_6$, toluene, room temp., (ii) HOAc, H_2O, THF (3:1:1), room temp., (n) 2,4,6-trichlorobenzoyl chloride, *i*-Pr_2Net, pyridine, toluene, room temp., (o) (i) Grubbs-II catalyst (20 mol %), toluene (0.5 mM), reflux (ii) HF'pyridine, THF, room temp.

Scheme 1.2 Total synthesis of migrastatin by Gaul *et al*. Adapted with permission from reference 17. Copyright © (2004) American Chemical Society.

The glutarimide aldehyde was reacted with the *β*-ketophosphonate in the presence of 1,8-diazabicycloundec-7-ene (DBU) and LiCl to yield the α,β-unsaturated carbonyl to form **19**. The conjugate enone was reduced using Stryker reagent. The TES ether was removed and the free alcohol was reacted with 2,6-heptadienoic acid under a modified Yamaguchi esterification forming **21**. Ring closing metathesis using Grubbs II catalyst afforded the ring closed product with an exclusively *E* olefin. The TBS protecting group was then removed with hydrofluoric acid (HF) –pyridine to yield migrastatin **1**.[17]

1.5.1.2 Reymond and Cossy total synthesis via CM and RCM

A total synthesis by Reymond in 2006 outlines the versatility and usefulness of ruthenium based catalysts in olefin synthesis. This paper reports the details of their approach and synthesis used. The synthesis began with commercially available (S)-(+)-2,2-dimethyl-1,3-dioxolane-4-carboxylate which was deprotected using acidic conditions. The primary alcohol was protected with a bulky *tert*-butyldiphenylsilyl (TBDPS) group and the secondary alcohol was methylated, followed by reduction of the ester moiety using DIBAL to form **24.** The resulting alcohol **24** was oxidised, using Swern conditions, followed by reacting the formed aldehyde, in the presence of $MgBr_2.Oet_2$ as a chelating agent, with but-2-enyl[tri(*n*-butyl)]stannane to furnish **25** diastereoselectivily (dr = 9:1) as shown in Scheme 1.3. The secondary alcohol was coupled to methacryloyl chloride in the presence of TEA, 4-dimethylaminopyridine (DMAP) in dichloromethane (DCM) to afford **26**. This was subsequently treated with Grubbs II catalyst to form the lactone with correct *Z* olefin stereochemistry. Next the lactone was opened with $LiBH_4$ and $CeCl_3 \cdot 7H_2O$ to form intermediate **28**. Both alcohols were protected with TBSOTf in the presence of base and the primary alcohol was selectively deprotected using mild acid conditions. The primary alcohol was then oxidised to the corresponding aldehyde **30** with MnO_2 .The aldehyde was treated directly with the highly face-selective crotyltitanium complex Ti-(*S*,*S*)-I to furnish two new chiral centres with high diastereoselectivity (dr = 9:1). The secondary alcohol was protected using TESCl to form **32**. The terminal alkene was transformed into an aldehyde chemoselectively using dihydroxylation-oxidative cleavage sequence, OsO_4, *N*-methylmorpholine *N*-oxide, and then $NaIO_4$. The secondary alcohol was coupled to methacryloyl chloride in the presence of TEA, 4-dimethylaminopyridine (DMAP) in dichloromethane (DCM) to afford **26**. This was subsequently treated with Grubbs II catalyst to form the lactone with correct *Z* olefin stereochemistry.

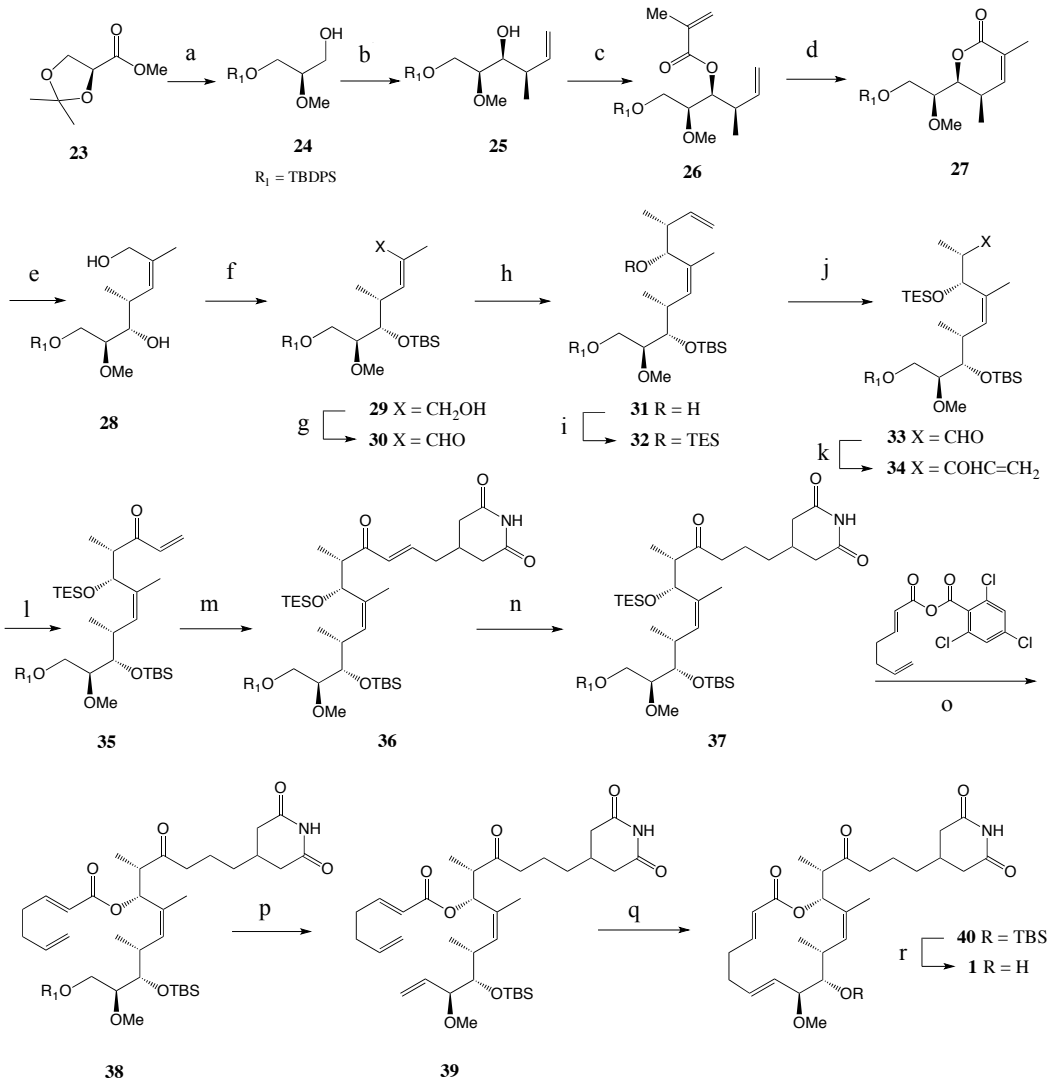

Reagents and conditions: (a) (i) *p*TsOH, MeOH/H_2O (1:1), room temp., (ii) TBDPSCl, imidazole, CH_2Cl_2, 0 °C to room temp., (iii) Ag_2O, MeI, MS 4 Å, Et_2O, 40 °C, (iv) DIBAL-H, CH_2Cl_2, –78 °C to room temp., (b) (i) $(COCl)_2$, DMSO, CH_2Cl_2, –78 °C, then Et_3N –78 °C to room temp., (ii) $MgBr_2 \cdot Oet_2$, CH_2Cl_2, –20 °C, then but-2-enyl- [(tri(*n*-butyl)]stannane, –60 °C, (c) methacryloyl chloride, Et_3N, DMAP, CH_2Cl_2, 0 °C to room temp., (d) [Ru]-**I** (16.5 mol%), CH_2Cl_2 40 °C, 144 h, (e) $LiBH_4$, $CeCl_3.7H_2O$, THF/H_2O (4:1), room temp., (f) (i) TBSOTf, 2,6-lutidine, CH_2Cl_2, 0 °C to room temp. (ii) THF/H_2O/AcOH (1:1:3), 36 h, room temp. (g) MnO_2, CH_2Cl_2, room temp., 16 h, (h) Ti-(*S*,*S*)-**I**, Et_2O, –78 °C, 24 h, (i) TESCl, CH_2Cl_2, room temp., 16 h, (j) (i) OsO_4 (4 mol-%), NMO, *t*BuOH/H_2O (1:1), room temp., 24 h, (ii) $NaIO_4$, THF/H_2O (1:1), room temp., 10 h, (k) vinylmagnesium chloride, –78 °C, THF, 0.5 h, (l) Dess– Martin periodinane, CH_2Cl_2, 0 °C to room temp. 1 h, (m) [Ru]-**II** (30 mol-%), glutarimide side chain, CH_2Cl_2, room temp., (n) Pd/C 5 % (5 mol-% Pd), EtOAc, room temp., 10h, (o) (i) THF/H_2O/AcOH, 36 h, room temp., (ii) mixed anhydride, pyridine, toluene, 48 h, room temp., (p) (i) NH_4F, MeOH, room temp., 24 h, (ii) Dess–Martin periodinane, CH_2Cl_2, 0 °C to room temp. 3 h, (iii) Zn, PbCl2 (cat), CH_2I_2, $Ti(OiPr)_4$, THF, room temp., (q) [Ru]-**I** (20 mol-%), toluene reflux, 0.3 h, I HF·pyr complex, THF, room temp., 24 h.

Scheme 1.3 Schematic overview of the total synthesis of **1** by Reymond employing cross metathesis and ring closing metathesis methodologies. Adapted with permission from reference 26. Copyright © 2006 WILEY-VCH Verlag GmbH & Co. KgaA, Weinheim.

The secondary alcohol was coupled to methacryloyl chloride in the presence of TEA, 4-dimethylaminopyridine (DMAP) in dichloromethane (DCM) to afford **26**. This was subsequently treated with Grubbs II catalyst to form the lactone with correct *Z* olefin stereochemistry. Next the lactone was opened with $LiBH_4$ and $CeCl_3 \cdot 7H_2O$ to form intermediate **28**. Both alcohols were protected with TBSOTf in the presence of base and the primary alcohol was selectively deprotected using mild acid conditions. The primary alcohol was then oxidised to the corresponding aldehyde **30** with MnO_2 .The aldehyde was treated directly with the highly face-selective crotyltitanium complex Ti-(*S*,*S*)-I to furnish two new chiral centres with high diastereoselectivity (dr = 9:1). The secondary alcohol was protected using TESCl to form **32**. The terminal alkene was transformed into an aldehyde chemoselectively using dihydroxylation-oxidative cleavage sequence, OsO_4, *N*-methylmorpholine *N*-oxide, and then $NaIO_4$ (sodium periodate). The aldehyde was reacted with vinylmagnesium chloride to form **34** and the alcohol was oxidised back to a ketone with DMP to form **35**. The resulting vinyl ketone was cross-linked with an allylglutarimide (synthesised over 5 steps from diethyl allylmalonate) via cross metastasis using Hoveyda-Grubbs catalyst. The resulting α,β-unsaturated ketone was selectively hydrogenated using 5% Pd/C. Next, the TES group was removed using mild acidic conditions. The secondary alcohol was coupled with freshly prepared mixed anhydride to form **38**. The TBDPS group was removed with NH_4F in methanol. The primary alcohol was oxidised to the aldehyde and this was subsequently treated under Takai conditions to afford alkene **39**. The ester was closed via ring closing metastasis to form **40** and the TBS protecting group was removed with HF/pyridine to yield migrastatin **1**.[26]

1.5.1.3 Danishefsky migrastatin analogues

The synthetic route toward migrastatin in the synthesis outlined by Gaul *et al*. furnished a key intermediate **14**. From this intermediate, a range of analogues were produced, shown in Figure 1.6. As previously mentioned, this diverted total synthesis approach in fact yielded more active compounds than the parent molecule **1**. The IC_{50} value for the synthetic migrastatin with 4T1 tumour cells was reported as 29 μM. The migrastatin core **41** showed an IC_{50} of 22 nM. By omitting the glutarimide side chain, an increase of ~ 1000 fold in activity was observed. This increase in potency was welcomed as the absence of the side chain allows for relatively easier synthesis and reduces the number of steps in the synthetic process. During a serum stability study, it was noted that the macrolactone **42** broke down in serum, likely due to endogenous esterases. The migrastatin core was a little

slower than the macrolactone at breaking down, perhaps due to the α,β-unsaturated carbonyl. The outcome of these tests shifted the attention onto more serum robust macrocycles, for example, macrolactam **43** and macroketone **44**. Compound **43** and **44** showed good inhibition results, 255 nM and 100 nM respectively, along with an increase in stability, relative to **41** in serum.[17]

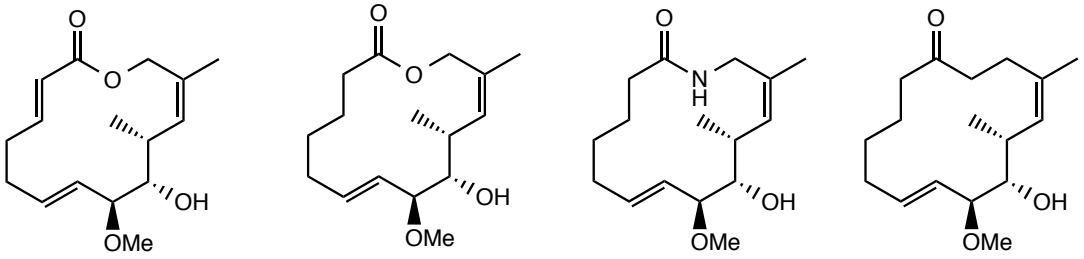

41 **42** **43** **44**

Figure 1.6 Danishefsky and co-worker's truncated migrastatin analogues.

Danishefsky and co-workers then focused on making an even simpler analogue, the macroether **45** and tested its inhibition potential. It showed an IC_{50} of 470 nM on 4T1 tumour cells. However, when tested against MDA-MB-231 and MDA-MB-435, human breast cancer cell lines, it had an increase in potency to 300 (±110) and 370 (±180) nM respectively. An IC_{50} of 408 (±80) μM was reported for normal human mammary epithelial MCF10A cells. This means a ~ 1000 fold increase in the concentration of **45** would be required to elicit the same inhibitory response of normal mammary epithelial cells. This observation is encouraging from a drug targeting and selectivity point of view. Both *in vivo* and *in vitro* studies suggested **45** mitigated metastasis, and if administered early at a high concentration, no detectable metastasis was observed. It should also be noted however that it did not reduce primary tumour growth.[37] Next, **45** and its analogue, macroether carboxylate **46**, were tested on lung cells A549. The IC_{50}'s were established as 1.93 μM and 660 nM respectively. The incorporation of the carboxylate group was envisaged to increase bioavailability and pharmacostability. Both compounds showed migratory inhibition in both *in vitro* and *in vivo* test models. Compound **46** in particular was four times more potent than its macroether counterpart **45** at low doses *in vivo*.[38] This data helps to support the hypothesis that the carboxylate moiety increases the bioavailability.

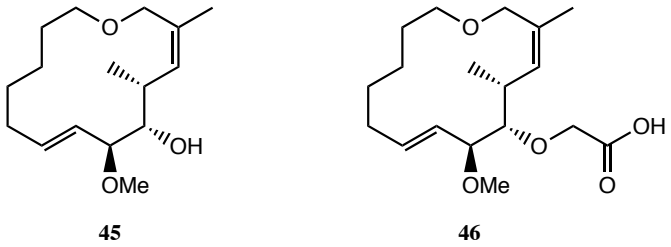

Figure 1.7 Macroether **45** and macroether carboxylate **46.**

1.5.1.4 Murphy migrastatin sugar derived analogues

The work carried out by Danishefsky illustrated that the macrocyclic core is important for inhibition of migration. With this in mind, previous work within the Murphy group focused on the development of migrastatin analogues derived from tri-*O*-acetal-D-glucal and D-xylose sugar units. These key intermediates from tri-*O*-acetal-D-glucal and D-xylose, **47** and **48** respectively, are shown in Figure 1.8. In the case of **47**, this resulted in inverted stereochemistry at C4, an omitted methyl group from the trisubstituted olefin and an additional alcohol group replacing a methyl group to that of the desired parent molecule **1**. Intermediate **48** retained the correct stereochemistry for all three chiral centers and had an alcohol in place of the methyl group. The differences between the analogues and the migrastatin are highlighted in red.[39]

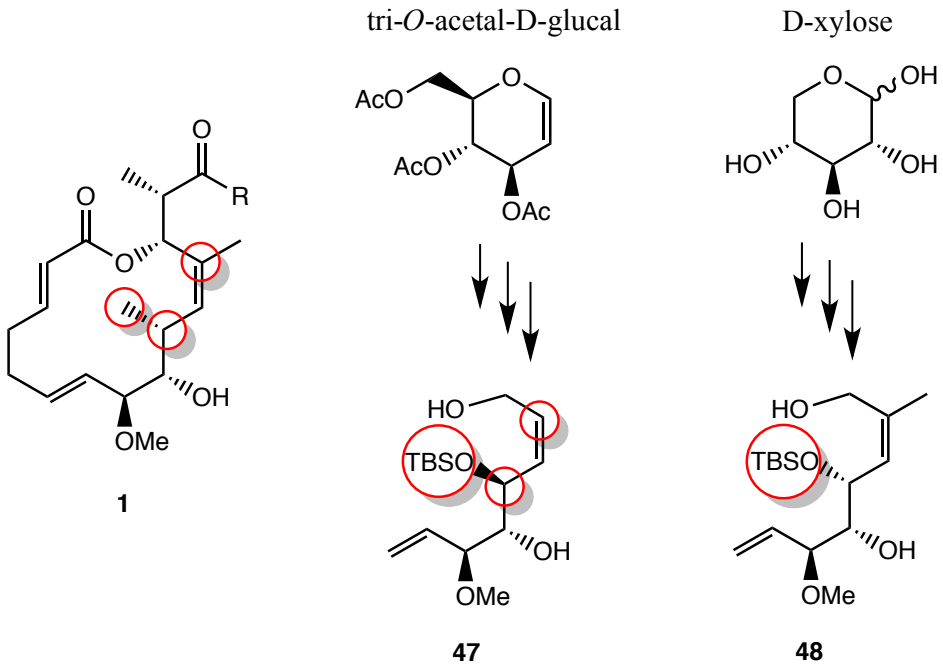

Figure 1.8 Sugar based intermediate derivatives of migrastatin by Zhou.

1.5.2 Migrastatin (macroketone / macrolactam) mode of action

One proposed mechanism, which is receiving much attention, describes migrastatin (macroketone) as binding to a protein called fascin. To understand this, we must first discuss the biological role fascin has and its link to metastatic tumour cells. The cytoskeleton of a cell is made up of actin filaments. These are microtubular in morphology and allow for rigidity of the cell. Cellular protrusions, for example microvilli, microspikes, filopodia or invadopodia, can vary in size and activity and are all composed of bundles of parallel actin. The amount of crosslinking protein to form these ordered structures can define the type of protrusion it is and subsequently its role. Invadopodia for example, possess the ability to help the cancerous cell invade other tissue by disassembling the extra cellular material and therefore work its way through the interstitial spaces of cells at the secondary location. Filopodia have a 55 KD crosslinking protein present called fascin. The fascin family consists of fascin-1, fascin-2 and fascin-3 with fascin-1 being more abundant in various regions of the body and the other members of the fascin family detected in the retina and testis respectively.[40,41] The presence of fascin-1, (from herein called fascin) has seen to be upregulated in tumour cells along with carcinoma cell lines, including breast and colon cancer cell lines, when compared to normal healthy cells.[42,43] The upregulation increases the cells motility and invasiveness power leading to the cell having an overall higher metastatic potential. A paper published by Chen *et al*. suggested that the macroketone does indeed bind to fascin however the crystallographic data was retracted from this article, although the authors still believe fascin is the target.[27] Work from Danishefsky and co-workers led to doubt to whether this could be the mode of action. As previously discussed, Gaul, Danishefsky and co-workers synthesised compound **46** with a carboxylic acid group present exhibiting high activity both *in vitro* and *in vivo*.[38] The addition of this carboxylic acid would have been expected to decrease the permeability of the compound into the cell. This suggests that the mode of action may well be targeting a receptor on the exterior of the cell and has raised questions about fascin being the primary target.

Another possible mechanism was reported by Murphy *et al*. whereby immobilised epithelial cadherin (E. Cadherin) dynamics were observed *in vivo* using a technique called FRAP (Fluorescence Recovery After Photobleaching).[29] This approach allows for the visualisation of protein dynamics around the phospholipid bilayer in the presence and absence of the chemotherapeutic agent being tested. The transmembrane protein E.

Cadherin, is involved in cell-cell junctions in epithelial cells and forms adhesive sites to which the cells can "stick" together.[44] This Ca^{2+} dependent binding between cells is part of epithelia formation and is a prerequisite for cell adhesion resulting in tissue structure.[45] The transmembrane protein complexes with β and γ catenins in the extra cellular environment and has a subunit in the cytoplasm that attaches to a α-catenin.[46] The complexation with α-catenin undergoes linking to a dynamic actin in the cytoskeleton which helps hold the linkage.[47] Freely moving E. Cadherin in the bilayer becomes tied up overtime in these cell-cell junctions and this cluster effect gives rise to a stronger bond between the cells.[48] It has been reported that the levels of E. Cadherin are down regulated or not produced in metastatic cells, thereby allowing cells to break way from one another and migrate.[49] By inhibiting the E. Cadherin dynamics in the cellular membrane, this could allow for better cell adhesion over a longer period of time and inhibit migration. The mechanism of migrastatin and its analogues remains unclear and not validated. The continued synthesis of more analogues of varying structures, for example through the inclusion of different atoms, may help elucidate the mechanism and increase the chance of future tailored designed therapeutics in inhibiting metastasis.

In addition to the sugar analogues of migrastatin previously mentioned in section 1.5.1.4, a synthetic method encompassing the three stereochemical carbons with the same stereo configuration to that of the parent molecule **1** was developed and previously used in the Murphy group. Truncated 13-membered migrastatin cyclic derivatives have shown good activity when tested against canine mammary cancer cells.[28] This work has led to high yields allowing a key intermediate and its precursors to be produced in good quantity, which has subsequently led to a wide variety of synthesised analogues and their biological evaluation.[50]

1.5.3 Objectives

The aim of this chapter was to create truncated analogues of compounds **1** and **2** and to evaluate them for biological evaluation. The derivative of compound **1** was made by focusing on the macrolactone ring and replacing the methyl substituent with an ethyl group at C-12 on the *Z*-tri-substituted alkene. The second part of this chapter focused on synthesising derivatives of compound **2**. The synthesis of these derivatives involved the formation of a macrolactone and macrolactam.

1.6 Results and Discussion

The previous work within the Murphy group formed the platform for the work outlined for this dissertation and the synthesis described herein. In conjunction with the synthetic route outlined for the migrastatin analogues, some important named chemical reactions will be discussed in more detail along the way during the course of this discussion. The aforementioned analogue differs to **1** with the incorporation of an ethyl group into the trisubstituted *Z* alkene instead of a methyl group. The synthesis starts with commercially available 2-methyl-1,3-propanediol which is selectively protected using vinyl benzoate in the presence of a zinc activated chiral catalyst, Trost (*S*,*S*)-bis-prophenol ligand, to give **48** with S configuration as shown in Scheme 1.4.[51] The primary alcohol was then oxidised to the aldehyde using diacetoxyiodobenzene (BAIB) and 2,2,6,6-Tetramethylpiperidinyloxy (TEMPO). This freshly prepared aldehyde was reacted quickly, to avoid epimerisation, with allyl methyl ether under basic conditions where it underwent a diastereoselective Brown alkoxyallyation (mechanism is shown in Figure 1.9) yielding a 7.8:1 mixture of diastereoisomers **50/51** after workup with 1M NaOH and 30 % H_2O_2 .

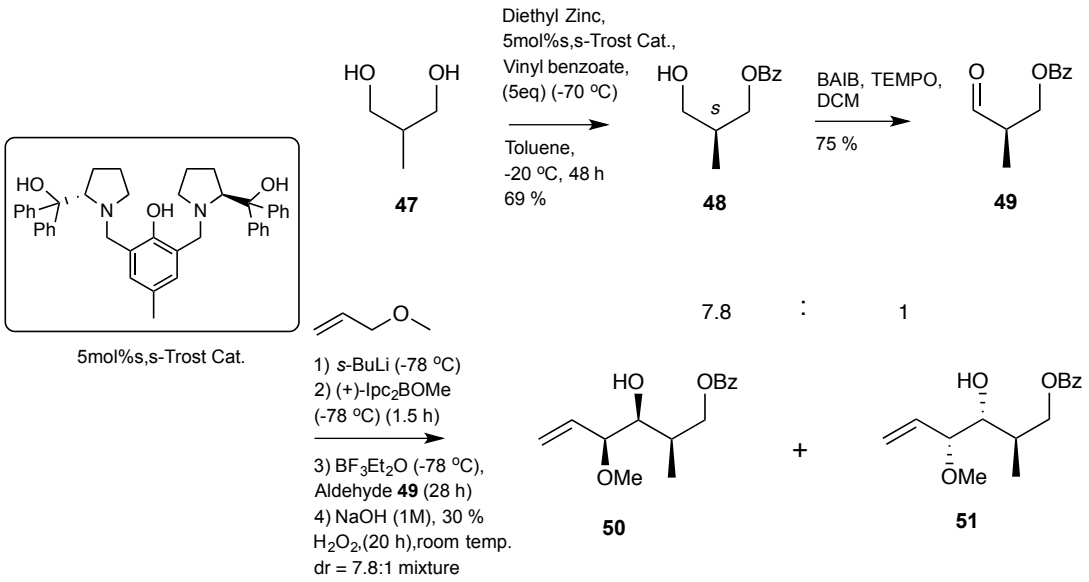

Scheme 1.4 Synthesis of diastereomeric mixture **50**/**51**.

1.6.1 Brown alkoxyallyation

When allyl methyl ether is treated with *sec*-Butyllithium (*sec*-BuLi), it forms a (*Z*)-allylic anion resulting in a five membered cyclic transition state. Reaction of this anion with a chiral borane group forms an overall stabilised complex where the borane is now attached to the allyl methyl ether group. Treatment of this complex with a Lewis acid, boron

trifluoride diethyl etherate, releases the methoxy group from the borane and as such the negative charge is removed. The newly created intermediate, (*B*)-(*Z*)-(*γ*)-alkoxyallyldiisopinocampheylborane, is reacted with an aldehyde resulting in the formation of two new chiral centers. Workup with NaOH and H_2O_2 releases the borane-oxygen complex furnishing the desired alcohol moiety.

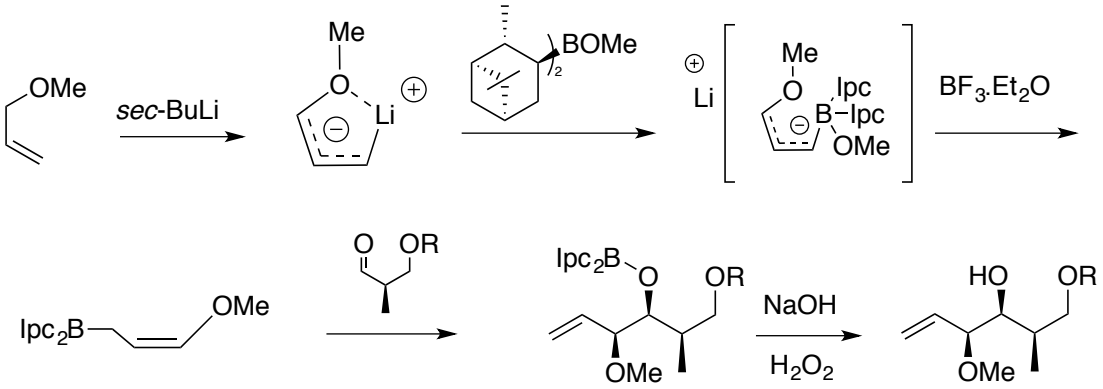

Figure 1.9. Overview of the Brown alkoxyallylboration mechanism.[52]

The workup of the reaction also produced a by-product pinenol and both products were taken on to the next step. Deprotection of the benzoate protecting group with K_2CO_3 in anhydrous methanol furnished the diol diastereomer mixture **52**/**53**. The mixture of **52**/**53** was fully protected with TBSOTf under basic conditions and the resulting compounds were selectively deprotected under mild acidic conditions, 10 mol % *para*-toluene sulfonic acid (*p*-TSA) to form the respective primary alcohols. At this point, flash chromatography was used to separate the two diastereomers yielding intermediate **54**. This alcohol intermediate was oxidised using DMP and pyridine to give the corresponding aldehyde **55**.

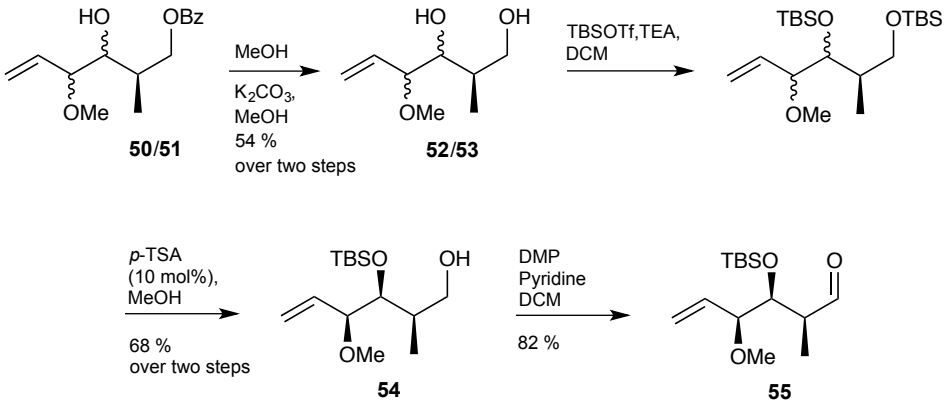

Scheme 1.5 Synthesis of aldehyde chiral aldehyde **55**.

It was observed that using non-anhydrous DCM improved the yield along with freshly prepared saturated solution of $Na_2S_2O_3$ as part of the quenching agent.

Again, this aldehyde was reacted quickly in a Horner Wadsworth Emmons (HWE) type reaction with an Ando phosphonate whereupon a *Z*-selective olefination reaction is favoured.

1.6.2 Horner Wadsworth Emmons

The HWE reaction is an efficient way of making *E* olefins using stabilised phosphonates. This reaction was developed to increase the reactivity of the phosphonate group compared to that of the phosphonium salt setup that is typically used in stabilised Wittig ylides. The introduction of an ester phosphonate moiety allows for enolate conjugation, which in turn allows for *E* selectivity. The resulting phosphonate moiety is polar and can be typically washed away with water unlike triphenyl phosphine, the by-product from the Wittig reaction. HWE reactions have played their part in the synthesis of natural products, in particular the formation of *E* α,β-unsaturated esters. The total synthesis of the natural marine compound palmerolide, an inhibitor of vacuolar ATPase and cytotoxic to melanoma cell lines, by Nicolaou *et al.* availed of the *E*-selective HWE olefination reaction.[53] A proposed mechanism showing the thermodynamic outcome is shown in Figure 1.10

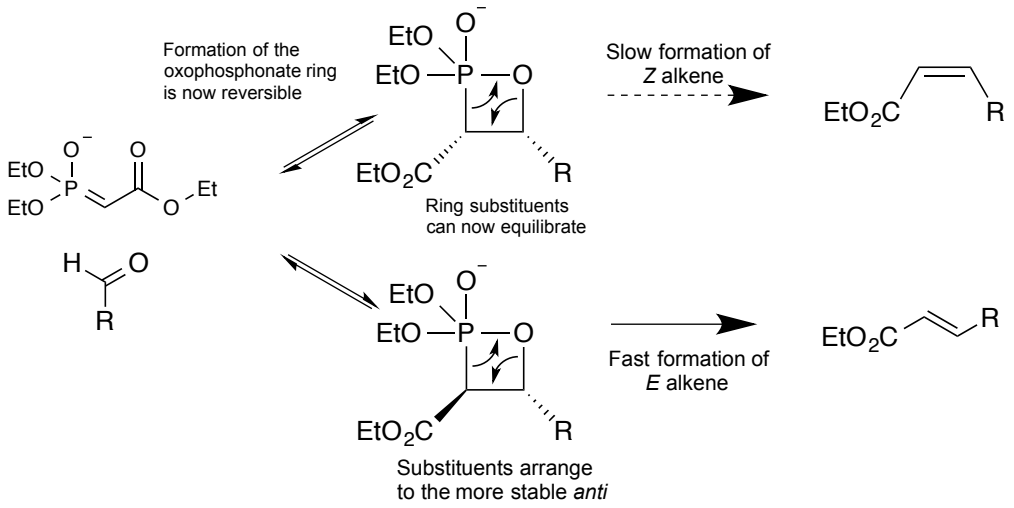

Figure 1.10 HWE reactions under thermodynamic control allowing more stable *anti* intermediate to form and give *E*-alkenes.

With an increase in conjugation about the α-carbon, the intermediate adducts can revert back to the precursors and in turn form the more thermodynamically stable *anti*. In this setup, the interconversion between the adducts and the starting material has to be faster than the elimination and thus the formation of the alkene. Typically strong bases are employed in deprotonating the α-proton from the ester phosphonate, for example NaH, BuLi. In the case of substrates that are not stable to these strong bases, the introduction of Masamune-Roush conditions can be implemented. Here weaker bases for example DBU or diisopropylethylamine (DIPEA), in addition with LiCl can still deprotonate the phosphonate ester to react with a carbonyl group.[54] The theory behind this breakthrough is the Li^+ salt acts as Lewis acid chelating to the two oxygens resulting in the α-proton becoming more acidic, as shown in Figure 1.11.

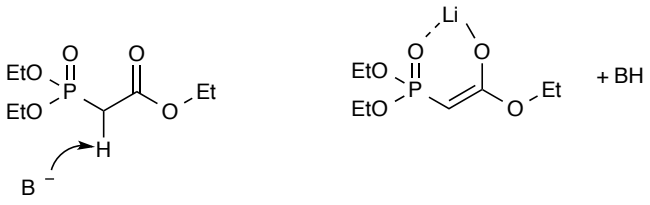

Figure 1.11 Proposed reaction using Masamune-Roush conditions.

Still and Gennari *et al.* worked on trying to achieve *Z*-selective olefinations based on the HWE reaction and developed a phosphonate that introduced triethylfluoro groups resulting in a more electronegative phosphorous. This trifluoroethylphosphonoester, accompanied by the base $KN(TMS)_2$ [(Potassium bis(trimethylsilyl)amide)] in the presence of 18-crown-6, resulted in selectivities ranging from 4:1 to > 50:1 for *Z*:*E*.[55] The concept was to interfere with the reversibility of the reaction back to the starting material and increase the outcome from the kinetically favoured pathway. The attack of the alkoxide anion into the now more electronegative phosphorus resulted in a faster formation of the ring followed by the spontaneous breakdown resulting in *Z*-selectivity. Ando *et al*. built on the idea of increasing electronegativity on the phosphorous atom to favour a kinetic pathway and replaced the triethylfluoro groups with phenyl groups. Ando however explained this outcome using the analogy of p*K*a strengths of respective alcohols. The stronger an electronegative substituent is next to an alcohol group, the more acidic it is due to the stabilisation of the anion. This is represented by the following; aryloxy group

(p*K*a(PhOH)) 10.0 vs (p*K*a (CF_3CH_2OH)) 12.4 vs (p*K*a(CH_3CH_2OH)) 16.[56] These higher ratio yielding *Z* Ando phosphonates[57] were analogously synthesised to include a *Z*-olefin into the migrastatin analogue core.

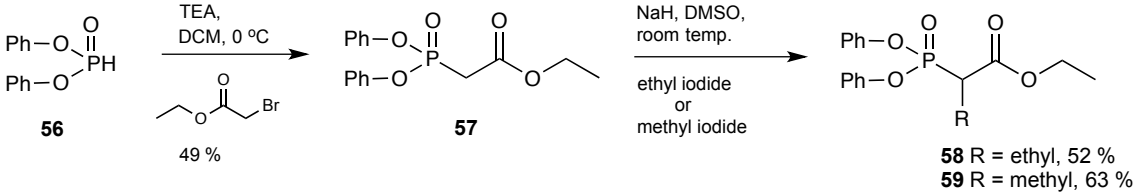

Scheme 1.6 Synthesis of Ando phosphonates **58** and **59**.

The Ando phosphonates were synthesised by treating diphenyl phosphite with TEA followed by the addition of bromo ethylacetate to yield intermediate **57**, as shown in Scheme 1.6, with a moderate yield of 49 %. With **57** in hand the opportunity to incorporate different alkyl halides was realised. NaH was used to deprotonate the α-proton and either ethyl iodide or methyl iodide was added resulting in compounds **58** and **59** respectively. Each reaction resulted in ~10 % disubstituted, 52 – 63 % mono-substituted (desired) and ~ 20 % unreacted starting material. The purification of compounds **58** and **59** using chromatography had to be performed with great care to ensure the purity of the desired compounds. Any small trace of unreacted starting material would give rise to a non-alkylated alkene in the following step. Ando phosphonate **58** was treated with NaH at −78 °C and freshly prepared **55** was added and the reaction worked to give **60** and **61**, with poor selectivity, *Z*:*E* 65:35 and a disappointing yield of 10 %. A major side product was formed, **62**, which contained a mixture of alkenes. This product contains an extra alkene with the elimination of the TBS ether group. The geometry of these two alkenes was not determined.

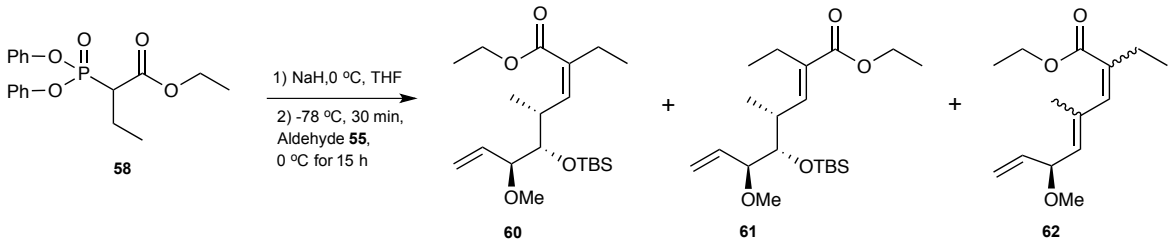

Scheme 1.7 Synthesis of *Z*-intermediate **60** and undesired products **61** and **62** that formed also.

The recovered mixture of product **60** and the undesired *E*-alkene isomer **61** was brought on to the next step as they were inseparable by chromatography at this stage. The isomeric mixture **60** and **61** was reduced to their respective primary alcohols using DIBAL, yielding the desired product **63**. This reaction had to be frequently monitored at 15 min intervals as removal of the TBS protecting group was once observed. In this instance, both alcohols were protected once again as TBS ethers and the primary alcohol was selectively desilylated. After effective ester reduction, both isomers were separated and the desired *Z* key intermediate **63** was taken forward to the next step.

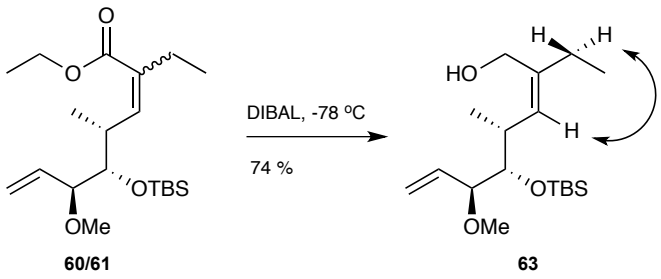

Scheme 1.8 Reduction of the isomeric mixture to form **63** and ^{1}H NMR 1D NOESY correlations confirming the *Z* isomer of desired intermediate **63**.

To confirm that **63** was the desired *Z*-isomer, ^{1}H 1D NMR NOESY (Nuclear Overhauser Effect Spectroscopy) experiments were performed as the alkene was trisubstituted and this information could not be extrapolated based on *J*-coupling data. The correlations between the source proton *S* and interest proton *I* is illustrated in Scheme 1.8

The next step was the addition of the aliphatic chain containing a terminal alkene and a carboxylic acid. This esterification was carried out under Mitsunobu conditions.

1.6.3 Mitsunobu Reaction

Mitsunobu observed that in the presence of triphenyl phosphine, diethyl azodicarboxylate (DEAD), an alcohol and a carboxylic acid, led to the formation of esters formation and has become one of the most used coupling reactions since.[58] Diisopropyl carboxylate (DIAD) as a coupling reagent is more stable and less explosive than DEAD and is therefore more commonly employed. The Mitsunobu reaction is an S_N2 reaction that leads to inversion of the incoming alcohol. This reaction utilises the nucleophilicity of the phosphorus atom

within triphenylphosphine, in combination with the less stable azo bond within the coupling reagent, DIAD. The formation of a strong P=O bond is the driving force of the reaction and results in the by-product triphenylphosphine oxide. The order of addition with regard to the reagents may some times have to be altered if no product is observed. This complication may arise as the two functional groups to be coupled both contain nucleophilic oxygen atoms.

The reaction starts with nucleophilic attack of the phosphorus atom to the less stable N=N π bond. The resulting complex generates a conjugated negative charge that is basic enough to deprotonate the proton from the carboxylic acid thus forming a carboxylate anion. The lone pair of electrons on the alcohol attacks the phosphorus atom that holds a positive charge as shown in Figure 1.13. The proton is removed from the alcohol allowing a P=O bond to form. This in turn results in the carboxylate anion attacking the electrophile C-O-P due to the positive charge on the oxygen. This results in triphenyl phosphine oxide and the desired ester.

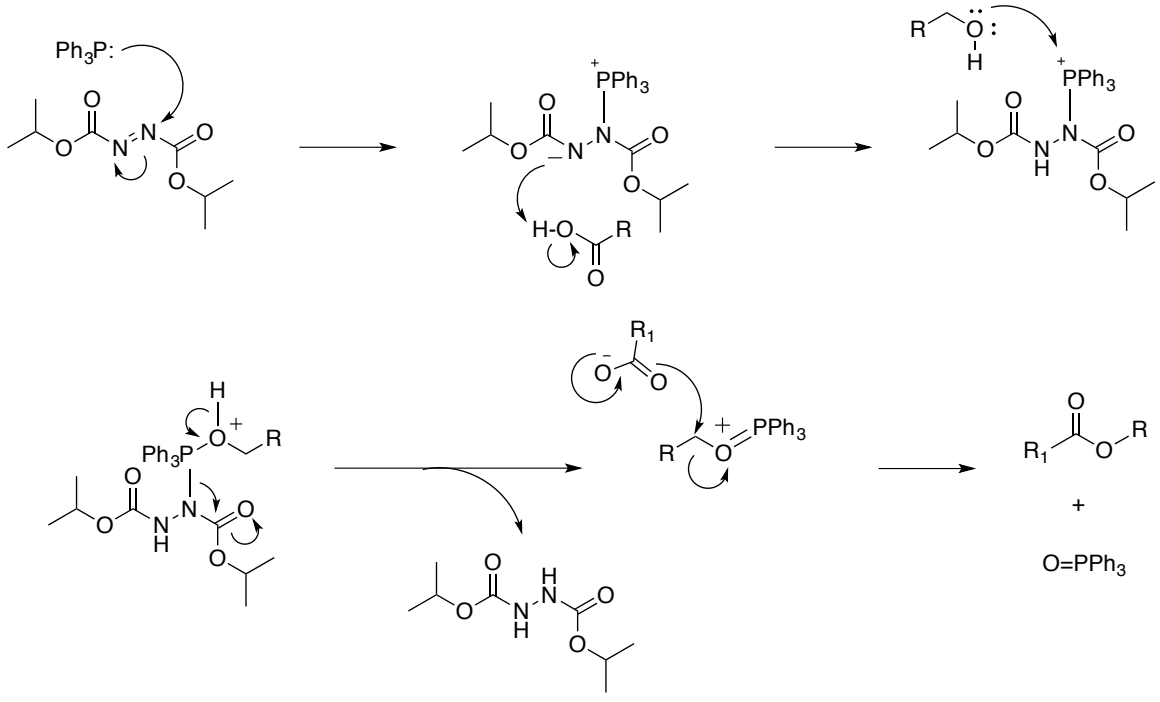

Figure 1.13 Mitsunobu reaction mechanism overview.

The key intermediate, **63**, was reacted with 6-heptenoic acid under the stated Mitsunobu conditions yielding ester **64** in a high yield of 79 %.

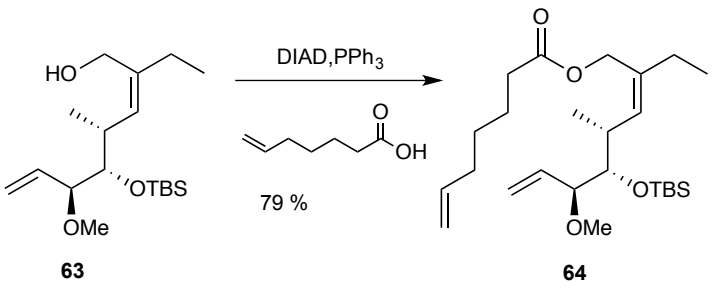

Scheme 1.9 Coupling of **63** to 6-heptenoic acid forming ester **64**.

The smooth esterification reaction yielded an ester with two terminal alkenes ideally positioned to setup the ring closing metathesis. These alkene cross couplings are suitable for creating carbon-carbon bonds leading to higher alkenes from simpler precursors. The resulting bond creates an olefin adding further diversity, depending on the substrate in question, by yielding a *Z* and/or an *E* geometric isomer. The newly formed olefin can also be reduced to a saturated compound based on one's end goal for their synthesis.

As this step is notably important, but none more so than the preceding steps to this stage, cross coupling and ring closing metastasis reactions will be further discussed in detail.

1.6.4 Ring Closing Metathesis

The in-depth research and contribution to the field of ruthenium and molybdenum 28arbine complexes by Schrock[59] and Grubbs[60] has paved the way forward by allowing chemists to have access to new synthetic routes via metathesis coupling reactions.

Olefin metathesis can be grouped into four major groups; (i) ring closing metathesis (RCM), (ii) ring opening metathesis (ROM), (iii) enyne metathesis (EnyneM) and (iv) cross coupling metathesis (CM), which can be further divided into hetero and homo dimerisation. Cross coupling metathesis has been previously employed in synthetic routes, for example in the total synthesis of migrastatin reported earlier by Reymond. However in this type of reaction, it can be hard to predict the outcome, whether it is the heterodimerised product or homodimerised product, along with predicting the stereochemistry of the alkene that is generated. Chatterjee *et al*. published alkenes into categories and developed some guidelines to help with predicting the outcomes. There are four types, ranging from type I, an alkene that readily homodimerises, to type IV, alkenes

that do not react but do not poison the catalyst or inhibit its activity.[61] Ring opening metathesis can be used to alleviate ring strain allowing these reaction outcomes to become more predictable.[62] In the case of enyne metathesis, this encompasses cross metathesis and ring opening and closing metathesis. The coupling of an alkyne and alkene leads to a final compound possessing two olefins. This reaction allows for complicated natural products and other difficult chemistry become accessible as outlined in a review by Mori.[63]

Ring closing metathesis allows for the cyclisation of linear olefin presenting substrates. The ability to create a more rigid scaffold adds reassurance that the conformation is retained and is more likely to interact better with a desired target. This reaction is carried out under high dilution, typically ~ 0.05 mM, to suppress undesirable acyclic diene metathesis (ADMET). The ring closing metathesis eliminates ethene as a by-product and can in principle furnish olefins with either *Z* or *E* geometry, depending on the ring size. Ring size matters in these ring closing metathesis. Due to ring strain, one isomer may be preferentially formed over the other. In some cases, as will be discussed later in this chapter, a mixture of *Z* and *E* may be formed.

The catalytic cycle, Chauvin mechanism, is shown in Figure 1.14 whereby the ligands on the ruthenium atom have been omitted for clarity purposes. The cycle starts with the ruthenium catalyst bound to a CH_2 group. This cycle does not show the initiation of the pre-catalyst step whereby the ancillary ligand has been exchanged with a CH_2 group. The newly formed active catalyst lines up with one of the alkenes from the incoming diene. A concerted *[2+2]* cycloaddition occurs resulting in a metallacyclobutane intermediate species. This ring subsequently breaks down with the elimination of ethene. The metallocarbene has formed part of the substrate and a second *[2+2]* cycloaddition occurs. This ring once again breaks down forming the ring closed product regenerating the catalyst for another cycle.

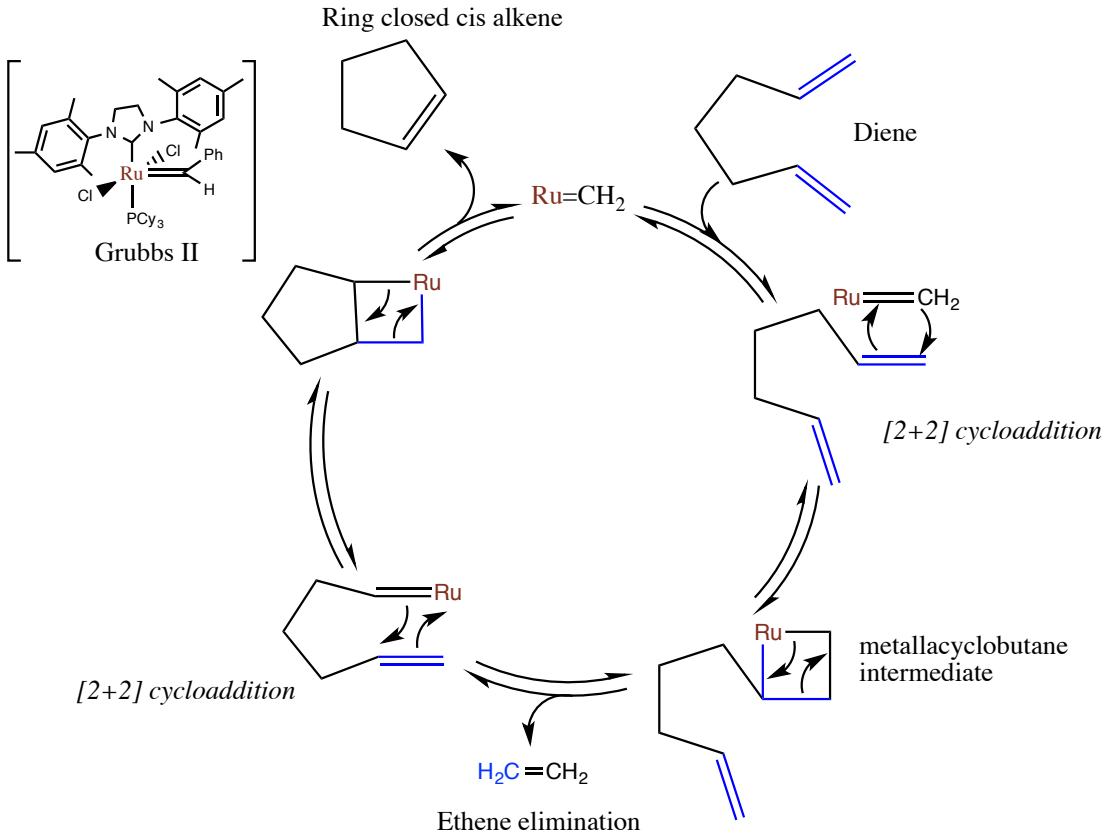

Figure 1.14 Catalytic cycle of ruthenium-catalysed olefin metathesis.

The oxidation state of the ruthenium multivalent compounds, for example Grubbs, starts off as pre-catalysts with a $16e^-$ species setup. These subsequently undergo a transitional change from the $16e^-$ species state to $14e^-$ species state as the "throw-away ligand" leaves in a dissociative fashion. Next, the alkene of the substrate binds to the $14e^-$ species and forms the active catalyst as a $16e^-$ species, which can go through the cycle illustrated above. This results in the elimination of one molecule of ethene and the formation of a new olefin along with the regeneration of the active catalyst.[64]

Returning to the synthetic discussion, compound **64** was closed via the ring closing metathesis reaction. This reaction gave exclusively an *E* alkene and resulted in the formation of the precursor **65**, to the final product with a high yield of 74 %. To deprotect the precursor and remove the TBS silyl group, **65** was first treated with the relatively less dangerous *tert*-butyl ammonium fluoride (TBAF) over a 24 h period however this returned a poor yield on the final product. This may be due to the bulky nature of the TBS group causing steric hindrance and the fact that it is a secondary alcohol. Next, the precursor was subjected to more harsh conditions using HF/pyridine under a controlled and safe

environment to yield the final product **66** in a much more satisfying yield of 88 % shown in Scheme 1.10. Compound **66** has an ethyl group present instead of a methyl offering slight diversity from that of **42**. It was subjected later to bioassays for biological evaluation and the results are reported in section 1.6.6.4.

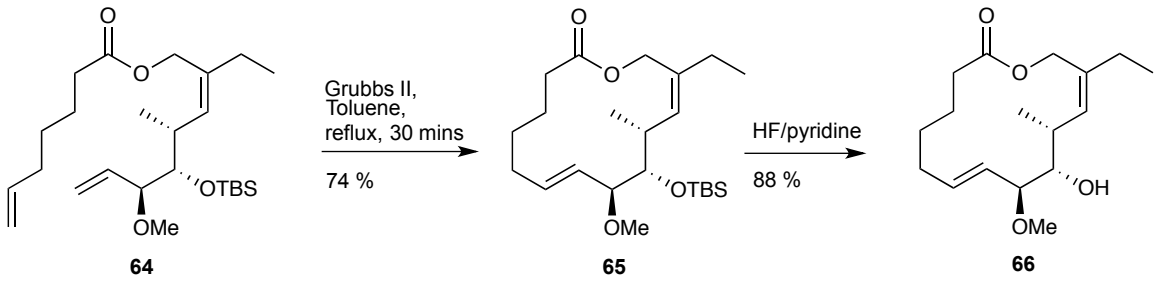

Scheme 1.10 Synthesis of the desired migrastatin analogue **66**.

While the synthesis of migrastatin analogues has previously been researched within our own group and other groups, the derivatisation of **2** has not been explored. As previously mentioned, **2** was tested against fungi and also showed to reverse the phenotype of transformed NIH/3T3 cells back to the morphology of normal cells. The back bone of compound **2** is the same as that of compound **1** however it is acyclic. The geometry of one of the double bonds has also changed from a *Z* to an *E* olefin. The synthesis of 'dorrigocin A' analogues was investigated due to the little attention the parent molecule has received in the literature and to see if the geometric isomer change has implications, good or bad, on anti-metastatic activity.

The synthesis began in the same fashion as before, introducing the three chiral centers with configurations matching **1**. The synthesis then arrived at intermediate **55** that was once again reacted quickly. Instead of carrying out a HWE with an Ando phosphonate as previously performed, a stabilised Wittig reagent was employed as the *E*-isomer was desired. This gave a high selectivity of *E*:*Z*, 44:1 and a moderate yield of 65 % to form intermediate **67**. Ester **67** was then reduced using the same DIBAL conditions as before and resulted in compound **68**.

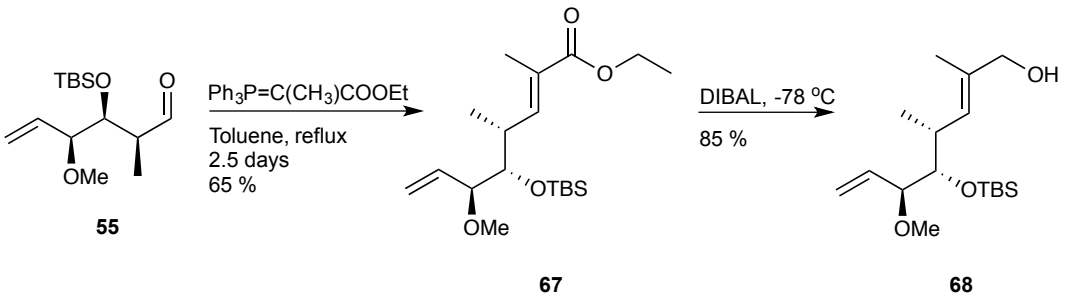

Scheme 1.11 Synthesis of intermediate **68** using the Wittig reagent.

The primary alcohol **68** was reacted under previously discussed Mitsunobu conditions to form **69** and allowed for the envisaged RCM.

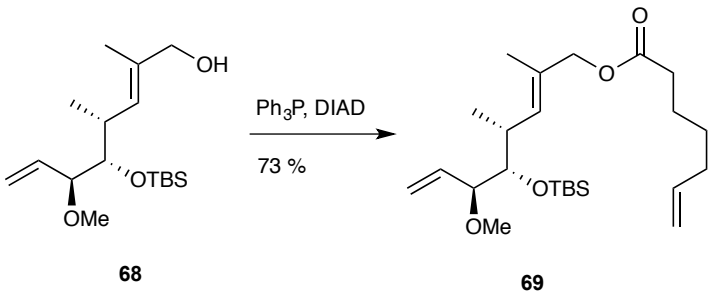

Scheme 1.12 Esterification of **68** to form **69**.

The introduction of the *E* olefin during ring closing metathesis gave rise to a lower yield relative to compound **65**. A mixture of *Z* **70** and *E* **71** olefins with a ratio of 1:1 over 45 min was also observed. These two isomers were inseparable by chromatography. The RCM was repeated under different reaction times to see if there was a change in the isomeric ratio, the results of which are represented in Table 1.1 and ^{1}H NMR spectra sample is shown in Figure 1.15.

Table 1.1 Reaction times of RCM using Grubbs II catalyst on intermediate **69**.

Reaction time (mins)	***Z* : *E* Ratio**	**Isolated Yield 70 + 71**
45	51 : 49	46 %
60	47 : 52	46 %
90	43 : 56	42 %

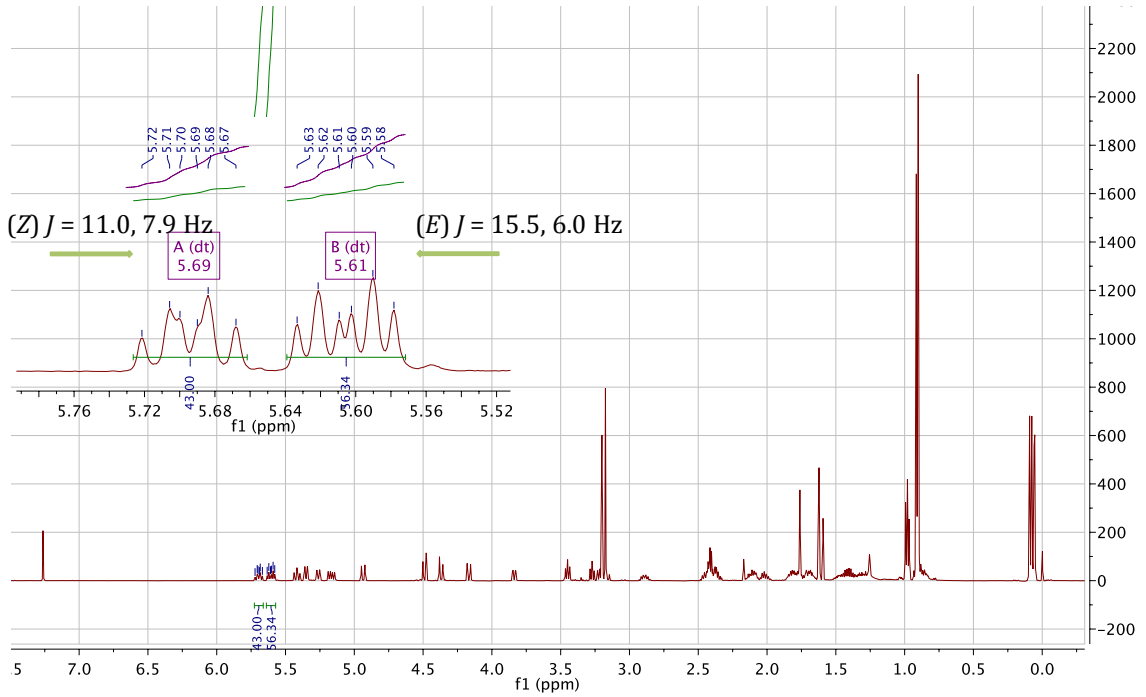

Figure 1.15 ^{1}H NMR spectra showing both *Z* and *E* isomers **70** and **71** are present in the mixture.

The increase in reaction time suggests that the more thermodynamically favoured product is the *E* isomer, however the yield started to suffer when the reaction was left on for 90 mins. The inseparable mixture of **70** and **71** was treated with HF/pyridine affording separable compounds **72** and **73** (89 % and 85 % respectively).

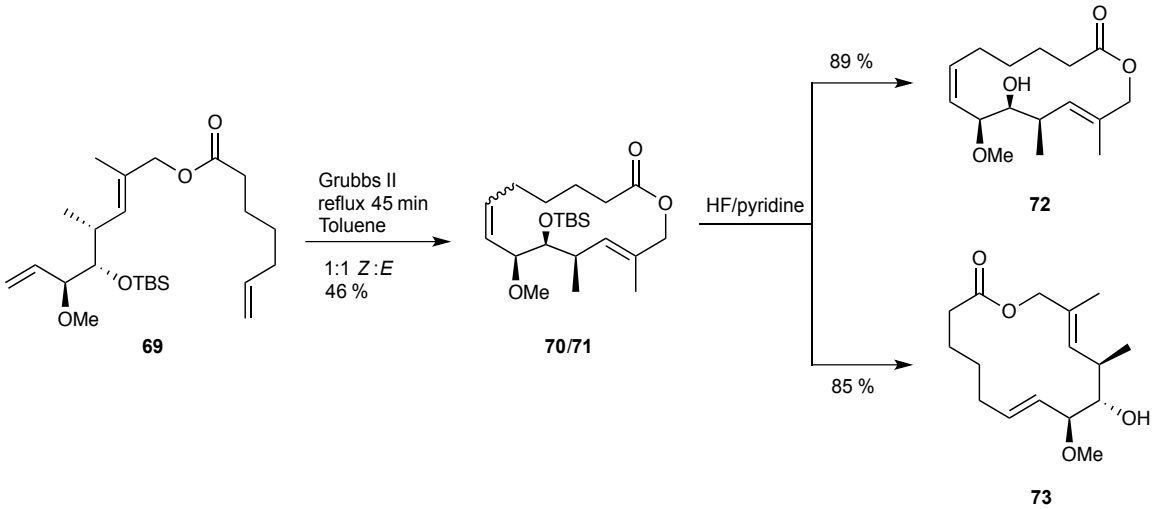

Scheme 1.13 Macrocyclisation of **69** to form a mixture of *E* and *Z*-isomers which are resolved after deprotection with HF/pyridine yielding desired compounds **72** and **73**.

As previously mentioned, the migrastatin analogue **42** showed a ~1000 fold increase in potency compared to migrastatin when the glutarimide side chain was omitted. With this in mind, 'dorrigocin A' analogues were synthesised based on the macrolactone core alone i.e. without the glutarimide side chain. As part of Gaul *et al.*'s work, they also reported that the open hydrolysed lactone form, shown in Scheme 1.14, showed activity at 378 nM. [17]

With this in mind, the synthesis of the acyclic analogue was investigated. A portion of material from **72** and **73** was subjected to saponification conditions using LiOH and a HCl workup. The first reaction conditions for the hydrolysis were tested at 10:1 MeOH:H_2O. This resulted in the methyl ester been observed. The ratio was then lowered to 1:1 forming the acyclic derivatives of **74** and **75** respectively, in moderate yields. The increase in water may have altered the chance of a methoxide anion attacking the ester as a nucleophile and opening it up to form the methyl ester via transesterification. The hydrolysis of the macrolactone is shown in Scheme 1.14.

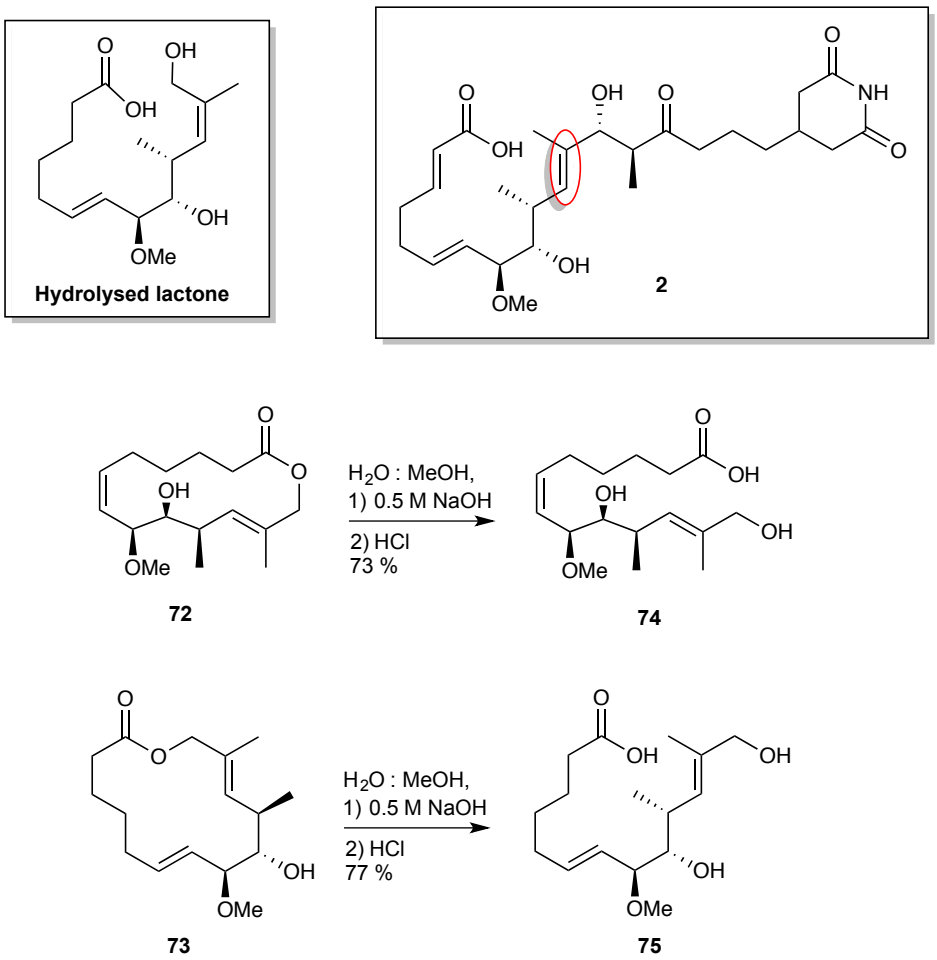

Scheme 1.14 Hydrolysis of lactone rings **72** and **73** to their respective acids **74** and **75**.

Hydrolysed lactone prepared by Gaul *et al*. and dorrigocin A **2** are shown in the boxes. The geometry of dorrigocin A olefin is highlighted for comparison purposes.

With the knowledge that the lactones could be successfully synthesised, albeit with a ratio of *Z* and *E* olefins after the RCM, the more serum stable macrolactams were explored. Danishefsky and co-workers report that indeed **43** is stable in mouse serum.[17] The synthesis of the macrolactams followed the same path to key intermediate **68**. The primary alcohol was transformed into the corresponding azide via an azido-transfer from diphenylphosphoryl azide (DPPA) under basic conditions to give a 1:1 ratio of **76** and **77**, shown in Scheme 1.15. The inclusion of the azide at this alpha position resulted in a low yield of desired *E* azide, **76** (45 % yield), due to allylic azide rearrangement which disrupted the integrity of the *E* olefin resulting in a mixture of isomers.[65] This rearrangement yielding the isomeric mixture was observed by NMR analysis and is illustrated in Figure 1.16.

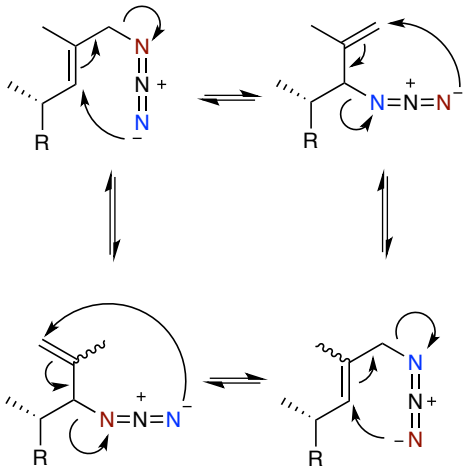

Figure 1.16 Allylic rearrangement mechanism showing that the olefin can reform to either geometric isomer after the rearrangement.

This isomeric mixture **76**/**77** was inseparable by chromatography and as such was taken on to the next step. The azide mixture was reduced via a Staudinger reaction to the corresponding primary amines **78** and **79**.

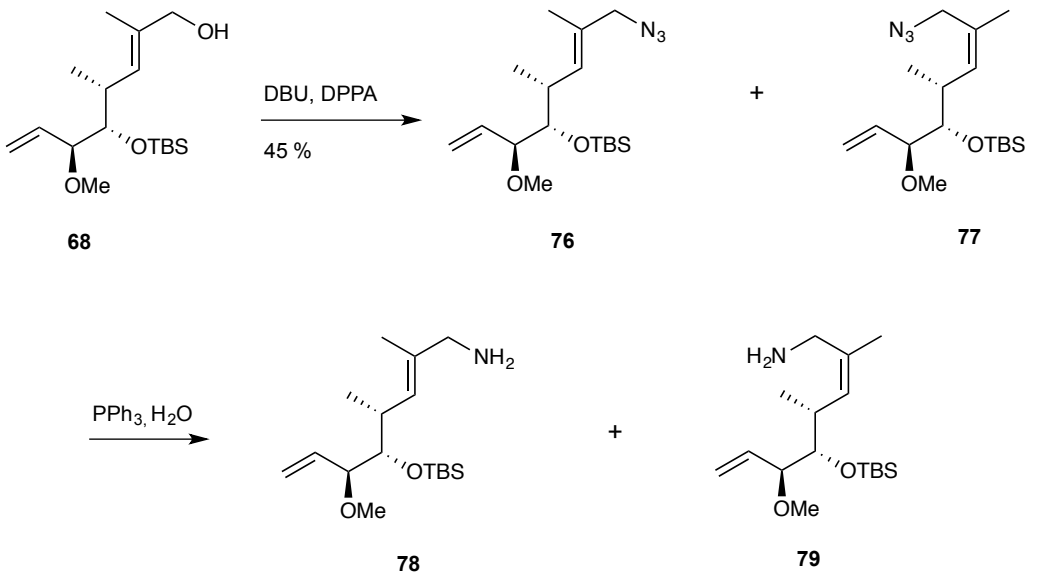

Scheme 1.15 Conversion of intermediate **68** to the primary amine isomeric mixture, **78** and **79**.

The resulting isomeric amine mixture of **78** and **79** was taken on crude to the next step. In the presence of a coupling reagent and base, N-(3-Dimethylaminopropyl)-N′-ethylcarbodiimide hydrochloride (EDC.HCl), and DIPEA, 6-hepteneoic acid was coupled to reveal the desired amide **80** with *E* geometry and a yield of 73 % (based on the ratio of *E* isomer from the starting azide) and amide **81**.

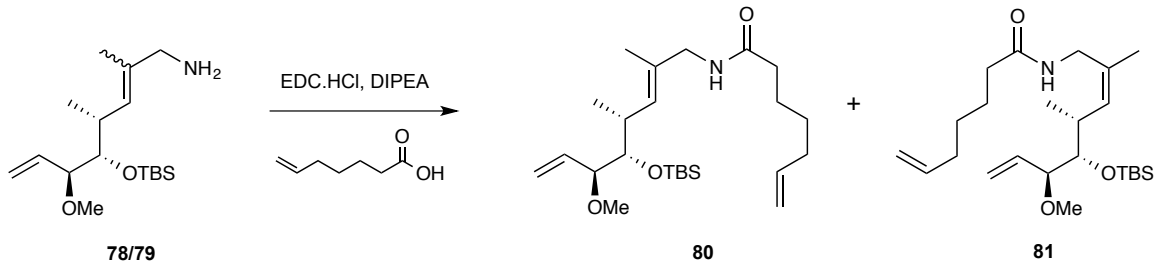

Scheme 1.16 Coupling of the isomeric mixture of **78** and **79** forming the desired amide **80** and the undesired amide **81**.

The two amides were separable at this point and intermediate **80** was subjected to RCM conditions using Grubbs II. Once again and similar to lactones **74** and **75**, *Z* and *E* macrocyclic products, **82** and **83** respectively, were formed in a moderate yield of 27 % and 23 % respectively. A ratio of 1.2:1 of *Z*:*E* was observed and both isomers were

separable and fully characterised independently. From the ^{1}H NMR spectrum it was clear that there were small multiplet peaks resembling those of the larger dominant signals in both spectra for both these compounds. Both **82** and **83** were treated with HF-pyridine to deprotect the TBS silyl group and the desired lactams **84** and **85** were obtained in high yield, 91 % and 90 % respectively. These smaller signals once again appeared in the products and the possibility that these were amide rotamers in the lactam was explored.

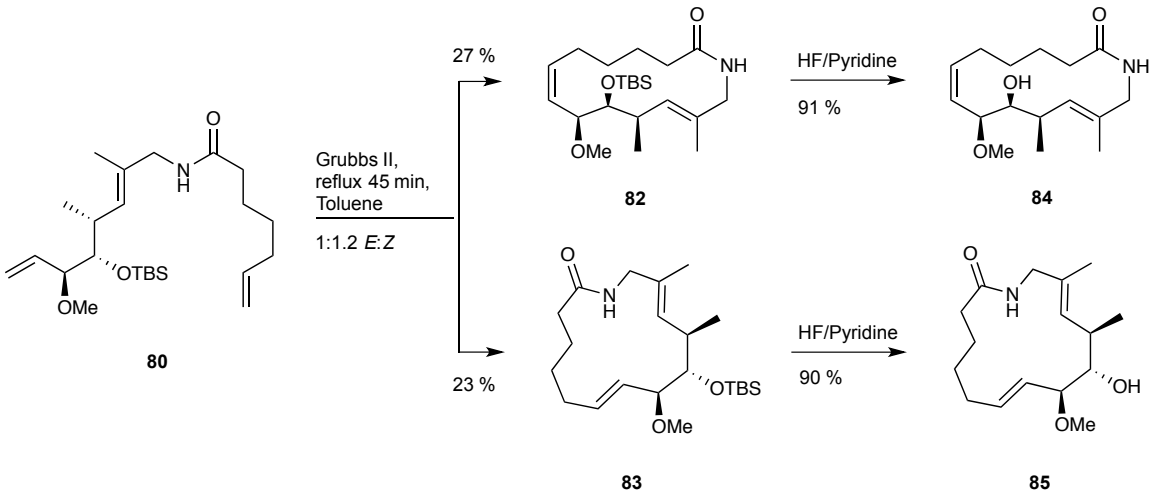

Scheme 1.17 Synthesis of macrolactams **84** and **85** from amide **80**.

1.6.5 Rotamers

The IUPAC definition of a rotamer states "*One of a set of conformers arising from restricted rotation about one single bond*". If in the case of the macrolactams that both the cis and trans amide were present, and not equilibrating fast enough, then they could be detected by NMR. The difference in intensities of the peaks suggests one conformer maybe favored over the other. A paper by Murphy and co-workers[66] showed how NOESY and ROESY (Rotating-frame Overhauser Spectroscopy) experiments can be used to determine the presence of rotamers. This technique is based on chemical exchange between the same hydrogen of the two conformers. Chemical exchange in NMR terms refers to any change a nucleus experiences between at least two different environments in which its NMR parameters are different e.g. the chemical shift parameter.[67] To further explain this, the theory of ^{1}H NMR NOESY will be addressed.

1.6.5.1 NOESY NMR

During an NMR experiment, when a proton is irradiated, it may give rise to an enhancement of intensity to spatially-close protons. This effect is called the Nuclear Overhauser Effect (NOE). This phenomenon is due to dipolar interactions between two nuclear spins. NOE experiments are unique compared to other NMR spectroscopy because the correlation is through space as oppose to through bond *J* couplings. This experiment is extremely important in elucidating the structure and conformation of a molecule by checking the spatial arrangement of protons and how close they are in proximity to one another. The spatial distance for NOE experiments has an upper limit to ~ 4 Å for small molecules < 600 Daltons, whereas large molecules > 1200 Daltons, can have an upper limit of ~ 5 Å. The source proton *S* is saturated with a specific radio frequency, the same as the one which causes it to resonate, so that the population difference of electrons between their high and low energy state is brought to zero. This perturbation of *S* tries to regain equilibrium of these two energy levels by employing electrons from protons that are close in spatial proximity; these are termed protons of interest *I*. As this occurs, *I* becomes perturbed with respect to its population difference and may have a different strength in signal intensity. Therefore, if a recording is taken after saturation period of *S*, the spectra may look different with peak intensities to that of the original ^{1}H spectra. The changes are typically small so the presence of the original ^{1}H spectra to cross-reference can help identify which chemical shifts seem different.[68]

To utilise this NOE phenomena, compound **84** was irradiated at one of the two similar looking peaks based on their multiplicity as shown in Figure 1.17. The chosen two peaks were relatively far apart (>30 Hz) from one another to ensure there was no overlap of irradiation leading to a false positive. After *S* was perturbed, the smaller further downfield signal *I* also inverted indicating chemical exchange was occurring.

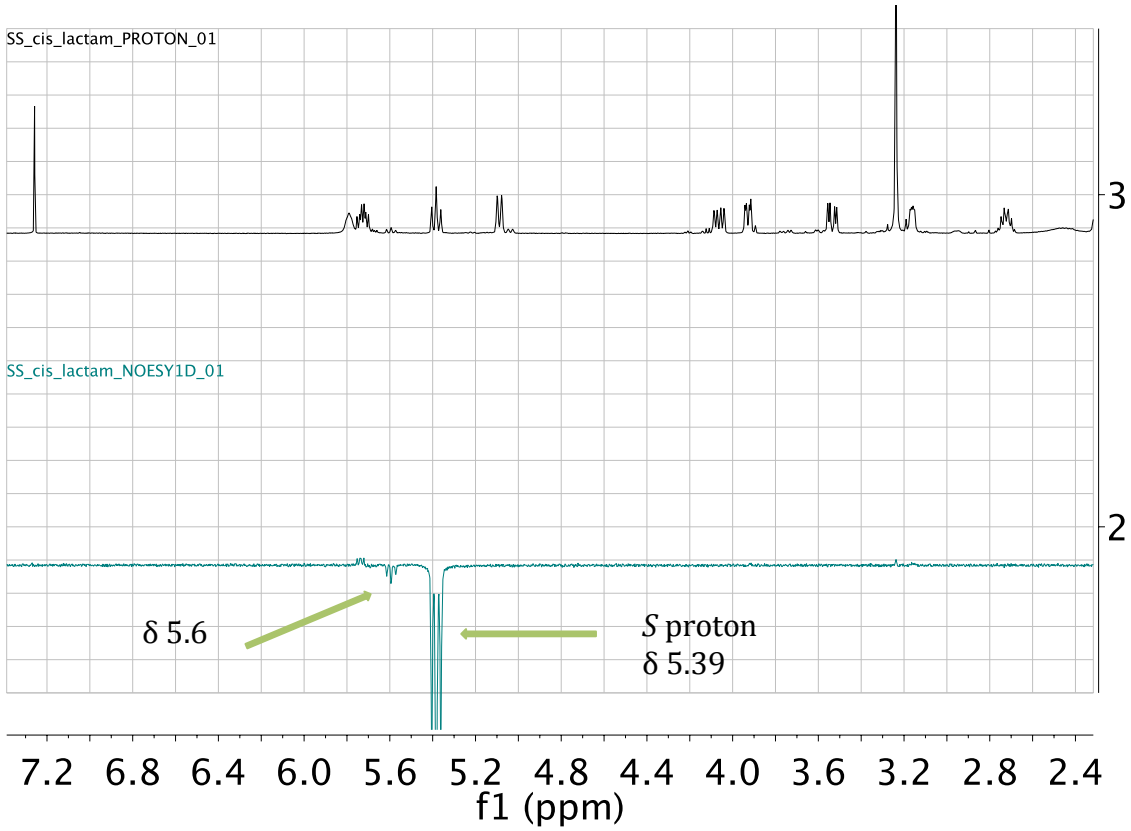

Figure 1.17 ^{1}H NMR 1D NOESY of compound **84**. The green spectra shows the *S* proton becoming inverted at δ 5.39 along with a smaller peak subsequently becoming inverted further downfield at δ 5.6. The black spectrum shows the original proton spectrum of compound **84**.

To gain further evidence for the presence of rotamers, a 2D NOESY experiment was performed. The 2 D experiment shows a proton spectrum on both axis and a diagonal correlation is observed with molecules in the same phase, represented by the blue colour shown in Figure 1.18. In small molecules < 600 Daltons, the effect of the NOE causes a change in phase and therefore it can be seen as a red colour. The observation of correlation points off the diagonal in red show the correlations of ^{1}H-^{1}H through space interactions. However, some points are observed off the diagonal and they correlate to the smaller peak intensities observed in the ^{1}H NMR spectra. These correlations are also in the same phase as the points on the diagonal, which are blue in colour. Taken together, the 1D and 2D NOESY experiments indicate that chemical exchange is occurring and therefore the presence of rotamers.

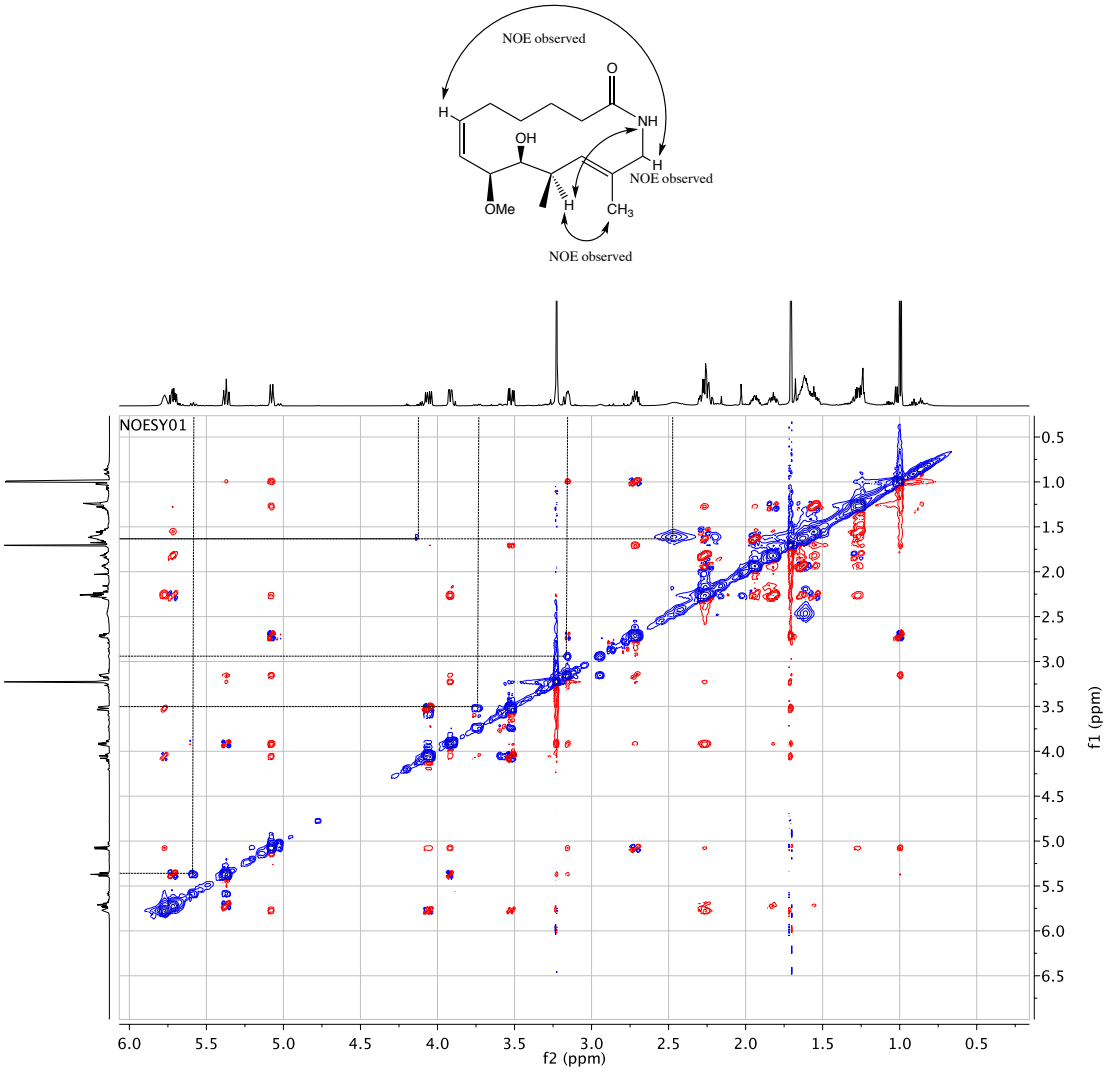

Figure 1.18 ^{1}H NMR 2D NOESY spectrum of compound **84** and observed NOE's. Two phases are observed off the diagonal, the negative with red correlation peaks show correlations between protons through space and the positive with blue correlations show the presence of chemical exchange.

During the workup and manipulation of compound **84**, a white glassy solid was observed. The material was subsequently crystallised from hot EtOAc at 60 °C and allowed to evaporate slowly over the course of three days. This resulted in white crystals that allowed an X-Ray crystal structure to be solved, shown in Figure 1.19. This crystal structure confirmed the structure of the macrocycle.

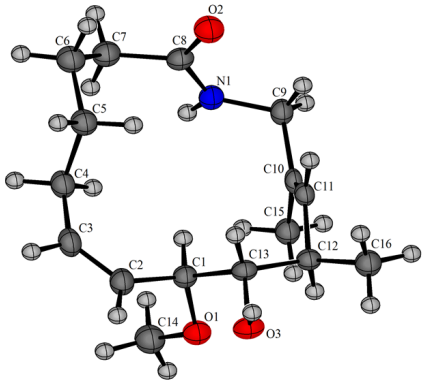

Figure 1.19 X-Ray crystal structure of **84**.

As these new macrocycles were to be biologically evaluated, the macrolactam **43** from Danishefsky's laboratory was prepared as a reference standard. The use of **43** to give new compounds was also exploited and will be discussed in more detail in Chapter 2. Intermediate **55** was utilised and reacted with Ando phosphonate **59** under basic conditions at -78 °C to give **86**, this time in high selectivity (97:3 *Z*:*E)* and yield of 78 %.

This is in contrast to the formation of **60**/**61** where there was poor selectivity and a disappointing yield. Compound **86** was reduced using DIBAL to form intermediate **14**, shown in Scheme 1.19.

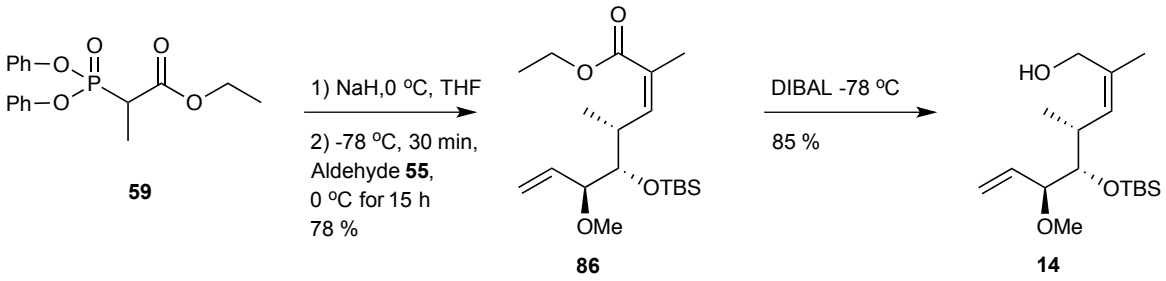

Scheme 1.19 Reaction of **59** with aldehyde **55** to form **86**. Reduction of **86** to form key intermediate **14**.

This intermediate underwent an azido-transfer to yield **77,** however this time there was only a trace amount of allylic rearrangement observed via NMR (~ 6 %). Compound **77** was quickly used in the next reduction step to yield primary amines **78**/**79**, where **79** was the desired isomer in this instance.

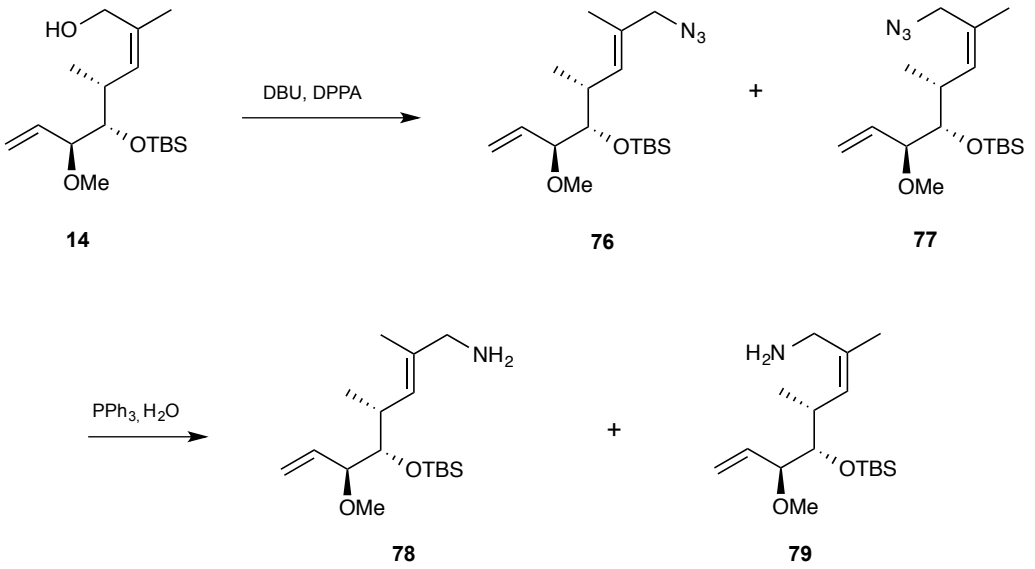

Scheme 1.20 Conversion of intermediate **14** to the primary amine isomeric mixture, **78** and **79**.

This isomeric mixture was coupled with 6-hepteneoic acid in the presence of EDC.HCl under basic conditions. After chromatographic purification, the rearrangement product **80** had increased to approximately 10 %. As the reduction involves heating to release the N_2 side product, it was believed that this is where further rearrangement had time to occur. Different addition times were explored between H_2O and triphenylphosphine (i) early addition of regents before the reaction was heated and (ii) when the reaction began to reflux. However, the rearrangement product (~ 10 %) was always observed when the corresponding amides were analysed. These two amides, **80** and the desired amide **81,** were inseparable this time via chromatography and as such were taken on to the next step to close the ring. Chromatographic purification, after the RCM reaction, yielded the desired macrolactam isomer **87** in a moderate yield of 53 % as a single isomer. The precursor **87** was treated with HF/pyridine to yield the desired compound **43**.

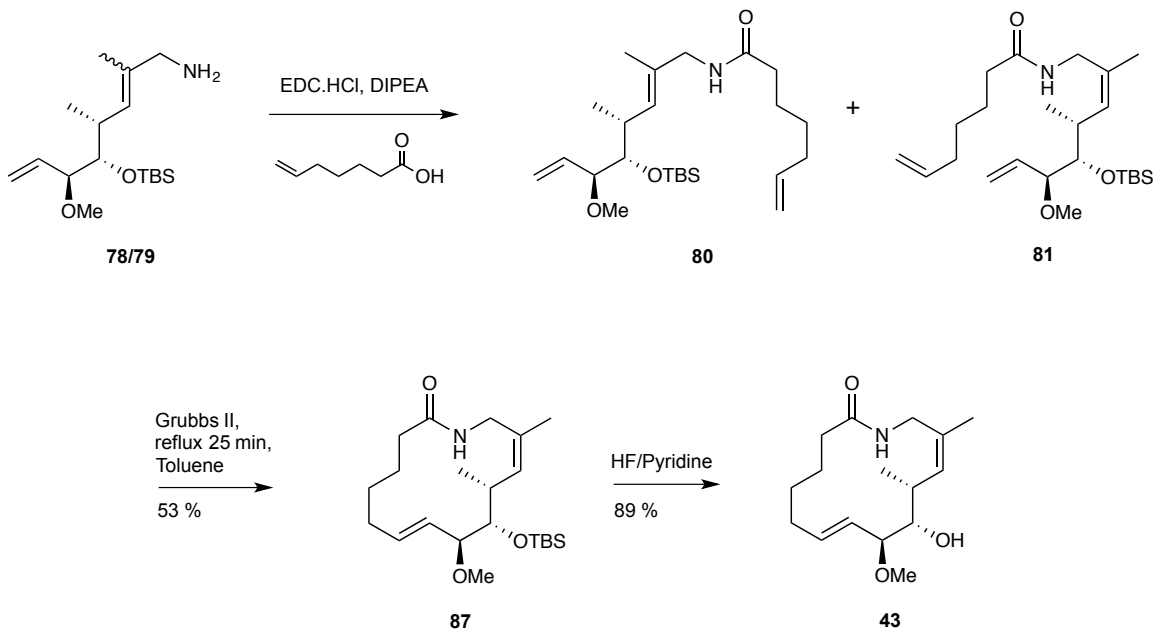

Scheme 1.21 Synthesis of macrolactam **43** as a biological reference standard.

Whilst exploring the synthesis of **43**, it became apparent that the α,β-unsaturated macrolactam was not present in published literature. Based on biological assays that the α,β-unsaturated macroketone, shown in Figure 1.20, was more effective when compared to the macroketone in anti-metastatic activity,[28] this inspired the synthesis of the α,β-unsaturated macrolactam to be undertaken.

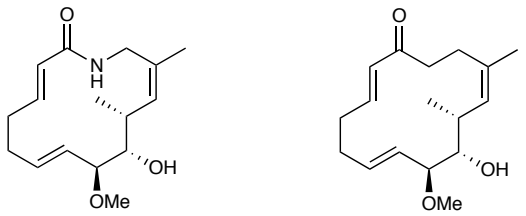

Figure 1.20 α,β-unsaturated macrolactam and α,β-unsaturated macroketone.

The route followed the same path as before that derives at the primary amines **78** and **79**. The crude amines were coupled to a pre-synthesised α,β-unsaturated acid **89.** Using a modified synthesis of **89** by Ryu *et al.*[69] , BAIB and TEMPO were added to commercially available 4-penten-1-ol. After vigorous stirring for 4 h, an activated Wittig reagent was added and was left for a further 16 h. This one pot method yielded the desired unsaturated

ester **88** with exclusively *E* geometry of the α,β-unsaturated ester in a moderate yield of 46 % over two steps and is shown in Scheme 1.22. This low boiling point intermediate was subjected to saponification techniques with LiOH at room temperature in a mixture of 1:1 THF: H_2O. This reaction formed a side impurity that was observed with the disappearance of the α,β-unsaturated and the incorporation of a hydroxyl group. Replacing the LiOH with a less reactive NaOH and keeping the ratio of the mixed solvent system the same, along with heating the reaction mixture, gave the desired product **89** in a satisfactory yield of 82 %.

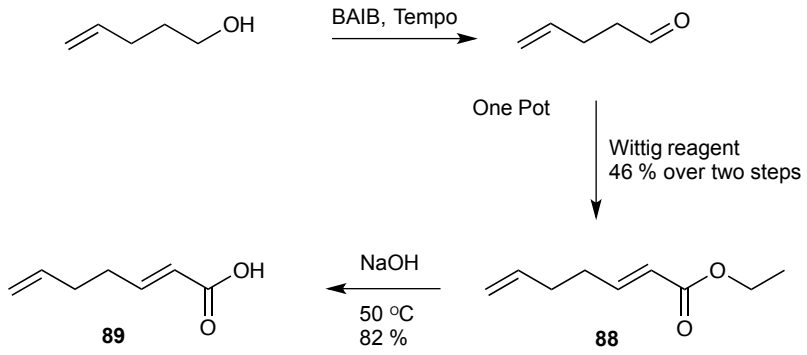

Scheme 1.22 Synthesis of α,β-unsaturated acid side chain **89**.

To help limit a possible side reaction whereby the nucleophilic amine may attack the activated α,β-unsaturated acid-carbodiimide complex, in a Michael addition style manner, the crude reaction mixture was lowered to 0 °C before the coupling reagents were added. The desired amide **90** was successfully obtained in an excellent yield of 80 % and successfully separated from its undesired amide isomer **91**.

An attempt to close the intermediate amide **90** via RCM was carried out. However, this did not lead to the ring closed product as envisaged but an array of side products and impurities. Reaction conditions were varied in order to close the ring, as shown in Scheme 1.23, but to no avail. The acyclic amide **90** was deprotected with HF/pyridine to furnish the acyclic amide with a free hydroxyl group, compound **91**.

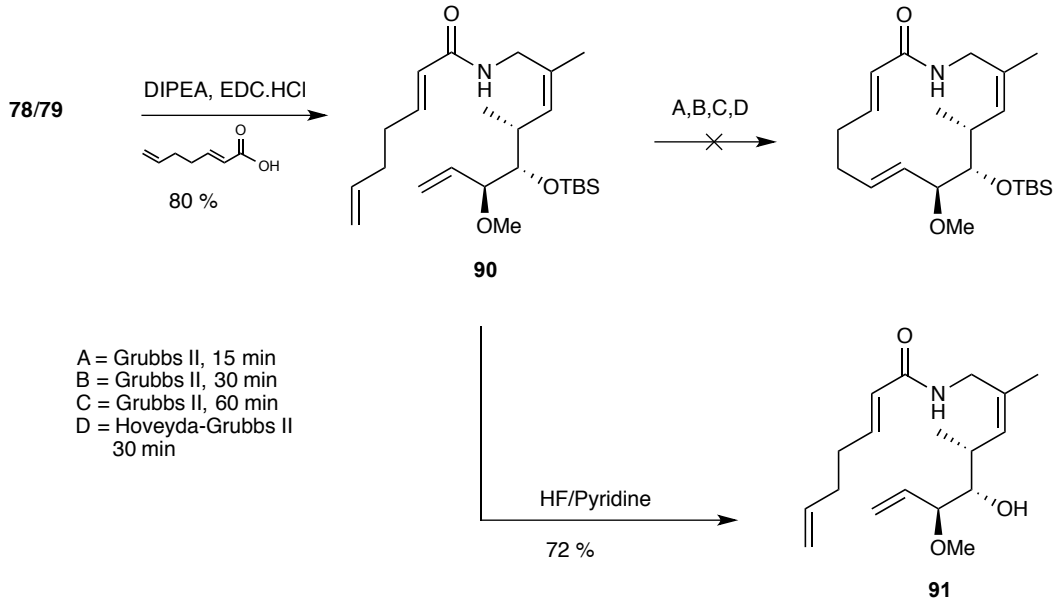

Scheme 1.23 Synthesis of acyclic α,β-unsaturated amide analogue **91**.

The closing of the ring proved inaccessible using the conditions applied as shown in Scheme 1.24. The acyclic compound was deprotected in any case to yield an open chain acyclic analogue. Migrastatin acyclic analogues have been published in the past. Dias *et al*. reported the synthesis of an acyclic migrastatin analogues as they too, in one case, were unable to ring close their migrastatin core analogue. Their activity reports show that the acyclic analogues still inhibited migration in the nM range when tested against MDA-MB 213 human breast tumor cells.[70]

1.6.6 Biological Evaluation

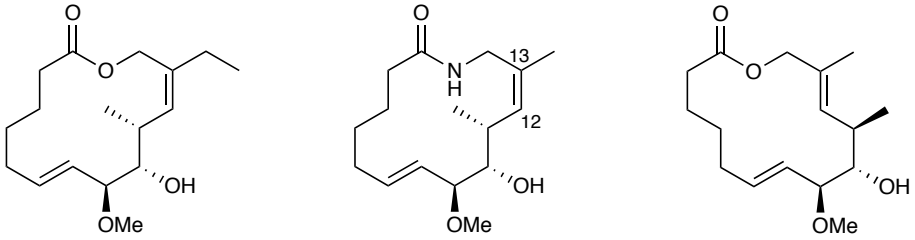

Figure 1.21 Selected compounds for biological evaluation **43**, **66** and **73**.

Two separate batches of biological experiments were carried out during the thesis work and related to the timing when products were available. The first analysis was chosen to check the activity of compounds **66** and **73** against the known reported compound **43**, on the cancer lung cell line A549. The compound selection was chosen to keep the parameters as closely related as possible and only to differ in the geometry of the olefin at C12-C13. The other portions of the molecule remained similar to one another. This work was carried out by our collaborators in the National Heart and Lung Institute, Imperial College London, UK. The second batch of test compounds includes **72**, **74**, **84** and **85**. These are currently under biological evaluation. The cell based assays performed in this experiment and the following batch of compounds are the same. Brief backgrounds to these bioassays are explained.

1.6.6.1 Cell Viability

Cell viability is one of the earliest initial assays to distinguish between safe and non-safe chemicals with respect to cell toxicity and death. There are many known and developed assays reported throughout the literature based on cell membrane permeability, enzyme activity, nucleotide uptake activity, cellular death markers etc. Many methods including tritium-labelled thymidine uptake and 3-(4,5-dimethylthiazol-2-yl)-2,5-diphenyltetrazolium bromide (MTT) are used in practice. Each assay has certain drawbacks ranging from storage problems of agents to stability issues. MTT is the more commonly used assay due to its relative ease in the manipulation of the reagents, high reproducibility and ease of quantification. The dissolved MTT, which is initially yellow, is transformed into an insoluble purple formazan by the cleavage of the tetrazolium ring by dehydrogenases. This colour change allows for an effective calorimetric method to determine cell viability. The transformation is only carried out by active mitochondrial hydrogenases in living cells and not in dead cells.

1.6.6.2 Wound Assay

Once the bioactive molecules have been deemed safe based on the cytotoxicity assay, the compounds can be further evaluated. This technique allows for the study of 2D movement of the cells to repair the wound. This is used typically first to investigate if the compound of interest has anti-migration properties. It is also relatively rapid and cheap however it cannot distinguish between proliferation of the cells if the test is ran over >24 h. The assay is performed by creating a scratch on a plate containing confluent cells giving rise to a gap

between the cells. A measurement of distance is taken of the initial gap at time 0 and the distance is then monitored and measured over time as the gap closes. This method can be studied under a microscope that is typically fitted with a camera to record the migration data.

1.6.6.3 Chamber Cell Migration

The transwell migration cell assay, also known as the Boyden chamber assay after its inventor, is a prerequisite assay to estimate the effectiveness of a bioactive molecule in cell migration inhibition. Two chambers are linked via a porous channel fitted with membrane filters that can be of various pore sizes, depending on the cell size of interest. Cells are added to the uppermost chamber and a cell attractant or simple media is added to the lower chamber. It is important to use a pore size that is smaller than the cells used to avoid spontaneous falling of the cells through the pores. The use of a smaller pore size allows for active migration and therefore a more accurate calculation can be obtained. Cells are typically fluorescently labelled and the ones that actively transmigrate are quantified using a fluorescent reader.

1.6.6.4 Interpretation of biological results

Interpretation of this data shows that all compounds tested, (Cmpd A = **66**), (Cmpd B = **43**) and (Cmpd C = **73**), showed no cytotoxicity in relation to cell viability, as shown in Figure 1.22. The wound repair study, shown in Figure 1.23 and Figure 1.24, showed active cell inhibition over 24 h with compounds **43** and **66** with less inhibition for **73**. The more comprehensive transwell migration assay, shown in Figure 1.25 and Figure 1.26, shows compound **43** has the highest % inhibition and is closely followed by **66**. Compound **73** has the least % inhibition in this cell line (A549). The stereochemistry of the *E* olefin at C12 – C13 in **73** may have reduced the activity of the macrocycle as both **43** and **66** contain a *Z* olefin at C12 – C13. This preliminary data suggests that **73** was less effective in lung cancer cell migration in the cell line A549 when compared to compounds **43** and **66**. Encouragingly, test compound **66** showed comparable inhibition effects to that of the known reported compound **43** against the cell line A549.

Table 1.2 IC_{50}'s from transwell cell migration study.

Compound	IC_{50} µM
66 (A)	16.7 ± 2.38
43 (B)	13.6 ± 3.21
73 (C)	ND

ND = not determinable at highest dose (> 100 µM)

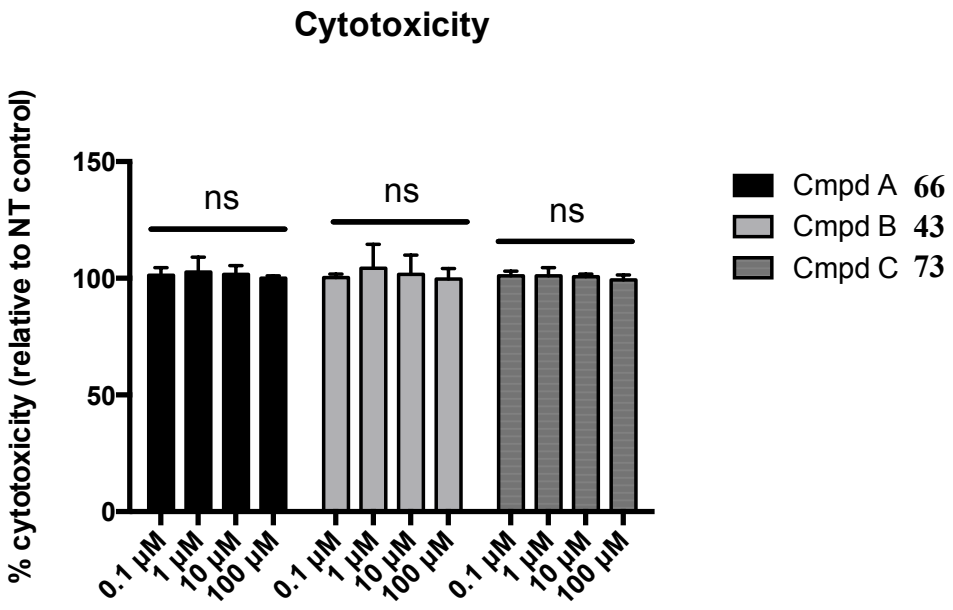

Figure 1.22 Cell viability assay representing the toxicity data of tested compounds **43**, **66** and **73**. The results show that no cytotoxicity was observed over the µM range when compared to the non-treated cells (control).

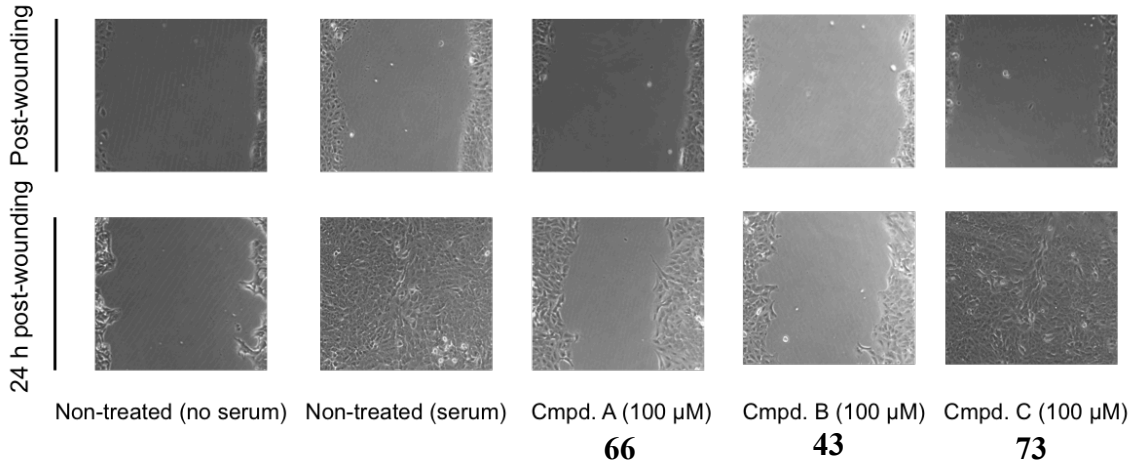

Figure 1.23 Wound assay at 100 μM shows post wounding at time = 0 and post wounding time = 24 h.

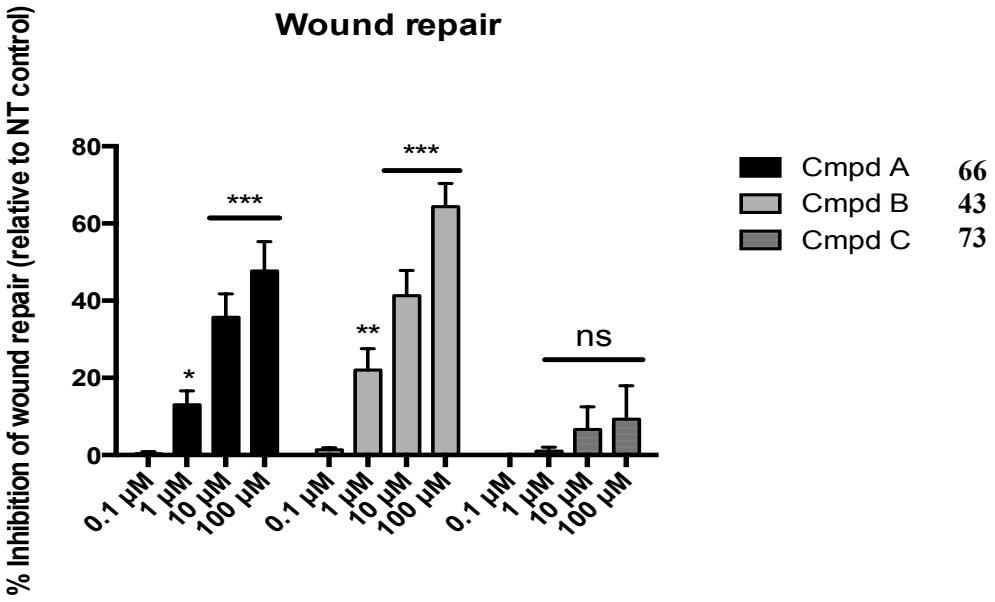

Figure 1.24 Wound repair chart shows % inhibition of the **43**, **66** and **73** ranging from 1-100 μM relative to the non-treated cells (control).

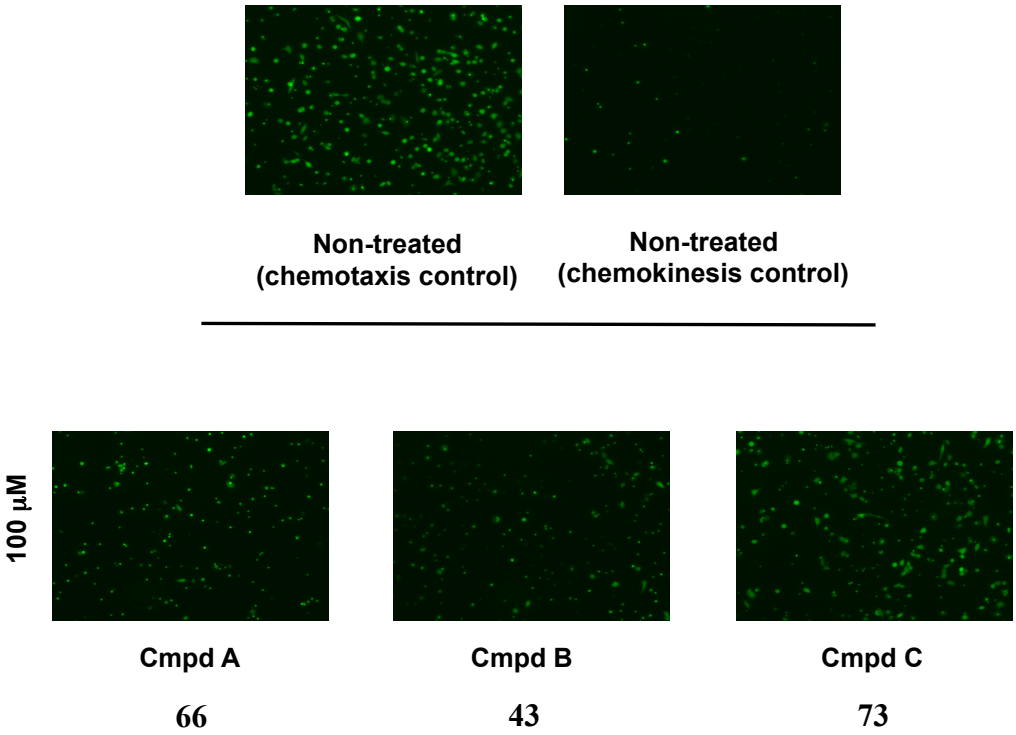

Figure 1.25 Transwell migration using fluorescently labelled cells at 100 μM of test compounds **43**, **66** and **73**. Non-treated cells (control) are shown on the top left in the presence of the chemo attractant. Non-treated cells (control) are shown on the top right in the absence of the chemo attractant.

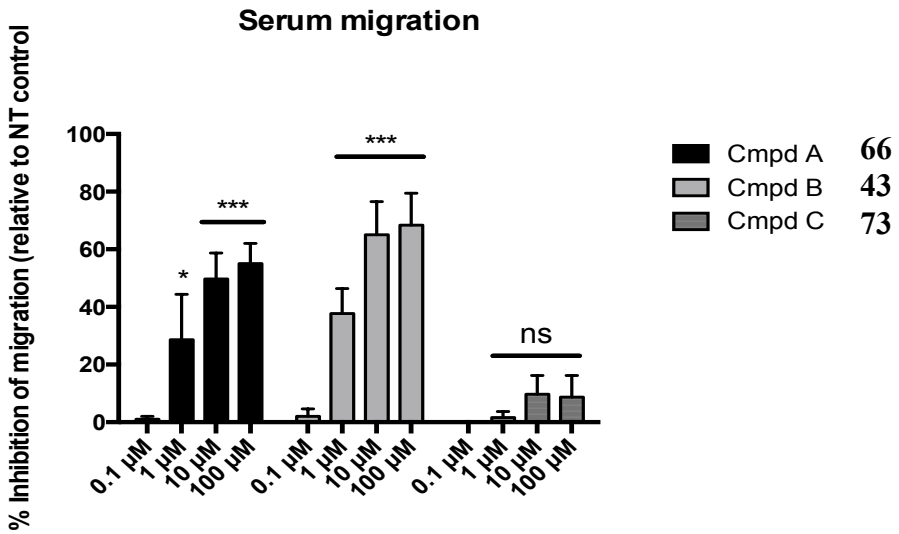

Figure 1.26 Serum migration chart shows % inhibition of the **43**, **66** and **73** at 100 μM relative to the non-treated cells (control).

1.7 Conclusion

Migrastatin and its derivatives have promise as anti-metastasis and more specifically tumour cell migration inhibition. A series of analogues were prepared as part of this study, including the benchmark macrolactam compound. This included macrolactone and macrolactam structures where an ethyl group forms part of the macrocycle **60** and where the alkene geometry at C-13 was changed from *Z* to *E*. Evidence for the presence of rotamers was obtained for the macrolactam derivatives. The macrolactone **73** showed a lower inhibition result when compared to both **43** and **66** for their effects on inhibition of migration of the cell line A549. A second batch of compounds are currently being tested and are being screened over a wider range of cell lines. Future work in this area could lead to attempts to gain evidence for the role of fascin in tumour cell migration, through structure based design of fascin inhibitors and thus more potent and bioavailable analogues being synthesised. Potentially, this could subsequently lead to the end goal of effective therapeutics for the treatment of tumour cell migration inhibition in cancer patients.

Bibliography

1. Mehlen, P.; Puisieux, A., *Nat Rev Cancer* **2006,** *6* (6), 449-458.
2. Keller, R., *Current Opinion in Cell Biology* **2005,** *17* (5), 533-541.
3. Friedl, P.; Weigelin, B., *Nat Immunol* **2008,** *9* (9), 960-969.
4. Lauffenburger, D. A.; Horwitz, A. F., *Cell* **1996,** *84* (3), 359-369.
5. Welch, M. D.; Mullins, R. D., *Annu. Rev. Cell Dev. Biol.* **2002,** *18* (1), 247-288.
6. Horwitz, A. R.; Parsons, J. T., *Science* **1999,** *286* (5442), 1102-1103.
7. Ewing, J., *Neoplastic Diseases; A Treatise on Tumors*. 2nd ed.; W.B. Saunders Co.: Philadelphia and London, 1922.
8. Paget, S., *The Lancet* **1889,** *133* (3421), 571-573.
9. Mathot, L.; Stenninger, J., *Cancer Science* **2012,** *103* (4), 626-631.
10. Berx, G.; Raspé, E.; Christofori, G.; Thiery, J.; Sleeman, J., *Clin Exp Metastasis* **2007,** *24* (8), 587-597.
11. Xue, C.; Plieth, D.; Venkov, C.; Xu, C.; Neilson, E. G., *Cancer Research* **2003,** *63* (12), 3386-3394.
12. Hay, E. D., *Developmental Dynamics* **2005,** *233* (3), 706-720.
13. Wang, Z.; Sandiford, S.; Wu, C.; Li, S. S.-C., *The EMBO Journal* **2009,** *28* (16), 2360-2373.
14. Christiansen, J. J.; Rajasekaran, A. K., *Cancer Research* **2006,** *66* (17), 8319-8326.
15. Garber, K., *Journal of the National Cancer Institute* **2008,** *100* (4), 232-239.
16. Chui, M. H., *International Journal of Cancer* **2013,** *132* (7), 1487-1495.
17. Gaul, C.; Njardarson, J. T.; Shan, D.; Dorn, D. C.; Wu, K.-D.; Tong, W. P.; Huang, X.-Y.; Moore, M. A. S.; Danishefsky, S. J., *J. Am. Chem. Soc.* **2004,** *126* (36), 11326-11337.
18. Dewick, P. M., *Medicinal natural products: a biosynthetic approach*. 2nd ed.; John Wiley & Sons: 2002.
19. Lahlou, M., *Pharmacology & Pharmacy* **2013,** *4* (3A), 17-31.
20. Haas, L. F., *Journal of Neurology, Neurosurgery, and Psychiatry* **1994,** *57* (11), 1333.
21. Molè-Bajer, J.; Bajer, A. S., *The Journal of Cell Biology* **1983,** *96* (2), 527-540.
22. McGivern, J. G., *Neuropsychiatric Disease and Treatment* **2007,** *3* (1), 69-85.
23. William, C. C., *Current Pharmaceutical Biotechnology* **2012,** *13* (6), 853-865.

24. Nakae, K.; Yoshimoto, Y.; Sawa, T.; Hamada, M.; Takeuchi, T.; Imoto, M., *The Journal of Antibiotics* **2000,** *53*, 1130.
25. Nakae, K.; Yoshimoto, Y.; Ueda, M.; Sawa, T.; Takashi, Y.; Naganawa, H.; Imoto, M., *The Journal of Antibiotics* **2000,** *53*, 1228.
26. Reymond, S.; Cossy, J., *Eur. J. Org. Chem.* **2006,** *2006* (21), 4800-4804.
27. Chen, L.; Yang, S.; Jakoncic, J.; Zhang, J. J.; Huang, X.-Y., *Nature* **2010,** *464* (7291), 1062-1066.
28. Majchrzak, K.; Lo Re, D.; Gajewska, M.; Bulkowska, M.; Homa, A.; Pawłowski, K.; Motyl, T.; Murphy, P. V.; Król, M., *PLoS one* **2013,** *8*, e76789.
29. Lo Re, D.; Zhou, Y.; Nobis, M.; Anderson, K. I.; Murphy, P. V., *ChemBioChem* **2014,** *15* (10), 1459-1464.
30. Woo, E. J.; Starks, C. M.; Carney, J. R.; Arslanian, R.; Cadapan, L.; Zavala, S.; Licari, P., *The Journal of Antibiotics* **2002,** *55*, 141.
31. Karwowski, J. P.; Jackson, M.; Sunga, G.; Sheldon, P.; Poddig, J.; Kohl, W. L.; Kadam, S.; , *The Journal of Antibiotics* **1994,** *47* (8), 862.
32. Mosmann, T., *Journal of Immunological Methods* **1983,** *65* (1), 55-63.
33. Hancock, J. F., *Nat Rev Mol Cell Biol* **2003,** *4* (5), 373-385.
34. Kadam, S.; McAlpine, J. B., *The Journal of Antibiotics* **1994,** *45* (8), 875.
35. Ju, J.; Lim, S.-K.; Jiang, H.; Shen, B., *J. Am. Chem. Soc.* **2005,** *127* (6), 1622-1623.
36. Gaul, C.; Danishefsky, S. J., *Tetrahedron Lett.* **2002,** *43* (50), 9039-9042.
37. Oskarsson, T.; Nagorny, P.; Krauss, I. J.; Perez, L.; Mandal, M.; Yang, G.; Ouerfelli, O.; Xiao, D.; Moore, M. A. S.; Massagué, J.; Danishefsky, S. J., *J. Am. Chem. Soc.* **2010,** *132* (9), 3224-3228.
38. Lecomte, N.; Njardarson, J. T.; Nagorny, P.; Yang, G.; Downey, R.; Ouerfelli, O.; Moore, M. A. S.; Danishefsky, S. J., *Proceedings of the National Academy of Sciences* **2011,** *108* (37), 15074-15078.
39. Zhou, Y.; Murphy, P. V., *Tetrahedron Lett.* **2010,** *51* (40), 5262-5264.
40. Saishin, Y.; Ishikawa, R.; Ugawa, S.; Guo, W.; Ueda, T.; Morimura, H.; Kohama, K.; Shimizu, H.; Tano, Y.; Shimada, S., *Investigative Ophthalmology & Visual Science* **2000,** *41* (8), 2087-2095.
41. Tubb, B.; Mulholland, D. J.; Vogl, W.; Lan, Z.-J.; Niederberger, C.; Cooney, A.; Bryan, J., *Experimental Cell Research* **2002,** *275* (1), 92-109.

42. Vignjevic, D.; Schoumacher, M.; Gavert, N.; Janssen, K.-P.; Jih, G.; Laé, M.; Louvard, D.; Ben-Ze'ev, A.; Robine, S., *Cancer Research* **2007,** *67* (14), 6844-6853.
43. Vergara, D.; Simeone, P.; del Boccio, P.; Toto, C.; Pieragostino, D.; Tinelli, A.; Acierno, R.; Alberti, S.; Salzet, M.; Giannelli, G.; Sacchetta, P.; Maffia, M., *Molecular BioSystems* **2013,** *9* (6), 1127-1138.
44. van Roy, F.; Berx, G., *Cell. Mol. Life Sci.* **2008,** *65* (23), 3756-3788.
45. Overduin, M.; Harvey, T.; Bagby, S.; Tong, K.; Yau, P.; Takeichi, M.; Ikura, M., *Science* **1995,** *267* (5196), 386-389.
46. Beavon, I. R. G., *European Journal of Cancer* **2000,** *36* (13), 1607-1620.
47. Ratheesh, A.; Yap, A. S., *Nat Rev Mol Cell Biol* **2012,** *13* (10), 673-679.
48. Adams, C. L.; Nelson, W. J., *Current Opinion in Cell Biology* **1998,** *10* (5), 572-577.
49. Wendt, M. K.; Taylor, M. A.; Schiemann, B. J.; Schiemann, W. P., *Molecular Biology of the Cell* **2011,** *22* (14), 2423-2435.
50. Lo Re, D.; Zhou, Y.; Mucha, J.; Jones, L. F.; Leahy, L.; Santocanale, C.; Krol, M.; Murphy, P. V., *Chemistry – A European Journal* **2015,** *21* (50), 18109-18121.
51. Trost, B. M.; Malhotra, S.; Mino, T.; Rajapaksa, N. S., *Chemistry – A European Journal* **2008,** *14* (25), 7648-7657.
52. Brown, H. C.; Jadhav, P. K.; Bhat, K. S., *J. Am. Chem. Soc.* **1988,** *110* (5), 1535-1538.
53. Nicolaou, K. C.; Sun, Y.-P.; Guduru, R.; Banerji, B.; Chen, D. Y. K., *J. Am. Chem. Soc.* **2008,** *130* (11), 3633-3644.
54. Blanchette, M. A.; Choy, W.; Davis, J. T.; Essenfeld, A. P.; Masamune, S.; Roush, W. R.; Sakai, T., *Tetrahedron Lett.* **1984,** *25* (21), 2183-2186.
55. Still, W. C.; Gennari, C., *Tetrahedron Lett.* **1983,** *24* (41), 4405-4408.
56. Ando, K., *The Journal of Organic Chemistry* **1997,** *62* (7), 1934-1939.
57. Ando, K., *The Journal of Organic Chemistry* **1998,** *63* (23), 8411-8416.
58. Mitsunobu, O.; Yamada, M., *Bull. Chem. Soc. Jpn* **1967,** *40* (10), 2380-2382.
59. Schrock, R. R.; Murdzek, J. S.; Bazan, G. C.; Robbins, J.; DiMare, M.; O'Regan, M., *J. Am. Chem. Soc.* **1990,** *112* (10), 3875-3886.
60. Nguyen, S. T.; Johnson, L. K.; Grubbs, R. H.; Ziller, J. W., *J. Am. Chem. Soc.* **1992,** *114* (10), 3974-3975.

61. Chatterjee, A. K.; Choi, T.-L.; Sanders, D. P.; Grubbs, R. H., *J. Am. Chem. Soc.* **2003,** *125* (37), 11360-11370.
62. Schrock, R. R., *Acc. Chem. Res.* **2014,** *47* (8), 2457-2466.
63. Mori, M., *Materials* **2010,** *3* (3), 2087.
64. Nelson, D. J.; Manzini, S.; Urbina-Blanco, C. A.; Nolan, S. P., *Chem. Commun.* **2014,** *50* (72), 10355-10375.
65. Gagneux, A.; Winstein, S.; Young, W. G., *J. Am. Chem. Soc.* **1960,** *82* (22), 5956-5957.
66. Bradley, H.; Fitzpatrick, G.; Glass, W. K.; Kunz, H.; Murphy, P. V., *Org. Lett.* **2001,** *3* (17), 2629-2632.
67. Kleckner, I. R.; Foster, M. P., *Biochim. Biophys. Acta* **2011,** *1814* (8), 942-968.
68. Williamson, M., The Nuclear Overhauser Effect. In *Modern Magnetic Resonance*, Webb, G., Ed. Springer Netherlands: 2006; pp 409-412.
69. Ryu, J.-S.; Marks, T. J.; McDonald, F. E., *The Journal of Organic Chemistry* **2004,** *69* (4), 1038-1052.
70. Dias, L. C.; Finelli, F. G.; Conegero, L. S.; Krogh, R.; Andricopulo, A. D., *Eur. J. Org. Chem.* **2010,** *2010* (35), 6748-6759.

Contents

Chapter 2: Coiled-coil scaffolds

2.1 Introduction

The four major classes of organic molecules are; (i) carbohydrates, (ii) proteins, (iii) lipids and (iv) nucleic acids. Neither one of these classes is any more important than the other with respect to a living organism. All of these molecule classes are required for biological processes and are required for an overall healthy organism. Whilst there is an array of knowledge of physiological processes, there is yet much to discover and this is an ongoing incentive for scientific research. An area of research that is increasing in importance is lectinology. This includes the design and synthesis of lectin (carbohydrate binding proteins) inhibitors/effectors that can act as modulators. These modulators can be used for understanding and determining the structure and biological functions of such lectins in both the plant and animal kingdoms.

2.1.1 Lectin background

Lectins are defined as carbohydrate binding proteins that specifically interact with carbohydrate moieties of glycoproteins and glycolipids. These protein-carbohydrate interactions are non-covalent, competitive and can be ion dependent and ion independent, based on the type of lectin in question. The term lectin is derived from Latin (*legere* - to pick, to select). Lectins are their own class of molecules and do not fall under the grouping of enzymes and antibodies, even though they are as highly specific as substrate-enzyme and antigen-antibody binding complexes. The discovery of these sugar-binding proteins was by Hermann Stillmark in 1888. Stillmark reported a compound isolated from castor-oil plant, which showed high toxicity and the aggregation of red blood cells.[1] This compound is now known as ricin (*Ricinus communis)* and interferes with protein production by targeting eukaryotic ribosomes, which are required for protein construction. However, whilst Stillmark had made this observation, it was reported that S. Weir Mitchell in 1860 had reported on the observation of an agent from rattlesnake venom that caused the agglutination of pigeon blood. This was nearly three decades before Stillmark had described the first discovery of a reported lectin and hence the start of lectinology. Extraction, isolation and crystallisation of pure, concanavalin A, was carried out by James B. Sumner in 1919.[2] William C. Boyd and Karl O. Renkonen independently built upon this

work in 1945 testing agglutinates on different blood types. It was demonstrated that lima beans extract preferentially bound to blood type A and not blood types B or O. This observation gave rise to the fact that lectins inherently have high sugar-specificity. Blood type A differs from blood type B by the substitution of a *N*-acetylgalactosamine with galactose, which is a minor structural difference with respect to the overall cell membrane make-up. The observation of these specific agglutinates pointed to a structural basis for blood types.

2.1.1.1 Plant lectins

Plant lectins, due to their abundance and relative ease of harvesting, have been tested for their therapeutic properties. *Polygonatum odoratum* lectin was isolated from the traditional Chinese herb (Mill.) druce and is a mannose-binding specific agglutinin. It has been found to induce apoptosis in lung cancer cells A549 without affecting normal human embryonic lung fibroblasts.[3] Another anti-cancer agent was found to exist in the mistletoe plant. Chinese mistletoe lectin-1 (CM-1) can induce apoptosis in colorectal cancer cells through the interference of the Wnt signalling pathway required for gene expression.[4]

As mentioned earlier, legume lectins arising from plants have been at the forefront of lectinology with various plant extracts that have been isolated. These plant lectins have given rise to crystallisation protocols and structure elucidation of blood types. Despite these discoveries, the exact function that these sugar-binding proteins have in plants is still unknown. These legume lectins are typically found in storage tissue such as fruits and seeds but have also been found in leaves and in the barks of trees. One theory suggests endogenous lectins have evolved for plant defence against predators and pathogens. Due to lectins holding similarities to antibodies, it also has been suggested that legume lectins are the plant antibodies against pathogens. These are however only theories and their physiological functions are still under examination.

2.1.1.2 Animal lectins

Lectins are involved in various biological roles including; (i) the clearance of glycopeptides from blood, (ii) points of adhesion for pathogens on host cells, (iii) signalling for leukocytes to points of inflammation. As such, endogenous lectins are important for healthy functioning physiological processes. This can be exemplified by the transmembrane lectin receptor, asialoglycoprotein, which is found largely in the

hepatocytes of the liver. This receptor is a C-type (a calcium dependent type of lectin that will be further discussed in section 2.1.1.3), lectin that carries out the clearance and the removal of glycoproteins from the blood.[5] This biological process forms part of the body's homeostasis in regulating glycoprotein levels in the circulatory system. Lectins are also found to play a role in the immune system. Here they act as homing and attractants for leukocytes to areas of inflammation and are regarded part of the immune system.[6] Another function of lectins that was previously mentioned is the attachment of pathogens to the host cell. This attachment is efficient for capturing pathogens and subsequently leading to phagocytosis and the removal of it from the host body. In the case of influenza however, the lectin moiety, called hemagglutinin, attaches to the cell via sialic acid and undergoes membrane-infusion. The cell then engulfs the rest of the virus allowing it to replicate within the host cell, lysing and repeating the process.[7] Therefore, although lectin binding can be favourable it can also be unfavourable, which opens up the ground for therapeutical intervention. One example of this therapeutic intervention was reported by Turnbull and co-workers in which a bacterial produced sugar-binding toxin, cholera (made up of a toxic subunit and five non-toxic subunits), was inhibited with activity in the pM range. The five non-toxic subunits, which had a strategically mutated residue, replacing tryptophan with glutamic acid, was used as a scaffold to project sugar moieties with the exact spatial arrangement to that of the wild type cholera toxin.[8] Animal lectins can be classified into four main groups, where they can be subdivided based on structural features. These four main groups encompass (i) C-type, (ii) S-type (now known to be Galectins), (iii) P-type, and (iv) I-type lectins.[9] These groups will be discussed in further detail.

2.1.1.3 Four main lectin groups

(i) C-type lectins

The term C-type is derived from the dependence on Ca^{2+} ions required for effective sugar binding. The inclusion of Ca^{2+} ions into the carbohydrate recognition domain (CRD) allows for coordination points between the shallow pocket of the protein and key hydroxyls of the sugar ring. C-type ligands can be further divided into groups based on structural similarities and functions. These lectins can be found in extracellular fluid and on cellular surfaces. The previously mentioned asialoglycoprotein receptor is of C-type lineage.

(ii) S-type Lectins

This term has now been abandoned and reassigned to galectins. The previous term was used as it was believed that free thiols were required for binding. Now it is understood that these lectins specifically bind to galactose based sugars, for example lactose, GalNAc, *N*-acetyllactosamine. These lectins share a cation independent binding affinity for β-galactosides. As these lectins are the main focus of this study, these will be discussed in further detail in section 2.1.1.4.

(iii) P-type lectins

Lectins within this group are specific in binding mannose-6-phosphate. The term P-type originates from the phosphate group. These lectins encompass both calcium dependant mannose-6-phosphonate receptor (CD-MPR) and calcium independent mannose-6-phosphonate receptor (CI-MPR).

(iv) I-Type lectins

These lectins are grouped together based on evolutionary structural motifs and were observed as binding carbohydrates through immunoglobulin domains and as such was assigned the term I-type. An example of members from the immunoglobulin lectins is the siglec family. These are involved in cell adhesion as part of sialic acid binding interactions, as previously discussed in relation to influenza attachment.

2.1.1.4 Galectin-3-binding protein and cell metastasis

As with a lot of nomenclature rules, there are always exceptions! Galectins form part of the superfamily C-type lectins, however, they are typically small, non-glycosylated and exist as Ca^{2+} independent extracellular and intracellular proteins.[10] Galectins partake in a high diversity of physiological processes and are mainly involved in immune system and inflammatory responses. Due to the various functions of galectins and subtypes of galectins, this is an attractive area for research. Galectins have fifteen known subtypes[11] to date and these can be grouped into three groups, shown in Figure 2.1, (i) prototypical type, which contains a single CRD and can form homodimers, (ii) chimeric type, that also contains a single CRD with an extended peptide tail however this type can self-assemble and form multivalent CRDs and (iii) tandem-repeat type, that consists of two non-identical CRDs joined together via a small peptide that form heterodimers. Galectin-1 (proto type) shows anti-inflammatory response by attenuating signalling pathways that lead to the

recruitment of leukocytes. Galectin-3 (chimeric type), however, shows the exact opposite response with pro-inflammatory activity that promotes the recruitment of leukocytes and macrophages.[12] This antagonistic outcome shows the diversity of galectins with respect to their biological roles.

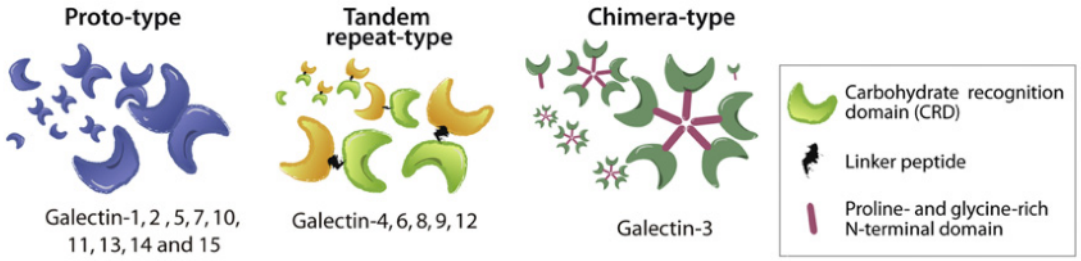

Figure 2.1 Galectin subtypes, (i) prototypical, (ii) chimeric and (iii) tandem-repeat. Adapted with permission from reference 11. Copyright © (2012) Elsevier Inc.

Galectin-3 is the only known chimeric type found in vertebrates to date. This chimeric type is expressed in many different cell types. Overexpression of galectin-3 has been observed when tumours are present. This could lead to the use of galectin-3 as a potential biomarker for tumour progression. Galectin-3 has also shown to be mechanistically intertwined in tumour metastasis with key steps involving angiogenesis, cell motility, cell adhesion and cell invasiveness. A tumour-associated antigen called 90K (now termed galectin-3-binding protein, Gal-3BP) has shown elevated levels in breast cancer patients and patients with metastatic breast cancer.[13] Gal-3BP is considered to form aggregates between homotypic cells leading to cancer development.[14] Lin *et al*. describes the structural elucidation of Gal-3BP. This study also uses MCF-7 and MDA-MB-231 cancer cell lines (these cell lines were previously mentioned in Chapter 1) to demonstrate that Gal-3BP-induced cell aggregates are carbohydrate-dependent. This suggests a role in that Gal-3BP has in metastatic breast cancer.[15]

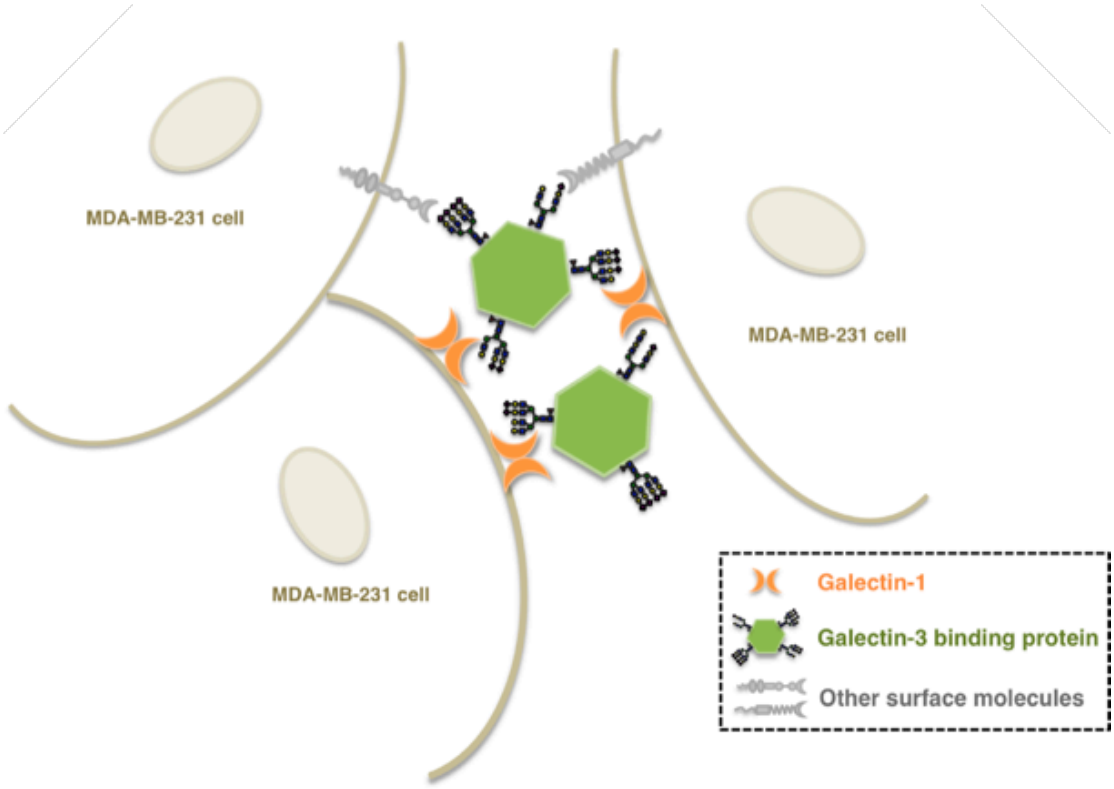

Figure 2.2 Illustration demonstrating the role of Gal-3BP has in forming cell aggregates. Adapted with permission from reference 15. Copyright © (2015) American Chemical Society.

2.1.2 Multivalency

Interactions of lectins with monosaccharide groups are typically weak. This is due to the structure of the CRDs, which have shallow binding pocket architecture. As these solvent exposed pockets are shallow, there are fewer interaction points between the lectin and the ligand. As a result of this, multiple protein-carbohydrate interactions need to occur in the recognition event. An example of this is shown by the reduction of glycopeptides from the circulatory system via the asialoglycoprotein receptor, if the concentration threshold of glycopeptide has been exceeded. This requirement for multiple sugars binding at the same time adds to the lectins affinity. Therefore the use of these multivalent ligands gives rise to an effect called the "glycosidic cluster effect".[16] This effect can be described as the increase in the activity of a multivalent ligand beyond what is expected, due to the increase in local sugar concentration alone.

The design and use of scaffolds to present multiple sugar headgroups can lead to functional avidity (the accumulated strength of multiple affinities of individual non-covalent binding interactions). The increase in valency however is not the only contributing factor to address in designing these scaffolds. Other factors such as the length of linker must also be addressed along with the geometry of the ligands and their displayed orientation. Designing scaffolds that meet all the criteria mentioned is challenging and exciting. Tailored scaffolds of varying backbones and valency can help with the elucidation of lectins and their physiological role. These tailored scaffolds may also be effective modulators that may disrupt signalling pathways resulting from tumour formation and subsequently metastasis.

2.2 Scaffolds

Scaffolds (chemical skeleton frameworks) are intrinsically important in drug discovery and drug design that allow for; (i) attachment of essential functional groups or ligands and other desired moieties to help with pharmacokinetics, (ii) the substitution of atoms with bioisosteres, (iii) a specific sequence of pharmacophoric groups and (iv) a fixed orientation that results in optimum target-receptor interaction. The scaffold is the framework that is inert to the target receptor. Bemis and Murcko proposed an approach that focuses on the dissection of a molecule leading to a term called frameworks. This concept suggests that a molecule can be broken down into four primary entities; (i) frameworks, (ii), side chains (iii) linkers and (iv) ring systems.[17] Bioactive molecules by their very nature have endogenous scaffolds displaying pharmacophoric regions. These initial active molecules may form a platform for lead compounds to be derived from. Scaffold diversity can generate a vast amount of compounds giving rise to compound libraries that can be screened for various diseases. Each scaffold chemotype can be evaluated and made more effective by increasing the pharmacological properties. Scaffold design may increase ligand/receptor activity and as a way to synthesise around patents.[18] Scaffold hoping or lead hopping, can be defined as identifying isofunctional molecular structures with different molecular backbones.[19]

2.2.1 Natural product scaffolds

Natural products and their derivatives have been and are still used as scaffolds for bioactive molecules. These scaffolds can be recognised throughout the range of regulatory approved anti-bacterial agents. They can be classified into structure classes including (i) β-lactam, (ii) daptomycin, (iii) macrolide, (iv) streptogramin and (v) tetracycline. Compounds from the above classes can range in their anti-bacterial mechanism from interfering with cell wall integrity though to interrupting protein synthesis.[20] Glycopeptide scaffolds can also be included as in the case of vancomycin. This is a Gram-positive anti-bacterial agent that inhibits the peptidoglycan biosynthesis. Vancomycin binds to the terminal D-Ala-D-Ala dipeptide of bacterial cell wall precursors resulting in loss of the cell structure that is a prerequisite for cell survival. As bacterial resistance is becoming more common, derivatives of vancomycin have been synthesised with retention of the parent scaffold core. The modifications and substitutions gives rise to effective anti-bacterial compounds.[21] The art of scaffold-hopping also allows for the manipulation of natural product entities to more pharmaceutically relevant compounds.

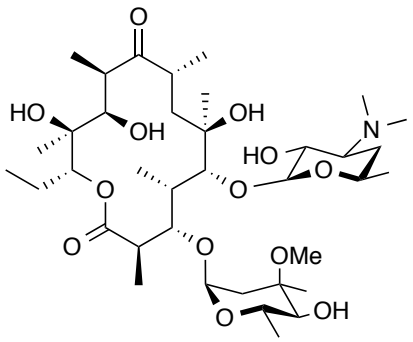

Figure 2.3 Anti-bacterial agent Erythromycin based on a macrolide scaffold.

2.2.3 Alkaloids

Alkaloids are an attractive option for scaffolds. Alkaloids may contain one or more primary, secondary and tertiary amines. The presence of these amines allows hydrogen bond acceptance or donation that can subsequently play an important role in the binding characteristics with potential targets. Many approved bioactive molecules currently on the pharmaceutical market are of alkaloid lineage.[22] A screening of five cyclin-dependent kinases 1-5 (CDK1, CDK2, CDK3, CDK4 and CDK5) for inhibition studies was performed. It was found that the introduction of a methylated alkaloid onto a naturally

occurring flavone chrysin, shown in Figure 2.4, increased the potency over 333 fold when tested against CDK1 and 200 fold when tested on CDK5, compared to the parent molecule, chrysin. In the same study it was also reported that the methylated alkaloid ring was more potent than the demethylated derivative.[23] This adds validity to the versatility of alkaloids with the presence of substituted and non-substituted amines.

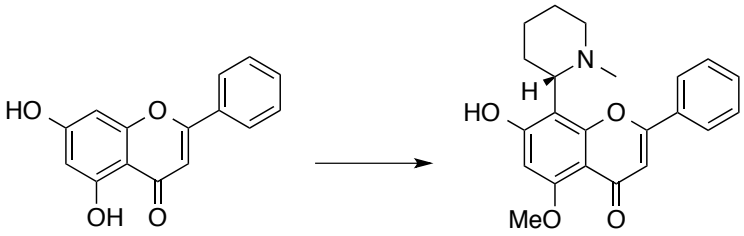

IC_{50} > 10 μM IC_{50} - 0.03μM

Figure 2.4 Chrysin (left) shows increase in activity after mono-methylation and inclusion of a methylated alkaloid ring (right). Adapted with permission from reference 23. Copyright © (2012) American Chemical Society.

2.2.4 Carbohydrate scaffolds

Carbohydrates in particular offer an excellent foundation for scaffolds due to their inherent fixed stereochemistry. Carbohydrates have hydroxyl groups that can be orthogonally protected and modified leading to great diversity. As there are five stereocenters and each stereocenter can either be axial or equatorial, this equates to thirty-two possibilities for displaying pharmacophores in different spatial orientations. Monosacharides can also offer an advantage with regard to ring size for example, furanose and pyranose rings. The ring oxygen can also be substituted for a nitrogen atom and as such are termed iminosugars. The development of peptidomimetics has increased the use of carbohydrate scaffold and will be discussed in further in Chapter 3. Another advantage of carbohydrates used as scaffolds is their multivalency and the fact they can be glycosidically linked to one another for example di, tri and tetrasaccharides etc. This allows for more attachment points to which pharmacophores can be chemically linked on to the scaffold. Various combinations of pharmacophores can also give rise to a substantial library of compounds which has been exploited by the Murphy group in the past.[24]

2.2.5 Previous scaffolds used in Murphy group

As previously mentioned, galectins form part of the cellular signalling system when they competitively and reversibly attach to glycans present on the cell surface. Interference of this docking could potentially lead to a therapeutic effect by blocking clinically unfavourable interactions, based on the physiological process in question, such as tumour progression. The increase in literature outlining the implications that carbohydrate-dependant protein interactions are involved in has given rise to the synthesis of potential lectin inhibitors. The scope of possible inhibitors varying in structural parameters such as; scaffold backbones, the type of sugar ligands to adopt, the geometry and orientation of ligands along with the spacing between ligands, attracted the Murphy group to this diverse field. The production of various scaffolds and sugar ligands may contribute to deciphering structure-activity relationships and thus pave the way for tailored inhibitors of medically important lectins. Galectins, as previously mentioned, contain one CRD as in the case of prototype, two CRDs in the case of tandem-repeat type and one or multiple CRDs as in the case of the chimera type.

Due to the different ranges of CRDs in different members of galectins, bivalent lactosides were first investigated. The synthesis of galectin inhibitors using bivalent (where two ligands were attached) scaffolds based on glycophanes, hydroquinone and terephtalamides were synthesised featuring lactose as the ligands. This panel of compounds gave rise to intriguing results. When the panel of bivalent compounds were tested against the ability to inhibit lectin-mediated haemagglutination, only one of the compounds showed comparable results to the control (lactose) whereas the rest of the compounds showed no inhibition properties respectively. A further assay based on surface-immobilised glycoprotein was carried out. This included four types of lectins; a plant toxin (VAA: Viscum album (a species of mistletoe), agglutinin/toxin which is galactoside specific), galectin-3, truncated galectin-3 and galectin-4. Only two compounds, **92** and **93**, shown in Figure 2.5, were potent inhibitors of these test galectins whereas the cyclic and more rigid glycophane **94** showed lower potency respectively to **92** and **93**. The flexibility factor in this case is preferred for binding and thus inhibiting galectin-3 and the plant toxin VAA.[25]

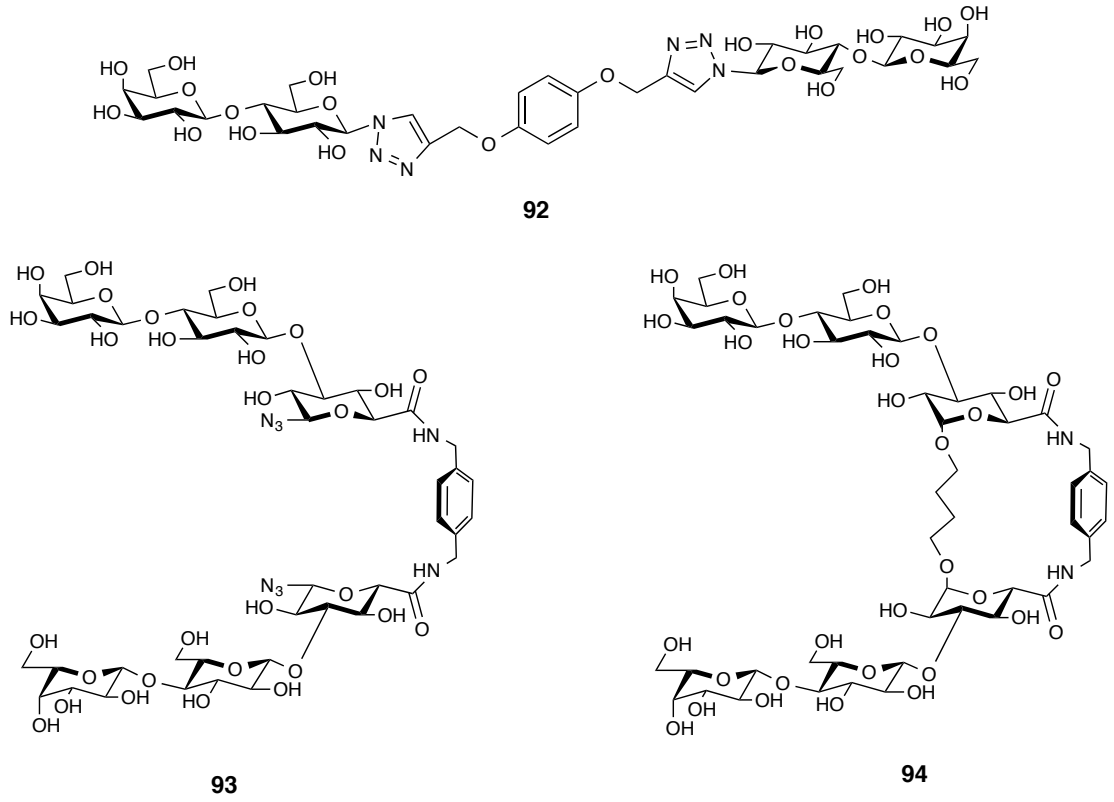

Figure 2.5 Example of multivalent compounds by Murphy and co-workers. Adapted with permission from reference 25. Copyright © (2009) American Chemical Society.

The findings from the previous assays prompted further studies that were carried out with a new range of compounds ranging from bi to tetravalent glycoclusters. Here Wang *et al*. synthesised a new panel of lactose based derivatives that additionally contained 2'-fucosyllactose (FucLac) to offer diversity within the headgroup of the ligand. The new panel of compounds were tested against plant lectins that included VAA toxin. The multivalent compounds were screened for their inhibitory effect on this plant toxin and in all cases bar one the inhibition was only slightly improved when compared to the disaccharide control, lactose. The panel was then subjected to lectins from the family of chicken galectins (CG) and two human galectins galectin-3 and galectin-4. The tetravalent compound **95** and the trivalent compound **96**, shown in Figure 2.6, were the most potent at inhibition with highest activity shown for CG-3 inhibition. Compound **96** containing FucLac headgroups showed the highest affinity, which adds weight to the fact that multivalency is not the only parameter to address when designing potential inhibitors. Once again when tested on human galectins-3 and -4, compound **95** and **96** showed the best inhibition, with the tetravalent compound **95** showing the highest activity.[26]

The positive outcomes of this data encouraged more research into the tailoring of the headgroups from lactose derivatives to *N*-acetylglucosamine (GlcNAc) and *N*-acetylgalactosamine (GalNAc) whilst ranging from bi to tetravalent compounds.

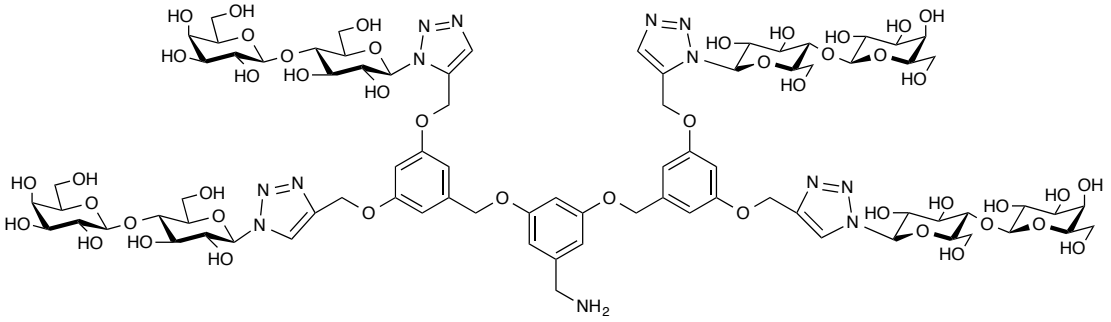

95

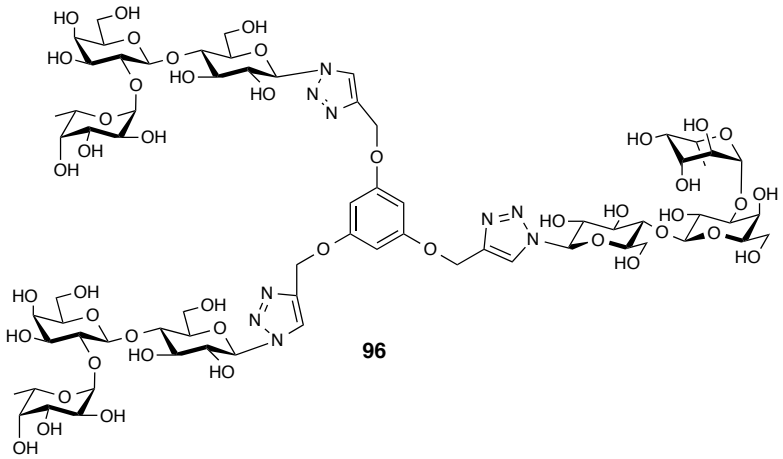

96

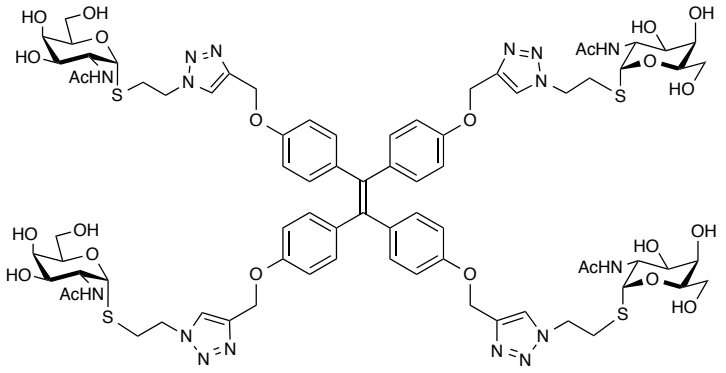

97

Figure 2.6 FucLac, lactose and *N*-acetylgalactosamine based sugar headgroups connected to different scaffolds. Adapted with permission from reference 26 and 27. Copyright © (2012) and (2015) Royal Society of Chemistry.

These compounds were evaluated against human macrophage galactose (-binding C)-type lectin MGL, as this is a site for viral uptake and therefore is of potential blocking interest. Compound **97** showed the highest activity with an IC_{50} in the nM region.[27]

2.2.6 Objectives

The aim of the first part of this chapter was to synthesise and evaluate self-assembling coiled-coil peptides as scaffolds. These peptides were *de novo* designed to form trimeric scaffolds for sugar ligand presentation, when exposed to aqueous conditions. The use of such self-assembling coiled coils can offer a more 3-dimensional scaffold increasing the topology when compared to the previously mentioned scaffolds. The second part of the chapter looked at forming a hybridised molecule using compound **43** as a scaffold.

2.3 Result/Discussion

The previous work carried out in the Murphy group on multivalent compounds as potential lectin inhibitors served as the foundation for the research described herein. The activities observed from these studies show that a wide range of scaffolds can be employed ranging from bi to tetravalent. These discussed scaffolds were typically of a flat nature due to the presence of the aromatic moieties and the triazole linker. The work carried out in this thesis describes the use of a self-assembling coiled-coil with an overall increase in the 3D morphology, relative to the 2D scaffolds previously synthesised.

2.3.1 Coiled Coils

Coiled coils are native protein architectures in which two or more α-helices are wound around each other forming a superhelical motif. It is estimated that 1.5 % of all protein amino acid residues are found in dimeric coiled coils and that 0.9 % form trimeric coiled coils.[28] These self-assembling structures were first noted back in the 1930's by William Astbury when he carried out X-Ray diffraction on natural fibres, for example, keratins from wool.[29] This observation however would take another ~20 years to fully extrapolate what the data was reporting. Various investigations were made by Linus Pauling and Robert Corey. In 1953 Francis Crick reported of 7/2 (3.5 residues per turn) configuration that would give rise to a structure, which had tightly packed α-helices, into coiled coils. The arrangement of these α-helices residues gave rise to the term "knobs and holes".[30] The secondary structure of an amphipathic α-helix has a turn every 3.6 residues and repeats the hydrophobic/hydrophilic alternately. The packing of right handed α-helices creates a left handed supercoil with a smaller pitch (distance between turns) to yield a setup where there are 3.5 residues per turn. Further structural investigations of coiled coils continued throughout the following years and identified the presence of a heptad repeat motif

$(abcdefg)_n$ which will be discussed later on.

2.3.1.1 Natural occurrences

A contractile protein, tropomyosin Ca^{2+}, from human cardiac tissue is made up of parallel dimers. This heterodimeric coiled-coil is formed between two differing subunits and is positioned on the actin filament.[31] Trimeric coiled coils are also observed on certain parts of viruses, for example haemagglutinin on influenza and glycoprotein41 found in human immunodeficiency virus.[32,33] Both these coiled coils form part of the docking and attachment to the host cell, which is a prerequisite for viral replication.

2.3.2 Sequence to structure

The knowledge and interest of these protein structures has led to the design and synthesis of these coiled coils motifs. The self-assembling properties of coiled coils are due to (i) hydrophobic, (ii) hydrophilic and (iii) salt bridge interactions. The incorporation of hydrophobic and hydrophilic residues gives rise to an amphipathic peptide. The hydrophobic residues bury themselves into the core of the coil trying to evade water molecules whilst the hydrophilic residues are embracing the water molecules. The formation of hydrogen bond interactions along with salt bridges increases the stability of the coiled coils. The construction of these coiled coils based on *de novo* (from the beginning) techniques gave rise to guidelines and rules of thumb as reported by Woolfson *et al*.[34] As previously mentioned in section 2.3.1, coiled coils are based on a heptad repeat motif where the coil turns every 3.5 residues (2 x 3.5 = 7). The overall sequence of these seven amino acids gives rise to what is known as a heptad. Within the heptad are seven positions (*a,b,c,d,e,f, and g*). Each position impacts on the folding capacity and the oligomerization state. As each turn of the coiled coil incorporates 3.5 residues, and with positions *a* and *d* (where hydrophobic residues are placed) being between three and four residues apart, this keeps all the hydrophobic amino acids on one side of the helix. The degree of oligomerization (the amount of α-helices wound together, for example dimeric, trimeric, tetrameric etc.) is dependent on the packing of the hydrophobic core. This is subsequently governed by the type of residues present and their geometric and space filling properties, in the *a* and *d* heptad repeat positions. Filling into positions *a* and *d* with combinations of isoleucine (Ile) and leucine (Leu), Harbury *et al*. reports the formation of a dimer, trimer and tetramer by incorporating Ile at *a* and Leu at *d*, Ile at both positions and

Leu at *a* and Ile at *d* respectively.[35] Positions *e* and *g* are typically polar and are of opposite charges. This allows the formation of interhelical salt bridges increasing the net stability of the superhelix. Lysine (Lys), which contains an NH_2 group on the side chain and glutamate (Glu), which contains a COOH group on its side chain, are frequently found in these positions in native proteins. Positions *b* and *c* may then be filled with alanine (Ala). This amino acid has a relatively small side chain, consisting of a methyl group, which encourages helical formation.[36] Position *f* is the final place to add an amino acid. This position is on the outer most surface of the coiled coil and is the most solvent exposed position. A polar residue, for example glutamine (Gln), typically occupies this place. The amine functionality helps with solubilising the coiled coils. As position *f* is not involved within the formation of the helix, this is the chosen position to incorporate mutations or modified amino acids. For quantification purposes, position *f* is where a chromophore can be included without it affecting the overall folding propensity of the superhelix. For example, the inclusion of tryptophan (Trp) into position *f* of one of the heptads, enables the concentration of the peptide to readily be determined by UV spectroscopy as Trp is a natural chromophore absorbing light at 280 nm (ε_{280} = 5690 M^{-1} cm^{-1}).

2.3.3 Coiled-Coil Scaffold synthesis

The mutation at position *f* with either an amino acid, as in the case of Trp, or indeed a modified ligand is of great interest. Not only is there a self-assembling multivalent scaffold capable of ligand presentation, it is also a native protein structure that may have the ability of further interaction with targeted receptors. Of course a scaffold by right should remain inert upon target binding, however this hybrid system could be of mechanistic interest. These scaffold glycoclusters therefore could help to study and elucidate multivalent lectin interactions. The work performed as part of this thesis focused on the design and synthesis of oligomeric trimers, whereby lactose was coupled onto aspartic acid forming lactosylated asparagine and the incorporation of such a glyco-amino acid into the coiled-coil structural motif.

The *de novo* peptide concept was based on the core heptad repeat motif totalling four heptads $(I_aA_bA_cI_dE_eQ_fK_g)_4$. The synthesis then incorporated glycine (Gly) to flank both the N and C-termini with the acetylation of the N-terminus, Ac-G$(I_aA_bA_cI_dE_eQ_fK_g)_4$G-$NH_2$. The acetylation was performed to help avoid ionic charges from the N-terminus amine interfering with the coiling of the superhelix. The heptad positions *a* and *d* were both filled

with Ile as a trimeric structure was desired. Ala was added to positions *b* and *c* as explained earlier. Lys was incorporated into position *g* and the oppositely charged Glu was added to position *e*. Gln was added to position *f* unless other wise stated.

Rink amide 4-methylbenzhydrylamine (MBHA) was used for the glycopeptide synthesis as it produced an amide on the C-terminus, upon the cleavage of the peptide from the resin. This was carried out to eliminate carboxylate ionic charges from forming and disrupting the coiled-coil formation. The elongation of the peptide chain was performed by automated microwave assisted solid phase peptide synthesis (SPPS) using (fluorenylmethyloxycarbonyl) Fmoc protected amino acids and standard coupling strategies. A brief introduction into solid phase peptide synthesis will be discussed.

2.3.3.1 Solid phase peptide synthesis

Bruce Merryfield introduced the concept of linking an amino acid to an insoluble solid support (now termed a resin) in which amino acids can be introduced in an iterative fashion.[37] As the solid supports are insoluble in the reaction solvent, a filtration technique can be applied. Excess reagents and side products can be washed away leaving behind the desired peptide at each step after the coupling of the sequential amino acid. After the final amino acid is added into the desired sequence, the peptide can be cleaved from the solid support (resin) along with the removal of temporary protecting groups on the side chains in one step. This process is outlined in Figure 2.7. This robust application for synthesising long peptides earned Merryfield the Nobel prize in chemistry in 1984.

This solid phase setup has many advantageous over the traditional solution peptide synthesis (SPS) including; (i) performing all the reactions in a single reaction vessel leads to a faster and simpler system (ii) lowers the potential of side product formation that results in large losses thus increasing the efficiency of the process and (iii) easier isolation and purification of the cleaved peptide. With more and more chemists using SPPS, a repertoire of resins and temporary protected amino acids are commercially available.

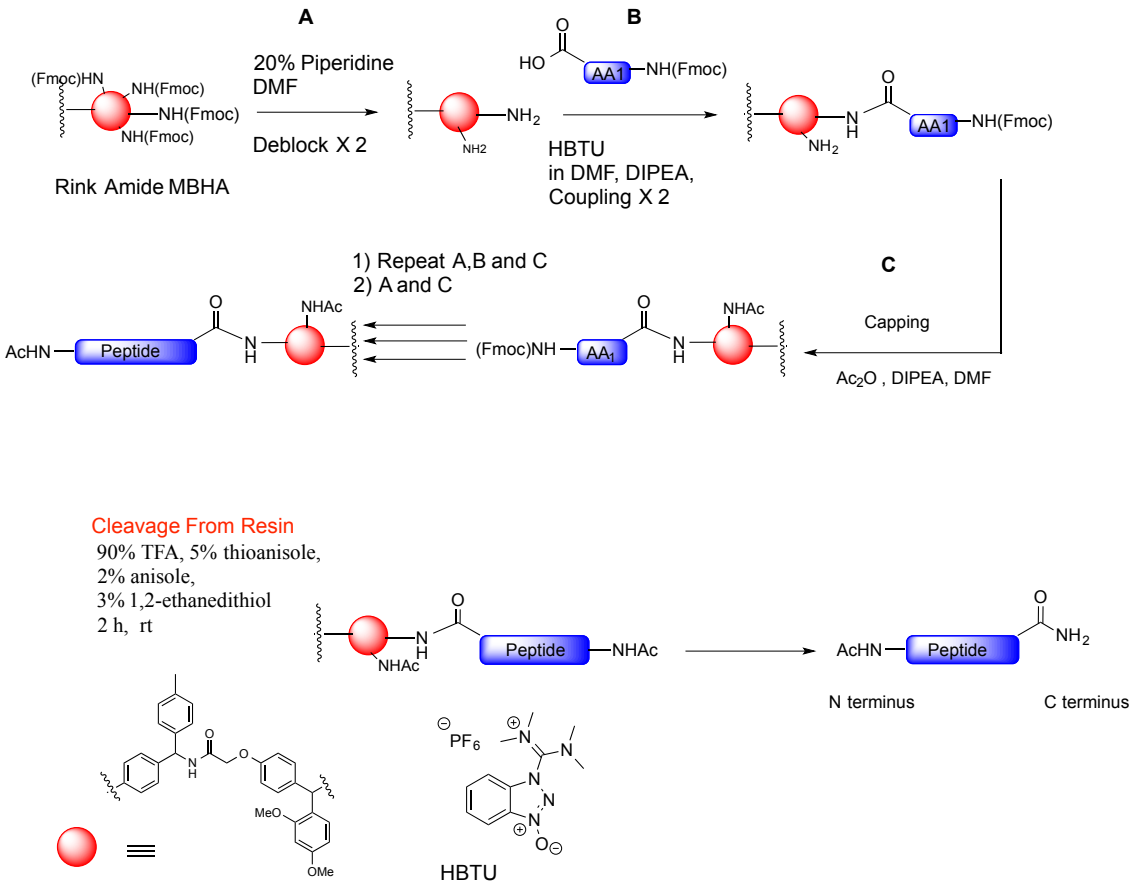

Figure 2.7 Outlining the steps involved in SPPS. (A) A commercially available resin (MBHA) is deblocked with a base, piperidine. (B) The incoming amino acid AA1 is attached to the resin using a coupling agent (HBTU) under basic conditions (DIPEA). (C) The resin is reacted with a capping solution (Ac_2O and DIPEA in DMF) to render any free amines unreactive. These steps (A, B and C) are repeated until the last amino acid has been added. The final amino acid is deblocked using step (A) and then capped using step (C). The peptide is then cleaved from the resin (under acidic conditions which also removes the protecting groups) and purified via preparative HPLC.

2.3.3.2 Coupling reagents

The coupling of the amino acids was done under basic conditions using HTBU (*O*-(Benzotriazol-1-yl)-*N,N,N′,N′*-tetramethyluronium hexafluorophosphate) and DIPEA. There are many types of amide coupling reagents at present to choose from. These include acyl chlorides, carbodiimides, phosphonium salts and uronium (guanidinium) salts. The latter two salts are generally used for SPPS as the acyl halides can lead to the formation of an oxazolone ring, which subsequently breaks down to form a racemic mixture losing the chiral integrity. Another disadvantage is the formation of a ketene when using the activated acid in the presence of base. Carbodiimides were previously discussed in Chapter 1. These are typically not used for SPPS as they are sensitisers and also lead to trace amounts of racemisation. Phosphonium salts are used in SPPS due to there fast coupling times. (Benzotriazol-1-yloxy)tris(dimethylamino)phosphonium hexafluorophosphate (BOP) is an efficient coupling reagent however it gives rise to hazardous size products. The next generation (Benzotriazol-1-yloxy)tripyrrolidinophosphonium hexafluorophosphate (PyBOP) dose not lead to hazardous side products and is used for difficult couplings. The use of uronium salts, now known to be guanidinium salts, are generally used as they are excellent coupling activators with low levels of racemisation. The term uronium salt comes from its discovery when chemists thought it contained a uronium structure, however Carpino *et al*. proved that it is in fact structurally based on guanidinium salts.[38] However, still to this present day, chemists with their nomenclature may refer to it as an uronium salt even though this is incorrect. The most common type used in SPPS is *N,N,N′,N′*-Tetramethyl-*O*-(1*H*-benzotriazol-1-yl)uronium hexafluorophosphate (HBTU) due to its relative low cost and excellent activity. The slight disadvantage of using guanidinium salts, is the potential for the N-terminus to couple to the coupling reagent resulting in guanidinylation and thus forming tetramethylguanidinium derivatives, as depicted in Figure 2.9. One way to avoid this side product and hence truncated guanidylated peptides, is through the use of lower equivalents of the coupling reagent compared to the incoming amino acid along with a pre-activation step. This ensures the entire coupling reagent has been used up, which prevents any unwanted nucleophilic attacks from the free amines.

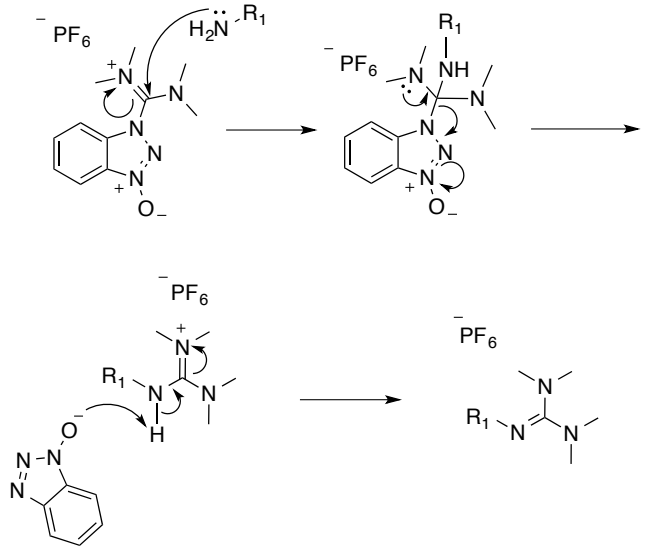

Figure 2.8 Potential guanidinylation mechanism involving guanidinium salts.

2.3.3.3 N-Terminus deprotection

There are two main types of protecting groups used in SPPS that are determined by the manner in which they are removed i.e. either using acidic or basic conditions. Classical SPPS used *tert*-butoxycarbonyl (Boc) to protect the amine functional group of the amino acid. Acidic conditions such as 50 % TFA in DCM is used for the cleavage of the Boc group. HF can then be used to cleave the peptide from the resin. MBHA resin shows a balance between its stability to TFA and labiality to HF.

Typically however, fluorenylmethyloxycarbonyl (Fmoc) protection is used due to the milder conditions required for synthesis and less specialised equipment is needed as in the case for Boc cleavage using HF. In this instance, Fmoc protecting groups are base labile (piperidine is generally used for deprotection) and the peptide is cleaved under acidic conditions for example 95 % TFA. It should be noted that the temporary protecting groups on the side chains are also removed upon cleavage of the peptide from the resin. Therefore, in Boc chemistry, the protecting groups are HF labile and in Fmoc chemistry, the protecting groups are acid labile. One of the disadvantages of Boc chemistry is the potential for these protecting groups to fall off during repeated TFA washes to remove the Boc group. In both cases, "scavangers" are added to the cleavage cocktail to 'mop up' the removed protecting groups so that no unwanted side reactions will occur. Fmoc chemistry was used as part of this work and the mechanism is illustrated in Figure 2.9.

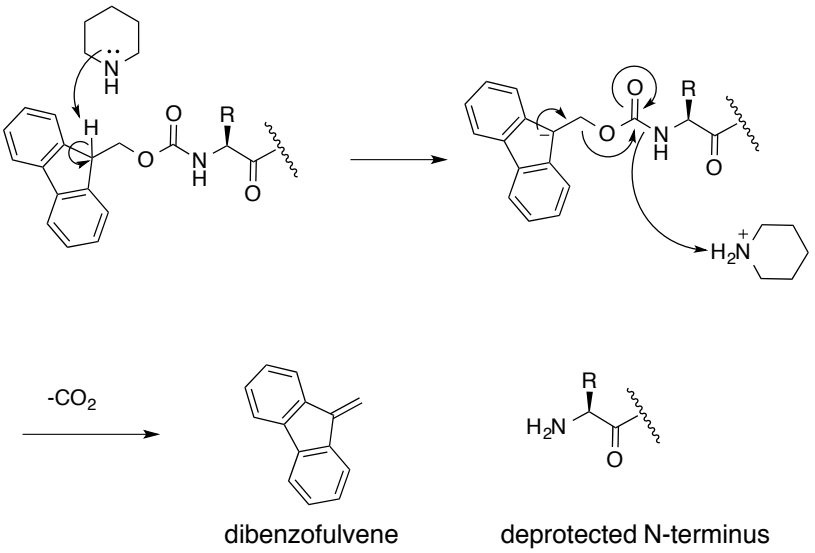

Figure 2.9 Deprotection of the Fmoc protecting group using piperidine resulting in the primary amine.

2.3.4 Lactosylated Asparagine

The design of these peptides required the incorporation of a modified glyco-amino acid. The peptide synthesis incorporated lactose as the sugar moiety, which was coupled to L-aspartic acid's side chain. This coupling resulted in a glyco amino acid building block that was Fmoc SPPS ready. The synthesis began with peracetylating lactose **98** to protect all the free hydroxyl groups to form **99**. Hydrogen bromide in 33 % acetic acid was used to introduce a bromine onto the glucose anomeric carbon of the disaccharide forming **100**. The bromine was displaced with sodium azide in the presence of a phase transfer catalyst as shown in Scheme 2.1 to reveal compound **101**.

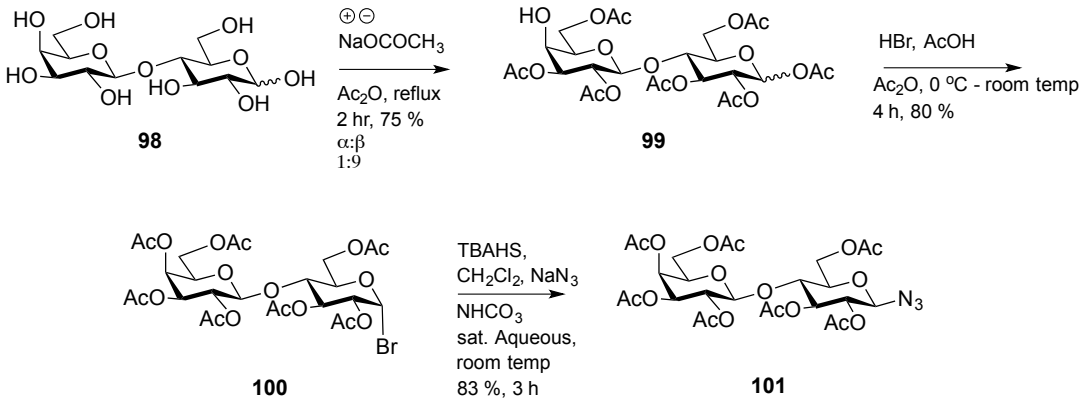

Scheme 2.1 Synthesis of **101** from lactose **98**.

The beta azide **101** was reduced successfully using palladium on carbon in ethyl acetate (EtOAc) and H_2 to the corresponding amine, shown in Scheme 2.2. This reduction however yielded a 9 : 1 ratio of beta : alpha anomers **102**/**103** that was an inseparable mixture. A different catalyst (Adams catalyst) and solvent (THF) were used to check if the anomeric outcome was solvent and/or catalyst dependent, however this once again yielded an anomeric mixture with a lower yield. Coupling of the mixture of amines, with appropriately protected aspartic acid (Scheme 2.2) in the presence of 2-ethoxy-1-ethoxycarbonyl-1,2-dihydroquinoline as the coupling agent afforded two anomeric amides **104** and **105**, that could be separated by chromatography.

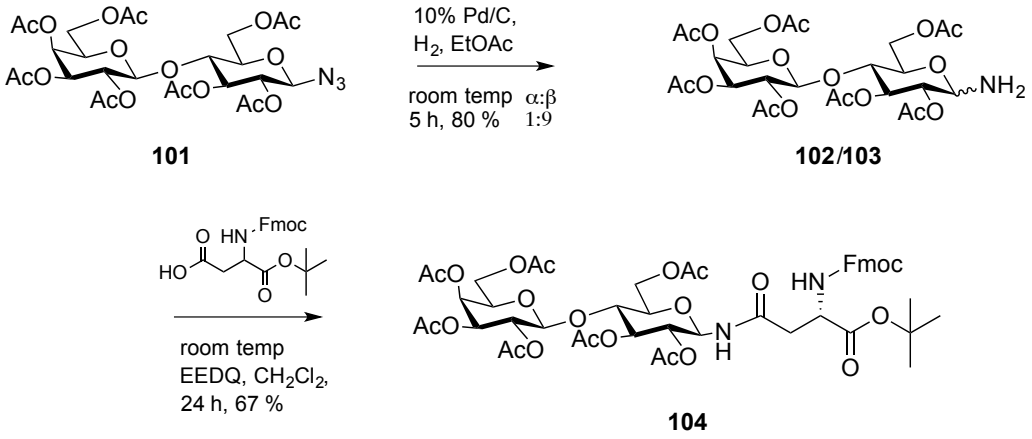

Scheme 2.2 Reduction of **101** to form the amine mixture **102**/**103** to form lactosylated asparagine precursor **104**.

The β-lactosamide was treated with TFA to afford the desired glyco-amino acid **106** as shown in Scheme 2.3. The preparation was carried out on an approximately 7 g scale.

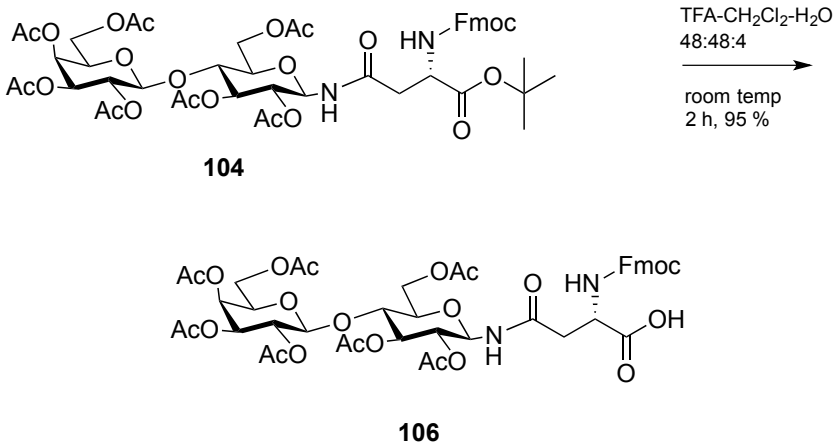

Scheme 2.3 Synthesis of lactosylated asparagine **106** using L-aspartic acid.

2.3.5 Glycoclusters

Automated SPPS synthesis was performed, for both glycoclusters, up to the point of the introduction of **106**. The insertion of the modified lactosylated amino acid **106** into the growing peptide was performed 'offline' in order to be able to carry out the coupling reaction of the lactose derivative over a longer reaction time. This also allowed the incorporation of **106** into the peptide to be monitored using the Kaiser test protocol. Acetylation "capping step" of the uncoupled free amines after the addition of the modified amino acid was performed so as to render any free amines unreactive. After incorporation of the lactosylated asparagine, the remaining peptide synthesises were accomplished by automated SPPS.

The first glycosylated peptide **107** (Ac-G IAAIEQK IAAIEQK IAAIE**X**K IAAIEWK G-NH_2, where X = lactosylated asparagine) was synthesised with the tryptophan (Trp) (natural chromophore) positioned in the fourth and final heptad and with the lactose positioned in the third heptad shown in Figure 2.10. The second glycosylated peptide **108** (Ac-G IAAIEQK IAAIEWK IAAIEQK IAAIE**X**K G-NH_2, X = lactosylated asparagine) had tryptophan positioned in the second heptad whilst the lactose was located in the fourth. The non-glycosylated peptide **109** (Ac-G IAAIEQK IAAIEQK IAAIEQK IAAIEWK G-NH_2) had the tryptophan located in the fourth heptad, analogous to **107**, as shown in Figure 2.11. It was found that the coupling of the lactosylated amino acid in **107** was slow and the yields were lower, based on HPLC analysis, when compared to amino acids that did not contain the lactose residue. Peptide aggregation and/or the bulky nature of the lactose moiety may have impaired the efficiency of the coupling. Therefore, **108** was synthesised, in which the lactosylated asparagine was introduced earlier on in the peptide synthesis (peptides are synthesised from the N-terminus to the C-terminus), as it was the first *f* site and the third amino acid residue, to be introduced. This led to enhanced coupling efficiency and an improved yield with respect to compound **107**.

After cleavage of the glycosylated peptides from their solid supports, both glycosylated peptides were subjected to reaction with NaOMe in methanol (pH 10), under stirring for 1h. These conditions facilitated the efficient removal of the acetate protecting groups from the lactose moieties. Amberlite H^+ resin was used to acidify the resulting mixture to pH 7 during the work up which was subsequently removed by filtration. The glycopeptides were purified via preparative C18 RP-HPLC and subsequently analysed by ESI-MS.

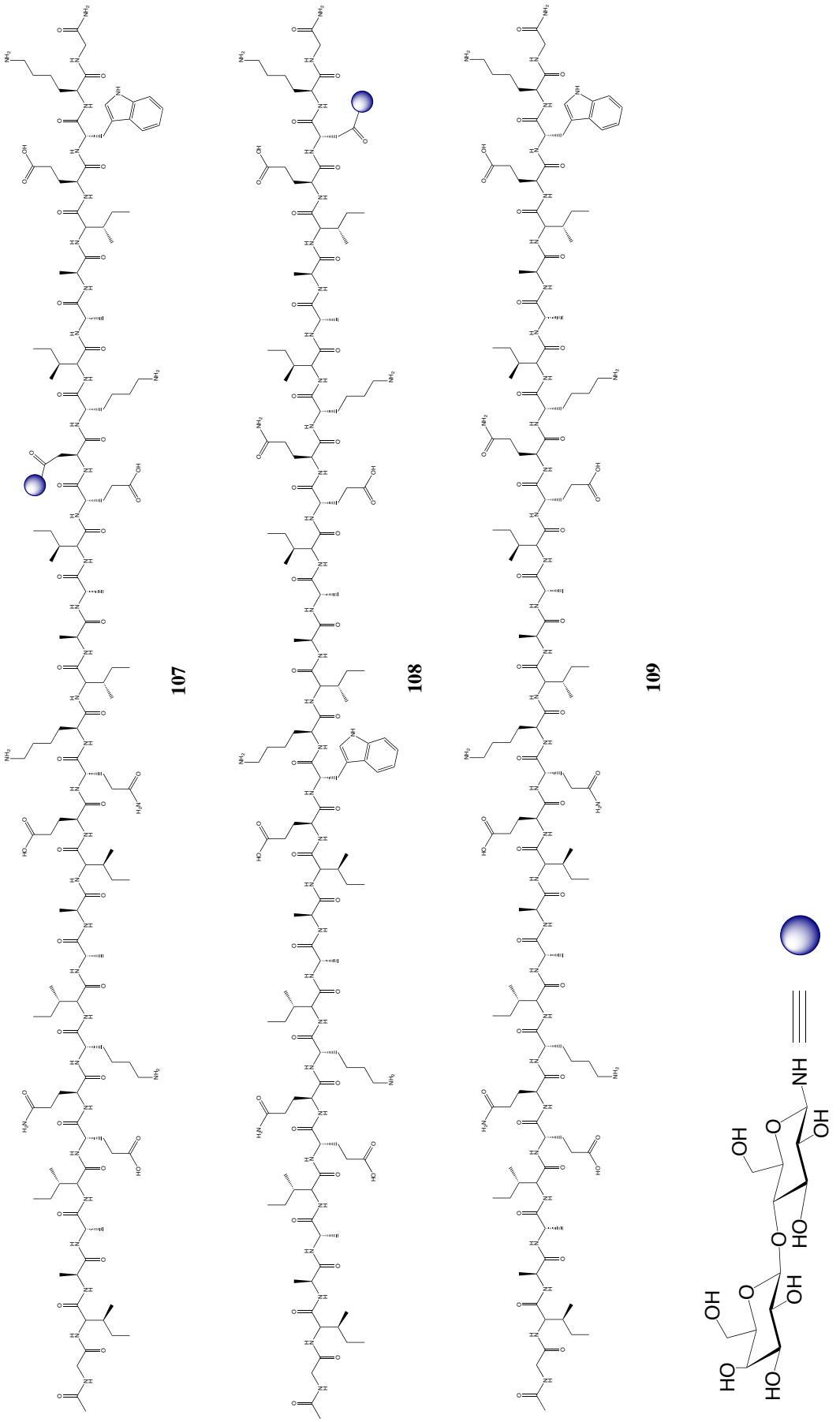

Figure 2.10 Synthesis of glycoclusters **107**, **108** and the non-glycosylated control **109**.

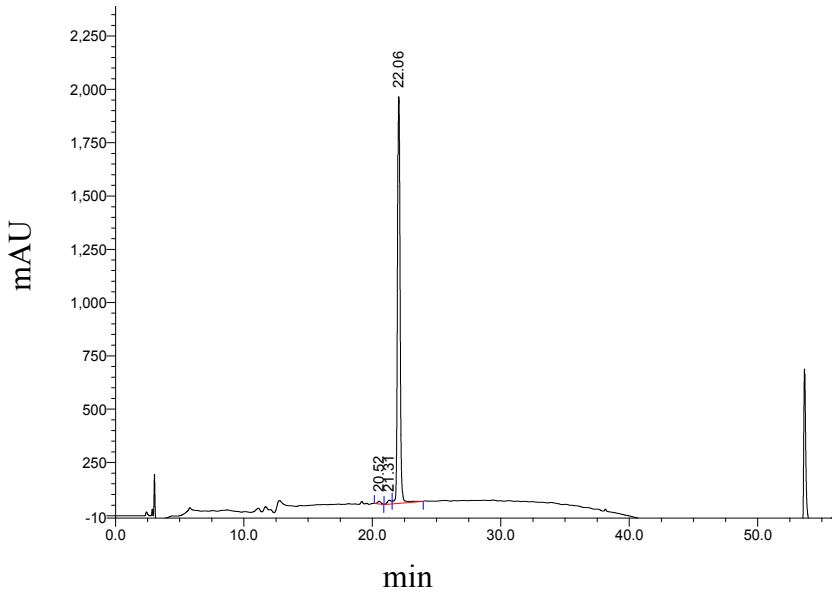

Figure 2.11 C18-analytical HPLC trace of pure **107** using a linear 0 to 100 % MeCN + 0.05 % TFA gradient in H_2O + 0.05 % TFA over 40 minutes.

Helical-wheel diagrams (Figures 2.12, 2.14 and 2.16) illustrate the heptad repeat helices with 3.5 residues per turn effectively forming the trimeric supercoil. Circles indicate the positions and amino acids present, and the respective heptads that they are located on; moving from inner to outer are heptads 1 to 4. Hydrophobic residues lie between the α-helix interfaces whilst hydrophilic residues are on the periphery of the coiled-coil.

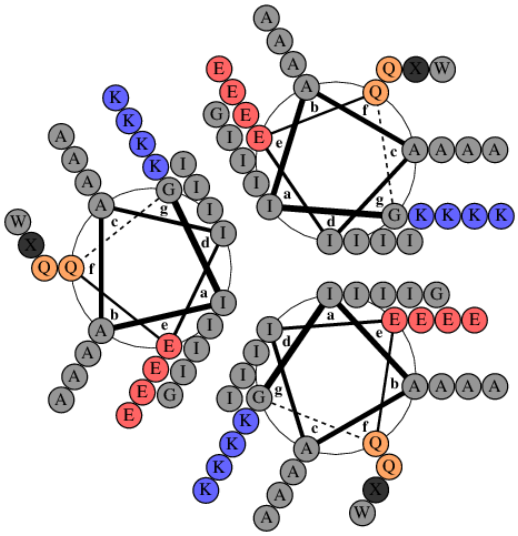

Figure 2.12 Helical-wheel diagram of **107** showing Trp located in the fourth heptad and the lactose moiety, represented by **X** in black, located in the third heptad.

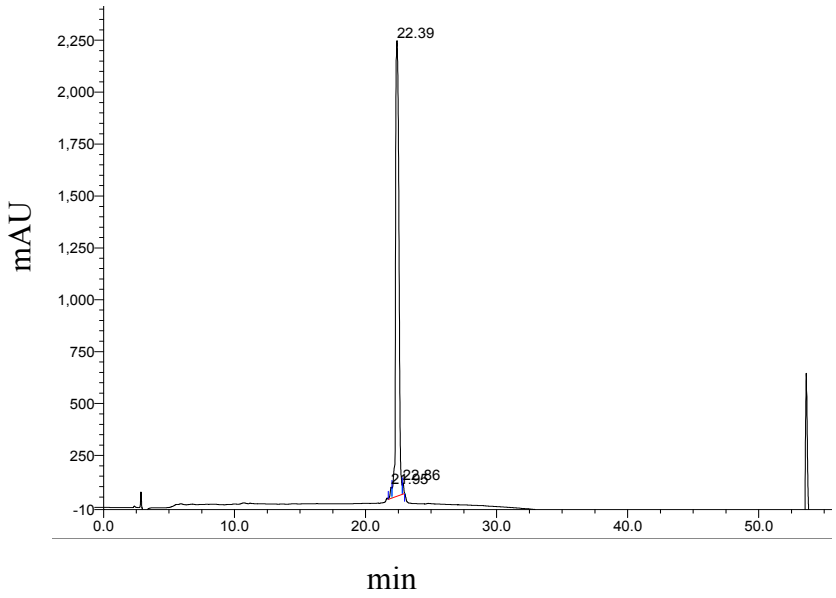

Figure 2.13 C18-analytical HPLC trace of pure **108** using a linear 0 to 100% MeCN + 0.05% TFA gradient in H_2O + 0.05% TFA over 40 minutes.

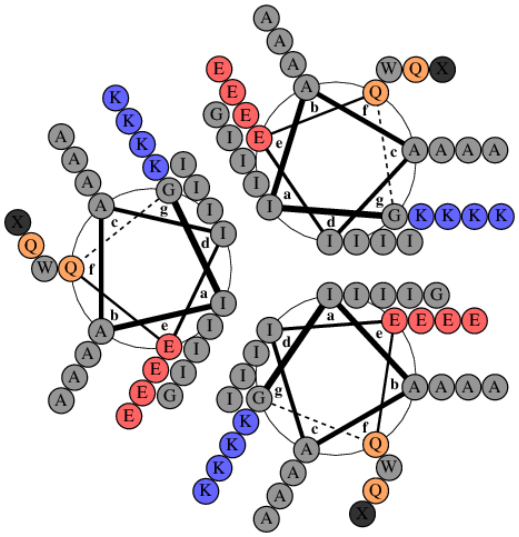

Figure 2.14 Helical-wheel diagram of **108** showing Trp located in the second heptad and the lactose moiety, represented by **X** in black, located in the fourth heptad.

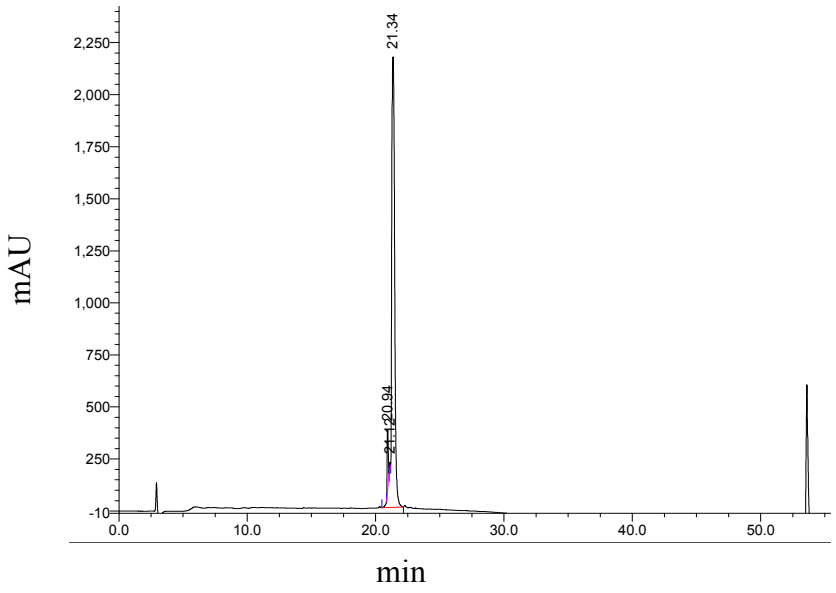

Figure 2.15 C18-analytical HPLC trace of pure **109** using a linear 0 to 100% MeCN + 0.05% TFA gradient in H_2O + 0.05% TFA over 40 minutes.

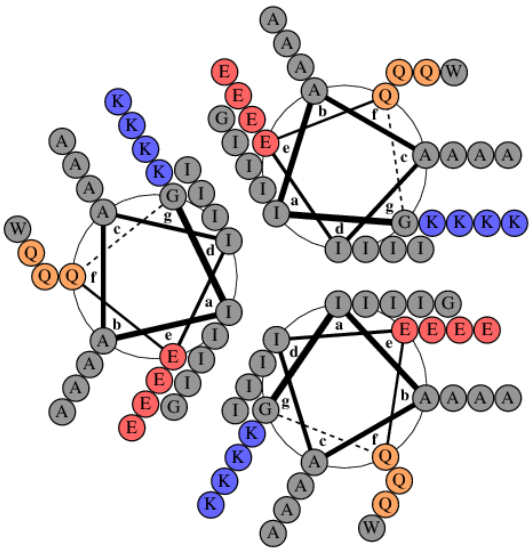

Figure 2.16 Helical-wheel diagram of **109** showing Trp located in the fourth heptad.

2.3.6 Circular Dichroism

Circular Dichroism (CD) is a spectroscopy technique used for determining the presence of secondary structures within proteins and peptides. This spectroscopic technique measures samples over a range of wavelengths. Linearly polarised light is transformed into a sinusoidal wave through either prisms or filters. This newly formed wave is helical in nature and is called circularly polarised light (CPL). As such, the sinusoidal wave can either be right-handed (R-CPL) spiralling clockwise or left-handed (L-CPL), spiralling in an anti-clockwise manner. The detector measures the intensity of both the R-CPL and the L-CPL. If both measured intensities are the same, then the detector will register zero. However, as chiral agents interact with polarised light differently, a chiral sample will absorb one of the helical waves more so than the other and therefore a difference in the detector will be observed. This output is then represented by peaks that can be positive and/or negative. Characteristic spectra for secondary structures can be observed including α-helix, β-sheet and β-turns. As the helical light interacts with the asymmetric sample, the post-sample light travelling to the detector takes on an elliptical form. The CD data can therefore can be reported in two forms, the difference (Δ) in absorption between R-CPL and L-CPL or the degree of ellipticity (θ) which is defined as the angle between the tangent of the ratio of the minor to major elliptical axis.

From the CD analysis of **107, 108** and **109**, the molar ellipticity (Θ_m) was determined using the calculation below;

$$\Theta_m = \frac{\Theta}{10 \times l \times c \times N_a}$$

Where Θ_m is the molar ellipticity, Θ is the ellipticity at 222 nm, l is the path length in cm, c is the concentration of monomer peptide in mol dm^{-3} and N_a is the number of amino acid residues in the peptide.

From this value (Θ_m), the percentage folding of all coiled coils, **107**, **108** and **109** was subsequently determined using the following equation;[39]

$$\% \text{ folding} = \left(\frac{\Theta_m - 640}{\left(-42500 \times \left(1 - \left(\frac{3}{N_a} \right) \right) \right) - 640} \right) \times 100$$

This work was carried out in Dr. Anna Peacock's research group, Birmingham, UK. The data obtained is represented in Figure 2.17 and Table 2.1.

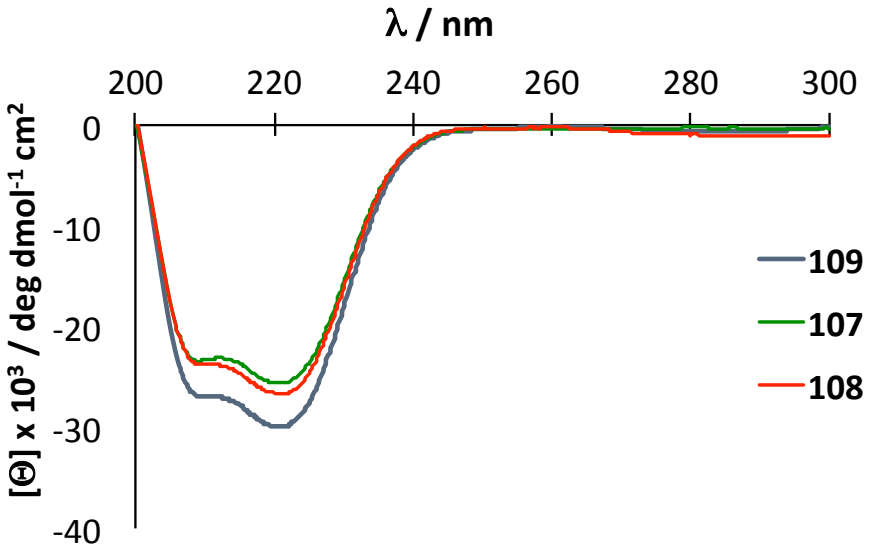

Figure 2.17 Circular dichroism spectroscopy of 30 µM solutions of **107**, **108** and **109** monomer, in 5 mM HEPES buffer at pH 7.

Table 2.1 Percentage folding of coiled coils **107**, **108** and **109**.

	222 nm	**Molar Ellipticity**	**% α -Helix Folded**
109	-29.772	-33080.444	86.7
107	-25.483	-28314.444	74.5
108	-26.585	-29539.333	77.6

This data shows that the coiled coils **107** and **108** tolerate the disaccharides with good overall % folding of 75 % and 78 % respectively, when compared to the non-glycosylated control **109** at 87 %.

2.3.7 Analytical Ultracentrifugation

Analytical ultracentrifugation (AUC) uses centrifugation forces along with spectroscopy techniques to measure sample concentration distribution at a given time. Solutes are dissolved up in an appropriate solvent and if they obey the Beer-Lambert equation, the absorbance is proportional to concentration. The dissolved sample is placed inside a cell, with a reference cell, containing solvent, next to it. The samples are rotated at speeds up to 60,000 rpm. Based through a series of calculations, the molecular weight of the protein or macromolecule samples can be determined. Solutes placed inside these cells undergo sedimentation during centrifugation. These particles undergo three separate forces at the same time; (i) sedimentation force or gravitational force which is proportional to the mass and gravitational force (ii) a buoyant force that takes into account Archimedes' principle, that is the solute is equal to the weight of fluid displaced and (iii) as the solute moves through the fluid, it will encounter a frictional force which is proportional to the velocity of the particle. Each force can be written into an equation, which can subsequently be rearranged to form an overall equation;

$$\frac{M(1-\nu\rho)}{Nf} = \frac{u}{\omega^2 r} \equiv s$$

This equation gives rise to the sedimentation coefficient, *S*. This coefficient, *S*, is obtained through two basic types of experiments using AUC; (i) sedimentation velocity and (ii) sedimentation equilibrium.

2.3.7.1 Sedimentation Velocity

This the most common technique used to determine molecular weights of solutes, either as monomers or oligomeric complexes, in their native states in solution. The solute in the sample cell is rotated rapidly which cause the sample to sediment to the bottom of the sample cell. This subsequently leads to a depletion of sample at the top meniscus of the cell and a boundary is observed between the depleted meniscus and the sedimenting solute at the bottom of the cell. The diffusion coefficient must be estimated accurately to determine *S* and hence characterise the molecular weight of the sample.

2.3.7.2 Sedimentation Equilibrium

In this experiment, the sample can be rotated at lower speeds than in sedimentation velocity. Here, the uniform solution in the sample cell is rotated and sedimentation starts to occur. However, as the concentration starts to build up at the bottom of the cell, some sample starts to oppose this action and begins to diffuse back toward the top of the cell. After time, the diffusion and sedimentation process finds an equilibrium whereupon the sample distribution is invariant with time. Measurements at different concentrations gives rise to molecular weight of the sedimenting solute.

For **107**, **108** and **109**, sedimentation equilibrium experiments were used to confirm monomer–dimer–trimer stoichiometry. Sedimentation equilibrium curves were analysed using a modified form of the INVEQ algorithm.[40] This experiment was ran due to the low molecular weight of the monomer which may have caused poor resolution if it was ran as a sedimentation velocity experiment. The trimeric coiled coils displaying lactose are illustrated in Figure 2.18. This work was carried out in Prof. Harding and Associate Prof. Adams' laboratories as part of The National Centre for Macromolecular Hydrodynamics in Nottingham, UK.

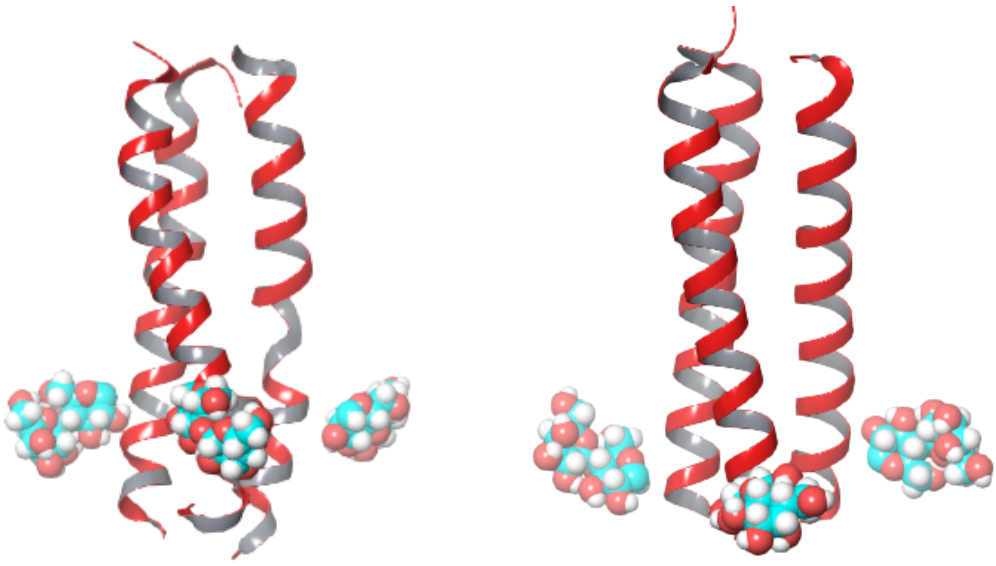

Figure 2.18 Graphical representations of **107** (left) and **108** (right) are shown, where the lactose residues project towards the exterior of the coiled coil. The models of **107** and **108** were built using Maestro and the structures were energy minimised in Macromodel using OPLSAA force field. Angle constraints (C1–C1–C1) were applied between the galactose

anomeric carbons of 60° during energy minimisation. The peptide backbone is depicted in ribbons with the conjugated *β*-lactose residues shown as space filling models. The distance between the galactose anomeric carbon atoms in both **107** and **108** is approximately 30 Å. The model on the left (**107**) shows slight distortion of the coiled-coil which could account for the lower % folding compared to **108** (right) and **109** shown by CD analysis.

2.3.8 Migrastatin derivative scaffold

Galectins are considered to play a role in the metastatic breast cells as previously mentioned in Section 2.1.1.4.[15] The reporting of these observations led to the development of a hybrid compound during the course of this work. The first part of the compound was designed using the macrolactam **43** from Chapter 1. This has shown anti-metastatic properties by the inhibition of migrating breast cancer cells [41] and was found to be stable in blood serum. The second part of the compound encompassed lactose through a triazole linker.

The synthesis of this hybridised compound began as outlined in Chapter 1 to form **43**. Next, the secondary alcohol was reacted with propargyl bromide to form propargyl ether **110**. A trial reaction was attempted to introduce the propargyl group onto the nitrogen involved in the amide bond, however the yields were low with little compound isolated shown in Scheme 2.4.

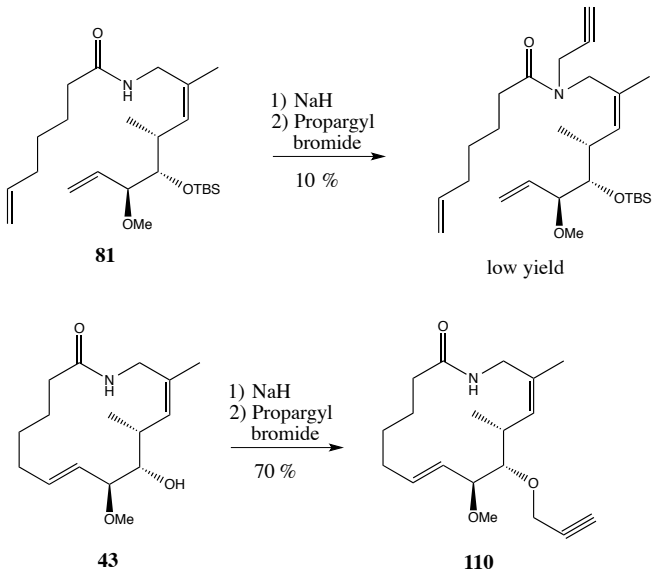

Scheme 2.4 Synthesis propargyl ether **110** from **43**. Reaction of **81** with propargyl bromide resulting in a low yield.

The next step involved a copper catalysed reaction involving the alkyne group from the propargyl ether and the azide moiety from **101** to form a 1,4 triazole linkage. This linkage is a common method for linking sugar moieties to scaffolds and peptides due to the similar atom placement i.e. nitrogen, and electronic effects such as dipole moments. The length of the 1,2,3 triazole bond increase the R_1-R_2 distance by approximately 1.1 Å [42], shown in Figure 2.19.

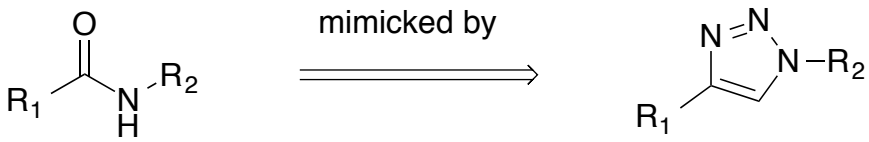

Figure 2.19 Amide distance between R_1 and R_2 is 3.9 Å. 1,4 triazole distance between R_1 and R_2 groups is 5 Å.[42]

As click chemistry is often used as a way to link two molecules, it will be further discussed in more detail.

2.3.9 Click Chemistry

This term was first coined by Sharpless and co-workers in 2001[43] and describes reactions that fit certain criteria including; (i) the reaction must be modular, (ii) have a wide scope, (iii) give very high yields and (iv) resulting by-products are easy to remove and are non-hazardous. Synthetic chemists strive to use these types of reactions. This reaction dates back to 1963 when Huisgen carried out a 1,3-dipolar cycloaddition using an azide and alkyne to form a five membered ring.[44] The formation of this ring is considered to be a concerted pericyclic cycloaddition mechanism. This reaction resulted in carbon-heteroatom connectivity. The drawback of this reaction however was poor selectivity forming a mixture of 1,4 and 1,5 traizoles and the need for high temperatures.

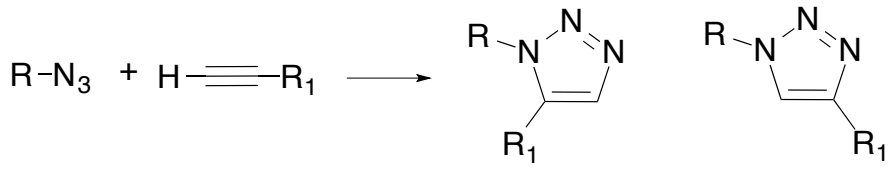

Figure 2.20 Huisgen 1,3-dipolar cycloaddition forming a 1,4 and 1,5 triazole mixture.

In 2002, Meldal and co-workers published a new copper activated derivative of the Huisgen 1,3-dipolar cycloaddition to yield a 1,4 triazole regioselectively on SPPS.[45] Sharpless and co-workers also published in the same year of a regioselective copper catalysed 1,4 triazole linkage.[46] Sharpless and co-workers proposed that the reaction started with the formation of a copper (I) acetylide. This copper complex forms a ligation with the 1,3 dipolar azide group which subsequently leads to a six membered intermediate. This intermediate then rearranges to a five membered group with the substitution of the Cu with a hydrogen as shown in Figure 2.21.

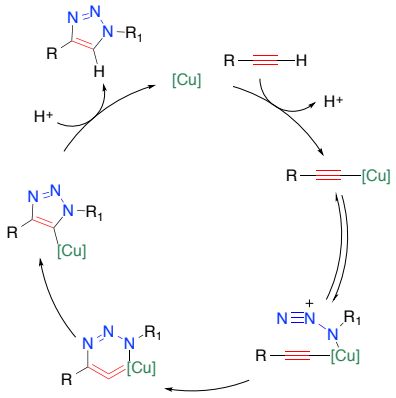

Figure 2.21 Proposed catalytic cycle for the Cu^{I}-catalysed ligation by Sharpless and co-workers. Adapted with permission from reference 46. Copyright © 2002 WILEY-VCH Verlag GmbH & Co. KGaA, Weinheim.

This regioselective reaction mechanism was further explored by Fokin and co-workers who showed the presence of a dinuclear copper intermediate giving rise to a new proposed mechanism.[47] This reaction mechanism is illustrated in Figure 2.22.

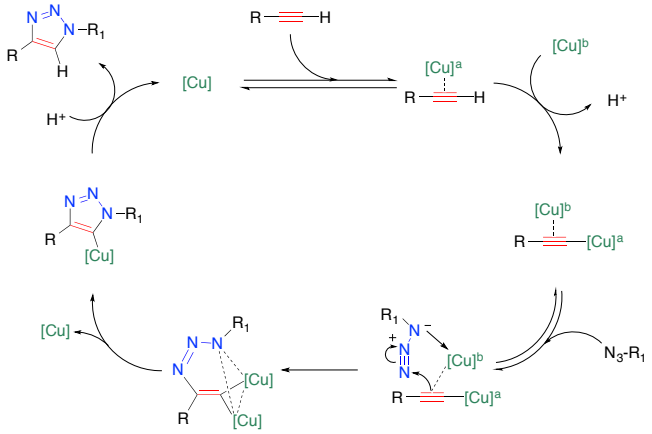

Figure 2.22 New proposed Cu^{I}-catalysed click reaction by Fokin. Adapted with permission from reference 47. Copyright © (2013) The American Association for the Advancement of Science.

The Cu-catalysed click reaction between **101** and **110** gave the desired 1,4 linkage regioselectively as shown in Scheme 2.5. Deacetylation of **111** furnished the final product **112** in excellent yield after reverse phase chromatographic purification.

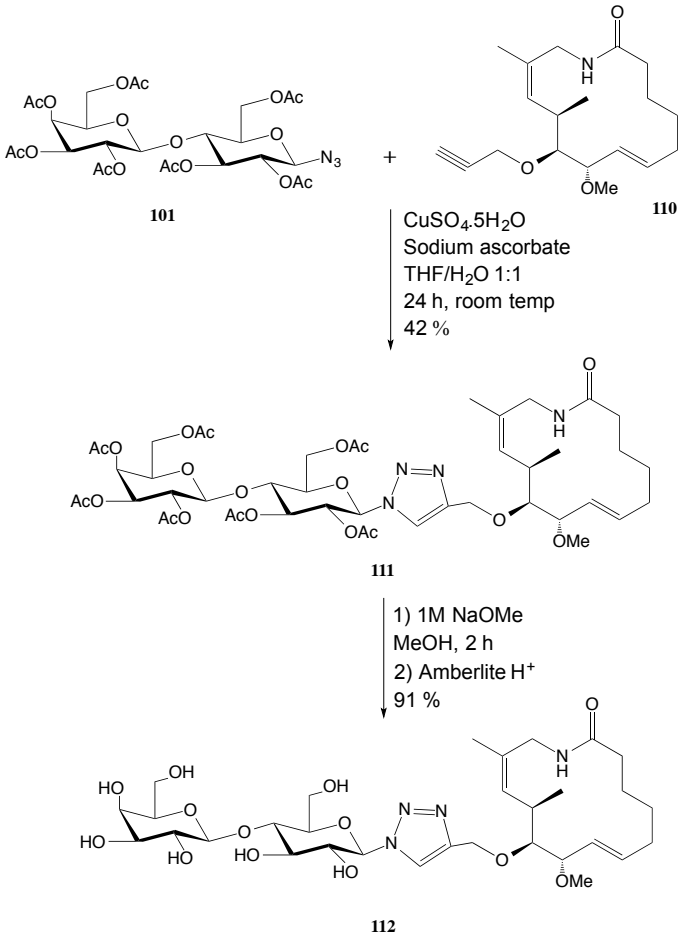

Scheme 2.5 Deacetylation of clicked substrate **111** to yield the final product **112**.

2.4 Conclusion

Whilst coiled-coil dimers have been reported for the presentation of simple sugars in the past by Koksch and co-workers,[48] the synthesis of novel trimeric coiled-coil scaffolds **107**, **108** and **109** were successfully carried out during the course of this thesis work. The location of the modified lactosylated asparagine was placed in two different heptads of the scaffold. This will be interesting to see if the location has an effect on the activity within lectin binding assays. The CD data indicates the coiled coils tolerate the addition of the lactose headgroups with a slightly less % folded superhelix when compared to the non-glycosylated coiled-coil **109**. In the case of **107**, the AUC data shows that 100 % trimeric coiled coils are formed indicating that the positioning of the lactose groups could

encourage the self-assembling propensity of the coiled-coil scaffold. These compounds are currently under biological evaluation.

The combining and hybridisation of the macrolactam **43** and *β*-lactosamide **101** was successfully performed to yield **112**. The use of compound **43** as a scaffold demonstrated the diversity of scaffolds that can be employed. This combination will be of medicinal interest as both regions of the molecule could potentially interfere with tumour progression. The lactose hydroxyl groups may also offer better bioavailability by increasing the solubilisation and hence the distribution of the macrolactam. This compound is currently being studied for biological activity.

Bibliography

1. Sharon, N.; Lis, H., *Glycobiology* **2004,** *14* (11), 53R-62R.
2. Sumner, J. B.; Howell, S. F., *Journal of Bacteriology* **1936,** *32* (2), 227-237.
3. Li, C.; Chen, J.; Lu, B.; Shi, Z.; Wang, H.; Zhang, B.; Zhao, K.; Qi, W.; Bao, J.; Wang, Y., *PLoS ONE* **2014,** *9* (7), e101526.
4. Li, L.-N.; Zhang, H.-D.; Zhi, R.; Yuan, S.-J., *British Journal of Pharmacology* **2011,** *162* (2), 349-364.
5. G Ashwell, a.; Harford, J., *Annual Review of Biochemistry* **1982,** *51* (1), 531-554.
6. Watanabe, N.; Kawashima, H.; Li, Y.-F.; Miyasaka, M., *Journal of Biochemistry* **1999,** *125* (4), 826-831.
7. D C Wiley, a.; Skehel, J. J., *Annual Review of Biochemistry* **1987,** *56* (1), 365-394.
8. Branson, T. R.; McAllister, T. E.; Garcia-Hartjes, J.; Fascione, M. A.; Ross, J. F.; Warriner, S. L.; Wennekes, T.; Zuilhof, H.; Turnbull, W. B., *Angewandte Chemie International Edition* **2014,** *53* (32), 8323-8327.
9. Gabius, H.-J., *European Journal of Biochemistry* **1997,** *243* (3), 543-576.
10. Ghazarian, H.; Idoni, B.; Oppenheimer, S. B., *Acta Histochemica* **2011,** *113* (3), 236-247.
11. Rabinovich, G. A.; Croci, D. O., *Immunity* **2012,** *36* (3), 322-335.
12. Vasta, G. R., *Nat Rev Micro* **2009,** *7* (6), 424-438.
13. Iacobelli, S.; Sismondi, P.; Giai, M.; D'Egidio, M.; Tinari, N.; Amatetti, C.; Di Stefano, P.; Natoli, C., *British Journal of Cancer* **1994,** *69* (1), 172-176.
14. Ulmer, T. A.; Keeler, V.; Loh, L.; Chibbar, R.; Torlakovic, E.; André, S.; Gabius, H.-J.; Laferté, S., *Journal of Cellular Biochemistry* **2006,** *98* (5), 1351-1366.
15. Lin, T.-W.; Chang, H.-T.; Chen, C.-H.; Chen, C.-H.; Lin, S.-W.; Hsu, T.-L.; Wong, C.-H., *Journal of the American Chemical Society* **2015,** *137* (30), 9685-9693.
16. Lee, Y. C., *Journal of Biochemistry* **1997,** *121* (5), 818-825.
17. Bemis, G. W.; Murcko, M. A., *Journal of Medicinal Chemistry* **1996,** *39* (15), 2887-2893.
18. Jenkins, J. L.; Glick, M.; Davies, J. W., *Journal of Medicinal Chemistry* **2004,** *47* (25), 6144-6159.
19. Schneider, G.; Schneider, P.; Renner, S., *QSAR & Combinatorial Science* **2006,** *25* (12), 1162-1171.
20. Butler, M. S.; Buss, A. D., *Biochemical Pharmacology* **2006,** *71* (7), 919-929.

21. Ge, M.; Chen, Z.; Russell, H.; Onishi; Kohler, J.; Silver, L. L.; Kerns, R.; Fukuzawa, S.; Thompson, C.; Kahne, D., *Science* **1999,** *284* (5413), 507-511.
22. Prasat, K.; Chulabhorn, M.; Somsak, R., *Current Topics in Medicinal Chemistry* **2014,** *14* (2), 239-252.
23. Nguyen, T. B.; Lozach, O.; Surpateanu, G.; Wang, Q.; Retailleau, P.; Iorga, B. I.; Meijer, L.; Guéritte, F., *Journal of Medicinal Chemistry* **2012,** *55* (6), 2811-2819.
24. Barron, S.; Murphy, P. V., *MedChemComm* **2014,** *5* (8), 1150-1158.
25. Leyden, R.; Velasco-Torrijos, T.; André, S.; Gouin, S.; Gabius, H.-J.; Murphy, P. V., *The Journal of Organic Chemistry* **2009,** *74* (23), 9010-9026.
26. Wang, G.-N.; Andre, S.; Gabius, H.-J.; Murphy, P. V., *Organic & Biomolecular Chemistry* **2012,** *10* (34), 6893-6907.
27. Andre, S.; O'Sullivan, S.; Koller, C.; Murphy, P. V.; Gabius, H.-J., *Organic & Biomolecular Chemistry* **2015,** *13* (14), 4190-4203.
28. Wolf, E.; Kim, P. S.; Berger, B., *Protein Science : A Publication of the Protein Society* **1997,** *6* (6), 1179-1189.
29. Hall, K., *Studies in History and Philosophy of Biological and Biomedical Sciences* **2011,** *42* (2), 119-128.
30. Crick, F. H. C., *Acta Crystallographica* **1953,** *6* (8-9), 689-697.
31. Bronson, D. D.; Schachat, F. H., *Journal of Biological Chemistry* **1982,** *257* (7), 3937-3944.
32. Yu, Y.; King, D.; Shin, Y., *Science* **1994,** *266* (5183), 274-276.
33. Yamamoto, D.; Li, G.-M.; Ikuta, K.; Goto, T., *Biochemical and Biophysical Research Communications* **2005,** *335* (1), 112-116.
34. Fletcher, J. M.; Boyle, A. L.; Bruning, M.; Bartlett, G. J.; Vincent, T. L.; Zaccai, N. R.; Armstrong, C. T.; Bromley, E. H. C.; Booth, P. J.; Brady, R. L.; Thomson, A. R.; Woolfson, D. N., *ACS Synthetic Biology* **2012,** *1* (6), 240-250.
35. Harbury, P. B.; Zhang, T.; Kim, P. S.; Alber, T., *Science* **1993,** *262* (5138), 1401-1407.
36. Pace, C. N.; Scholtz, J. M., *Biophysical Journal* **1998,** *75* (1), 422-427.
37. Merrifield, R. B., *Journal of the American Chemical Society* **1963,** *85* (14), 2149-2154.
38. Carpino, L. A.; Imazumi, H.; El-Faham, A.; Ferrer, F. J.; Zhang, C.; Lee, Y.; Foxman, B. M.; Henklein, P.; Hanay, C.; Mügge, C.; Wenschuh, H.; Klose, J.;

Beyermann, M.; Bienert, M., *Angewandte Chemie International Edition* **2002,** *41* (3), 441-445.

39. Myers, J. K.; Pace, C. N.; Scholtz, J. M., *Proceedings of the National Academy of Sciences* **1997,** *94* (7), 2833-2837.
40. Rowe, A. J., *Methods* **2011,** *54* (1), 157-166.
41. Shan, D.; Chen, L.; Njardarson, J. T.; Gaul, C.; Ma, X.; Danishefsky, S. J.; Huang, X.-Y., *Proceedings of the National Academy of Sciences of the United States of America* **2005,** *102* (10), 3772-3776.
42. Bock, V. D.; Hiemstra, H.; van Maarseveen, J. H., *European Journal of Organic Chemistry* **2006,** *2006* (1), 51-68.
43. Kolb, H. C.; Finn, M. G.; Sharpless, K. B., *Angewandte Chemie International Edition* **2001,** *40* (11), 2004-2021.
44. Huisgen, R., *Angewandte Chemie International Edition in English* **1963,** *2* (10), 565-598.
45. Tornøe, C. W.; Christensen, C.; Meldal, M., *The Journal of Organic Chemistry* **2002,** *67* (9), 3057-3064.
46. Rostovtsev, V. V.; Green, L. G.; Fokin, V. V.; Sharpless, K. B., *Angewandte Chemie International Edition* **2002,** *41* (14), 2596-2599.
47. Worrell, B. T.; Malik, J. A.; Fokin, V. V., *Science* **2013,** *340* (6131), 457-460.
48. (a) Falenski, J. A.; Gerling, U. I. M.; Koksch, B., *Bioorganic & Medicinal Chemistry* **2010,** *18* (11), 3703-3706; (b) Zacco, E.; Hütter, J.; Heier, J. L.; Mortier, J.; Seeberger, P. H.; Lepenies, B.; Koksch, B., *ACS Chemical Biology* **2015,** *10* (9), 2065-2072.

Contents

Chapter 3: Somatostatin peptidomimetics

3.1 Introduction

Controlled cellular signalling pathways are a prerequisite for life. Within the milieu of signalling pathways, peptides and proteins, amongst other classes of organic compounds, are typically found as chemical modulators for single transduction. Mutations in DNA sequences or tumour growths can affect these pathways and therefore may lead to different diseases. Control of such diseases allows for therapeutic intervention. The previous chapter discussed the importance of scaffolds and scaffold design. The work carried out as part of this thesis uses peptidomimetics to mimic an endocrine hormone, somatostatin, through the stabilisation of a β-turn via a glycosylated asparagine, for the treatment of acromegaly (abnormal growth of hands, feet and facial features).

3.1.1 Peptidomimetics

A peptidomimetic is a small-protein like chain that has been designed to accommodate molecular properties to that of the native peptide/protein of interest. Peptides and proteins are involved in a range of biological functions including structure, catalysis, signaling etc. Protein and peptide biological roles are carried out ubiquitously throughout life and significantly contribute to an overall functioning organism. The demand for protein-protein interaction (PPI) inhibitors and effectors allows for a medical application.[1] The pharmacological properties, including bioavailability and biostability of certain peptides and/or proteins, make it challenging for effective drug administration.[2] Medically relevant peptides can be replaced with smaller synthetic analogues offering enhanced receptor-ligand interaction, a longer half-life, increased pharmacological properties etc. Peptidomimetics also have the ability to either promote or to suppress secondary structures that are found within the native peptide through drug design and functional group manipulation. The art of synthesising such mimics involves the investigation of a peptide's and/or protein's active site to ascertain the key residues in a the specific sequence that correlate to its biological activity.[3] An array of structural modifications can be created from the native peptide or protein, which are used as templates. These include; (i) isoteric replacements within the backbone of the peptide, (ii) side-chain substitution, (iii) amide alkylation and (iv) change of residue chirality from L to D.[4] These structural alterations of the endogenous peptides circumvent physicochemical challenges that may arise.

3.1.2 Non-peptide peptidomimetics

The Murphy group has carried out research in non-peptide peptidomimetics. This class of peptidomimetic carbohydrate scaffolds, based on β-D-mannopyranosides and 1-deoxynojirimycin, has resulted in putative ligands for their respective targets. The orthogonal display of protecting groups resembling amino acids have demonstrated activity as HIV-1 protease inhibitors in the μM region.[5,6] The grafting of key amino-acid residues onto 1-deoxynojirimycin scaffold, shown in Figure 3.1, has given rise to potent somatostatin mimics for the potential treatment of acromegaly.[7]

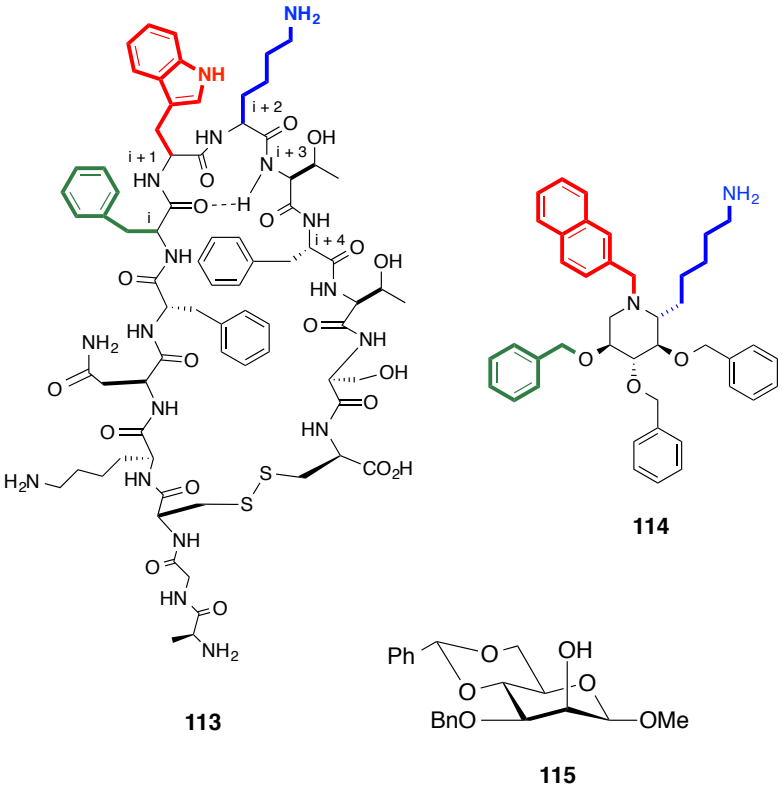

Figure 3.1 Somatostatin (**113**), its mimetic (**114**) based on 1-deoxynojirimycin scaffold and a HIV protease inhibitor **115** based on β-D-mannopyranoside.

3.1.3 Acromegaly

Abnormal growth and development by overexpression of a growth hormone by the hormone producing pituitary gland is termed acromegaly. Acromegaly is considered a rare disease with approximately 60 cases per 1 million people, however recent studies suggests acromegaly cases are increasing.[8] Symptoms typically manifest as enlarged hands and feet, however facial enlargement has also been observed. Other clinical side effects can arise including, sleep apnea and diabetes.[9] The pituitary gland is made up of somatotropic cells which normally express growth hormone (somatotropin). Adenomas (benign tumours) are

formed when these cells start to proliferate uncontrollably leading to a hormonal disorder and an imbalance. Tumours that have formed elsewhere in the body can generate growth-hormone releasing hormone that signals the release of somatotropin.[10] Due to signalling cascades, the increased somatotropic cells start to produce elevated amounts of somatotropin. This has a systematic knock on effect by increasing the concentration of somatotropin throughout the body. Somatotropin then binds and acts on growth-hormone receptors that are mainly found in the liver. Secondary messaging occurs intracellularly that triggers the synthesis of insulin-like growth factor 1 (IGF-1).[11] IGF-1 is typically found at higher levels in adolescents and less so in adults. IGF-1 is required for normal biological function and development. A higher increase in IGF-1 than normal can lead to accelerated growth and gigantism. As in most cases within the body, homeostasis keeps regulating hormonal balance and thus releases a growth hormone inhibitor (somatostatin). This endocrine inhibitor is secreted from the hypothalamus, located near to the pituitary gland, and peripheral tissues. Native somatostatin has a relatively short half-life, approximately three minutes, and low receptor specificity.[12] This has led to the design and synthesis of long half-life somatostatin analogues. One particular case showed that long term treatment with one of these analogues has stabilised tumor growth, which resulted in a prolonged time to tumor progression of neuroendocrine tumours.[13]

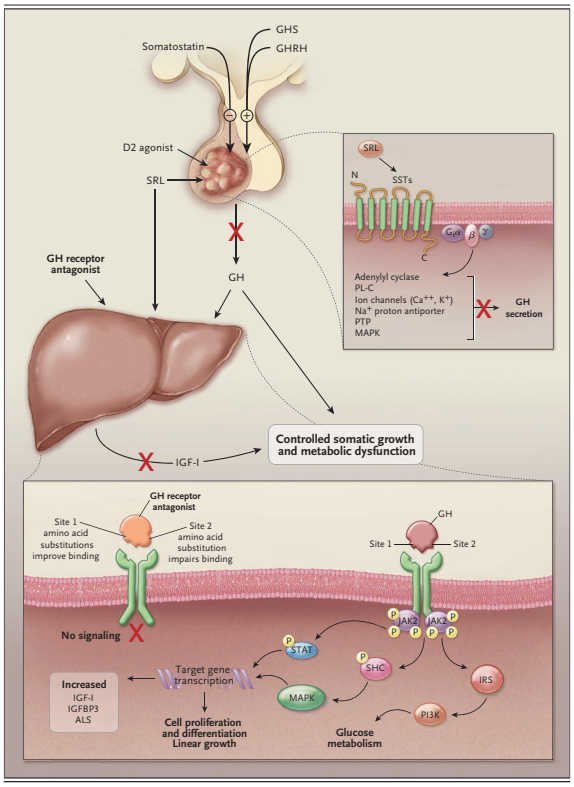

Figure 3.2 Illustration of endocrine hormone released from the pituitary gland and their respective targets. Reproduced with permission from reference 14, Copyright Massachusetts Medical Society.[14]

3.1.3.1 Somatostatin receptor subtypes

There are five somatostatin receptor (SSTR) subtypes, SSTR 1-5. These five subtypes are spread ubiquitously throughout the body including the brain, pituitary gland, stomach, gastrointestinal tract, liver and pancreas. SSTR4 however is the only receptor not found on the pituitary.[15] SSTR1 and SSTR5 compose 90-95 % of the SST receptors on the pituitary gland.[16] Each of these SST receptors are G-protein coupled receptors. When a ligand binds to the extracellular domain of the G-protein receptor, inhibition of adenyl cyclase occurs. This stops the formation of cyclic adenosine monophosphate (cAMP), a secondary messenger, which subsequently corresponds to a loss in signaling transduction. A reduction in intracellular Ca^{2+} also occurs and this in turn prevents exocytosis of somatotropin from the somatotropic cells.[17,18]

3.1.3.2 Approved treatments

Somatostatin endogenously exists in two forms, a 14-membered amino acid cyclic peptide and a 28-membered amino acid chain. Both peptides are cyclised through a disulphide bond. Peptidomimetics of somatostatin has given rise to proprietary therapeutics that includes octreotide (Novartis, Switzerland) and lanreotide (Ipsen, France), shown in Figure 3.3. Such analogues incorporate the active portion of somatostatin, with four key residues making up the pharmacophoric portion. These residues are connected from N to C terminus, Phe-Trp-Lys-Tyr.[19] Clinically approved drugs have omitted certain amino acids, performed minor isoteric substitution to key residues and changed the chirality of native L-Trp to D-Trp. This has given rise to potent compounds, which have a longer half-life compared to the parent molecule somatostatin.[12]

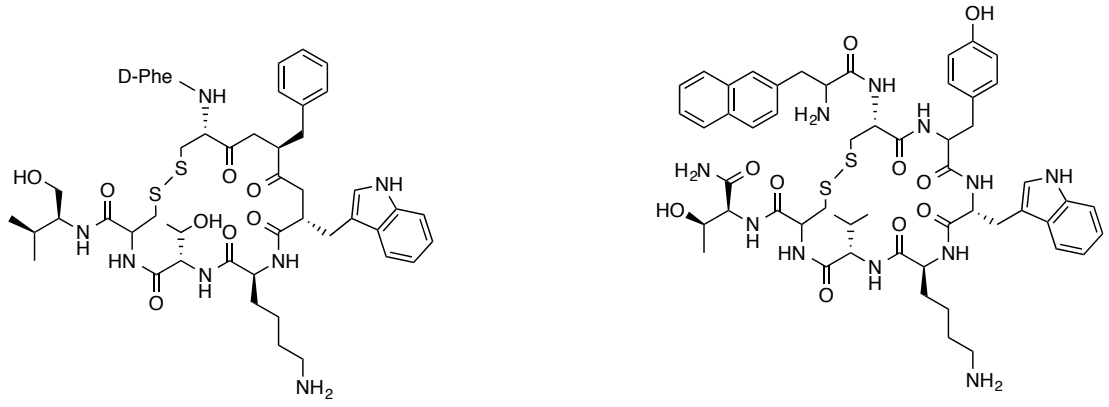

Figure 3.3 Approved drugs used to treat acromegaly.

These truncated peptides offer better resistance to proteolytic cleavage and thus increase the half-life. Typically, administration is through a sub-cutaneous injection ranging from three times daily to once every four weeks. Depending on patient acceptability, other routes of administration such as oral and topical gels have arisen while still trying to maintain a long lasting therapeutic drug.[20,21]

An alternative clinical approach is targeting the blocking of somatotropin receptor antagonistically. A growth hormone receptor antagonist, pegvisomant, has shown to lower the production of IGF-1. Using somatotropin as a scaffold, pegvisomant was developed by making small mutations of amino acids in the binding site. This allowed the antagonist to have better affinity and a longer half-life than somatotropin. On binding to the growth hormone receptor, pegvisomant interferes with dimerisation of two subunits thus inhibiting signal transduction.[22]

For patients that show no therapeutic benefit when somatostatin analogues are administered, some chimeric somatostatin and dopamine hybridised compounds have been synthesised. These hybrids contain structural elements from each agonist and are called dopastatins. Activation of dopamine receptors (D2R) has shown to lower somatotropin secretion in patients with somatotropin hypersecretion.[23]

3.1.4 Secondary Structures

Endogenous somatostatin encompasses a β-turn that is required for effective binding. This secondary structure is an important structural feature that ensures that the three key residues are freely exposed to interact with their target receptor. The stabilisation of this β-turn could lead to an increased binding affinity and thus increase the potency of the bioactive compound. Secondary structures arise from hydrogen bonds between backbone amino and carbonyl groups. Here the nitrogen of the amide group acts as a hydrogen bond donor and the carbonyl group acts as a hydrogen bond acceptor. The use of hydrogen bonds allows primary structures to adopt a more stable secondary structure that is capable of subsequent biological roles for example signalling. There are three main types of secondary structures. These are α-helices, β-sheets and β-turns, all of which owe their structure to hydrogen bonding.

- **α-helix** - Peptide sequences that participate in intra-hydrogen bonding between a carbonyl group of one residue, *i*, and the amide proton from another residue that is four residues away, *i* + *4*, adopts an α-helical motif.

- **β-sheets** - Another type of secondary structure that involves inter-hydrogen bonds, once again between carbonyls and amide protons, are called β-sheets. Here, strands of linear sequenced peptides can lie parallel or anti-parallel to one another creating a sheet.

- **β-turns** – These emerge from four consecutive amino acid residues where a bond from carbonyl, *i*, interacts with the amide proton three amino acids away, *i* + *3*. β-strands fold back on themselves creating a reverse turn. This facilities hydrogen bonding to occur between the two strands.

Whilst β-turns are required for a polypeptide/protein to fold into a compact structure, they also help with ligand-receptor binding.[24] For example, as previously mentioned, somatostatin contains this β-turn structural feature that includes the key residue sequence Phe-Trp-Lys-Thr. This is illustrated in Figure 3.4.

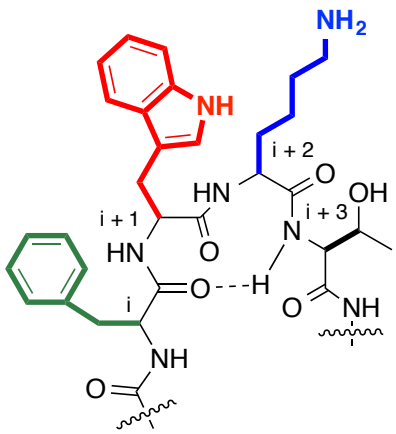

Figure 3.4 Cropped somatostatin (**113**) structure showing β-turn hydrogen bonding between *i* and *i* + *3*.

3.1.5 Objectives

The objective of this chapter was to synthesise somatostatin mimetics with the inclusion of a glycosylated asparagine. The stabilisation of a beta-turn, which is a structural feature present in somatostatin, was previously reported by the introducing a glycosylated asparagine three positions from a phenylalanine. Cyclic and non-cyclic glycosylated mimetics were developed.

3.2 Results and Discussion

As discussed in Section 3.1.1, peptidomimetics tries to capture structural elements that are needed for ligand-receptor affinity and efficacy. Along with key residues for binding, secondary structures are also important element for defined orientation and displaying of the residues in a specific way

A paper published by Kelly and co-workers[25] outlined that reverse β-turns can be stabilised with the inclusion of a glycosylated asparagine two or three places after a phenylalanine residue, *i*, through a carbohydrate-π interaction.[26] This stabilisation concept prompted the synthesis of N-glycosylated peptidomimetics of somatostatin where the glycosylated asparagine was located three places after the phenylalanine (*i* + *3*), which is one of the key residues in receptor binding.

3.2.1 Glycosylated asparagine

The synthesis started by peracetylating commercially available *N*-acetylglucosamine with freshly distilled acetyl chloride. This formed the peracetylated sugar and a chlorine, present on the anomeric position, in tandem. This α-halide was subjected to sodium azide in anhydrous DMF which gave intermediate **117**, shown in Scheme 3.1.

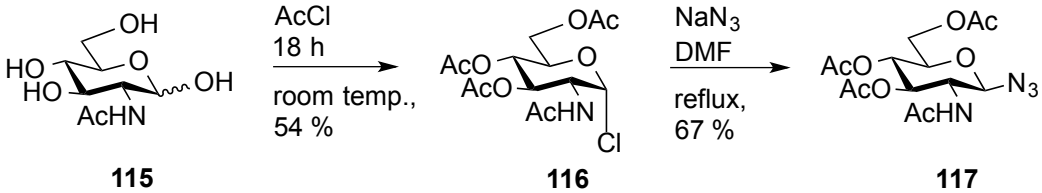

115 **116** **117**

Scheme 3.1 Synthesis of β-azide **117** from *N*-Acetylglucosamine **115**.

Reduction of the **117** with Adams catalyst afforded compound **118,** shown in Scheme 3.2. This intermediate was coupled to Fmoc-aspartic acid in which the C terminus was protected resulting in compound **119**.

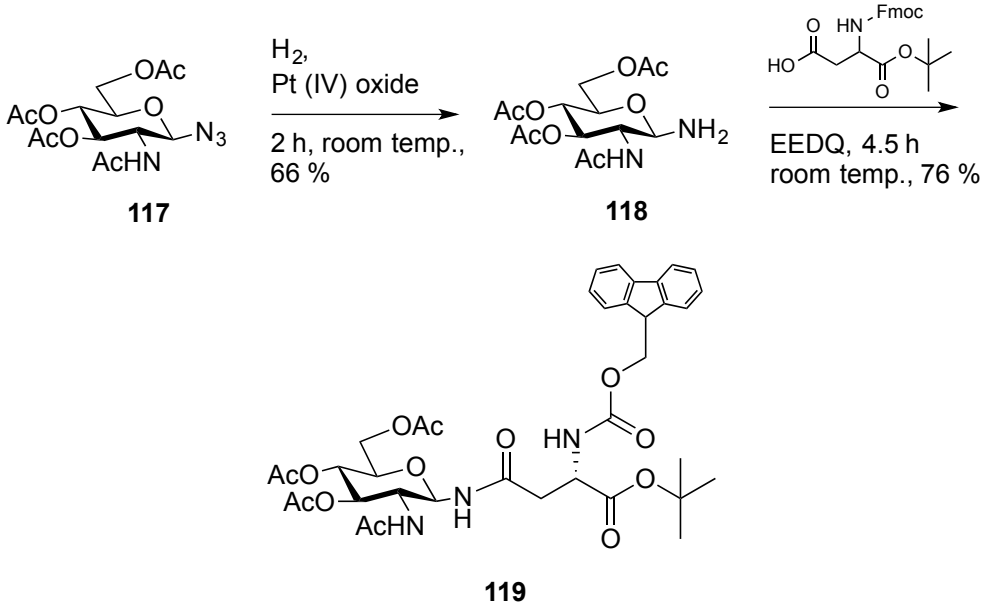

Scheme 3.2 Amide coupling of **118** to appropriately protected aspartic acid to form **119**.

Intermediate **119** was treated with trifluoroacetic acid that resulted in the glyco-amino acid building block **120** in high yield ready for use in SPPS, shown in Scheme 3.3.

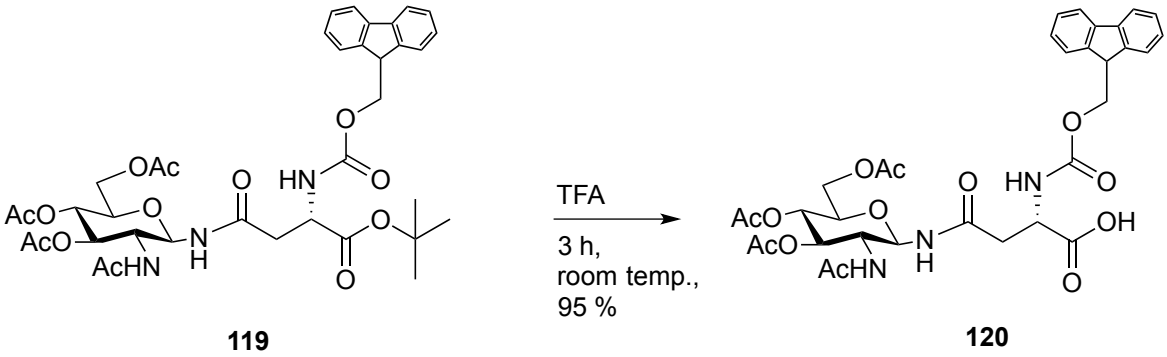

Scheme 3.3 Deprotection of *t*-butyl ester to yield glyco-amino acid **120**.

3.2.2 Linear glycosylated and non-glycosylated peptides

Linear non-glycosylated peptides (**121** and **122**) and glycosylated peptide (**124**) were synthesised using SPPS technique using Rink amide (as previously outlined in Chapter 2). *O*-(6-Chlorobenzotriazol-1-yl)-*N*,*N*,*N*′,*N*′-tetramethyluronium hexafluorophosphate

(HCTU) and DIPEA was used for each amino acid coupling along with a preactivation time. After peptide chain elongation and acetylation of the N-terminus, the peptides were cleaved from the solid support with a cleavage cocktail of TFA : thioansole : EDT : anisole (90 : 5 : 3 : 2 v/v/v/v). These were then precipitated with cold diethyl ether and subsequently non-glycosylated (**121** and **122**) peptides were purified via preparative HPLC. The fully protected glycosylated peptides **123** and **127**, after precipitation from cold diethyl ether, were subjected to freshly prepared sodium methoxide in MeOH to facilitate the removal of the acetate protecting groups. Glycosylated peptide **124** was then worked up using acidic Amberlite H^+ ion exchange resin, shown in Scheme 3.4, and purified via preparative HPLC.

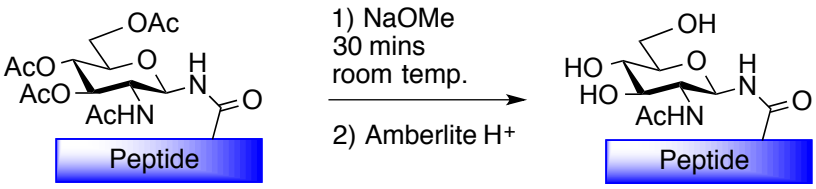

Scheme 3.4 General method for the deacetylation of glycopeptides.

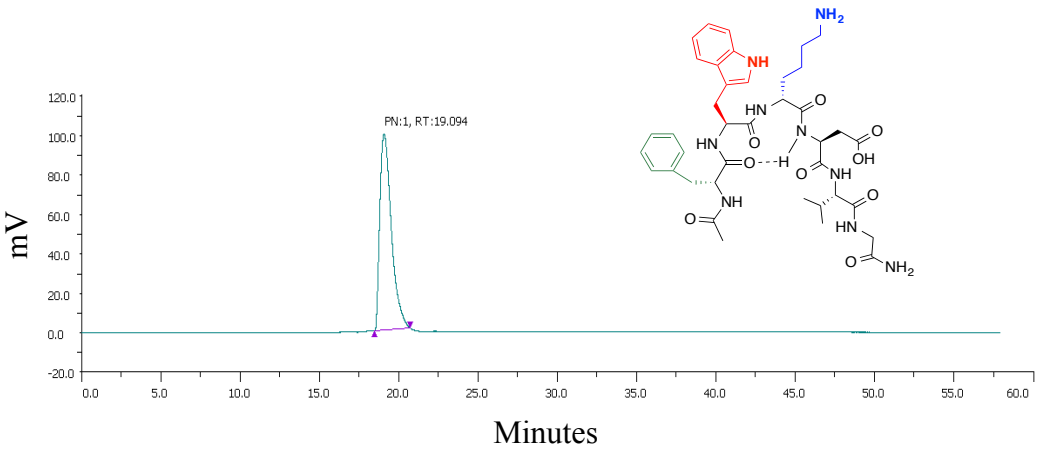

Figure 3.5 HPLC trace of purified compound **121**, retention time 19.1, with a linear gradient of H_2O (0.1 % TFA) and CH_3CN (0.1 % TFA) from 25 to 60 % of CH_3CN in 60 minutes.

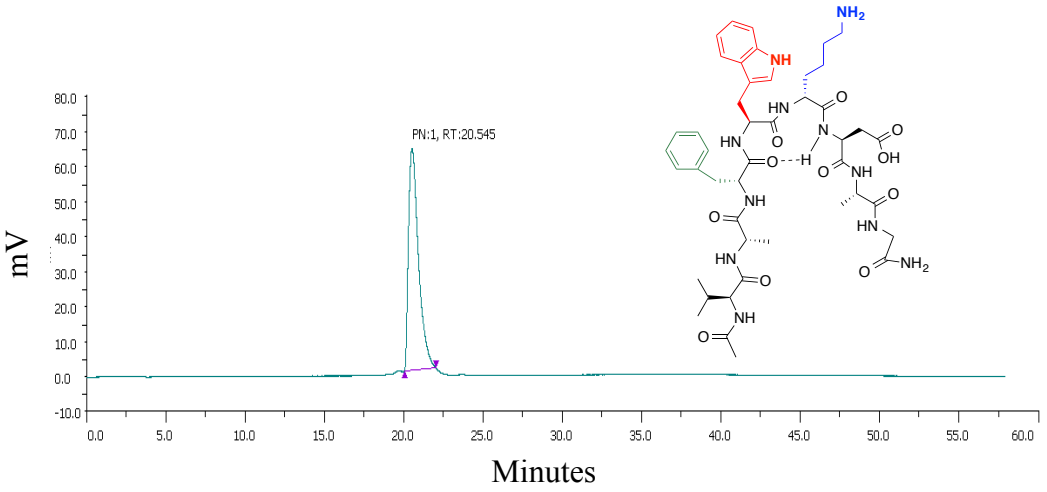

Figure 3.6 HPLC trace of purified compound **122**, retention time 20.5, with a linear gradient of H_2O (0.1 % TFA) and CH_3CN (0.1 % TFA) from 25 to 60 % of CH_3CN in 60 minutes.

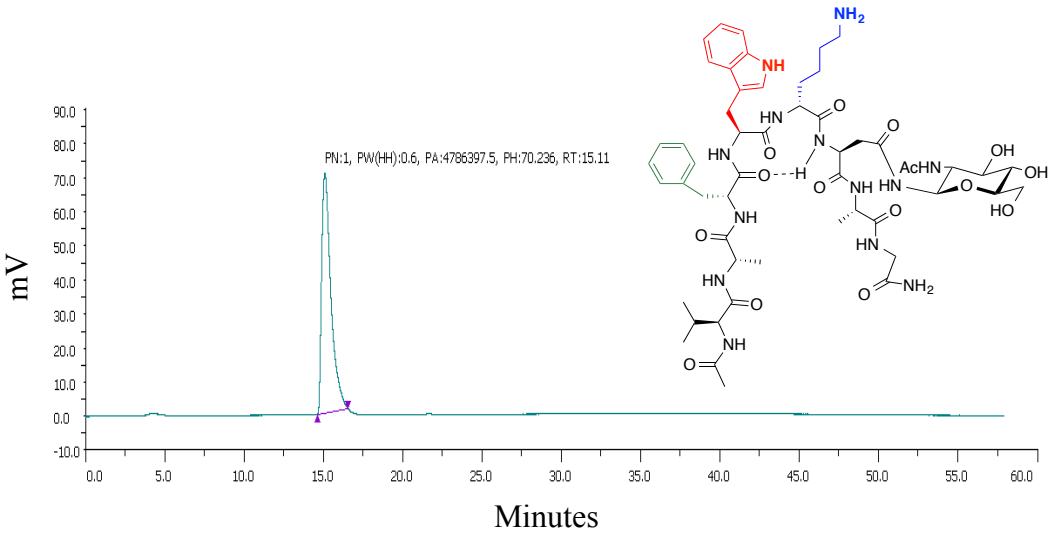

Figure 3.7 HPLC trace of purified compound **124**, retention time 15.1, with a linear gradient of H_2O (0.1 % TFA) and CH_3CN (0.1 % TFA) from 25 to 60 % of CH_3CN in 60 minutes.

3.2.3 Cyclic glycosylated and non-glycosylated peptides

Crude peptide **125** was dissolved up in H_2O with 5 % acetic acid (AcOH) and the pH was adjusted to pH 6 with $(NH_4)CO_3$. DMSO was added as an oxidant to create the disulphide linkage as shown in Scheme 3.5. A shorter retention time was observed for peptide **126** from that of the linear cysteine peptide **125**. This cyclised peptide was purified by preparative HPLC.

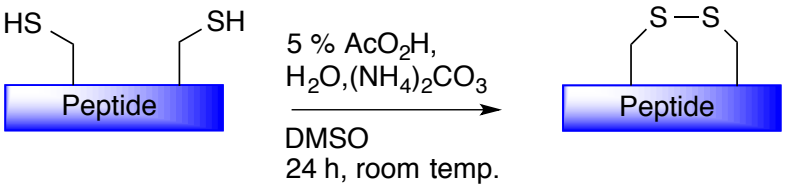

Scheme 3.5 General method for the formation of disulfide bonds.

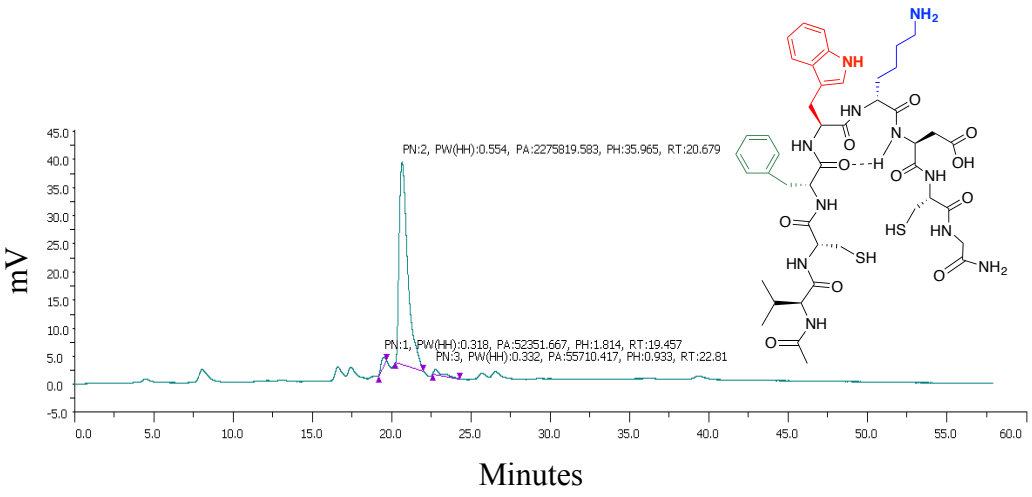

Figure 3.8 HPLC trace of crude compound **125**, retention time 20.7, with a linear gradient of H_2O (0.1 % TFA) and CH_3CN (0.1 % TFA) from 25 to 60 % of CH_3CN in 60 minutes.

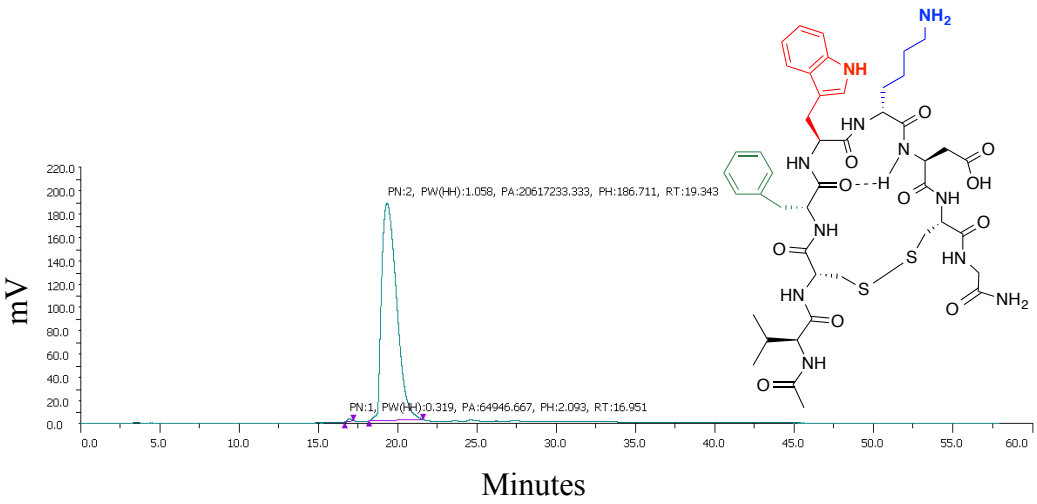

Figure 3.9 HPLC trace of purified compound **126**, retention time 19.3, with a linear gradient of H_2O (0.1 % TFA) and CH_3CN (0.1 % TFA) from 25 to 60 % of CH_3CN in 60 minutes.

3.2.3.1 Desulfurised impurity

Crude protected glycosylated peptide **127** was deacetylated using the same procedure outlined in Section 3.2.3, to form compound **128**. This however also gave rise to an impurity that was observed using mass spectrometry. A paper by Galande *et al*. outlined the desulfurisation of cyclic disulphide linked peptides under basic conditions, shown in Figure 3.10.[27] This research outlined that proton abstraction from the peptide backbone resulted in β-elimination forming a dehydroalanine residue. This residue in turn could be attacked by the remaining sulphur, through an intramolecular Michael addition reaction as shown in in Figure 3.10. This formed a thioether linkage reducing the ring size by one and a loss of -32 MW. Cyclic peptides containing cysteine residues placed at the *i* position, and *i* + n positions, were explored ranging in ring sizes from *i* + 2 to *i* + 4. In all cases of the varying ring sizes, desulfurisation was observed. The glycosylated somatostatin analogue in this case had cysteine placed at *i* and *i* + 5. This added further scope to Galande *et al*.'s paper in which desulfurisation occurs on larger ring sizes than that of which had been tested.

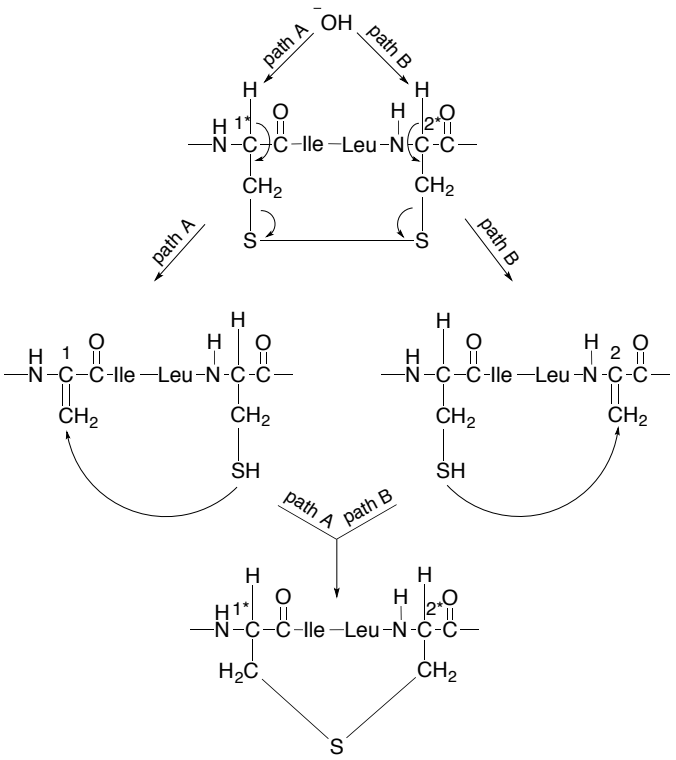

Figure 3.10 Proposed desulfurisation mechanism in which either α-proton, path A or path B, from cysteine can be abstracted leading to β-elimination and subsequent Michael addition. Adapted from reference 27 with permission. Copyright © 2003 WILEY-VCH Verlag GmbH & Co. KGaA, Weinheim.

In all cases the ring was formed first via a disulphide bond and then β-elimination occurred. As such, this prompted the degassing of the MeOH solvent to remove any oxygen present to prevent random air oxidation and hence lead to a disulphide linkage first. The deacetylation was then carried out in degassed methanol and worked up using Amberlite H^+ once again yielding **128**. No impurity was observed during mass spectrometry analysis and the linear peptide was subjected to the same oxidative conditions as before to close the ring via a disulphide linkage. This yielded the desired compound **129**.

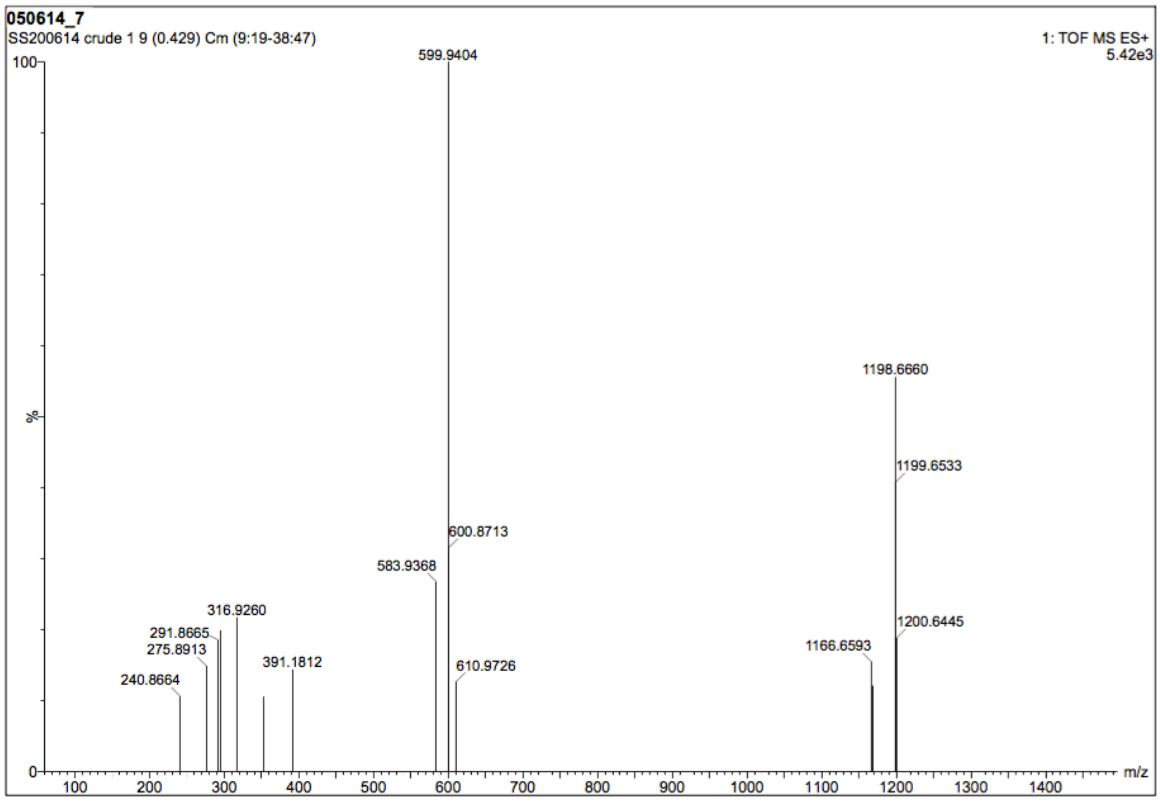

Figure 3.11 Mass spectrum showing crude glycosylated cyclic product **129** ((M+H$^+$;1198) and (M+2H)$^{2+}$;599) and the desulfurised cyclic impurity ((M+H$^+$;1166) and (M+2H)$^{2+}$;583). This spectrum shows a loss of -32 MW when non-degassed methanol was used during deacetylation.

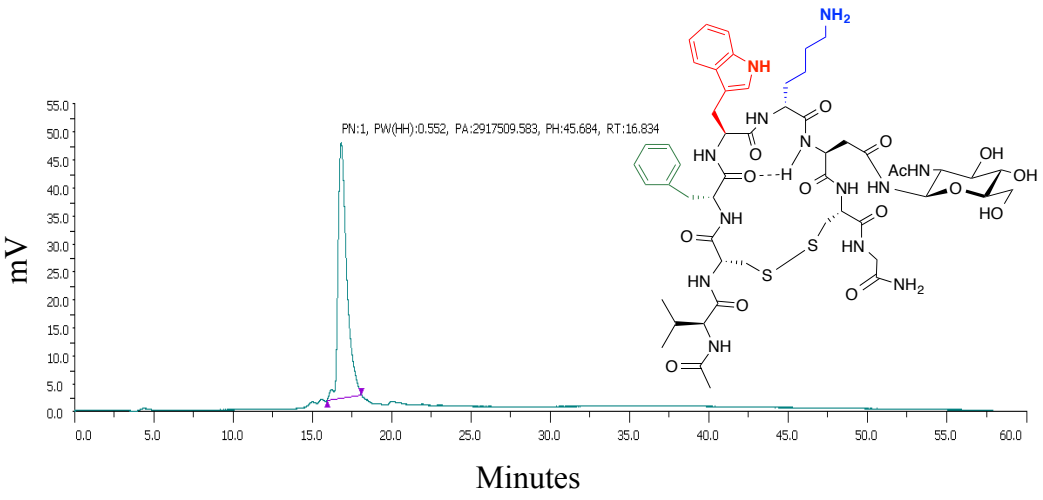

Figure 3.12 HPLC trace of purified compound **129**, retention time 16.8, with a linear gradient of H_2O (0.1 % TFA) and CH_3CN (0.1 % TFA) from 25 to 60 % of CH_3CN in 60 minutes.

3.2.4 Biological results

Compounds **124**, **126** and **129** were evaluated for their ability to inhibit the binding of radiolabelled somatostatin-14 to human SSTR4 and SSTR5 receptor subtypes *in vitro*. These assays were carried out by Cerep and the results are reported in Table 3.1. Somatostatin displayed K_i values of <2.0 nM for these receptor subtypes. Compounds **126** and **129** showed moderate affinity for SSTR4 and SSTR5 with K_i values in the μM range, however compound **124** showed no measurable affinity.

Table 3.1 Binding of compounds **126** and **129** to somatostatin receptors.

Compound	K_i [μM] hSSTR4	K_i [μM] hSSTR5
124	-	-
126	7.2	20
129	10	3.4
Somatostatin (ref)	0.00082	0.0015

3.4 Conclusion

Glycosylated-peptides **124** and **129** were successfully synthesised along with non-glycosylated peptides, **121**, **122** and **126**. Compounds **124**, **126** and **129** were selected for biological evaluation. Compound **124** showed low activity and a K_i value was not determinable. Cyclic glycosylated peptide **129** and non-glycosylated peptide **126** showed moderate activity for SSTR4 and SSTR5 somatostatin receptor subtypes. The fact that the linear glycosylated peptide showed low to no activity indicated the necessity for a cyclic scaffold and hence a cyclic peptide. Compound **129** showed to be more potent for the receptor subtype SSTR5 with a K_i of 3.4 μM where as compound **126** showed an increase in potency for the SSTR4 subtype. While the activity was moderate for both compounds **126** and **129**, the inclusion of the glycosylated asparagine with *N*-acetylglucosamine into the peptide sequence changed the receptor preference from SSTR4 to SSTR5. Further glycosylated analogues with different $i + n$ positions and different sugar moieties could be explored with a view to increase activity and selectivity for specific somatisation receptor subtypes.

Bibliography

1. Milroy, L.-G.; Grossmann, T. N.; Hennig, S.; Brunsveld, L.; Ottmann, C., *Chemical Reviews* **2014,** *114* (9), 4695-4748.
2. Antosova, Z.; Mackova, M.; Kral, V.; Macek, T., *Trends in Biotechnology* **2009,** *27* (11), 628-635.
3. Vagner, J.; Qu, H.; Hruby, V. J., *Current opinion in chemical biology* **2008,** *12* (3), 292-296.
4. Avan, I.; Hall, C. D.; Katritzky, A. R., *Chemical Society Reviews* **2014,** *43* (10), 3575-3594.
5. Murphy, P. V.; O'Brien, J. L.; Gorey-Feret, L. J.; Smith Iii, A. B., *Bioorganic & Medicinal Chemistry Letters* **2002,** *12* (13), 1763-1766.
6. Murphy, P. V.; O'Brien, J. L.; Gorey-Feret, L. J.; Smith Iii, A. B., *Tetrahedron* **2003,** *59* (13), 2259-2271.
7. Barron, S.; Murphy, P. V., *MedChemComm* **2014,** *5* (8), 1150-1158.
8. Chanson, P.; Salenave, S.; Kamenicky, P.; Cazabat, L.; Young, J., *Best Practice & Research Clinical Endocrinology & Metabolism* **2009,** *23* (5), 555-574.
9. Holdaway, I. M.; Rajasoorya, C., *Pituitary 2* (1), 29-41.
10. Biermasz, N. R.; Smit, J. W. A.; Pereira, A. M.; Frölich, M.; Romijn, J. A.; Roelfsema, F., *Pituitary* **2007,** *10* (3), 237-249.
11. Roith, D. L.; Scavo, L.; Butler, A., *Trends in Endocrinology & Metabolism* **2001,** *12* (2), 48-52.
12. Modlin, I. M.; Pavel, M.; Kidd, M.; Gustafsson, B. I., *Alimentary Pharmacology & Therapeutics* **2010,** *31* (2), 169-188.
13. Rinke, A.; Müller, H.-H.; Schade-Brittinger, C.; Klose, K.-J.; Barth, P.; Wied, M.; Mayer, C.; Aminossadati, B.; Pape, U.-F.; Bläker, M.; Harder, J.; Arnold, C.; Gress, T.; Arnold, R., *Journal of Clinical Oncology* **2009,** *27* (28), 4656-4663.
14. Melmed , S., *New England Journal of Medicine* **2006,** *355* (24), 2558-2573.
15. Patel, Y. C.; Srikant, C. B., *Trends in Endocrinology & Metabolism 8* (10), 398-405.
16. Fleseriu, M.; Delashaw, J. B.; Cook, D. M., *Neurosurgical Focus* **2010,** *29* (4), E15.
17. Toro, M. J.; Birnbaumer, L.; Redon, M. C.; Montoya, E., *Horm. Res.* **1988,** *29*, 59-64.

18. Sims, S. M.; Lussier, B. T.; Kraicer, J., *The Journal of Physiology* **1991,** *441*, 615-637.
19. Shimon, I., *Endocrine 20* (3), 265-269.
20. Melmed, S.; Popovic, V.; Bidlingmaier, M.; Mercado, M.; Lely, A. J. v. d.; Biermasz, N.; Bolanowski, M.; Coculescu, M.; Schopohl, J.; Racz, K.; Glaser, B.; Goth, M.; Greenman, Y.; Trainer, P.; Mezosi, E.; Shimon, I.; Giustina, A.; Korbonits, M.; Bronstein, M. D.; Kleinberg, D.; Teichman, S.; Gliko-Kabir, I.; Mamluk, R.; Haviv, A.; Strasburger, C., *The Journal of Clinical Endocrinology & Metabolism* **2015,** *100* (4), 1699-1708.
21. Tutuncu, Y.; Berker, D.; Isik, S.; Ozuguz, U.; Akbaba, G.; Kucukler, F. K.; Aydin, Y.; Guler, S., *Pituitary* **2011,** *15* (3), 398-404.
22. Kopchick, J. J.; Parkinson, C.; Stevens, E. C.; Trainer, P. J., *Endocrine Reviews* **2002,** *23* (5), 623-646.
23. Ferone, D.; Saveanu, A.; Culler, M. D.; Arvigo, M.; Rebora, A.; Gatto, F.; Minuto, F.; Jaquet, P., *European Journal of Endocrinology* **2007,** *156* (suppl 1), S23-S28.
24. Suat, K. K.; Seetharama, D. S. J., *Current Pharmaceutical Design* **2003,** *9* (15), 1209-1224.
25. Culyba, E. K.; Price, J. L.; Hanson, S. R.; Dhar, A.; Wong, C.-H.; Gruebele, M.; Powers, E. T.; Kelly, J. W., *Science (New York, N.Y.)* **2011,** *331* (6017), 571-575.
26. Laughrey, Z. R.; Kiehna, S. E.; Riemen, A. J.; Waters, M. L., *Journal of the American Chemical Society* **2008,** *130* (44), 14625-14633.
27. Galande, A. K.; Trent, J. O.; Spatola, A. F., *Peptide Science* **2003,** *71* (5), 534-551.

Contents

Chapter 4: Experimental data

4.1 General Experimental conditions

Compounds that are known in the literature already have been cited herein. Unless otherwise stated analytical data e.g.^{1}H NMR and/or ^{13}C NMR, obtained during this thesis work has been found to be in agreement with previously published data.

NMR spectra were recorded with 500 & 600 MHz Varian spectrometers. Chemical shifts are reported relative to $CDCl_3$ (δ 7.26) or CD_3OD (δ 3.31) or DMSO (δ 2.50) for ^{1}H and $CDCl_3$ (δ 77.16) or CD_3OD (δ 49.00) or DMSO (δ 39.52) for ^{13}C. NMR spectra were processed and analysed using MestReNova software. ^{1}H NMR signals were assigned with the aid of gCOSY and TOCSY. ^{13}C NMR signals were assigned with the aid of DEPT, gHSQC and/or gHMBC. Coupling constants are reported in Hertz, with all *J* values reported uncorrected. Low and high resolution mass spectra were measured on a Waters LCT Premier XE Spectrometer, measuring in both positive and/or negative mode as, using MeCN, H_2O and/or MeOH as solvent. FT-IR spectra were recorded with a Perkin Elmer Spectrum 100 FTIR Spectrometer with a polarized UATR (Universal Attenuated Total Reflectance) accessory. Optical rotations were determined at the sodium D line at 20°C with a Schmidt & Haensch Unipol L 1000 polarimeter, using the solvent indicated (i.e. $CHCl_3$). Thin layer chromatography (TLC) was performed on aluminium sheets precoated with silica gel 60 (HF254, E. Merck) and spots visualized by UV and heating with H_2SO_4-EtOH (1:20), or cerium molybdate. Flash chromatography was carried out with silica gel 60 (0.040-0.630 mm, E. Merck or Aldrich) and using a stepwise solvent polarity gradient (starting with the conditions indicated in each case and increasing the polarity as required). Chromatography solvents, Petroleum ether (fraction with b.p. 40 - 60°C), EtOAc, CH_2Cl_2 and MeOH were used as obtained from suppliers (Fisher Scientific and Sigma-Aldrich). Reverse phase chromatography was carried out with C18-reversed phase silica gel (100 Å pore size, Fluka) The MeCN used was HPLC grade and used as obtained from suppliers (Lab-Scan), while the H_2O used was distilled. Reactions solvents for anhydrous conditions were obtained from a Pure SolvTM Solvent Purification System.

4.2 Experimental data - Chapter 1

(4*R*,5*S*,6*S*,*Z*)-5-((*tert*-butyldimethylsilyl)oxy)-6-methoxy-2,4-dimethylocta-2,7-dien-1-ol (14)[1]

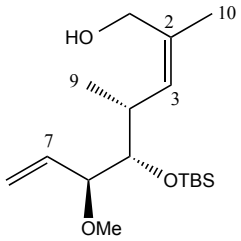

DIBAL (16.1 mL, 16.1 mmol, 1.0 M solution in hexane) was added to a solution of compound **86** (1.64 g, 4.60 mol) in anhydrous DCM (200 mL) at -78 °C. The resulting solution was stirred at -78 °C for 5 h. The reaction was quenched with saturated aqueous potassium sodium tartrate (50 mL), diluted with DCM (40 mL) and was vigorously stirred at room temperature for 3 h to break up the emulsion. The aqueous phase was extracted with DCM (4 × 50 mL). The organic portion was dried over Na_2SO_4 and the solvent was removed *in vacuo*. Chromatography (Petroleum ether/EtOAc, 10:1) afforded the title compound (1.23 g, 85 %) as a colourless oil.

^{1}H NMR (500 MHz, Chloroform-d) δ 5.70 (ddd, *J* = 17.5, 10.6, 7.4 Hz, 1H, H-7), 5.32 – 5.23 (m, 3H, H-8 and H-3, overlapping peaks), 4.12 (d, *J* = 11.8 Hz, 1H, H-1a), 4.00 (d, *J* = 11.9 Hz, 1H, H-1b), 3.51 – 3.41 (m, 2H, H-6 and H-5, overlapping peaks), 3.22 (s, 3H, OMe), 2.66 (dqd, *J* = 10.1, 6.8, 3.4 Hz, 1H, H-4), 1.79 (d, *J* = 1.4 Hz, 3H, H-10), 1.65 (br s, 1H, OH), 0.93 – 0.90 (m, 12H, H-9 and TBS group (3 x CH_3), overlapping peaks), 0.06 (s, 3H, CH_3), 0.04 (s, 3H, CH_3).

^{13}C NMR (126 MHz, Chloroform-d) δ 135.3 (C-7), 133.3 (C-3), 133.2 (C-2), 118.7 (C-8), 86.1 (C-6 or C-5), 78.5 (C-6 or C-5), 62.0 C-1), 56.3 (O*C*H$_3$), 34.4 (C-4), 26.3 (C(*C*H$_3$)$_3$), 21.7 (CH$_3$ C-10), 18.7 (*C*(CH$_3$)$_3$), 15.5 (C-9), -3.7 (Si*C*H$_3$), -4.5 (Si*C*H$_3$).
IR (ATR) cm^{-1}: 3365, 2930, 1250, 1079, 830, 774

ESI/MS$^-$ (*m/z*) (M+Na$^+$); 337.2 HRMS-ESI: cacld for $C_{17}H_{34}O_3NaSi$: 337.2175; Found 337.2173.

(7*E*,9*S*,10*S*,11*R*,12*Z*)-10-hydroxy-9-methoxy-11,13-dimethylazacyclo-tetradeca-7,12-dien-2-one (43)[2]

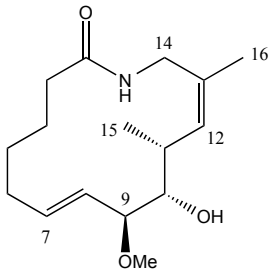

Compound **87** (33 mg, 0.083 mmol) was dissolved up in THF (2 mL) and transferred to a plastic falcon tube. HF in pyridine (70 %, 220 µL) was carefully added dropwise and the resulting mixture was stirred for 24 h at room temperature. The temperature of the reaction vessel was reduced to 0 °C and methoxytrimethylsilane (2.5 mL, 18.1 mmol) was added dropwise to quench the reaction. The newly formed mixture was stirred for a further 30 min at room temperature. The mixture was concentrated and flash chromatography (EtOAc, 100 %) afforded the title compound (20.7 mg, 89 %) as a clear oil.

^{1}H NMR (500 MHz, Chloroform-d) δ 5.76 (ddd, *J* = 15.1, 8.6, 6.0 Hz, 1H, H-7), 5.67 (d, *J* = 10.1 Hz, 1H, H-12), 5.24 (dd, *J* = 15.8, 7.5 Hz, 1H, H-8), 5.11 (br s, 1H, NH), 3.92 (dd, *J* = 13.7, 4.3 Hz, 1H, H-14a), 3.49 (dd, *J* = 13.7, 4.4 Hz, 1H, H-14b), 3.44 (apt t, *J* = 9.2, 7.5 Hz, 1H, H-9), 3.35 – 3.29 (m, 4H, OMe and H-10, overlapping peaks), 2.89 (s, 1H, OH), 2.59 – 2.51 (m, 1H, H-11), 2.33 – 2.23 (m, 2H, H-6a and H-3a, overlapping peaks), 2.18 – 2.10 (m, 1H, H-3b), 1.98 – 1.88 (m, 1H, H-6b), 1.77 (d, *J* = 1.5 Hz, 3H, H-16), 1.63 – 1.51 (m, 3H, H-4 and H-5a), 1.41 – 1.32 (m, 1H, H-5b), 0.95 (d, *J* = 6.8 Hz, 3H, H-15).

^{13}C NMR (126 MHz, Chloroform-d) δ 173.5 (C-2), 135.7 (C-7), 133.9 (C-12), 130.1 (C-13), 128.9 (C-8), 83.4 (C-9), 76.6 (C-10), 56.6 (O*C*H$_3$), 41.6 (C-14), 36.1 (C-3), 32.4 (C-11), 30.0 (C-6), 27.2 (C-5), 25.0 (C-4), 24.6 (C-16), 13.2 (C-15).

IR (ATR) cm^{-1}: 3282, 2930, 1635, 1535, 1257, 978, 658

ESI/MS$^-$ (*m/z*) (M+Na$^+$); 304.2 HRMS-ESI: cacld for $C_{16}H_{27}NO_3Na$: 304.1889; Found 304.1893.

$[\alpha]_D$ +88.1° (*c* 0.66, $CHCl_3$) obtained for **43**;

$[\alpha]_D$ +101.3° (*c* 1.00, $CHCl_3$)[2]

The alpha D obtained shows an e.e of ~88 % when compared to the alpha D reported by Danishefsky and co-workers.

(*S*)-3-hydroxy-2-methylpropyl benzoate (48)[1]

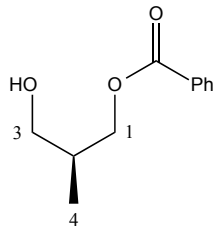

Diethyl Zinc (1 M) (9.4 mL, 9.40 mmol) was added dropwise to a solution of (*S*,*S*)-(+)-2,6-Bis[2-(hydroxydiphenylmethyl)-1-pyrrolidinyl-methyl]-4-methylphenol (3 g, 4.70 mmol) in anhydrous toluene (17 mL) under an N_2 environment whilst stirring. This solution was stirred for 1 h at room temperature and then stored in the fridge at 4 °C. Anhydrous toluene (560 mL) was added to a flame dried 1 Ltr round bottom flask containing vinyl benzoate (65 mL, 469.4 mmol) and compound 47 (8.34 mL, 93.9 mmol) at room temperature. The reaction flask was lowered to -70 °C. The stock solution of chiral catalyst, from above, was added dropwise to the reaction flask under positive N_2 pressure via cannula under stirring. The contents were stirred at this temperature for 15 min and allowed to warm gradually to – 20 °C whereupon they were stirred for 48 h at this temperature. The solvent was removed under diminished pressure. Flash chromatography (Petroleum Ether/EtOAc, 100:1) gave the desired title compound (12.5 g, 69 %) as a yellow oil.

^{1}H NMR (500 MHz, Chloroform-d) δ 8.04 (dd, *J* = 8.4, 1.3 Hz, 2H, ArH), 7.59 – 7.55 (m, 1H, ArH), 7.47 – 7.43 (m, 2H, ArH), 4.39 (dd, *J* = 11.1, 5.1 Hz, 1H, H-1a), 4.31 (dd, *J* = 11.1, 6.4 Hz, 1H, H-1b), 3.67 – 3.54 (m, 2H, H-3), 2.19 – 2.09 (m, 1H, H-2), 2.02 (t, *J* = 5.6 Hz, 1H, OH), 1.05 (d, *J* = 7.0 Hz, 3H, H-4).

^{13}C NMR (126 MHz, Chloroform-d) δ 167.2 (Ar*C*H), 133.2 (Ar*C*H), 130.2 (Ar*C*H), 129.8 (Ar*C*H), 128.6 (Ar*C*H), 66.6 (C-1), 64.6 (C-3), 35.9 (C-2), 13.8 (C-4).

IR (ATR) cm^{-1}: 3422, 2964, 1716, 1271, 707

(*R*)-2-methyl-3-oxopropyl benzoate (49)[1]

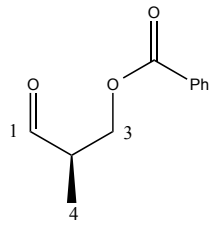

Compound **48** (12.51 g, 64.5 mmol) was dissolved in anhydrous DCM (110 mL). To this reaction mixture was added BAIB (22.8 g, 70.8 mmol) and the reaction was stirred for 10 min at room temperature. TEMPO (1.01g, 6.46 mmol) was subsequently added and the mixture was vigorously stirred for 3 h. The mixture was quenched with saturated aqueous NH_4Cl (160 mL). The organic phase was separated and the aqueous phase was back extracted with DCM (2 x 100 mL). The combined organic layers were dried over Na_2SO_4. The solution was filtered and reduced under diminished pressure. The residue was purified by chromatography (Petroleum Ether/EtOAc, 30:1) and gave the title compound (9.3 g, 75 %) as a yellow oil.

^{1}H NMR (500 MHz, Chloroform-d) δ 9.79 (d, *J* = 1.3 Hz, 1H, H-1), 7.99 (dd, *J* = 8.3, 1.4 Hz, 2H, ArH), 7.56 (t, *J* = 7.5 Hz, 1H, ArH), 7.43 (t, *J* = 7.8 Hz, 2H, ArH), 4.58 – 4.51 (m, 2H, H-3), 2.90 – 2.81 (m, 1H, H-2), 1.25 (d, *J* = 7.2 Hz, 3H, H-4).

^{13}C NMR (126 MHz, Chloroform-d) δ 202.1 (C-1), 166.4 (Ar*C*H), 133.3 (Ar*C*H), 129.7 (Ar*C*H), 128.5 (Ar*C*H), 64.1 (C-3), 46.0 (C-2), 10.8 C-4).
IR (ATR) cm^{-1}: 2969, 1720, 1271, 711

(2*R*,3*S*,4*S*)-4-methoxy-2-methylhex-5-ene-1,3-diol (52)[1]

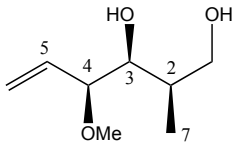

Sec-Butyllithium in cyclohexane (52 mL, 65.5 mmol, 1.26 M) was added to a solution of allyl methyl ether (7.7 mL, 82.0 mmol) in THF (113 mL) at -78°C over the course of 30 min under stirring in an N_2 inert environment. The mixture was stirred at -78 °C for a further 40 min. (+)-*B*-methoxydiisopinocampheylborane (24.2 g, 76.5 mmol) in THF (115 mL) was added dropwise through a cannula. The reaction mixture was stirred at -78 °C for 1.5 h, then boron trifluoride diethyl etherate (12.5 mL, 101.3 mmol) was added slowly at -78 °C. After this, a solution of compound **49** (9.34 g, 48.6 mmol) in THF (113 mL) was added via cannula, and the mixture was stirred at -78.8 °C for a further 28 h. Aqueous NaOH (1 M, 33 mL) was added followed by H_2O_2 (30 %, 33 mL). The resulting biphasic mixture was allowed to slowly equilibrate to room temperature. After stirring for an additional 16 h, the mixture was diluted with diethyl ether and the organic layer was separated and washed with saturated aqueous NH_4Cl. The organic portion was dried over Na_2SO_4 and the solvent was removed under reduced pressure. Flash chromatography (Petroleum Ether/EtOAc, 6:1) afforded a diastereomeric mixture of **50** and **51** including a side product pinenol (total weight = 32.2 g), which was used directly in the next deprotection step. The mixture of compounds (32.2 g) was dissolved in anhydrous methanol (100 mL), K_2CO_3 (7.4 g, 53.5 mmol) was added and the mixture was stirred at room temperature for 64 h. The solvent was removed under reduced pressure and the residue was taken up in a mixture of H_2O and EtOAc (200 mL), and the organic layer was isolated. The aqueous layer was further extracted with EtOAc (10 x 100mL) and the combined organic extracts were dried over Na_2SO_4. The solvent was removed under reduced pressure. The residue was purified by chromatography (Petroleum Ether/EtOAc,

2:1) to give a 7.8:1 mixture of desired title compound **52** and incorrect diastereomer **53** (4.20 g, 54 %, yield is based from the starting compound **49**) as a colourless oil.

^{1}H NMR (500 MHz, Chloroform-d) δ 5.58 (ddd, *J* = 17.1, 10.6, 8.3 Hz, 1H, H-5), 5.37 – 5.32 (m, 2H, H-6), 3.70 (d, *J* = 8.5 Hz, 2H, H-3 and H-1a, overlapping peaks), 3.63 (dd, *J* = 10.8, 6.2 Hz, 1H, H-1b), 3.49 (t, *J* = 8.3 Hz, 1H, H-4), 3.31 (s, 3H, OMe), 2.93 (s, 1H, OH), 2.53 (s, 1H, OH), 1.79 – 1.72 (m, 1H, H-2), 0.94 (d, *J* = 7.0 Hz, 3H, H-7).

^{13}C NMR (126 MHz, Chloroform-d) δ 134.4 (C-5), 120.5 (C-6), 85.1 (C-4), 75.5 (C-3), 67.3 (C-1), 56.4 (O*C*H$_3$), 35.8 (C-2), 9.7 (C-7).

IR (ATR) cm^{-1}: 3387, 2879, 1642, 1088, 1060, 990, 927

ESI/MS^{-} (*m/z*) (M+Na^{+}); 183.1 HRMS-ESI: cacld for $C_8H_{16}O_3Na$: 183.0997; Found 183.0988.

(2*R*,3*S*,4*S*)-3-((*tert*-butyldimethylsilyl)oxy)-4-methoxy-2-methylhex-5-en-1-ol (54)[1]

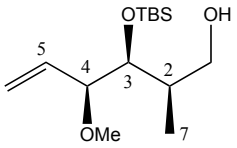

The diol mixture **52** and **53** (4.2 g, 26.2 mmol) was dissolved in anhydrous DCM (250 mL) and treated with TEA (11 mL, 78.9 mmol) and TBSOTf (14.5 mL, 63.1 mmol) at 0 °C. The reaction mixture was stirred at 0 °C for 2 h and quenched with saturated aqueous NH_4Cl. The aqueous layer was extracted with DCM (2 x 15 mL). The combined organic layers were dried over Na_2SO_4, filtered and concentrated under reduced pressure. The crude residue was taken up in anhydrous methanol (200 mL) and lowered to 0 °C. To this mixture was added *p*-TSA (0.5 g, 2.63 mmol). The flask was allowed to warm up to room temperature and stirred for 1 h. The reaction was quenched with TEA (330 µL) to pH 7. The reaction mixture was concentrated and purified by flash chromatography (Petroleum Ether/EtOAc, 10:1) to yield the title compound (4.3 g, 68 %, theoretical yield calculated from ratio of desired diastereomer 7.8:1) as a colourless oil.

^{1}H NMR (500 MHz, Chloroform-d) δ 5.67 (ddd, *J* = 17.2, 10.5, 7.9 Hz, 1H, H-5), 5.31 – 5.23 (m, 2H, H-6), 3.74 (dd, *J* = 6.3, 3.7 Hz, 1H, H-3), 3.60 – 3.54 (m, 1H, H-1a, overlapping peaks), 3.54 – 3.49 (m, 2H, H-1b and H-4), 3.26 (s, 3H, OMe), 2.12 (s, 1H, OH), 1.85 – 1.76 (m, 1H, H-2), 0.89 (s, 9H, TBS group (3 x CH_3)), 0.86 (d, *J* = 6.9 Hz, 3H, H-7), 0.08 (s, 3H, CH_3), 0.07 (s, 3H, CH_3).

^{13}C NMR (126 MHz, Chloroform-d) δ 135.0 (C-5), 118.9 (C-6), 86.0 (C-4), 75.4 (C-3), 65.8 (C-1), 56.4 (O*C*H_3), 38.5 (C-2), 26.2 (C(*C*H_3)$_3$), 18.6 (*C*(CH_3)$_3$), 11.4 (C-7), -3.8 (Si*C*H_3), -4.8 (Si*C*H_3).

IR (ATR) cm^{-1}: 3356, 2929, 1033, 928, 828, 773

ESI/MS$^-$ (*m/z*) (M+ACN+Na$^+$); 338.2 HRMS-ESI: cacld for $C_{16}H_{33}O_3NaSi$: 338.2127; Found 338.2111.

(2*S*,3*S*,4*S*)-3-((*tert*-butyldimethylsilyl)oxy)-4-methoxy-2-methylhex-5-enal (55)[1]

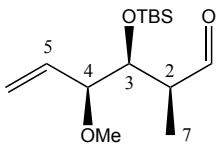

Pyridine (0.94 mL, 11.6 mmol) and DMP (1.86 g, 4.39 mmol) were sequentially added to a solution of compound **54** (1.0 g, 3.65 mmol) in DCM (50 mL) at 0 °C. The solution was stirred at room temperature for 16 h and quenched with saturated aqueous $NaHCO_3$ and $Na_2S_2O_3$ (1:1, 100 mL). After vigorous stirring for 1.5 h, the separated aqueous layer was extracted with DCM (3 x 80 mL). The combined organic layers was washed with saturated brine and dried over Na_2SO_4. The solvent was removed under reduced pressure. The residue was purified by flash chromatography (Petroleum Ether/EtOAc, 20:1) to give the title compound (0.81 g, 82 %) as a colourless oil.

^{1}H NMR (500 MHz, Chloroform-d) δ 9.72 (s, 1H, H-1), 5.69 (ddd, *J* = 17.5, 10.5, 7.8 Hz, 1H, H-5), 5.33 – 5.27 (m, 2H, H-6), 4.12 (dd, *J* = 6.0, 3.8 Hz, 1H, H-3), 3.51 (dd, *J* = 7.7, 6.0 Hz, 1H, H-4), 3.22 (s, 3H, OMe), 2.43 (apt qd, *J* = 6.9, 3.8 Hz, 1H, H-2), 1.07 (d, *J* = 7.0 Hz, 3H, H-7), 0.86 (s, 9H, TBS group (3 x CH_3)), 0.08 (s, 3H, CH_3), 0.06 (s, 3H, CH_3).

^{13}C NMR (126 MHz, Chloroform-d) δ 203.8 (C-1), 134.9 (C-5), 119.4 (C-6), 84.9 (C-4), 74.6 (C-3), 56.5 (O*C*H$_3$), 49.6 (C-2), 26.0 (C(*C*H$_3$)$_3$), 18.4 (*C*(CH$_3$)$_3$), 8.3 (C-7), -4.0 (Si*C*H$_3$), -4.9 (Si*C*H$_3$).

IR (ATR) cm^{-1}: 2930, 1727, 932, 832, 777

ESI/MS$^-$ (*m/z*) (M+Na$^+$); 295.2 HRMS-ESI: cacld for $C_{14}H_{28}O_3NaSi$: 295.1705; Found 295.1692.

ethyl 2-(diphenoxyphosphoryl)acetate (57)[3]

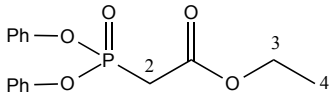

Diphenyl phosphite (2.25 mL, 11.8 mmol) was dissolved in anhydrous DCM (10 mL). The solution was lowered to 0 °C and TEA (1.97 mL, 14.1 mmol) was added dropwise and stirred for 10 min. Ethyl bromoacetate (1.16 mL, 10.5 mmol) was added dropwise at 0 °C. After the addition, the mixture was allowed to warm to room temperature and stirred for 3 h. The reaction was quenched with H_2O (20 mL) and the organic layer was separated. The aqueous layer was extracted with DCM (2 x 20 mL). The combined organic layers were extracted with H_2O (2 x 20 mL) and finally extracted with brine (20 mL). The organic layer was dried over Na_2SO_4 and concentrated. Flash chromatography (Petroleum Ether/EtOAc, 4:1) afforded the title product (1.63 g, 49 %).

^{1}H NMR (500 MHz, Chloroform-d) δ 7.34 (ddd, *J* = 8.8, 7.3, 0.6 Hz, 4H, ArH), 7.25 – 7.17 (m, 6H, ArH), 4.23 (q, *J* = 7.1 Hz, 2H, H-3), 3.26 (apt d, *J* = 21.6 Hz, 2H, H-2), 1.28 (t, *J* = 7.1 Hz, 3H, H-4).

^{13}C NMR (126 MHz, Chloroform-d) δ 164.9 (Ar*C*H), 164.9 (Ar*C*H), 150.2 (Ar*C*H), 150.1 (Ar*C*H), 130.0 (Ar*C*H), 125.7 (Ar*C*H), 120.8 (Ar*C*H), 120.8 (Ar*C*H), 62.1 (C-3), 34.3 (C-2), 14.2 (C-4).

IR (ATR) cm^{-1}: 2984, 1735, 1283,1208, 759

ESI/MS$^-$ (*m/z*) (M+Na$^+$); 384.1 HRMS-ESI: cacld for $C_{18}H_{20}O_5NaP$: 384.0977; Found 384.0990.

ethyl 2-(diphenoxyphosphoryl)butanoate (58)

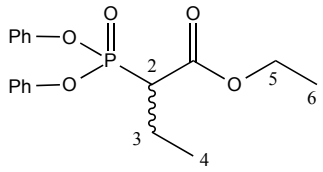

To a solution of compound **57** (1.62g, 5.06 mmol) in DMSO (6 mL) at 15 °C was added NaH (60 % dispersion in mineral oil, 200 mg, 5.0 mmol) portionwise. The mixture was stirred at 15 °C for 25 min. Ethyl iodide (0.88 mL, 10.9 mmol) was added at room temperature and the resulting mixture was stirred for 1.5 h. The reaction was quenched with saturated aqueous NH_4Cl (40 mL). The aqueous layer was separated and back extracted with EtOAc (3 x 20 mL). The combined organics were washed with H_2O (2 x 20 mL) and dried over Na_2SO_4. The solution was concentrated and purified via flash chromatography (Petroleum Ether/EtOAc, 8:1) to yield the title compound (0.92 g, 52 %) as a yellow oil.

^{1}H NMR (500 MHz, Chloroform-d) δ 7.34 – 7.28 (m, 4H, ArH), 7.22 – 7.14 (m, 6H, ArH), 4.30 – 4.20 (m, 2H, H-5), 3.19 (ddd, *J* = 22.5, 10.6, 4.2 Hz, 1H, H-2), 2.26 – 2.07 (m, 2H, H-3), 1.28 (t, *J* = 7.1 Hz, 3H, H-6), 1.07 (dt, *J* = 7.3, 0.9 Hz, 3H, H-4).

^{13}C NMR (126 MHz, Chloroform-d) δ 168.3 (Ar*C*H), 168.3 (Ar*C*H), 150.5 (Ar*C*H), 150.4 (Ar*C*H), 129.9 (Ar*C*H), 125.4 (Ar*C*H), 125.4 (Ar*C*H), 125.4 (Ar*C*H), 120.8 (Ar*C*H), 120.7 (Ar*C*H), 61.9 (C-5), 47.5 (C-2), 20.9 (C-3), 14.3 (C-6), 13.2 (C-4).

ESI/MS$^-$ (*m/z*) (M+Na$^+$); 412.1 HRMS-ESI: cacld for $C_{20}H_{24}O_5NaP$: 412.1290; Found 412.1299.

ethyl 2-(diphenoxyphosphoryl)propanoate (59)[4]

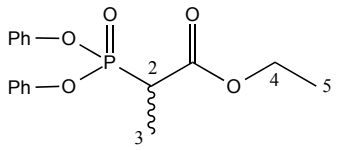

To a solution of compound **57** (9.34 g, 29.2 mmol) in DMSO (28.6 mL) at 15 °C was carefully added NaH (60 % dispersion in mineral oil, 1.16 g, 29.0 mmol) portionwise. The mixture was stirred at 15 °C for 25 min. Methyl iodide (3.8 mL, 61.0 mmol) was added at 0 °C and the resulting mixture was stirred for 2 h. The reaction was quenched with saturated aqueous H_2O (100 mL). The aqueous layer was separated and back extracted with EtOAc (5 x 100 mL). The combined organics were washed with H_2O (2 x 20 mL) and dried over Na_2SO_4. The solution was concentrated and purified via flash chromatography (Petroleum Ether/EtOAc, 8:1) to afford the title compound (6.15 g, 63 %) as a yellow oil.

^{1}H NMR (500 MHz, Chloroform-d) δ 7.34 – 7.29 (m, 4H, ArH), 7.21 – 7.15 (m, 6H, ArH), 4.29 – 4.16 (m, 2H, H-4), 3.37 (apt dq, *J* = 23.6, 7.3 Hz, 1H, H-2), 1.64 (apt dd, *J* = 19.2, 7.3 Hz, 3H, H-3), 1.26 (apt dt, *J* = 7.1, 0.6 Hz, 3H, H-5).

^{13}C NMR (126 MHz, Chloroform-d) δ 168.9 (Ar*C*H), 168.8 (Ar*C*H), 150.5 (Ar*C*H), 150.4 (Ar*C*H), 150.4 (Ar*C*H), 150.3 (Ar*C*H), 129.9 (Ar*C*H), 129.7 (Ar*C*H), 125.4 (Ar*C*H), 125.4 (Ar*C*H), 125.4 (Ar*C*H), 125.4 (Ar*C*H), 120.7 (Ar*C*H), 120.7 (Ar*C*H), 120.6 (Ar*C*H), 62.0 (C-4), 39.5 (C-2), 14.2 (C-5), 11.9 (C-3).

IR (ATR) cm^{-1}: 2985, 1732, 1276, 760

ESI/MS$^-$ (*m/z*) (M+Na$^+$); 335.1 HRMS-ESI: cacld for $C_{17}H_{20}O_5P$: 335.1048; Found 335.1045.

ethyl (4*R*,5*S*,6*S*,*Z*)-5-((*tert*-butyldimethylsilyl)oxy)-2-ethyl-6-methoxy-4-methylocta-2,7-dienoate (60)

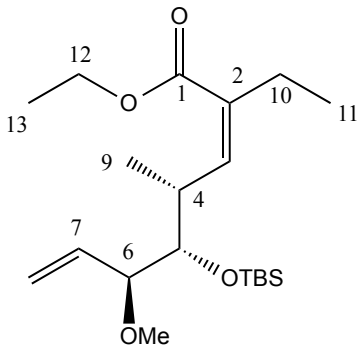

To a solution of compound **58** (0.896 g, 2.57 mmol) in anhydrous THF (40 mL) was added NaH (60 % dispersion in mineral oil, 122 mg, 3.05 mmol) portionwise at 0 °C and stirred for 1 h. The mixture was reduced to -78 °C, and a solution of compound **55** (0.700 g, 2.57 mmol) in THF (20 mL) was then finally added. Stirring was continued for 30 min at -78 °C. The resulting mixture was warmed to 0 °C and left at this temperature for 17 h under stirring. The reaction was quenched with saturated aqueous NH_4Cl (40 mL), and the aqueous layer was extracted with EtOAc (4 x 100 mL). The combined organic layers was dried over Na_2SO_4, and the solvent was removed under diminished pressure. Chromatography (Petroleum Ether/EtOAc, 30:1) of the residue afforded the title compound as an isomeric mixture of desired compound **60** and undesired compound **61** (95 mg, 10 %, ratio of *Z*:*E* = 65:35) as a colourless oil. Compound **62** was formed as the major product.

^{1}H NMR (500 MHz, Chloroform-d) δ 5.87 (d, *J* = 9.8 Hz, 1H, H-3), 5.63 (ddd, *J* = 17.2, 10.4, 8.3 Hz, 1H, H-7), 5.33 – 5.20 (m, 2H, H-8) 4.22 – 4.14 (m, 2H, H-12), 3.60 (dd, *J* = 7.6, 2.6 Hz, 1H, H-5), 3.37 (apt t, *J* = 8.0 Hz, 1H, H-6), 3.20 (s, 3H, OMe), 3.15 – 3.10 (m, 1H, H-4), 2.30 – 2.21 (m, 2H, H-10, overlapping peaks), 1.30 – 1.27 (m, 3H, H-13, overlapping peaks), 1.02 (t, *J* = 7.4 Hz, 3H, H-11), 0.93 (d, *J* = 6.0 Hz, 3H, H-9, overlapping peaks), 0.91 (s, 9H, TBS group (3 x CH_3)), 0.06 (s, 3H, CH_3), 0.02 (s, 3H, CH_3).

^{13}C NMR (126 MHz, Chloroform-d) δ 168.3 (C-1), 143.9 (C-3), 135.1 (C-7), 132.1 (C-2), 118.8 (C-8), 86.8 (C-6), 77.7 (C-5), 60.1 (C-12), 56.1 (O*C*H$_3$), 35.5 (C-4), 27.8 (C-10), 26.3 (C(*C*H$_3$)$_3$), 18.7 (*C*(CH$_3$)$_3$), 14.4 (C-13), 13.6 (C-11), 13.3 (C-9), -3.6 (Si*C*H$_3$), -4.8 (Si*C*H$_3$).

IR (ATR) cm^{-1}: 2929, 1712, 1120, 928, 832, 775

ESI/MS$^-$ (*m/z*) (M+Na$^+$); 393.2 HRMS-ESI: cacld for $C_{20}H_{38}O_4NaSi$: 393.2437; Found 393.2441.

ethyl (*S, Z or E*)-2-ethyl-6-methoxy-4-methylocta-2,4,7-trienoate (62)

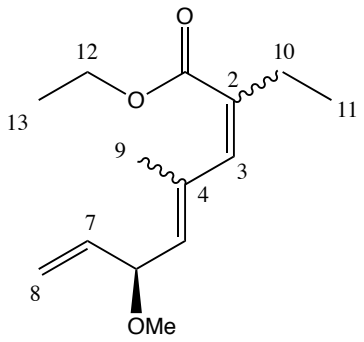

Compound **62** was observed as a yellow oil and was the major product observed from the modified HWE reaction. The stereochemistry of the olefins was not elucidated.

^{1}H NMR (500 MHz, Chloroform-*d*) δ 6.03 (d, *J* = 1.7 Hz, 1H, H-3), 5.73 (ddd, *J* = 17.1, 10.3, 6.5 Hz, 1H, H-7), 5.36 (apt dt, *J* = 8.4, 1.4 Hz, 1H, H-5), 5.27 – 5.13 (m, 2H, H-8), 4.36 (apt ddt, *J* = 7.8, 6.5, 1.1 Hz, 1H, H-6), 4.18 (apt qd, *J* = 7.2, 2.7 Hz, 2H, H-12), 3.28 (s, 3H, OMe), 2.31 (apt qd, *J* = 7.5, 1.5 Hz, 2H, H-10), 1.78 (d, *J* = 1.3 Hz, 3H, H-9), 1.28 (t, *J* = 7.2 Hz, 3H, H-13), 1.06 (t, *J* = 7.5 Hz, 3H, H-11).

^{13}C NMR (126 MHz, Chloroform-d) δ 170.4 (C=O), 137.0 (C-7), 135.7 (C-2), 135.2 (C-4), 134.0 (C-3), 131.0 (C-5), 116.4 (C-8), 79.0 (C-6), 60.7 (C-12), 55.9 (O*C*H$_3$), 28.7 (C-10), 15.7 (C-9), 14.3 (C-13), 12.9 (C-11).

ESI/MS$^-$ (*m/z*); calcd, 261.16 (M+Na$^+$); Found 261.16

(4*R*,5*S*,6*S*,*Z*)-5-((*tert*-butyldimethylsilyl)oxy)-2-ethyl-6-methoxy-4-methylocta-2,7-dien-1-ol (63)

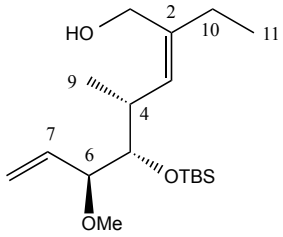

DIBAL (0.27 mL, 0.27 mmol, 1.0M in DCM) was added to the ester mixture of **60** and **61** (*Z*/*E* = 65:35, 76 mg, 0.21 mmol) in DCM (10 mL) at -78 °C. After stirring at -78 °C for 1 h, the reaction was quenched with saturated aqueous potassium sodium tartrate (10 mL). The mixture was diluted with DCM (30 mL) and vigorously stirred at room temperature for 2 h. The aqueous layer was extracted with DCM (3 x 10 mL). The combined organic portion was dried with Na_2SO_4. The solvent was removed under diminished pressure. Flash chromatography (Petroleum Ether/EtOAc, 10:1) gave the key intermediate title compound (32 mg, 74 %, yield based on the ratio of starting *Z* isomer) as a colourless oil.

^{1}H NMR (500 MHz, Chloroform-d) δ 5.71 (ddd, *J* = 17.3, 10.5, 7.5 Hz, 1H, H-7), 5.31 – 5.23 (m, 3H, H-8 and H-3, overlapping peaks), 4.15 (d, *J* = 11.8 Hz, 1H, H-1a), 3.99 (d, *J* = 11.7 Hz, 1H, H-1b), 3.51 – 3.45 (m, 2H, H-6 and H-5, overlapping peaks), 3.22 (s, 3H, OMe), 2.74 – 2.65 (m, 1H, H-4), 2.16 – 2.10 (m, 2H, H-10), 1.77 (s, 1H, OH), 1.03 (t, *J* = 7.5 Hz, 3H, H-11), 0.95 – 0.89 (m, 12H, H-9 and TBS group (3 x CH_3), overlapping peaks), 0.07 (s, 3H, CH_3), 0.05 (s, 3H, CH_3).

^{13}C NMR (126 MHz, Chloroform-d) δ 139.0 (C-2), 135.3 (C-7), 131.8 (C-3), 118.7 (C-8), 86.1 (C-6 or C-5), 78.5 (C-6 or C-5), 60.7 (C-1), 56.3 (O*C*H$_3$), 34.4 (C-4), 28.4 (C-10), 26.3 (C(*C*H$_3$)$_3$), 18.7 (*C*(CH$_3$)$_3$), 15.9 (C-9), 12.9 (C-11), -3.7 (Si*C*H$_3$), -4.5 (Si*C*H$_3$).

IR (ATR) cm^{-1}: 3363, 2959, 928, 830, 774

ESI/MS$^-$ (*m/z*) (M+Na$^+$); 351.2 HRMS-ESI: cacld for $C_{18}H_{36}O_3NaSi$: 351.2331; Found 351.2339.

(4*R*,5*S*,6*S*,*Z*)-5-(((*tert*-butyldimethylsilyl)oxy)-2-ethyl-6-methoxy-4-methylocta-2,7-dienyl)hept-6-enoate (64)

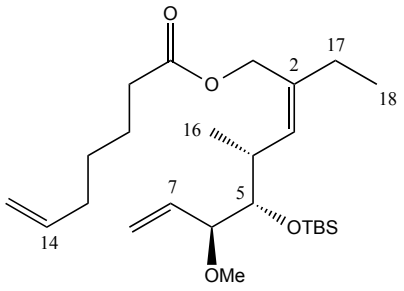

Compound **63** (20 mg, 0.061 mmol) was dissolved in toluene (1.4 mL). To this solution was added 6-heptenoic acid (170 μL, 1.25 mmol) and triphenylphosphine (47 mg, 0.18 mmol). The reaction was stirred for 25 min at room temperature. Diisopropyl azodicarboxylate (35.8 μL, 0.18 mmol) was added dropwise and the mixture was stirred for a further 3 h. The reaction was quenched with saturated aqueous NH_4Cl (8 mL). The organic layer was removed and the aqueous phase was extracted with EtOAc (4 x 8 mL). Combined organics were dried over Na_2SO_4 and concentrated. Flash chromatography (Petroleum Ether/EtOAc, 50:1) of the residue afforded the desired title compound (21 mg, 79 %).

^{1}H NMR (500 MHz, Chloroform-d) δ 5.79 (ddt, *J* = 17.0, 10.2, 6.7 Hz, 1H, H-14), 5.63 (ddd, *J* = 17.2, 10.4, 8.2 Hz, 1H, H-7), 5.45 (d, *J* = 9.7 Hz, 1H, H-3), 5.30 – 5.22 (m, 2H, H-8), 5.03 – 4.93 (m, 2H, H-15), 4.58 (d, *J* = 12.0 Hz, 1H, H-1a), 4.54 (d, *J* = 12.0 Hz, 1H, H-1b), 3.47 (dd, *J* = 7.2, 2.9 Hz, 1H, H-5), 3.40 – 3.36 (m, 1H, H-6), 3.20 (s, 3H, OMe), 2.65 – 2.57 (m, 1H, H-4), 2.31 (t, *J* = 7.5 Hz, 2H, H-10), 2.06 (apt q, *J* = 7.2 Hz, 4H, H-17 and H-13, overlapping peaks), 1.68 – 1.61 (m, 2H, H-11), 1.45 – 1.38 (m, 2H, H-12), 1.00 (t, *J* = 7.4 Hz, 3H, H-18), 0.94 – 0.88 (m, 12H, H-16 and TBS group (3 x CH_3), overlapping peaks), 0.06 (s, 3H, CH_3), 0.03 (s, 3H, CH_3).

^{13}C NMR (126 MHz, Chloroform-d) δ 173.8 (C-9), 138.6 (C-14), 135.3 (C-7), 134.4 (C-3), 133.8 (C-2), 118.9 (C-8), 114.8 (C-15), 86.5 (C-6), 78.5 (C-5), 62.1 (C-1), 56.2 (O*C*H$_3$), 34.4 (C-10 or C-4), 34.3 (C-10 or C-4), 33.5 (C-17 or C-13), 28.5 (C-12), 28.2 (C-17 or C-13), 26.3 (C(*C*H$_3$)$_3$), 24.6 (C-11), 18.7 (*C*(CH$_3$)$_3$), 14.3 (C-16), 12.7 (C-18), -3.6 (Si*C*H$_3$), -4.6 (Si*C*H$_3$).

IR (ATR) cm^{-1}: 2929, 1736, 1251, 1124, 831, 775

ESI/MS$^-$ (*m/z*) (M+Na$^+$); 461.3 HRMS-ESI: cacld for $C_{25}H_{46}O_4NaSi$: 461.3063; Found 461.3077.

(7*E*,9*S*,10*S*,11*R*,12*Z*)-10-((*tert*-butyldimethylsilyl)oxy)-13-ethyl-9-methoxy-11-methyloxacyclotetradeca-7,12-dien-2-one (65)

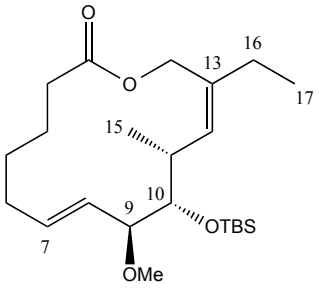

Compound **64** (20 mg, 0.046 mmol) was dissolved up in anhydrous degassed toluene (160 mL). The reaction flask was brought to reflux under gentle stirring. Grubbs-II generation catalyst (7 mg, 0.008 mmol) was dissolved in anhydrous degassed toluene (10 mL) and directly cannulated under positive nitrogen pressure to the reaction flask. This was heated to reflux for 45 min and the contents was concentrated. Chromatography (Petroleum Ether/EtOAc, 100:1) afforded the title compound (13.9 mg, 74 %) as a clear oil.

^{1}H NMR (500 MHz, Chloroform-d) δ 5.70 (dt, *J* = 15.6, 6.8 Hz, 1H, H-7), 5.58 (d, *J* = 9.9 Hz, 1H, H-12), 5.29 (dd, *J* = 15.8, 8.1 Hz, 1H, H-8), 4.51 (d, *J* = 12.8 Hz, 1H, H-14a), 4.38 (d, *J* = 12.8 Hz, 1H, H-14b), 3.47 (dd, *J* = 7.7, 2.6 Hz, 1H, H-10), 3.40 (apt t, *J* = 7.8 Hz, 1H, H-9), 3.19 (s, 3H, OMe), 2.83 – 2.75 (m, 1H, H-11), 2.43 – 2.35 (m, 1H, H-3a), 2.30 – 2.22 (m, 1H, H-3b), 2.20 – 2.12 (m, 1H, H-6a), 2.10 – 1.98 (m, 3H, H-6a and H-16, overlapping peaks), 1.80 – 1.70 (m, 1H, H-4a), 1.64 – 1.57 (m, 1H, H-4b), 1.56 – 1.49 (m, 1H, H-5a), 1.48 – 1.36 (m, 1H, H-5b), 1.00 (t, *J* = 7.4 Hz, 3H, H-17), 0.93 – 0.89 (m, 12H, H-15 and TBS group (3 x CH_3), overlapping peaks), 0.08 (s, 3H, CH_3), 0.06 (s, 3H, CH_3).

^{13}C NMR (126 MHz, Chloroform-d) δ 174.1 (C-2), 134.1 (C-12), 133.9 (C-7), 132.2 (C-13), 128.9 (C-8), 85.6 (C-9), 78.0 (C-10), 64.3 (C-14), 56.1 (O*C*H_3), 34.8 (C-3), 34.2 (C-11), 30.2 (C-16), 29.5 (C-6), 27.8 (C-5), 26.4 (C(*C*H_3)$_3$), 23.7 (C-4), 18.8 (*C*(CH_3)$_3$), 14.0 (C-15), 12.9 (C-17), -3.5 (Si*C*H_3), -4.8 (Si*C*H_3).

IR (ATR) cm^{-1}: 2928, 1734, 1251, 1128, 976, 832, 775

ESI/MS^{-} (*m/z*) (M+Na^{+}); 433.3 HRMS-ESI: cacld for $C_{23}H_{42}O_4NaSi$: 433.2750; Found 433.2750.

(7*E*,9*S*,10*S*,11*R*,12*Z*)-13-ethyl-10-hydroxy-9-methoxy-11-methyloxacyclotetradeca-7,12-dien-2-one (66)

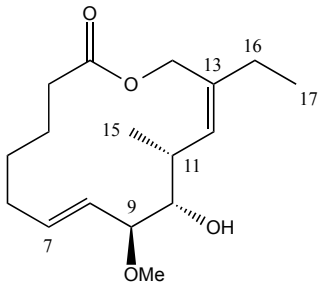

Compound **65** (11.1 mg, 0.027 mmol) was dissolved up in THF (1.5 mL) and transferred to a nalgene vessel. HF in pyridine (70 %, 110 µL) was slowly added dropwise and the resulting mixture was stirred for 19 h. The reaction was lowered to 0 °C and methoxytrimethylsilane (2.5 mL, 18.1 mmol) was slowly added dropwise to quench the reaction. The mixture was stirred for 30 min at room temperature to ensure complete quenching. The solution was concentrated and chromatography (Petroleum Ether/EtOAc, 10:1) furnished the title compound (7 mg, 88 %) as a clear oil.

^{1}H NMR (500 MHz, Chloroform-d) δ 5.76 – 5.68 (m, 2H, H-7 and H-12, overlapping peaks), 5.24 (ddt, *J* = 15.8, 7.7, 1.2 Hz, 1H, H-8), 4.54 (d, *J* = 12.6 Hz, 1H, H-14a), 4.33 (d, *J* = 12.6 Hz, 1H, H-14b), 3.48 – 3.39 (m, 2H, H-9 and H-10, overlapping peaks), 3.31 (s, 3H, OMe), 2.79 (s, 1H, OH), 2.78 – 2.72 (m, 1H, H-11), 2.46 – 2.39 (m, 1H, H-3a), 2.27 – 2.18 (m, 2H, H-3b and H-6a), 2.10 – 2.02 (m, 2H, H-16), 2.01 – 1.93 (m, 1H, H-6b), 1.80 – 1.70 (m, 1H, H-4a), 1.61 – 1.57 (m, 1H, H-4b), 1.57 – 1.51 (m, 1H, H-5a), 1.35 – 1.29 (m, 1H, H-5b), 1.01 (t, *J* = 7.4 Hz, 3H, H-17), 0.95 (d, *J* = 6.9 Hz, 3H, H-15).

^{13}C NMR (126 MHz, Chloroform-d) δ 174.0 (C-2), 135.4 (C-7 or C-12), 133.8 (C-7 or C-12), 133.2 (C-13), 129.3 (C-8), 83.9 (C-9 or C-10), 76.0 (C-10 or C-9), 63.8 (C-14), 56.5 (O*C*H$_3$), 34.6 (C-3), 32.2 (C-11), 30.4 (C-16), 30.1 (C-6), 27.5 (C-5), 23.7 (C-4), 13.0 (C-17), 13.0 (C-15).

IR (ATR) cm^{-1}: 3478, 2929, 1730, 1253, 1115, 981

ethyl (4*R*,5*S*,6*S*,*E*)-5-((*tert*-butyldimethylsilyl)oxy)-6-methoxy-2,4-dimethylocta-2,7-dienoate (67)[5]

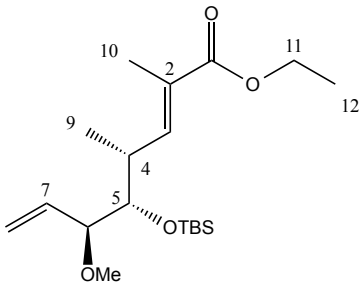

(Carbethoxyethylidene)triphenylphosphorane (1.53 g, 4.22 mmol) was added to the compound **55** (770 mg, 2.83 mmol) in anhydrous toluene (50 mL) and the mixture was refluxed under stirring for 48 h. The solvent was removed *in vacuo* and chromatography of the residue (Petroleum Ether/EtOAc, 100:1) gave the title compound (654 mg, 65 %, ratio of *E*:*Z* = 44:1) as a colourless oil.

^{1}H NMR (500 MHz, Chloroform-d) δ 6.78 (dd, *J* = 9.9, 1.4 Hz, 1H, H-3), 5.63 (ddd, *J* = 16.9, 10.4, 8.2 Hz, 1H, H-7), 5.34 - 5.25 (m, 2H, H-8), 4.24 - 4.11 (m, 2H, H-11), 3.53 (dd, *J* = 7.2, 2.9 Hz, 1H, H-5), 3.42 (apt t, *J* = 7.6 Hz, 1H, H-6), 3.22 (s, 3H, MeO), 2.69 - 2.60 (m, 1H, H-4), 1.80 (d, *J* = 1.4 Hz, 3H, H-10), 1.28 (t, *J* = 7.1 Hz, 3H, H-12), 0.97 (d, *J* = 6.7 Hz, 3H, H-9), 0.92 (s, 9H, TBS group (3 x CH_3)), 0.07 (s, 3H, CH_3), 0.04 (s, 3H, CH_3).

^{13}C NMR (126 MHz, Chloroform-d) δ 168.5 (C-1), 146.1 (C-3), 135.1 (C-7), 126.2 (C-2), 119.1 (C-8), 86.3 (C-6), 77.1 (C-5), 60.5 (C-11), 56.3 (O*C*H_3), 35.5 (C-4), 26.3 (C(*C*H_3)$_3$), 18.7 (*C*(CH$_3$)$_3$), 14.4 (C-12), 13.1 (C-9), 12.6 (C-10), -3.7 (Si*C*H_3), -4.8 (Si*C*H_3).

IR (ATR) cm^{-1}: 2930, 1710, 1248, 1075, 994, 832, 775

ESI/MS^{-} (*m/z*) (M+Na^{+}); 379.2 HRMS-ESI: cacld for $C_{19}H_{36}O_4NaSi$: 379.2281; Found 379.2294.

(4*R*,5*S*,6*S*,*E*)-5-((*tert*-butyldimethylsilyl)oxy)-6-methoxy-2,4-dimethylocta-2,7-dien-1-ol (68)[5]

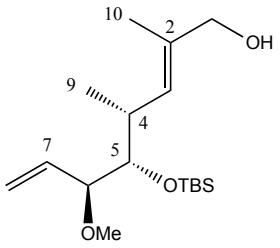

To compound **67** containing a small trace of cis isomer (*E:Z* = 44:1, 0.625 g, 1.75 mmol) in anhydrous DCM (90 mL), DIBAL (6.2 mL, 6.20 mmol, 1.0 M solution in hexane) was added at -78 °C and the resulting solution was stirred at -78 °C for 5 h. The reaction was quenched with saturated aqueous potassium sodium tartrate (50 mL), diluted with DCM (40 mL) and was vigorously stirred at room temperature for 3 h. The aqueous layer was extracted with dichloromethane (4 × 50 mL). The combined organic layers were dried over Na_2SO_4 and the solvent was removed *in vacuo*. Chromatography (Petroleum Ether/EtOAc, 10:1) gave the title compound (0.469 g, 85 %) as a colourless oil.

^{1}H NMR (500 MHz, Chloroform-d) δ 5.65 (ddd, *J* = 17.5, 10.4, 8.1 Hz, 1H, H-7), 5.43 (d, *J* = 9.3 Hz, 1H, H-3), 5.30 - 5.23 (m, 2H, H-8), 3.98 (s, 2H, H-1), 3.49 (dd, *J* = 7.0, 3.3 Hz, 1H, H-5), 3.40 (t, *J* = 7.5 Hz, 1H, H-6), 3.21 (s, 3H, OMe), 2.56 (apt dp, *J* = 9.9, 6.7, 3.2 Hz, 1H, H-4), 1.64 (s, 3H, H-10), 0.94 - 0.87 (m, 12H, TBS group (3 x CH_3), and H-9), 0.06 (s, 3H, CH_3), 0.02 (s, 3H, CH_3).

^{13}C NMR (126 MHz, Chloroform-d) δ 135.5 (C-7), 133.2 (C-2), 131.2 (C-3), 118.7 (C-8), 86.4 (C-6), 78.1 (C-5), 69.3 (C-1), 56.3 (O*C*H$_3$), 34.3 (C-4), 26.3 (C(*C*H$_3$)$_3$), 18.7 (*C*(CH$_3$)$_3$), 14.1 (C-9), 13.9 (C-10), -3.6 (Si*C*H3), -4.6 (Si*C*H3).

IR (ATR) cm^{-1}: 3327, 2928, 928, 832, 775

ESI/MS$^-$ (*m/z*) (M+Na$^+$); 337.2 HRMS-ESI: cacld for $C_{17}H_{34}O_3NaSi$: 337.2175; Found 337.2177.

(4*R*,5*S*,6*S*,*E*)-5-(((*tert*-butyldimethylsilyl)oxy)-6-methoxy-2,4-dimethylocta-2,7-dienyl)hept-6-enoate (69)

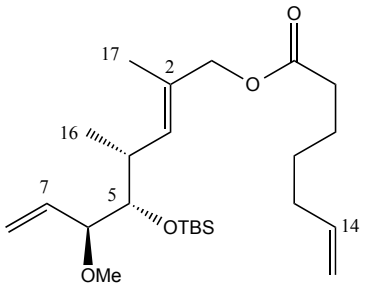

To a solution of compound **68** (150 mg, 0.48 mmol) in anhydrous toluene (15 mL) was added 6-heptenoic acid (130 µL, 0.96 mmol) and triphenylphosphine (352 mg, 1.34 mmol) under stirring. Diisopropyl azodicarboxylate (264 µL, 1.34 mmol) was added dropwise to the stirred solution and the reaction was left to stir for 3 h. The reaction was quenched with saturated aqueous NH_4Cl (30 mL). The aqueous phase was back extracted with EtOAc (3 x 20 mL). The combined organic layers were dried over Na_2SO_4 and concentrated. Flash chromatography (Petroleum Ether/EtOAc, 50:1) afforded the title product (149 mg, 73 %). as a yellow oil.

^{1}H NMR (500 MHz, Chloroform-d) δ 5.79 (ddt, *J* = 17.0, 10.2, 6.7 Hz, 1H, H-14), 5.64 (ddd, *J* = 17.2, 10.4, 8.1 Hz, 1H, H-7), 5.48 (apt dq, *J* = 9.4, 1.3 Hz, 1H, H-3), 5.32 - 5.22 (m, 2H, H-8), 5.03 - 4.93 (m, 2H, H-15), 4.44 (ABq, 2H, H-1a and H-1b), 3.49 (dd, *J* = 7.0, 3.1 Hz, 1H, H-5), 3.39 (apt t, *J* = 7.9, 1H, H-6), 3.21 (s, 3H, MeO), 2.56 (apt dqd, *J* = 9.8, 6.7, 3.1 Hz, 1H, H-4), 2.32 (t, *J* = 7.5 Hz, 2H, H-10), 2.09 - 2.04 (m, 2H, H-12), 1.68 - 1.63 (m, 2H, H-11), 1.61 (d, *J* = 1.4 Hz, 3H, H-17), 1.46 - 1.39 (m, 2H, H-13), 0.92 (d, *J* = 6.7 Hz, 3H, H-16), 0.90 (s, 9H, TBS group (3 x CH_3)), 0.06 (s, 3H, CH_3), 0.01 (s, 3H, CH_3).

^{13}C NMR (126 MHz, Chloroform-d) δ 173.7 (C-9), 138.6 (C-14), 135.4 (C-7), 134.1 (C-3), 128.6 (C-2), 118.7 (C-8), 114.8 (C-15), 86.4 (C-6), 78.0 (C-5), 70.1 (C-1), 56.3 (O*C*H_3), 34.4 (C-4), 34.3 (C-10), 33.5 (C-12), 28.5 (C-13), 26.3 (C(*C*H_3)$_3$), 24.6 (C-11), 18.7 (*C*(CH_3)$_3$), 14.2 (C-17), 13.8 (C-16), -3.6 (Si*C*H_3), -4.6 (Si*C*H_3).

IR (ATR) cm^{-1}: 2929, 1737, 1641, 1248, 1126, 993, 832, 775

ESI/MS$^-$ (*m/z*) (M+Na$^+$); 447.3 HRMS-ESI: cacld for $C_{24}H_{44}O_4NaSi$: 447.2907; Found 447.2902.

(7*E*/*Z*,9*S*,10*S*,11*R*,12*E*)-10-((*tert*-butyldimethylsilyl)oxy)-9-methoxy-11,13-dimethyloxacyclotetradeca-7,12-dien-2-one (70) and (71)

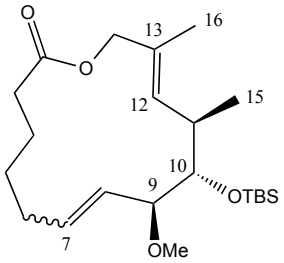

Compound **69** (100 mg, 0.24 mmol) was dissolved up in anhydrous degassed toluene (250 mL). The reaction flask was heated to reflux under stirring. Grubbs-II generation catalyst (41 mg, 0.048 mmol) was dissolved in anhydrous degassed toluene (30 mL) and cannulated under positive nitrogen pressure to the reaction flask. This was heated for 45 min under reflux. The contents was concentrated and flash chromatography (Petroleum Ether/EtOAc, 100:1) afforded a mixture of products with the same R_f (44 mg, 46 %, ratio of *Z*:*E* = 1:1) as a clear oil.

IR (ATR) cm^{-1}: 2928, 1735, 1250, 1145, 972,834, 775, 665

ESI/MS$^-$ (*m/z*): (M+Na$^+$); 419.3 HRMS-ESI: cacld for $C_{22}H_{40}O_4NaSi$: 419.2594; Found 419.2586.

(7*Z*,9*S*,10*S*,11*R*,12*E*)-10-hydroxy-9-methoxy-11,13-dimethyloxacyclotetradeca-7,12-dien-2-one (72)

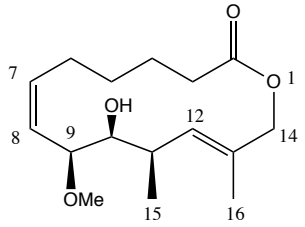

The cis and trans lactone mixture **70** and **71** (22 mg, 0.056 mmol) was dissolved up in THF (3 mL) and transferred to a plastic vessel. HF in pyridine (70 %, 220 µL) was added dropwise and the resulting mixture was stirred for 24 h. The reaction was lowered to 0 °C and methoxytrimethylsilane (2.5 mL, 18.1 mmol) was added dropwise to quench the reaction. This was stirred for 30 mins to ensure complete quenching. The mixture was concentrated and chromatography (Petroleum Ether/EtOAc 10:1) afforded the title compound (7.7 mg, 89 %).

^{1}H NMR (500 MHz, Chloroform-d) δ 5.77 (ddd, *J* = 11.1, 8.8, 6.9 Hz, 1H, H-7), 5.49 (apt t, *J* = 10.5 Hz, 1H, H-8), 5.25 (d, *J* = 10.2 Hz, 1H, H-12), 4.98 (d, *J* = 11.7 Hz, 1H, H-14a), 4.12 (d, *J* = 11.7 Hz, 1H, H-14b), 3.91 (d, *J* = 10.0 Hz, 1H, H-9), 3.25 (s, 3H, MeO), 2.98 (apt t, *J* = 9.2 Hz, 1H, H-10), 2.69 (apt tq, *J* = 9.9, 6.7 Hz, 1H, H-11), 2.40 (qdd, *J* = 15.5, 8.5, 3.9 Hz, 2H, H-3), 2.25 (d, *J* = 9.6 Hz, 1H, OH), 2.18 (tdd, *J* = 13.5, 9.0, 4.8 Hz, 1H, H-6a), 1.89 - 1.81 (m, 1H, H-4a, overlapping peaks), 1.80 (s, 3H, H-16, overlapping peaks), 1.79 - 1.72 (m, 1H, H-6b, overlapping peaks), 1.63 (tdd, *J* = 15.1, 8.1, 4.2 Hz, 1H, H-4b), 1.51 - 1.42 (m, 1H, H-5a), 1.24 - 1.16 (m, 1H, H-5b), 1.05 (d, *J* = 6.7 Hz, 3H, H-15).

^{13}C NMR (126 MHz, Chloroform-d) δ 173.1 (C-2), 133.8 (C-7), 133.5 (C-12), 132.1 (C-13), 128.4 (C-8), 78.8 (C-10), 74.3 (C-9), 68.7 (C-14), 55.7 (O*C*H$_3$), 36.5 (C-11), 32.8 (C-3), 28.3 (C-5), 27.1 (C-6), 24.7 (C-4), 17.3 (C-15), 15.7 (C-16).

IR (ATR) cm^{-1}: 3535, 2928, 1732, 1258, 1145, 973

ESI/MS$^-$ (*m/z*): (M+Na$^+$); 305.2 HRMS-ESI: cacld for $C_{16}H_{26}O_4Na$: 305.1729; Found 305.1735.

(7*E*,9*S*,10*S*,11*R*,12*E*)-10-hydroxy-9-methoxy-11,13-dimethyloxacyclo-tetradeca-7,12-dien-2-one (73)

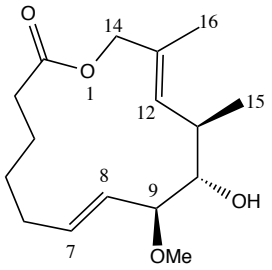

From the previous deprotection reaction of compounds **70** and **71** using HF in pyridine, flash chromatography afforded the title compound (6.7 mg, 85 %).

^{1}H NMR (500 MHz, Chloroform-d) δ 5.63 (ddd, *J* = 15.6, 6.5, 5.2 Hz, 1H, H-7), 5.30 - 5.27 (m, 1H, H-12), 5.13 (ddt, *J* = 15.6, 7.9, 1.7 Hz, 1H, H-8), 4.44 (dd, *J* = 12.3, 1.1 Hz, 1H, H-14a) 4.36 (d, *J* = 12.4 Hz, 1H, H-14b), 3.40 (s, 1H, OH), 3.28 (apt t, *J* = 8.8 Hz, 8.7, 1H, overlapping peaks, H-10), 3.25 (s, 3H, overlapping peak, MeO), 3.20 (apt t, *J* = 8.3, 8.1 Hz, 1H, H-9), 2.46 - 2.40 (m, 1H, H-11), 2.38 (t, *J* = 6.7 Hz, 2H, H-3), 2.20 - 2.11 (m, 1H, H-6a), 2.05 - 1.96 (m, 1H, H-6b), 1.80 - 1.73 (m, 1H, H-4a), 1.73 - 1.66 (m, 1H, H-4b), 1.65 (d, *J* = 0.93 Hz, 3H, H-16), 1.46 - 1.38 (m, 2H, H-5), 1.08 (d, *J* = 6.7 Hz, 3H, H-15).

^{13}C NMR (126 MHz, Chloroform-d) δ 173.5 (C-2), 134.9 C-7), 132.7 (C-12), 128.2 (C-13), 126.4 (C-8), 86.6 (C-9), 77.6 (C-10), 69.4 (C-14), 55.8 (O*C*H$_3$), 37.7 (C-11), 34.1 (C-3), 29.5 (C-6), 26.1 (C-5), 23.6 (C-4), 18.6 (C-15), 15.1 (C-16).

IR (ATR) cm^{-1}: 3535, 2928, 1728, 1258, 1145, 973

ESI/MS$^-$ (*m/z*): (M+Na$^+$); 305.2 HRMS-ESI: cacld for $C_{16}H_{26}O_4Na$: 305.1729; Found 305.1719.

(6*Z*,8*S*,9*S*,10*R*,11*E*)-9,13-dihydroxy-8-methoxy-10,12-dimethyltrideca-6,11-dienoic acid (74)

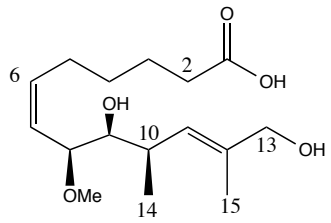

Compound **72** (3 mg, 0.011 mmol) was dissolved in a mixture (1:1 MeOH/H_2O) at room temperature. To it was added NaOH (180 µL, 0.09 mmol, 0.5 M). After stirring for 16 h, the mixture was concentrated and taken up in DCM. The mixture was acidified to pH 1 with 1 M HCl under stirring. The aqueous layer was separated and the organic layer was dried over Na_2SO_4 and concentrated to yield the furnished title compound (2.4 mg, 73 %) as a clear oil.

^{1}H NMR (600 MHz, Chloroform-d) δ 5.71 (dt, *J* = 11.1, 7.4 Hz, 1H, H-6), 5.41 - 5.33 (m, 2H, H-7 and H-11, overlapping peaks), 4.04 (s, 2H, H-13), 3.91 (apt dd, *J* = 9.7, 4.5 Hz, 1H, H-8), 3.25 (s, 3H, OMe), 3.22 (apt dd, *J* = 6.5, 4.5 Hz, 1H, H-9), 2.65 (dp, *J* = 9.7, 6.8 Hz, 1H, H-10), 2.35 (t, *J* = 7.1 Hz, 2H, H-2), 2.11 (apt q, *J* = 7.7 Hz, 2H, H-5), 1.70 - 1.64 (m, 5H, H-3 and H-15, overlapping peaks), 1.45 (p, *J* = 7.5 Hz, 2H, H-4), 1.00 (d, *J* = 6.6 Hz, 3H, H-14).

^{13}C NMR (151 MHz, Chloroform-d) δ 177.4 (C-1), 134.9 (C-6), 134.5 (C-12), 128.8 (C-7 or C-11), 127.8 (C-7 or C-11), 78.1 (C-9), 76.8 (C-8), 68.6 (C-13), 56.1 (O*C*H_3), 34.9 (C-10), 33.7 (C-2), 29.0 (C-4), 27.6 (C-5), 24.4 (C-3), 16.0 (C-14), 13.9 (C-15).

ESI/MS- (m/z): ($M-H^+$); 304.2 HRMS-ESI: cacld for $C_{16}H_{27}O_5$: 299.1858; Found 299.1854.

(6*E*,8*S*,9*S*,10*R*,11*E*)-9,13-dihydroxy-8-methoxy-10,12-dimethyltrideca-6,11-dienoic acid (75)

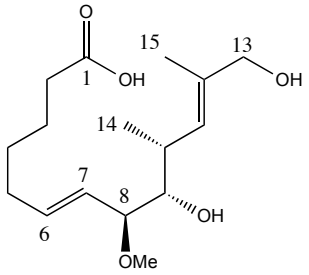

To a solution of compound **73** (3.5 mg, 0.012 mmol) in a solvent mixture (1:1 MeOH/H_2O) at room temperature was added NaOH (210 µL, 0.105 mmol, 0.5 M). After stirring for 16 h, the reaction mixture was concentrated under diminished pressure and taken up in DCM. This solution was subsequently acidified to pH 1 with 1 M HCl. The organic layer was separated, dried over Na_2SO_4 and concentrated to afford the title compound (2.8 mg, 77 %) as a clear oil.

^{1}H NMR (600 MHz, Chloroform-d) δ 5.69 (dtd, *J* = 17.3, 7.1, 3.9 Hz, 1H, H-6), 5.42 - 5.33 (m, 2H, H-7 and H-11, overlapping peaks), 4.01 (s, 2H, H-13), 3.46 - 3.39 (m, 1H, H-8), 3.27 (apt t, *J* = 5.6 Hz, 1H, H-9, overlapping peaks), 3.25 - 3.23 (m, 3H, OMe, overlapping peaks), 2.61 (apt dp, *J* = 9.7, 6.7 Hz, 1H, H-10), 2.35 (apt q, *J* = 12.6, 7.3 Hz, 2H, H-2), 2.12 (apt t, *J* = 6.8, 6.3 Hz, 2H, H-5), 1.69 - 1.63 (m, 5H, H-3 and H-15, overlapping peaks), 1.51 - 1.43 (m, 2H, H-4), 0.99 (d, *J* = 6.8 Hz, 3H, H-14).

^{13}C NMR (151 MHz, Chloroform-d) δ 177.7 (C-1), 135.8 (C-6), 134.5 (C-12), 129.4 (C-7 or C-11), 127.6 (C-7 or C-11), 83.4 (C-8), 77.5 (C-9), 69.0 (C-13), 56.1 (O*C*H$_3$), 34.4 (C-10), 33.7 (C-2), 32.0 (C-5), 28.6 (C-4), 24.3 (C-3), 15.3 (C-14), 13.9 (C-15).

IR (ATR) cm^{-1}: 3440, 2929, 1729, 1185, 973

ESI/MS- (m/z): (M-H$^+$); 304.2 HRMS-ESI: cacld for $C_{16}H_{27}O_5$: 299.1858; Found 299.1865.

(((3*S*,4*S*,5*R*,*E*/*Z*)-8-azido-3-methoxy-5,7-dimethylocta-1,6-dien-4-yl)oxy)(*tert*-butyl)dimethylsilane (76) and (77)

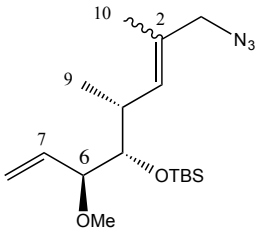

To a solution of compound **68** (520 mg, 1.65 mmol) in anhydrous toluene (5 mL) was added diphenylphosphoryl azide (536 µL, 2.49 mmol) and DBU (372 µL, 2.49 mmol) under stirring at room temperature. After stirring for 5 h, the reaction was quenched with saturated aqueous NH_4Cl solution and diluted with Et_2O (30 mL). The organic layer was separated and the aqueous layer was extracted with Et_2O (3 x 20 mL). The combined organic layers were dried over Na_2SO_4 and concentrated under diminished pressure. Purification of the crude product by flash chromatography (Petroleum Ether/EtOAc, 30:1) afforded a mixture of the desired compound **76** and double bond isomerised product **77** (252 mg, 45 %, ratio of *E*:*Z* = 65:35, yield was based on desired product **76**) as a colourless oil.

IR (ATR) cm^{-1}: 2929, 2097, 1246, 930, 835, 775

ESI/MS^- (*m/z*): ($M+Na^+$); 362.2 HRMS-ESI: cacld for $C_{17}H_{33}N_3O_2SiNa$: 362.2240; Found 362.2227.

(((3*S*,4*S*,5*R*,*Z*)-8-azido-3-methoxy-5,7-dimethylocta-1,6-dien-4-yl)oxy)(*tert*-butyl)dimethylsilane (77)[2]

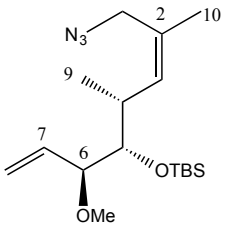

At room temperature, diphenylphosphoryl azide (425 µL, 1.96 mmol) and DBU (294 µL, 1.97 mmol) were added to a solution of compound **14** (0.410 g, 1.30 mmol) in anhydrous toluene (7 mL). After stirring for 5 h at room temperature, the reaction was quenched with saturated aqueous NH_4Cl solution and diluted with Et_2O (7 mL). The top organic layer was separated and the aqueous layer was extracted with Et_2O (3 x 20 mL). The combined organic layers were dried over Na_2SO_4 and concentrated under diminished pressure. Purification of the crude product by flash chromatography (Petroleum Ether/EtOAc, 50:1) afforded the title compound and a trace amount of **76** (420 mg, 95 %, ratio of *Z*:*E* = 94:6, yield includes both isomers) as a clear oil.

^{1}H NMR (500 MHz, Chloroform-d) δ 5.64 (ddd, *J* = 17.2, 10.4, 8.0 Hz, 1H, H-7), 5.52 (d, *J* = 10.0 Hz, 1H, H-3), 5.36 – 5.23 (m, 2H, H-8), 3.81 (d, *J* = 13.0 Hz, 1H, H-1a), 3.66 (d, *J* = 13.0 Hz, 1H, H-1b), 3.45 (dd, *J* = 7.1, 3.0 Hz, 1H, H-5), 3.41 – 3.37 (m, 1H, H-6), 3.21 (s, 3H, OMe), 2.55 (dqd, *J* = 9.7, 6.7, 3.0 Hz, 1H, H-4), 1.77 (d, *J* = 1.4 Hz, 3H, H-10), 0.99 – 0.83 (m, 12H, H-9 and TBS group (3 x CH_3), overlapping peaks), 0.06 (s, 3H, CH_3), 0.04 (s, 3H, CH_3).

^{13}C NMR (126 MHz, Chloroform-d) δ 136.1 (C-3), 135.4 (C-7), 127.4 (C-2), 118.9 (5.36), 86.2 (C-6), 78.6 (C-5), 56.3 (O*C*H_3), 51.6 (C-1), 34.6 (C-4), 26.3 (C(*C*H_3)$_3$), 22.4 (C-10), 18.7 (*C*(CH_3)$_3$), 14.6 (C-9), -3.6 (Si*C*H_3), -4.6 (Si*C*H_3).

IR (ATR) cm^{-1}: 2930, 2096, 1247, 832, 774, 671

ESI/MS$^-$ (*m/z*) (M+H$^+$); 340.2 HRMS-ESI: cacld for $C_{17}H_{34}N_3O_2Si$: 340.2420; Found 340.2414.

_N_-((4_R_,5_S_,6_S_,_E_)-5-((_tert_-butyldimethylsilyl)oxy)-6-methoxy-2,4-dimethylocta-2,7-dien-1-yl)hept-6-enamide (80)

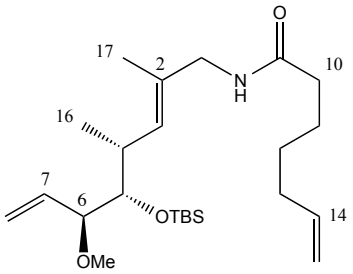

The reacting mixture containing desired product **76** and isomerised product **77** (503 mg, 1.48 mmol) was dissolved up in THF (15 mL). The reaction content's was brought to reflux and triphenylphosphine (0.679 g, 2.59 mmol) and H_2O (133 µL, 7.39 mmol) was added. The reaction was refluxed for 6 h under stirring. THF (10 mL) was added and dried over Na_2SO_4 and concentrated under diminished pressure. The residue was taken up in anhydrous DCM (10 mL) and DIPEA (1.03 mL, 5.91 mmol), EDC.HCl (567 mg, 2.96 mmol) and 6-heptenoic acid (401 µL, 2.96 mmol) were added sequentially. The mixture was stirred for 1 h and concentrated to circa 2 mL. Purification of the residual solution by flash chromatography (Petroleum Ether/EtOAc, 6:1) afforded the desired title product (229 mg, 73 %, based on the ratio of starting *E* isomer **76** present in the reacting mixture) as a clear oil.

^{1}H NMR (500 MHz, Chloroform-d) δ 5.79 (ddt, *J* = 17.0, 10.2, 6.7 Hz, 1H, H-14), 5.63 (ddd, *J* = 17.2, 10.4, 8.0 Hz, 1H, H-7), 5.34 (br s, 1H, NH, overlapping peak), 5.33 - 5.22 (m, 3H, H-8, H-3, overlapping peaks), 5.03 - 4.92 (m, 2H, H-15), 3.81 (dd, *J* = 14.7, 6.0 Hz, 1H, H-1a), 3.72 (dd, *J* = 14.7, 5.5 Hz, 1H, H-1b), 3.46 (dd, *J* = 7.0, 3.2 Hz, 1H, H-5), 3.39 (apt t, *J* = 7.5 Hz, 1H, H-6), 3.2 (s, 3H, OMe), 2.53 (apt dqd, *J* = 9.8, 6.8, 3.2 Hz, 1H, H-4), 2.20 - 2.15 (m, 2H, H-10), 2.10 - 2.03 (m, 2H, H-13), 1.71 - 1.62 (m, 2H, H-11), 1.57 (d, *J* = 1.4 Hz, 3H, H-17), 1.42 (apt p, *J* = 7.5 Hz, 2H, H-12), 0.91 - 0.88 (m, 12H, H-16 and TBS group (3 x CH_3), overlapping peaks), 0.06 (s, 3H, CH_3), 0.01 (s, 3H, CH_3).

^{13}C NMR (126 MHz, Chloroform-d) δ 172.8 (C-9), 138.6 (C-14), 135.3 (C-7), 131.7 (C-3), 130.3 (C-2), 118.7 (C-8), 114.8 (C-15), 86.4 (C-6), 78.1 (C-5), 56.3 (O*C*H$_3$), 47.0 (C-1), 36.9 (C-10), 34.5 (C-4), 33.6 (C-13), 28.7 (C-12), 26.3 (C(*C*H$_3$)$_3$), 25.4 (C-11), 18.7 (*C*(CH$_3$)$_3$), 14.8 (C-17), 14.1 (C-16), -3.6 (Si*C*H$_3$), -4.6 (Si*C*H$_3$).

IR (ATR) cm^{-1}: 3288, 2929, 1643, 1553, 1247, 993, 830, 775

ESI/MS$^-$ (*m/z*): (M+Na$^+$); 446.3 HRMS-ESI: cacld for $C_{24}H_{45}NO_3SiNa$: 446.3066; Found 446.3066.

N-((4*R*,5*S*,6*S*,*Z*)-5-((*tert*-butyldimethylsilyl)oxy)-6-methoxy-2,4-dimethylocta-2,7-dien-1-yl)hept-6-enamide (81)[2]

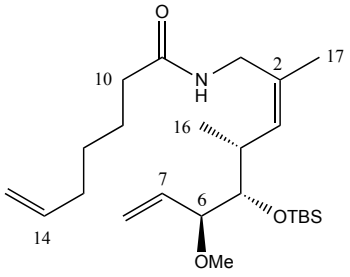

The reacting mixture containing desired product **77** and isomerised product **76** (0.420 g, 1.24 mmol) was solubilised in THF (10 mL) and the reaction contents were brought to reflux. Triphenylphosphine (0.576 g, 2.20 mmol) and H_2O (112 µL, 6.22 mmol) was added. The reaction was refluxed for 5.5 h under stirring THF (10 mL) was added and dried over Na_2SO_4. The mixture was subsequently concentrated under diminished pressure. The residue was taken up in anhydrous DCM (10 mL) and DIPEA (865 µL, 4.97 mmol), EDC.HCl (474 mg, 2.47 mmol) and 6-heptenoic acid (336 µL, 2.48 mmol) were added sequentially. The mixture was stirred for 8 h and concentrated to circa 1 mL. Purification by flash chromatography (Petroleum Ether/EtOAc, 6:1) afforded the desired amide **81** and 10 % undesired amide **80** (388 mg, 74 %, ratio of *Z*:*E* = 9:1, yield includes both isomers) as a clear oil.

^{1}H NMR (500 MHz, Chloroform-d) δ 5.79 (ddt, *J* = 16.9, 10.2, 6.7 Hz, 1H, H-14), 5.67 (ddd, *J* = 17.7, 10.5, 7.7 Hz, 1H, H-7), 5.41 (br s, 1H, NH), 5.35 – 5.22 (m, 3H, H-8 and H-3, overlapping peaks), 5.04 – 4.92 (m, 2H, H-15), 3.86 (dd, *J* = 14.0, 5.7 Hz, 1H, H-1a), 3.79 (dd, *J* = 14.0, 5.5 Hz, 1H, H-1b), 3.46 (dd, *J* = 6.8, 3.2 Hz, 1H, H-5), 3.41 (apt t, *J* = 7.2 Hz, 1H, H-6), 3.22 (s, 3H, OMe), 2.63 – 2.55 (m, 1H, H-4), 2.17 (t, *J* = 7.6 Hz, 2H, H-10), 2.06 (apt q, *J* = 7.1 Hz, 2H, H-13), 1.69 (d, *J* = 1.4 Hz, 3H, H-17, overlapping peak), 1.68 – 1.62 (m, 2H, H-11), 1.45 – 1.38 (m, 2H, H-12), 0.90 (s, 12H, H-1 and TBS group (3 x CH_3)), 0.06 (s, 3H, CH_3), 0.03 (s, 3H, CH_3).

^{13}C NMR (126 MHz, Chloroform-d) δ 173.0 (C-9), 138.6 (C-14), 135.3 (C-7), 134.1 (C-3), 130.0 (C-2), 118.8 (C-8), 114.8 (C-15), 86.2 (C-6), 78.4 (C-5), 56.3 (OCH_3), 40.0 (C-1), 36.8 (C-10), 34.4 (C-4), 33.6 (C-13), 28.7 (C-12), 26.3 ($C(CH_3)_3$), 25.4 (C-11), 22.1 (C-17), 18.7 ($C(CH_3)_3$), 14.9 (C-16), -3.7 ($SiCH_3$), -4.6 ($SiCH_3$).

IR (ATR) cm^{-1}: 3283, 2929, 1641, 1547, 1249, 832, 774, 671

ESI/MS^{-} (*m/z*) ($M+Na^{+}$); 446.3 HRMS-ESI: cacld for $C_{24}H_{45}NO_3NaSi$: 446.3066; Found 446.3080.

(7*Z*,9*S*,10*S*,11*R*,12*E*)-10-((*tert*-butyldimethylsilyl)oxy)-9-methoxy-11,13-dimethylazacyclotetradeca-7,12-dien-2-one (82)

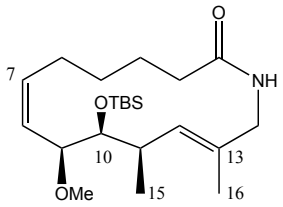

Compound **81** (80 mg, 0.19 mmol) was dissolved up in anhydrous degassed toluene (250 mL). The reaction flask was heated to reflux under stirring. Grubbs-II generation catalyst (34 mg, 0.040 mmol) was dissolved in anhydrous degassed toluene (30 mL) and added to the reaction flask via cannula. This was heated for 45 min under reflux. The contents of the flask was concentrated under diminished pressure and flash chromatography (Petroleum Ether/EtOAc, 3:1) afforded the title product and compound **83** (1.2:1 respectively). Flash chromatography yielded the title compound (20.3 mg, 27 %) as a white solid.

^{1}H NMR (500 MHz, Chloroform-d) δ 5.85 (dd, *J* = 7.2, 4.1 Hz, 1H, NH), 5.65 (td, *J* = 10.4, 5.5 Hz, 1H, H-7), 5.26 (t, *J* = 10.6 Hz, 1H, H-8), 5.08 (d, *J* = 10.3 Hz, 1H, H-12), 4.20 (dd, *J* = 16.2, 8.4 Hz, 1H, H-14a), 3.83 (dd, *J* = 10.2, 5.3 Hz, 1H, H-9), 3.44 - 3.35 (m, 2H, H-14b and H-10, overlapping peaks), 3.18 (s, 3H, OMe), 2.83 - 2.74 (m, 1H, H-11), 2.38 - 2.28 (m, 2H, H-3a and H-6a, overlapping peaks), 2.22 (ddd, *J* = 14.3, 10.6, 3.6 Hz, 1H, H-3b), 2.00 (dtd, *J* = 13.8, 6.4, 3.2 Hz, 1H, H-5a), 1.84 (tt, *J* = 13.6, 4.9 Hz, 1H, H-6b), 1.67 (s, 3H, H-16), 1.65 - 1.51 (m, 2H, H-5b and H-4a, overlapping peaks), 1.35 (dtt, *J* = 13.8, 9.4, 5.0 Hz, 1H, H-4b), 0.94 (d, *J* = 7.3 Hz, 3H, H-15), 0.89 (s, 9H, TBS group (3 x CH_3)), 0.06 (s, 6H, 2 X CH_3).

^{13}C NMR (126 MHz, Chloroform-d) δ 172.0 (C-2), 133.3 (C-7), 132.9 (C-13), 128.4 (C-8), 125.8 (C-12), 80.4 (C-10), 78.0 (C-9), 55.8 (O*C*H_3), 44.8 (C-14), 37.8 (C-11), 35.2 (C-3), 27.7 (C-4), 27.1 (C-6), 26.3 (C(*C*H_3)$_3$), 24.6 (C-5), 18.9 (C-15), 18.7 (*C*(CH_3)$_3$), 16.1 (C-16), -3.8 (Si*C*H_3), -4.1 (Si*C*H_3).

IR (ATR) cm^{-1}: 3253, 2925, 1638, 1548, 1247, 832, 775

ESI/MS$^-$ (*m/z*): (M+Na$^+$); 418.3 HRMS-ESI: cacld for $C_{22}H_{41}NO_3SiNa$: 418.2753; Found 418.2754.

(7*E*,9*S*,10*S*,11*R*,12*E*)-10-((*tert*-butyldimethylsilyl)oxy)-9-methoxy-11,13-dimethylazacyclotetradeca-7,12-dien-2-one (83)

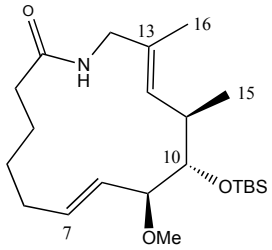

From the ring closing reaction using compound **81**, whereby compound **82** was formed, flash chromatography also afforded the title compound (17.3 mg, 23 %) as a white solid.

^{1}H NMR (500 MHz, Chloroform-d) δ 5.67 (dt, *J* = 14.1, 6.6 Hz, 1H, H-7), 5.47 (t, *J* = 5.8 Hz, 1H, NH), 5.33 - 5.24 (m, 2H, H-8 and H-12, overlapping peaks), 3.83 (dd, *J* = 15.3, 6.9 Hz, 1H, H-14a), 3.62 (dd, *J* = 15.6, 5.1 Hz, 1H, H-14b), 3.56 (apt t, *J* = 6.6 Hz, 1H, H-10), 3.36 - 3.31 (m, 1H, H-9), 3.21 (s, 3H, OMe), 2.55 - 2.47 (m, 1H, H-11), 2.33 - 2.20 (m, 2H, H-3), 2.11 - 2.04 (m, 2H, H-6), 1.77 - 1.68 (m, 2H, H-4), 1.61 (d, *J* = 1.2 Hz, 3H, H-16), 1.55 - 1.45 (m, *J* = 7.0, 6.3 Hz, 2H, H-5), 0.97 (d, *J* = 7.1 Hz, 3H, H-15), 0.91 - 0.87 (m, 9H, TBS group (3 x CH_3)), 0.08 (s, 3H, CH_3), 0.07 (s, 3H, CH_3).

^{13}C NMR (126 MHz, Chloroform-d) δ 172.6 (C-2), 133.2 (C-7), 131.1 (C-13), 128.5 (C8 or C-12), 127.3 (C8 or C-12), 87.9 (C-9), 78.8 (C-10), 56.2 (O*C*H$_3$), 45.8 (C-14), 38.4 (C-11), 36.1 (C-3), 30.6 (C-6), 26.8 (C-5), 26.2 (C(*C*H$_3$)$_3$), 24.2 (C-4), 19.1 (C-16), 18.5 (*C*(CH$_3$)$_3$), 16.1 (C-16), -4.0 (Si*C*H$_3$), -4.5 (Si*C*H$_3$).

IR (ATR) cm^{-1}: 3260, 2926, 1638, 1248, 832, 775

ESI/MS$^-$ (*m/z*): (M+Na$^+$); 418.3 HRMS-ESI: cacld for $C_{22}H_{41}NO_3SiNa$: 418.2753; Found 418.2752.

(7*Z*,9*S*,10*S*,11*R*,12*E*)-10-hydroxy-9-methoxy-11,13-dimethylazacyclo-tetradeca-7,12-dien-2-one (84)

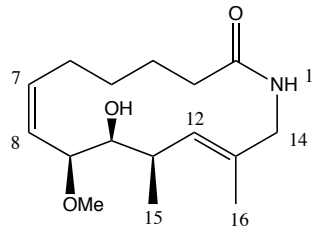

Compound **82** (18.1 mg, 0.046 mmol) was dissolved up in THF (3 mL) and transferred to a plastic reaction vessel. HF in pyridine (70 %, 220 μL) was added dropwise and the resulting mixture was stirred for a further 24 h. The reaction temperature was reduced to 0 °C and methoxytrimethylsilane (2.5 mL, 18.1 mmol) was added dropwise to quench the reaction. This was stirred for a further 30 min at room temperature. The mixture was concentrated and chromatography (EtOAc, 100 %) afforded the desired compound (11.7 mg, 91 %) as a white solid. This was then re-crystallised from hot EtOAc to yield a crystalline material.

^{1}H NMR (500 MHz, Chloroform-d) δ 5.77 (br s, 1H, NH, overlapping peak), 5.73 (td, *J* = 10.4, 6.1 Hz, 1H, overlapping peak, H-7), 5.39 (apt t, *J* = 10.6 Hz, 1H, H-8), 5.09 (d, *J* = 10.1 Hz, 1H, H-12), 4.07 (dd, *J* = 15.9, 7.7 Hz, 1H, H-14a), 3.93 (dd, *J* = 10.0, 3.6 Hz, 1H, H-9), 3.54 (dd, *J* = 16.0, 5.3 Hz, 1H, H-14b), 3.24 (s, 3H, OMe), 3.16 (dd, *J* = 7.4, 3.5 Hz, 1H, H-10), 2.72 (apt dp, *J* = 10.2, 7.2 Hz, 1H, H-11), 2.47 (s, 1H, OH) 2.31 - 2.24 (m, 3H, overlapping peaks, H-3 and H-6a), 1.99 - 1.91 (m, 1H, H-4a), 1.83 (ddt, *J* = 13.2, 10.0, 4.9 Hz, 1H, H-6b), 1.72 (s, 3H, H-16), 1.68 - 1.52 (m, 2H, overlapping peaks, H-5a and H-4b), 1.29 (dtt, *J* = 13.5, 8.9, 4.4 Hz, 1H, H-5b), 1.01 (d, *J* = 7.0 Hz, 3H, H-15).

^{13}C NMR (126 MHz, Chloroform-d) δ 172.0 (C-2), 134.2 (C-7), 133.7 (C-13), 128.0 (C-8), 126.8 (C-12), 79.3 (C-10), 75.9 (C-9), 55.8 (O*C*H$_3$), 45.0 (C-14), 36.3 (C-11), 35.4 (C-3), 28.1 (C-5), 27.5 (C-6), 24.6 (C-4), 18.0 (C-15), 16.1 (C-16).

IR (ATR) cm^{-1}: 3399, 3327, 2929, 1644, 1554, 1236, 753

ESI/MS$^-$ (*m/z*): (M+Na$^+$); 304.2 HRMS-ESI: cacld for $C_{16}H_{27}NO_3Na$: 304.1889; Found 304.1888.

(7*E*,9*S*,10*S*,11*R*,12*E*)-10-hydroxy-9-methoxy-11,13-dimethylazacyclotetradeca-7,12-dien-2-one (85)

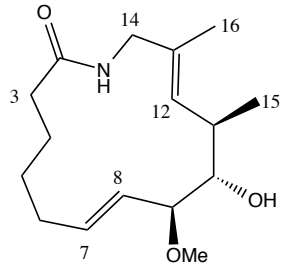

Compound **83** (16 mg, 0.041 mmol) was dissolved up in THF (3 mL) and transferred to a nalgene falcon tube. HF in pyridine (70 %, 220 µL) was added dropwise and the resulting mixture was stirred for 24 h at room temperature. The temperature was reduced to 0 °C via an ice bath and methoxytrimethylsilane (2.5 mL, 18.1 mmol) was added dropwise to quench the reaction. This was stirred for a further 30 min at room temperature. The mixture was concentrated and chromatography (EtOAc, 100 %) afforded the desired title compound (10.3 mg, 90 %) as a white solid.

^{1}H NMR (500 MHz, Chloroform-d) δ 5.63 (ddd, *J* = 15.6, 7.5, 5.1 Hz, 1H, H-7), 5.46 (apt s, 1H, NH), 5.18 (dd, *J* = 15.4, 7.6 Hz, 1H, H-8), 5.10 (d, *J* = 9.6 Hz, 1H, H-12), 4.00 (dd, *J* = 15.5, 7.7 Hz, 1H, H-14a), 3.47 (dd, *J* = 15.3, 4.4 Hz, 1H, H-14b), 3.29 - 3.26 (m, 1H, H-10), 3.25 (s, 3H, OMe), 3.20 (apt t, *J* = 7.9 Hz, 1H, H-9), 2.43 (apt dp, *J* = 16.1, 9.6, 7.0 Hz, 1H, H-11), 2.29 - 2.22 (m, 2H, H-3, overlapping peak), 2.21 - 2.15 (m, 1H, H-6a, overlapping peak), 2.07 - 1.95 (m, 1H, H-6b), 1.80 - 1.73 (m, 1H, H-4a), 1.69 - 1.64 (m, 1H, H-4b), 1.63 (s, 3H, H-16), 1.60 - 1.47 (m, 2H, H-5), 1.06 (d, *J* = 6.7 Hz, 3H, H-15).

^{13}C NMR (126 MHz, Chloroform-d) δ 172.8 (C-2), 134.3 (C-7), 131.1 (C-13), 128.7 (C-12), 126.7 (C-8), 86.2 (C-9), 78.4 (C-10), 55.9 (O*C*H$_3$), 45.5 (C-14), 37.2 (C-11), 36.2 (C-3), 30.0 (C-6), 26.2 (C-5), 24.3 (C-4), 18.8 (C-15), 16.2 (C-16).

IR (ATR) cm^{-1}: 3323, 3194, 1641, 1557,1247, 962

ESI/MS^- (*m/z*): ($M+Na^+$); 304.2 HRMS-ESI: cacld for $C_{16}H_{27}NO_3Na$: 304.1889; Found 304.1883.

ethyl (4*R*,5*S*,6*S*,*Z*)-5-((*tert*-butyldimethylsilyl)oxy)-6-methoxy-2,4-dimethylocta-2,7-dienoate (86)[1]

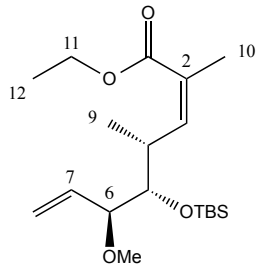

To a solution of compound **59** (1 g, 2.99 mmol) in anhydrous THF (45 mL) was added NaH (60 % dispersion in mineral oil, 142 mg, 3.55 mol) portionwise at 0 °C and under stirring for 1 h. The mixture temperature was lowered to -78 °C, where upon a solution of compound **55** (0.810 g, 2.98 mmol) in THF (25 mL) was then slowly added and stirring was continued for 30 min at -78 °C. The resulting mixture was warmed to 0 °C and stirred for 17 h at this temperature. The reaction was quenched with saturated aqueous NH_4Cl (40 mL). The aqueous phase was extracted with EtOAc (4 x 100 mL). The combined organic layers were dried over Na_2SO_4, and the solvent was removed *in vacuo*. Chromatography (Petroleum Ether/EtOAc, 30:1) of the residue afforded the title compound (0.828 g, 78 %, ratio of *Z*:*E* = 97:3) as a colourless oil.

^1H NMR (500 MHz, Chloroform-d) δ 5.96 (apt dd, *J* = 9.7, 1.5 Hz, 1H, H-3), 5.64 (ddd, *J* = 17.2, 10.4, 8.5 Hz, 1H, H-7), 5.30 – 5.21 (m, 2H, H-8), 4.18 (apt dq, *J* = 7.1, 0.9 Hz, 2H, H-11), 3.61 (dd, *J* = 7.6, 2.5 Hz, 1H, H-5), 3.37 (apt t, *J* = 8.1 Hz, 1H, H-6), 3.27 – 3.21 (m, 1H, H-4), 3.20 (s, 3H, OMe), 1.88 (d, *J* = 1.4 Hz, 3H, H-10), 1.28 (t, *J* = 7.1 Hz, 3H, H-12), 0.93 (d, *J* = 6.7 Hz, 3H, H-9), 0.90 (s, 9H, TBS group (3 x CH_3)), 0.06 (s, 3H, CH_3), 0.01 (s, 3H, CH_3).

^{13}C NMR (126 MHz, Chloroform-d) δ 168.1 (C-1), 147.1 (C-3), 135.1 (C-7), 125.5 (C-2), 118.8 (C-8), 86.8 (C-6), 77.7 (C-5), 60.2 (C-11), 56.1 (O*C*H$_3$), 35.5 (C-4), 26.3 (C(*C*H$_3$)$_3$), 20.9 (C-10), 18.7 (*C*(CH$_3$)$_3$), 14.5 (C-12), 13.1 (C-9), -3.6 (Si*C*H$_3$), -4.8 (Si*C*H$_3$).

IR (ATR) cm^{-1}: 2930, 1714, 1645, 1247, 1117, 830, 774

ESI/MS$^-$ (*m/z*) (M+Na$^+$); 379.2 HRMS-ESI: cacld for $C_{19}H_{36}O_4NaSi$: 379.2281; Found 379.2270.

(7*E*,9*S*,10*S*,11*R*,12*Z*)-10-((*tert*-butyldimethylsilyl)oxy)-9-methoxy-11,13-dimethylazacyclotetradeca-7,12-dien-2-one (87)[2]

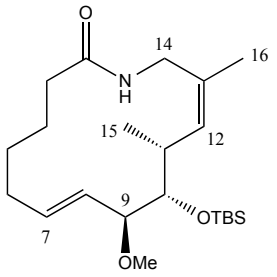

The mixture of compounds, **80** (~ 10 %) and **81** (~ 90 %) (57 mg, 0.135 mmol) was dissolved up in anhydrous degassed toluene (220 mL) and added to the reaction flask. The solution was heated to reflux under stirring and Grubbs-II generation catalyst (23 mg, 0.027 mmol), dissolved in anhydrous degassed toluene (30 mL), was added via cannula. This mixture was heated for 25 min under reflux. The content's of the flask was concentrated under diminished pressure. The residue was flushed though a plug of silica (Petroleum Ether/EtOAc, 1:1) to remove the catalyst. Flash chromatography (Petroleum Ether/EtOAc, 2:1) afforded the title compound (28 mg, 53 %) as a clear oil.

^{1}H NMR (500 MHz, Chloroform-d) δ 5.78 (dt, *J* = 15.5, 6.9 Hz, 1H, H-7), 5.47 (d, *J* = 9.9 Hz, 1H, H-12), 5.39 – 5.33 (m, 2H, NH and H-8, overlapping peaks), 3.77 (dd, *J* = 13.9, 3.6 Hz, 1H, H-14a), 3.66 (dd, *J* = 13.9, 5.5 Hz, 1H, H-14b), 3.48 – 3.44 (m, 2H, H-9 and H-10, overlapping peaks), 3.21 (s, 3H, OMe), 2.63 – 2.56 (m, 1H, H-11), 2.27 – 2.14 (m, 3H, H-3 and H-6a, overlapping peaks), 2.10 – 2.02 (m, 1H, H-6b), 1.74 (d, *J* = 1.5 Hz, 3H, H-16), 1.65 – 1.57 (m, 3H, H-5 and H-4a, overlapping peaks), 1.48 – 1.40 (m, 1H, H-4b), 0.96 – 0.88 (m, 12H, H-15 and TBS group (3 x CH_3)), 0.07 (s, 3H, CH_3), 0.06 (s, 3H, CH_3).

^{13}C NMR (126 MHz, Chloroform-d) δ 173.4 (C-2), 134.3 (C-12), 134.1 (C-7), 129.2 (C-13), 128.7 (C-8), 85.0 (C-9 or C-10), 77.6 (C-9 or C-10), 56.5 (O*C*H_3), 41.6 (C-14), 36.2 (C-3), 34.7 (C-11), 29.8 (C-6), 27.6 (C-4), 26.3 (C(*C*H_3)$_3$), 24.9 (C-4), 24.5 (C-16), 18.7 (*C*(CH_3)$_3$), 15.1 (C-15), -3.7 (Si*C*H_3), -4.8 (Si*C*H_3).

IR (ATR) cm^{-1}: 3243, 2928, 1637, 1245, 981, 832, 776, 670

ESI/MS^- (*m/z*) ($M+Na^+$); 418.2 HRMS-ESI: cacld for $C_{22}H_{41}NO_3NaSi$: 418.2753; Found 418.2749.

ethyl (*E*)-hepta-2,6-dienoate (88)[6]

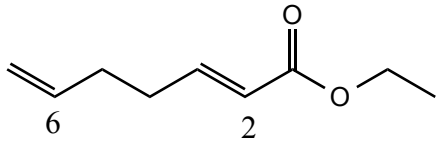

To a solution of 4-penten-1-ol (1.2 mL, 11.6 mmol) in anhydrous DCM (50 mL) was added BAIB (4.5 g, 14.0 mmol) and stirred for 10 min. TEMPO (181 mg, 1.16 mmol) was added and the reaction was vigorously stirred for 4 h at room temperature. After 4 h, (Carbethoxymethylene)triphenylphosphorane (5.25 g, 15.1 mmol) was added and the reaction mixture was stirred for 16 h. The reaction was quenched with H_2O (30 mL). The organic phase was removed and the aqueous phase was back extracted with DCM (3 x 100 mL). The combined organic layers were dried over Na_2SO_4. And concentrated *in vacuo*. Care was taken whilst drying it as the compound has a low boiling point. Flash chromatography (Petroleum Ether/EtOAc, 50:1) furnished the title compound (0.824 g, 46 %, yield was based on 4-penten-1-ol) as a clear oil.

^1H NMR (500 MHz, Chloroform-d) δ 6.95 (dt, *J* = 15.6, 6.7 Hz, 1H, H-3), 5.85 – 5.73 (m, 2H, H-6 and H-2, overlapping peaks), 5.07 – 4.97 (m, 2H, H-7), 4.17 (q, *J* = 7.1 Hz, 2H, H-8), 2.34 – 2.26 (m, 2H, H-4), 2.25 – 2.14 (m, 2H, H-5), 1.27 (t, *J* = 7.1 Hz, 3H, H-9).

^{13}C NMR (126 MHz, Chloroform-d) δ 166.7 (C-1), 148.3 (C-3), 137.2 (C-6 or C-2), 121.8 (C-6 or C-2), 115.6 (C-7), 60.3 (C-8), 32.2 (C-4 or C-5), 31.6 (C-4 or C-5), 14.4 (C-9).

IR (ATR) cm^{-1}: 2981, 1718, 1655, 1264, 988

(*E*)-hepta-2,6-dienoic acid (89)

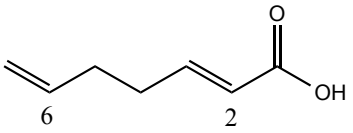

Compound **88** (700 mg, 4.55 mmol) was dissolved up in a mixed solvent system (THF/H_2O, 18 mL). The solution was vigorously stirred and heated to 50 °C. To the solution was added NaOH (1.82 g, 45.5 mmol) portionwise and stirred for 5 h. The mixture was acidified to pH 1 with HCl (1 M). The organic layer was removed and the aqueous phase was back extracted with EtOAc (3 x 40 mL). The combined organics were washed with brine and dried over Na_2SO_4. The solvent was removed under diminished pressure and flash chromatography (Petroleum Ether/EtOAc, 1:1) afforded the title product (470 mg, 82 %) as a clear oil.

^{1}H NMR (500 MHz, Chloroform-d) δ 7.09 (dt, *J* = 15.6, 6.8 Hz, 1H, H-3), 5.86 (d, *J* = 15.7 Hz, 1H, H-2, overlapping peak with H-6), 5.84 – 5.76 (m, 1H, H-6, overlapping peak with H-2), 5.10 – 5.01 (m, 2H, H-7), 2.40 – 2.31 (m, 2H, H-4), 2.29 – 2.21 (m, 2H, H-5).

^{13}C NMR (126 MHz, Chloroform-d) δ 172.0 (C-1), 151.4 (C-3), 137.0 (C-6 or C-2), 121.2 (C-6 or C-2), 115.9 (C-7), 32.0 (C-5 or C-4), 31.7 (C-5 or C-4).

IR (ATR) cm^{-1}: 2981, 1691, 1650, 1417, 1285, 988, 910

ESI/MS$^-$ (*m/z*) (M-H$^+$); 125.1 HRMS-ESI: cacld for $C_7H_9O_2$: 125.0603; Found 125.0607.

(*E*)-*N*-((4*R*,5*S*,6*S*,*Z*)-5-((*tert*-butyldimethylsilyl)oxy)-6-methoxy-2,4-dimethylocta-2,7-dienyl)hepta-10,14-dienamide (90)

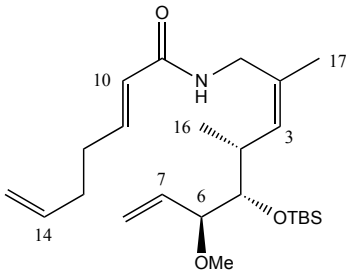

The reacting mixture containing desired product **77** and isomerised product **76** (270 mg, 0.796 mmol) was reduced in the same manner as compound **80**. The residue containing reduced primary amine and triphenylphosphine oxide was taken up in anhydrous DCM (7 mL) and the reaction was lowered to 0 °C. To this solution was added DIPEA (555 µL, 3.19 mmol), EDC.HCL (305 mg, 1.59 mmol) and compound **89** (200 mg, 1.59 mmol) sequentially. The mixture was allowed to warm back up to room temperature and was stirred for 4 h. The reaction was then concentrated to circa 1.5 mL. Purification of the residual solution by flash chromatography (Petroleum Ether/EtOAc, 6:1) afforded the title compound (268 mg, 80 %, the yield was based on the ratio of starting *Z* isomer **77** present in the reacting mixture) as a clear oil.

^{1}H NMR (500 MHz, Chloroform-d) δ 6.83 (dt, *J* = 15.2, 6.7 Hz, 1H, H-11), 5.85 – 5.73 (m, 2H, H-14 and H-10, overlapping peaks), 5.67 (ddd, *J* = 17.2, 10.5, 7.7 Hz, 1H, H-7), 5.48 (br s, 1H, NH), 5.38 – 5.22 (m, 3H, H-8 and H-3, overlapping peaks), 5.08 – 4.96 (m, 2H, H-15), 3.93 (dd, *J* = 14.0, 5.8 Hz, 1H, H-1a), 3.84 (ddd, *J* = 14.0, 5.5, 1.0 Hz, 1H, H-1b), 3.46 (dd, *J* = 6.7, 3.3 Hz, 1H, H-5), 3.44 – 3.40 (m, 1H, H-6), 3.22 (s, 3H, OMe), 2.61 (dqd, *J* = 9.9, 6.7, 3.3 Hz, 1H, H-4), 2.30 – 2.24 (m, 2H, H-12), 2.23 – 2.18 (m, 2H, H-13), 1.70 (d, *J* = 1.4 Hz, 3H, H-17), 0.92 – 0.89 (m, 12H, H-16 and TBS group (3 x CH_3)), 0.06 (s, 3H, CH_3), 0.03 (s, 3H, CH_3).

^{13}C NMR (126 MHz, Chloroform-d) δ 166.0 (C-9), 143.8 (C-11), 137.5 (C-10 or C-14), 135.2 (C-7), 134.1 (C-3), 130.0 (C-2), 124.0 (C-10 or C-14), 118.8 (C-8), 115.5 (C-15), 86.1 (C-6 or C-5), 78.4 (C-6 or C-5), 56.3 (O*C*H$_3$), 40.0 (C-1), 34.5 (C-4), 32.4 (C-13), 31.5 (C-12), 26.3 (C(*C*H$_3$)$_3$), 22.1 (C-17), 18.7 (*C*(CH$_3$)$_3$), 15.0 (C-16), -3.7 (Si*C*H$_3$), -4.6 (Si*C*H$_3$).

IR (ATR) cm^{-1}: 3277, 2929, 1669, 1628, 1547, 1248, 927, 830, 775, 671

ESI/MS$^-$ (*m/z*) (M+Na$^+$); 444.3 HRMS-ESI: cacld for $C_{24}H_{43}NO_3NaSi$: 444.2910; Found 444.2925.

(*E*)-*N*-((4*R*,5*S*,6*S*,*Z*)-5-hydroxy-6-methoxy-2,4-dimethylocta-2,7-dien-1-yl)hepta-10,14-dienamide (91)

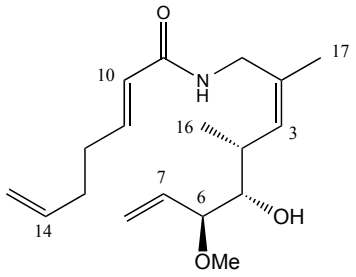

Compound **90** (22 mg, 0.052 mmol) was dissolved up in THF (1.1 mL) and transferred to a plastic reaction vessel. To this was added HF in pyridine (70 %, 210 µL) dropwise and the mixture was stirred for 20 h at room temperature. The temperature was reduced to 0 °C and quenched with methoxytrimethylsilane (2.5 mL, 18.1 mmol) which was added slowly. This was stirred for a further 30 min at room temperature. The mixture was concentrated *in vacuo* and flash chromatography (Petroleum Ether/EtOAc, 3:1) afforded the title compound (11.5 mg, 72 %) as a clear oil.

^{1}H NMR (500 MHz, Chloroform-d) δ 6.82 (dt, *J* = 15.3, 6.7 Hz, 1H, H-11), 5.88 – 5.60 (m, 4H, H-14, H-10, H-7 and NH, overlapping peaks), 5.42 – 5.23 (m, 3H, H-8 and H-3, overlapping peaks), 5.11 – 4.95 (m, 2H, H-15), 3.96 (dd, *J* = 14.1, 5.9 Hz, 1H, H-1a), 3.86 (dd, *J* = 14.0, 5.1 Hz, 1H, H-1b), 3.49 (dd, *J* = 8.1, 5.7 Hz, 1H, H-6), 3.31 (apt q, *J* = 5.2 Hz, 1H, H-5), 3.27 (s, 3H, OMe), 2.75 – 2.66 (m, 1H, H-4), 2.58 (d, *J* = 4.5 Hz, 1H, OH), 2.30 – 2.24 (m, 2H, H-12), 2.22 – 2.17 (m, 2H, H-13)
1.74 (d, *J* = 1.5 Hz, 3H, H-17), 1.00 (d, *J* = 6.8 Hz, 3H, H-16).

^{13}C NMR (126 MHz, Chloroform-d) δ 166.0 (C-9), 143.8 (C-11), 137.5 (C-14 or C-10 or C-7), 135.3 (C-14 or C-10 or C-7), 132.0 (C-2), 131.8 (C-3), 124.1 (C-14 or C-10 or C-7), 119.9 (C-8), 115.5 (C-15), 83.7 (C-6), 77.5 (C-5), 56.3 (O*C*H$_3$), 40.0 (C-1), 35.0 (C-4), 32.5 (C-13), 31.5 C-12), 22.6 (C-17), 16.5 (C-16).

IR (ATR) cm^{-1}: 3288, 2930, 1669, 1626, 1542, 1230, 983

ESI/MS$^-$ (*m/z*) (M+Na$^+$); 330.2 HRMS-ESI: cacld for $C_{18}H_{29}NO_3Na$: 330.2045; Found 330.2053.

4.3 Experimental data - Chapter 2

2,3,4,6-Tetra-O-acetyl-β-D-galactopyranosyl-(1→4)-1,2,3,6-tetra-O-acetyl-α/β-D-glucopyranoside (99)[7]

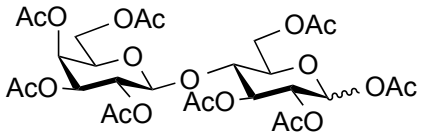

Acetic anhydride (135 mL) and sodium acetate (10.55 g, 128.6 mmol) was added to a dry round bottom flask. The suspension was gently heated to reflux under stirring. After 10 min at reflux, D-Lactose (40 g, 116.9 mmol) was added carefully ~1 g/min. Once all the lactose was added, the reaction was refluxed for a further 30 min. Chloroform (400 mL) was added to the mixture and the mixture was lowered to 0 °C. Ice (20 g) was then added to the reaction flask portionwise under stirring. Ice H_2O (300 mL) was added and the flask contents were transferred to a separating funnel. The layers were separated and the organic portion was further washed with ice H_2O (3 x 200 mL). Cold $NaHCO_3$ (300 mL) was added to the organic portion. The organic portion was further washed with cold $NaHCO_3$ (3 x 200 mL). The organics was then dried over Na_2SO_4 and concentrated under reduced pressure. Chromatography (EtOAc, 100 %) afforded the title product (41.2 g, 52 %) as a white solid, as a mixture of anomers (β:α 9:1).

^{1}H NMR (500 MHz, Chloroform-d) δ 5.64 (d, *J* = 8.3 Hz, 1H, H-1), 5.31 (dd, *J* = 3.5, 1.2 Hz, 1H, H-4'), 5.21 (apt t, *J* = 9.2 Hz, 1H, H-3), 5.07 (dd, *J* = 10.4, 7.9 Hz, 1H, H-2'), 5.01 (dd, *J* = 9.4, 8.3 Hz, 1H, H-2), 4.92 (dd, *J* = 10.4, 3.5 Hz, 1H, H-3'), 4.46 – 4.40 (m, 2H, H-1' and H-6a, overlapping peaks), 4.13 – 4.02 (m, 3H, H-6' and H-6b, overlapping peaks), 3.88 – 3.78 (m, 2H, H-4 and H-5', overlapping peaks), 3.73 (ddd, *J* = 9.9, 4.9, 2.0 Hz, 1H, H-5), 2.12 (s, 3H, $COCH_3$), 2.08 (s, 3H, $COCH_3$), 2.06 (s, 3H, $COCH_3$), 2.01 (apt dd, *J* = 11.6, 7.3 Hz, 12H, 4 x $COCH_3$), 1.93 (s, 3H, $COCH_3$).

^{13}C NMR (126 MHz, Cloroform-d) δ 170.4 (C=O), 170.4 (C=O), 170.2 (C=O), 170.1 (C=O), 169.7 (C=O), 169.6 (C=O), 169.1 (C=O), 168.9 (C=O), 101.0 (C-1'), 91.6 (C-1), 75.7 (C-4 or C-5'), 73.6 (C-5), 72.7 (C-3), 71.0 (C-3'), 70.8 (C-4 or C-5'), 70.6 (C-2), 69.1 (C-2'), 66.7 (C-4'), 61.8 (C-6), 60.9 (C-6'), 20.9 (CH_3), 20.9 (CH_3), 20.9 (CH_3), 20.8 (CH_3), 20.7 (CH_3), 20.7 (CH_3), 20.7 (CH_3), 20.6 (CH_3).

IR (ATR) cm^{-1}: 1739, 1209, 1041

ESI/MS^- (*m/z*) ($M+NH_4^+$); 696.2 HRMS-ESI: cacld for $C_{28}H_{42}NO_{19}$: 696.2351; Found 696.2348.

2,3,4,6-Tetra-O-acetyl-β-D-galactopyranosyl-(1→4)-2,3,6-tri-O-acetyl-α-D-glucopyranoside bromide (100)[8]

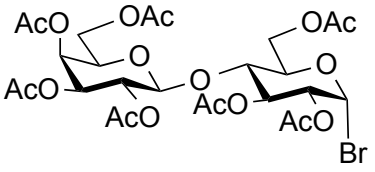

To a stirred solution of compound **99** (25 g, 36.9 mmol) was added glacial acetic acid (7.5 mL) and acetic anhydride (7.5 mL) at 0 °C. HBr (33 wt.% in acetic acid, 25 mL) dropwise. The reaction was stirred overnight at 0 °C and diluted with chloroform (400 mL). Ice (17 g) was then added to the reaction flask portionwise under stirring. Ice H_2O (300 mL) was added and the flask content's was transferred to a separating funnel. The organic portion was further washed with ice H_2O (3 x 200 mL). Cold $NaHCO_3$ (300 mL) was added to the organic portion. The organic portion was further washed with cold $NaHCO_3$ (3 x 200 mL) to neutralise the excess acid. The organic layer was then dried over Na_2SO_4 and concentrated under reduced pressure. Chromatography (EtOAc, 100 %) gave the title compound (11.2 g, 43 %) as a white solid.

^{1}H NMR (500 MHz, Chloroform-d) δ 6.52 (d, *J* = 4.0 Hz, 1H, H-1), 5.55 (t, *J* = 9.6 Hz, 1H, H-3), 5.35 (dd, *J* = 3.5, 1.2 Hz, 1H, H-4'), 5.12 (dd, *J* = 10.4, 7.9 Hz, 1H, H-2'), 4.96 (dd, *J* = 10.4, 3.5 Hz, 1H, H-3'), 4.76 (dd, *J* = 10.0, 4.1 Hz, 1H, H-2), 4.53 – 4.47 (m, 2H, H-6a and H-1', overlapping peaks), 4.23 – 4.05 (m, 4H, H-5, H-6b and H-6', overlapping peaks), 3.91 – 3.83 (m, 2H, H-5' and H-4, overlapping peaks), 2.16 (s, 3H, $COCH_3$), 2.13 (s, 3H, $COCH_3$), 2.07 – 2.04 (m, 9H, 3 x $COCH_3$), 1.96 (s, 3H, $COCH_3$).

^{13}C NMR (126 MHz, Chloroform-d) δ 170.5 (C=O), 170.3 (C=O), 170.3 (C=O), 170.2 (C=O), 170.1 (C=O), 169.4 (C=O), 169.1 (C=O), 100.9 (C-1'), 86.5 (C-1), 75.1 (C-4 or C-5'), 73.1 (C-5), 71.2 (C-3'), 71.0 (C-2), 70.9 (C-4 or C-5'), 69.8 (C-3), 69.2 (C-2'), 66.8 (C-4'), 61.2 (C-6), 61.0 (C-6'), 21.0 (CH_3), 20.9 (CH_3), 20.8 (CH_3), 20.8 (CH_3), 20.8 (CH_3), 20.8 (CH_3), 20.6 (CH_3).

IR (ATR) cm^{-1}: 1736, 1211, 1036

2,3,4,6-Tetra-O-acetyl-β-D-galactopyranosyl-(1→4)-2,3,6-tetra-O-acetyl-β-D-glucopyranoside-1-azido (101)[9]

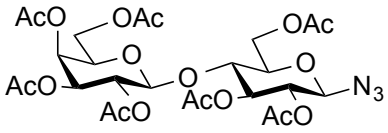

To a stirred solution of compound **100** (25 g, 35.8 mmol) and tetrabutylammonium hydrogensulfate (12.1 g, 35.6 mmol) in a solvent mixture consisting of DCM (250 mL) and saturated $NaHCO_3$ (250 mL) at room temperature was added NaN_3 (11.6 g, 178.4 mmol). The reaction stirred vigorously for 4 h. The mixture was then transferred a separating funnel and the aqueous phase back extracted with DCM (3 x 100 mL). The combined organics were dried over Na_2SO_4 and concentrated under reduced pressure. The residue was purified by chromatography (Petroleum Ether/EtOAc, 1:1) to yield the title compound (19.6 g, 83 %) as a white solid.

^{1}H NMR (500 MHz, Chloroform-d) δ 5.31 (apt d, *J* = 3.4 Hz, 1H, H-4'), 5.17 (apt t, *J* = 9.3 Hz, 1H, H-3), 5.06 (dd, *J* = 9.9, 8.1 Hz, 1H, H-2'), 4.95 – 4.88 (m, 1H, H-3'), 4.86 – 4.78 (m, 1H, H-2), 4.60 (d, *J* = 8.8 Hz, 1H, H-1), 4.50 – 4.44 (m, 2H, H-1' and H-6a, overlapping peaks), 4.16 – 4.01 (m, 3H, H-6' and H-6b, overlapping peaks), 3.88 – 3.82 (m, 1H, H-5'), 3.78 (apt td, *J* = 9.4, 8.8, 1.0 Hz, 1H, H-4), 3.71 – 3.65 (m, 1H, H-5), 2.11 (s, 3H, $COCH_3$), 2.10 (s, 3H, $COCH_3$), 2.04 – 2.00 (m, 12H, 4 x $COCH_3$), 1.92 (s, 3H, $COCH_3$).

^{13}C NMR (126 MHz, Chloroform-d) δ 170.4 (C=O), 170.3 (C=O), 170.1 (C=O), 170.1 (C=O), 169.6 (C=O), 169.5 (C=O), 169.1 (C=O), 101.1 (C-1'), 87.7 (C-1), 75.8 (C-4), 74.9 (C-5), 72.6 (C-3), 71.0 (C-3' or C-2), 71.0 (C-3' or C-2), 70.8 (C-5'), 69.1 (C-2'), 66.7 (C-4'), 61.8 (C-6), 60.9 (C-6'), 20.8 (CH_3), 20.8 (CH_3), 20.7 (CH_3), 20.7 (CH_3), 20.7 (CH_3), 20.6 (CH_3), 20.5 (CH_3).

IR (ATR) cm^{-1}: 2941, 2119, 1740, 1211, 1042

ESI/MS$^-$ (*m/z*) (M+Na$^+$); 684.2 HRMS-ESI: cacld for $C_{26}H_{35}N_3O_{17}Na$: 684.1864; Found 684.1873.

2,3,4,6-Tetra-O-acetyl-β-D-galactopyranosyl-(1→4)-2,3,6-tetra-O-acetyl-α/β-D-glucopyranoside-1-amine (102)[10] and (103)

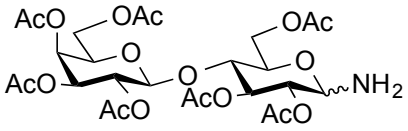

To a solution of compound **101** (9 g, 13.6 mmol) in anhydrous degassed EtOAc (100 mL) was added 10 wt.% Pd/C (1.4 g, 1.32 mmol). A H_2 filled balloon was inserted via a needle and rubber septum. The reaction was stirred vigorously for 5 h and the reaction mixture was passed through Celite to remove the catalyst. The residue was purified by flash chromatography (EtOAc, 100 %) to give the title compound (6.9 g, 80 %) as an off white solid, as a mixture of anomers (β:α 9:1).

^{1}H NMR (500 MHz, Chloroform-d) δ 5.32 (dd, *J* = 3.4, 1.2 Hz, 1H, H-4'), 5.20 (apt t, *J* = 9.4 Hz, 1H, H-3), 5.07 (dd, *J* = 10.4, 7.9 Hz, 1H, H-2'), 4.92 (dd, *J* = 10.4, 3.5 Hz, 1H, H-3'), 4.70 (dd, *J* = 9.7, 9.0 Hz, 1H, H-2), 4.52 – 4.40 (m, 2H, H-1' and H-6a, overlapping peaks), 4.16 – 4.01 (m, 4H, H-1, H-6b and H-6'), 3.85 (ddd, *J* = 7.4, 6.2, 1.3 Hz, 1H, H-5'), 3.70 (apt t, *J* = 9.5 Hz, 1H, H-4), 3.57 (ddd, *J* = 9.9, 5.2, 2.1 Hz, 1H, H-5), 2.10 (s, 3H, $COCH_3$), 2.05 – 2.01 (m, 12H, 4 x $COCH_3$), 1.93 (s, 3H, $COCH_3$).

^{13}C NMR (126 MHz, Chloroform-d) δ 170.5 (C=O), 170.5 (C=O), 170.4 (C=O), 170.2 (C=O), 170.1 (C=O), 169.7 (C=O), 169.1 (C=O), 101.1 (C-1'), 84.7 (C-1), 76.7 (C-4), 73.8 (C-5), 73.1 (C-3), 72.6 (C-2), 71.1 (C-3'), 70.7 (C-5'), 69.2 (C-2'), 66.7 (C-4'), 62.5 (C-6), 60.9 (C-6'), 21.0 (CH_3), 20.9 (CH_3), 20.9 (CH_3), 20.7 (CH_3), 20.7 (CH_3), 20.6 (CH_3), 20.6 (CH_3).

IR (ATR) cm^{-1}: 2945, 1736, 1211, 1042

ESI/MS^- (*m/z*) ($M+H^+$); 636.2 HRMS-ESI: cacld for $C_{26}H_{38}NO_{17}$: 636.2140; Found 636.2134.

2,3,4,6-Tetra-O-acetyl-β-D-galactopyranosyl-(1→4)-2,3,6-tetra-O-acetyl-β-D-glucopyranoside-1-fluorenylmethyloxycarbonyl-L-asparagine *tert*-butyl ester (104)[11]

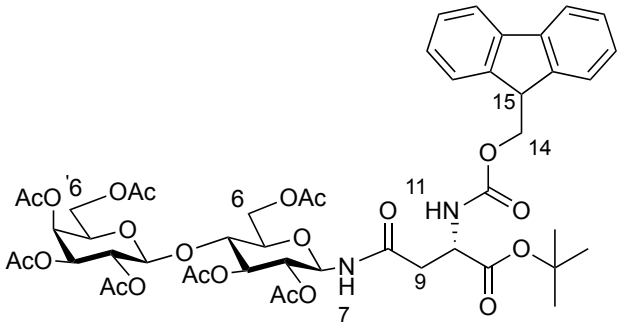

Fmoc aspartic acid with the C-terminus protected (647 mg, 1.57 mmol) and 2-ethoxy-1-ethoxycarbonyl-1,2-dihydroquinoline (427 mg, 1.73 mmol) were added sequentially to a solution of 9:1 anomeric compounds **102** and **103** respectively (1 g, 1.57 mmol) in DCM (40 mL). The reaction was stirred for 5 h and the solvent was removed via reduced pressure to yield a white solid. The solid was purified by chromatography (Petroleum Ether/EtOAc, 1:1) yielding the titled compound (0.835 g, 52 %) as a white solid.

^{1}H NMR (500 MHz, Chloroform-d) δ 7.72 (d, *J* = 7.5 Hz, 2H, ArH), 7.59 – 7.55 (m, 2H, ArH), 7.36 (apt t, *J* = 7.5 Hz, 2H, ArH), 7.31 – 7.22 (m, 2H, ArH), 6.58 (d, *J* = 9.2 Hz, 1H, NH, H-7), 5.97 (d, *J* = 8.6 Hz, 1H, NH, H-11), 5.32 (dd, *J* = 3.5, 1.1 Hz, 1H, H-4'), 5.29 – 5.24 (m, 1H, H-3), 5.18 (apt t, *J* = 9.3 Hz, 1H, H-1), 5.07 (dd, *J* = 10.4, 7.9 Hz, 1H, H-2'), 4.92 (dd, *J* = 10.4, 3.5 Hz, 1H, H-3'), 4.81 (apt t, *J* = 9.6 Hz, 1H, H-2), 4.46 – 4.42 (m, 2H, H-10 and H-1', overlapping peaks), 4.41 – 4.35 (m, 2H, H-6a and H-14a, overlapping peaks), 4.27 (dd, *J* = 10.6, 7.4 Hz, 1H, H-14b), 4.19 (t, *J* = 7.2 Hz, 1H, H-15), 4.13 – 4.07 (m, 2H, H-6b and H-6a', overlapping peaks), 4.04 (dd, *J* = 11.1, 7.3 Hz, 1H, H-6b'), 3.84 (apt t, *J* = 7.1 Hz, 1H, H-5'), 3.74 (apt t, *J* = 9.4 Hz, 1H, H-4), 3.69 (ddd, *J* = 10.0, 4.8, 1.9 Hz, 1H, H-5), 2.82 (dd, *J* = 16.5, 4.7 Hz, 1H, H-9a), 2.65 (dd, *J* = 16.4, 4.4 Hz, 1H, H-9b), 2.12 (s, 3H, $COCH_3$), 2.02 (apt d, *J* = 6.9 Hz, 12H, 5 x $COCH_3$), 1.93 (s, 3H, $COCH_3$), 1.41 (s, 9H, *t*-Bu).

^{13}C NMR (126 MHz, Chloroform-d) δ 171.2 (C=O), 170.7 (C=O), 170.4 (C=O), 170.3 (C=O), 170.2 (C=O), 170.1 (C=O), 169.8 (C=O), 169.4 (C=O), 169.0 (C=O), 156.2 (ArC), 143.9 (ArC), 143.8 (ArC), 141.3 (ArC), 127.7 (Ar*C*H), 127.7 (Ar*C*H), 127.1 (Ar*C*H), 125.2 (Ar*C*H), 125.2 (Ar*C*H), 120.0 (Ar*C*H), 100.9 (C-1'), 82.4 (*C*(CH_3)$_3$), 77.9 (C-1), 75.9 (C-5), 74.6 (C-4), 72.5 (C-3), 71.0 (C-3' or C-2), 70.9 (C-3' or C-2), 70.7 (C-5'), 69.0 (C-2'), 67.2 (C-14), 66.7 (C-4'), 62.0 (C-6), 60.9 (C-6'), 51.1 (C-10), 47.1 (C-15), 38.0 (C-9), 27.9 (C(*C*H_3)$_3$), 20.8 (CH_3), 20.8 (CH_3), 20.7 (CH_3), 20.7 (CH_3), 20.6 (CH_3), 20.5 (CH_3).

IR (ATR) cm^{-1}: 3287, 1734, 1679, 1559, 1234, 1050, 766

ESI/MS$^-$ (*m/z*) (M+Na$^+$); 1051.4 HRMS-ESI: cacld for $C_{49}H_{60}N_2O_{22}Na$: 1051.3535; Found 1051.3538.

2,3,4,6-Tetra-O-acetyl-β-D-galactopyranosyl-(1→4)-2,3,6-tetra-O-acetyl-β-D-glucopyranoside-1-fluorenylmethyloxycarbonyl-L-asparagine (106)[11]

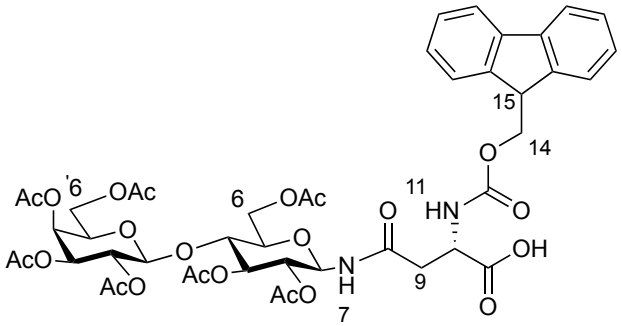

Compound **104** (475 mg, 0.46 mmol) was dissolved in a mixture of DCM (5 mL) and trifluoroacetic acid (5 mL). The solution was stirred for 2 h at room temperature and then azeotroped with toluene to dryness to yield the desired title compound (434 mg, 97 %) as a white solid.

^{1}H NMR (500 MHz, Chloroform-d) δ 7.74 (d, *J* = 7.6 Hz, 2H, ArH), 7.66 – 7.55 (m, 2H, ArH), 7.37 (apt t, *J* = 7.5 Hz, 2H, ArH), 7.30 – 7.26 (m, 2H, ArH), 6.86 (d, *J* = 9.3 Hz, 1H, NH, H-7), 6.29 (d, *J* = 8.2 Hz, 1H, H-11), 5.36 (dd, *J* = 3.4, 1.2 Hz, 1H, H-4'), 5.34 – 5.23 (m, 2H, H-1 and H-3, overlapping peaks), 5.09 (dd, *J* = 10.4, 7.9 Hz, 1H, H-2'), 4.94 (dd, *J* = 10.4, 3.4 Hz, 1H, H-3'), 4.83 (apt t, *J* = 9.5 Hz, 1H, H-2), 4.62 – 4.55 (m, 1H, H-10), 4.48 (d, *J* = 7.9 Hz, 1H, H-1'), 4.45 – 4.36 (m, 2H, H-6a and H-14a, overlapping peaks), 4.32 (dd, *J* = 10.6, 7.3 Hz, 1H, H-14b), 4.20 (t, *J* = 7.3 Hz, 1H, H-15), 4.17 – 4.11 (m, 2H, H-6b and H-6a'), 4.03 (dd, *J* = 11.1, 7.6 Hz, 1H, H-6b'), 3.90 (apt t, *J* = 7.0 Hz, 1H, H-5'), 3.81 – 3.71 (m, 2H, H-4 and H-5, overlapping peaks), 2.93 – 2.88 (m, 1H, H-9a), 2.76 (dd, *J* = 16.7, 5.0 Hz, 1H, H-9b), 2.14 (s, 3H, $COCH_3$), 2.09 – 2.00 (m, 15H, 5 x $COCH_3$), 1.96 (s, 3H, $COCH_3$).

^{13}C NMR (126 MHz, Chloroform-d) δ 173.0 (C=O), 171.5 (C=O), 171.4 (C=O), 170.7 (C=O), 170.6 (C=O), 170.3 (C=O), 170.3 (C=O), 169.8 (C=O), 169.4 (C=O), 156.5 (ArC), 143.9 (ArC), 143.7 (ArC), 141.4 (ArC), 127.9 (Ar*C*H), 127.2 (Ar*C*H), 125.3 (Ar*C*H), 120.1 (Ar*C*H), 101.0 (C-1'), 77.9 (C-1), 76.1 (C-4 or C-5), 74.8 (C-4 or C-5), 72.8 (C-3), 71.1 (C-3' or C-2), 71.1 (C-3' or C-2), 70.6 (C-5'), 69.2 (C-2'), 67.6 (C-14), 66.7 (C-4'), 62.2 (C-6), 60.8 (C-6'), 50.4 (C-10), 47.1 (C-15), 37.7 (C-9), 21.0 (CH_3), 20.9 (CH_3), 20.8 (CH_3), 20.7 (CH_3), 20.7 (CH_3), 20.7 (CH_3).

IR (ATR) cm^{-1}: 3313, 1741, 1529, 1215, 1043, 740

ESI/MS^{-} (*m/z*) ($M-H^{+}$); 971.3 HRMS-ESI: cacld for $C_{45}H_{51}N_2O_{22}$: 971.2933; Found 971.2960.

4.3.1 General synthesis and purification of Coiled coils

Peptides were synthesized on a CEM Liberty Blue automated peptide synthesizer on MBHA resin (0.25 mmol scale), using 3 equivalents of introduced Fmoc amino acid, 2.9 equivalents of HBTU and 6 equivalents of DIPEA, per coupling. Couplings and deprotections of all Fmoc-L-amino acids were performed using a standard double coupling programme (25 W, 75 °C, 5 min) with washings (30–40 mL DMF) in between. The introduction of the modified lactosylated amino acid was performed 'offline' to monitor the coupling reaction over an increased period of time using the Kaiser test protocol. An acetylation capping step after the addition of the modified amino acid was carried out. After the inclusion of the modified amino acid and the capping step, the remaining peptide synthesis was accomplished by automated SPPS. The peptide's N-terminus was acetylated manually using 1 M Ac_2O and 0.4 M DIPEA solution in DMF. The peptide was then cleaved from the resin using 90 % TFA, 5 % thioanisole, 2 % anisole, 3 % 1,2-ethanedithiol for 2 h at room temp.. During the cleavage step, the removal of acid labile protecting groups simultaneously occurred. The resin was removed by filtration and the crude peptides were precipitated out of solution on addition into cold diethyl ether. Crude peptides, both glycosylated and non-glycosylated, were purified using preparative HPLC reverse phase C18 column.

Analysis of the purified peptides was performed on Shimadzu HPLC instrument using a C18 column with a linear gradient of H_2O (0.05 % TFA) and CH_3CN (0.05 % TFA) from 0 to 100 % of CH_3CN in 40 minutes. Characterisation using mass spectrometry in conjunction with HPLC analysis confirmed the structures.

Compound 107

Ac-G IAAIEQK IAAIEQK IAAIE**X**K IAAIEWK G-NH_2

ESI/MS^- (*m/z*) calcd 3554.94 ($M+H^+$); Found 3556.72

Retention Time (min) 22.06

Compound 108

Ac-G IAAIEQK IAAIEWK IAAIEQK IAAIE**X**K G-NH_2

ESI/MS^- (*m/z*) calcd 3554.94 ($M+H^+$); Found 3555.8

Retention Time (min) 21.34

Compound 109

Ac-G IAAIEQK IAAIEQK IAAIEQK IAAIEWK G-NH_2

ESI/MS^- (*m/z*) calcd 3244.85 ($M+H^+$); Found 3245.85

Retention Time (min) 22.39

(7*E*,9*S*,10*S*,11*R*,12*Z*)-9-methoxy-11,13-dimethyl-10-(prop-2-yn-1-yloxy)azacyclotetradeca-7,12-dien-2-one (110)

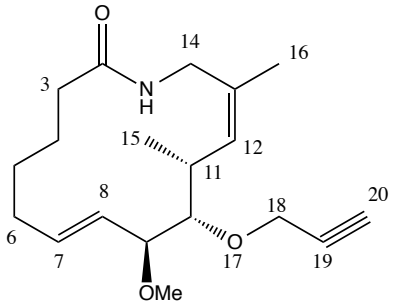

To a flame dried flask was added a solution of compound **43** (33 mg, 0.107 mmol) dissolved in THF (0.5 mL). NaH (60 % dispersion in mineral oil, 7 mg, 0.176 mmol) was added portionwise at 0°C to the flask. The resultant mixture was stirred for 30 min. To this was then added propargyl bromide solution (80 wt.% in toluene, 20 µL, 0.176 mmol) and the mixture was stirred for a further 18 h at room temperature. Saturated aqueous NH_4Cl (3 mL) was added to quench the reaction. The reaction mixture was back extracted with EtOAc (2 x 5 mL). The organic phase was washed with brine and dried over Na_2SO_4. The solvent was reduced under diminished pressure and flash chromatography (Petroleum Ether/EtOAc, 1:1) gave the title compound (26 mg, 70 %) as yellow oil.

^{1}H NMR (500 MHz, Chloroform-d) δ 5.77 (dt, *J* = 14.6, 6.9 Hz, 1H, H-7), 5.57 (d, *J* = 9.9 Hz, 1H, H-12), 5.38 – 5.28 (m, 2H, H-8 and NH, overlapping peaks), 4.43 (dd, *J* = 15.9, 2.4 Hz, 1H, H-18a), 4.35 (dd, *J* = 15.8, 2.3 Hz, 1H, H-18b), 3.81 (dd, *J* = 13.8, 3.8 Hz, 1H, H-14a), 3.70 (apt t, *J* = 7.7 Hz, 1H, H-9), 3.61 (dd, *J* = 13.8, 4.9 Hz, 1H, H-14b), 3.34 – 3.24 (m, 4H, OMe and H-10, overlapping peaks), 2.64 – 2.55 (m, 1H, H-11), 2.41 (t, *J* = 2.4 Hz, 1H, H-20), 2.30 – 2.23 (m, 1H, H-3a), 2.22 – 2.15 (m, 2H, H-3b and H-6a, overlapping peaks), 2.06 – 1.96 (m, 1H, H-6b), 1.76 (d, *J* = 1.4 Hz, 3H, H-16), 1.65 – 1.52 (m, 3H, H-4 and H-5a, overlapping peaks), 1.46 – 1.38 (m, 1H, H-5b), 0.95 (d, *J* = 7.2 Hz, 3H, H-15).

^{13}C NMR (126 MHz, Chloroform-d) δ 173.4 (C-2), 134.6 (C-7), 133.6 (C-12), 129.7 (C-13), 128.8 (C-8), 84.8 (C-9), 83.6 (C-10), 80.9 (C-19), 74.0 (C-20), 59.8 (C-18), 56.7 (O*C*H$_3$), 41.5 (C-14), 36.1 (C-3), 33.4 (C-11), 29.6 (C-6), 27.4 (C-4), 24.7 (C-5), 24.4 (C-16), 15.0 (C-15).

IR (ATR) cm^{-1}: 3288, 2931, 1635, 1536, 1076, 977

ESI/MS$^-$ (*m/z*) (M+Na$^+$); 342.2 HRMS-ESI: cacld for $C_{19}H_{29}NO_3Na$: 342.2045; Found 342.2054.

2,3,4,6-Tetra-O-acetyl-β-D-galactopyranosyl-(1→4)-2,3,6-tetra-O-acetyl-β-D-glucopyranoside--(7*E*,9*S*,10*S*,11*R*,12*Z*)-9-methoxy-11,13-dimethyl-10-oxyazacyclotetradeca-7,12-dien-2-one (111)

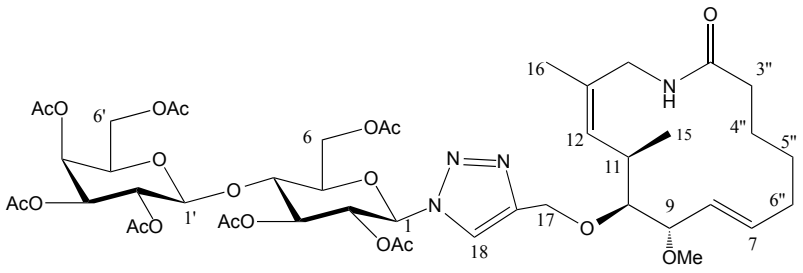

Compound **110** (25 mg, 0.0783 mmol) in THF/H_2O 1:1 (2.8 mL) was treated compound **101** (72.7 mg, 0.11 mmol) and stirred for 4 min. Sodium ascorbate (18.6 mg, 0.094 mmol) and $CuSO_4.5H_2O$ (23.5 mg, 0.094 mmol) was sequentially added and the reaction was stirred for 24 h. The reaction was concentrated to remove the THF and the aqueous phase was extracted with EtOAc (3 x 30 mL). The organic portion was washed with H_2O (2 x 10 mL) and was dried over Na_2SO_4. The solvent was concentrated under reduced vacuum and chromatography (Petroleum Ether/EtOAc, 1:1 to 1:1.5) afforded the title compound (32 mg, 42 %) as a white solid.

^{1}H NMR (500 MHz, Chloroform-d) δ 7.71 (s, 1H, H-18), 5.86 – 5.80 (m, 1H, H-1), 5.78 (apt t, *J* = 7.5 Hz, 1H, H-7), 5.43 – 5.39 (m, 2H, H-4 and H-2, overlapping peaks), 5.39 – 5.34 (m, 4H, H-8, H-12, NH and H-4', overlapping peaks), 5.14 (dd, *J* = 10.4, 7.8 Hz, 1H, H-2'), 5.00 – 4.93 (m, 2H, H-3' and H-17a, overlapping peaks), 4.74 (d, *J* = 12.4 Hz, 1H, H-17b), 4.53 (d, *J* = 7.9 Hz, 1H, H-1'), 4.48 (dd, *J* = 12.3, 1.9 Hz, 1H, H-6a), 4.18 – 4.12 (m, 2H, H-6b and H-6a', overlapping peaks), 4.09 (dd, *J* = 11.2, 7.4 Hz, 1H, H-6b'), 4.00 – 3.94 (m, 1H, H-3), 3.94 – 3.88 (m, 2H, H-5 and H-5', overlapping peaks), 3.79 (dd, *J* = 13.8, 3.8 Hz, 1H, H-14a), 3.71 (apt t, *J* = 7.5 Hz, 1H, H-9), 3.58 (dd, *J* = 13.8, 5.2 Hz, 1H, H-14b), 3.31 (dd, *J* = 7.8, 2.9 Hz, 1H, H-10), 3.28 (s, 3H, OMe), 2.66 – 2.56 (m, 1H, H-11), 2.29 – 2.22 (m, 1H, H-3a''), 2.21 – 2.14 (m, 5H, H-3b'', H-6a'' and $COCH_3$ overlapping peaks), 2.10 (s, 3H, $COCH_3$), 2.08 – 2.04 (m, 9H, 3 x $COCH_3$), 2.05 – 1.99 (m, 1H, H-6b''), 1.97 (s, 3H, $COCH_3$), 1.87 (s, 3H, $COCH_3$), 1.70 (d, *J* = 1.5 Hz, 3H, H-16), 1.66 – 1.54 (m, 3H, H-4'' and 5a'', overlapping peaks), 1.41 (apt t, *J* = 7.3 Hz, 1H, H-5b''), 0.93 (d, *J* = 6.8 Hz, 3H, H-15).

^{13}C NMR (126 MHz, Chloroform-d) δ 173.4 (C=O), 170.5 (C=O), 170.3 (C=O), 170.2 (C=O), 170.2 (C=O), 169.6 (C=O), 169.3 (C=O), 169.2 (C=O), 146.7 (CHN=*C*CN), 134.5 (C-7), 133.5 (C-12), 130.0 (C-13), 128.8 (C-8), 121.0 (C-18), 101.3 (C-1'), 85.7 (C-1), 84.8 (C-10), 84.6 (c-9), 76.1 (C-5 or C-5'), 75.8 (C-3), 72.8 (C-4'), 71.1 (C-3'), 71.0 (C-5 or C-5'), 70.7 (C-4), 69.2 (C-2'), 66.7 (C-2), 66.1 (C-17), 61.9 (C-6), 60.9 (C-6'), 56.8 (O*C*H_3), 41.4 (C-14), 36.2 (C-3''), 33.9 (C-11), 29.7 (C-6''), 27.5 (C-5''), 24.7 (C-4''), 24.4 (C-16), 20.9 (CH_3), 20.9 (CH_3), 20.8 (CH_3), 20.8 (CH_3), 20.8 (CH_3), 20.7 (CH_3), 20.4 (CH_3), 15.2 (CH_3).

IR (ATR) cm^{-1}: 2935, 1748, 1649, 1529, 1216, 104

ESI/MS^{-} (*m/z*) ($M+H^{+}$); 981.4 HRMS-ESI: cacld for $C_{45}H_{65}NO_{20}$: 981.4192; Found 981.4169.

β-D-galactopyranosyl-(1→4)-1-(1,2,3-triazol-1,4)-β-D-glucopyranoside-(7*E*,9*S*,10*S*,11*R*,12*Z*)-9-methoxy-11,13-dimethyl-10-oxyazacyclotetradeca-7,12-dien-2-one (112)

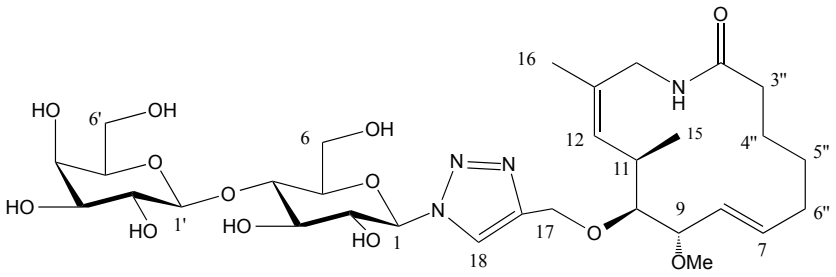

To a solution of compound **111** (32 mg, 0.033 mmol) in methanol (3.3 mL) was added freshly prepared NaOMe (0.2 mL, 0.20 mmol, 1 M). The reaction was stirred for 2 h and quenched with the addition of Amberlite H^+ to pH 6. The ion-exchange resin was filtered off and the solvent was reduced *in vacuo*. The compound, dissolved in a minimal amount of water was loaded onto the column, with the elution carried out as follows: 3 volumes of water were flushed through the column first to ensure salt removal which was subsequently followed by a 1:1 MeCN-H_2O mixture. This gave the title compound (20.5 mg, 91 %) as an off-white foam solid.

^{1}H NMR (500 MHz, Methanol-d_4) δ 8.18 (s, 1H, H-18), 5.75 (ddd, *J* = 15.8, 8.3, 5.6 Hz, 1H, H-7), 5.66 (d, *J* = 9.3 Hz, 1H, H-1), 5.41 – 5.32 (m, 2H, H-8 and H-12, overlapping peaks), 4.98 (d, *J* = 12.2 Hz, 1H, H-17a), 4.72 (d, *J* = 12.2 Hz, 1H, H-17b), 4.44 (d, *J* = 7.7 Hz, 1H, H-1'), 4.00 (apt t, *J* = 9.1 Hz, 1H, H-2), 3.91 (d, *J* = 2.9 Hz, 2H, H-6), 3.88 (d, *J* = 15.0 Hz, 1H, H-14a), 3.85 – 3.83 (m, 1H, H-4', overlapping peaks), 3.82 – 3.76 (m, 2H, H-6a' and H-4, overlapping peaks), 3.76 – 3.71 (m, 3H, H-5, H-3 and H-6b', overlapping peaks), 3.68 (apt t, *J* = 8.2 Hz, 1H, H-9), 3.65 – 3.61 (m, 1H, H-5', overlapping peaks), 3.60 – 3.57 (m, 1H, H-2', overlapping peaks), 3.52 (dd, *J* = 9.7, 3.3 Hz, 1H, H-3'), 3.41 (d, *J* = 14.8 Hz, 1H, H-14b), 3.34 (d, *J* = 2.4 Hz, 1H, H-10), 3.28 (s, 3H, OMe), 2.77 – 2.66 (m, 1H, H-11), 2.31 – 2.18 (m, 2H, H-3a'' and H-6a'', overlapping peaks), 2.16 – 2.04 (m, 2H, H-3b'' and H-6b'', overlapping peaks), 1.74 – 1.66 (m, 4H, H-16 and H-4a'', overlapping peaks), 1.65 – 1.56 (m, 1H, H-5a''), 1.55 – 1.49 (m, 1H, H-4b''), 1.48 – 1.41 (m, 1H, H-5b''), 0.88 (d, *J* = 6.8 Hz, 3H, H-15).

^{13}C NMR (126 MHz, Methanol-d_4) δ 176.6 (C-2), 146.8 (CHN=*C*CN), 135.8 (C-7), 133.7 (C-12), 130.4 (C-13), 129.9 (C-8), 124.2 (C-18), 105.1 (C-1'), 89.3 (C-1), 86.8 (C-9), 85.9 (C-10), 79.7 (C-4'), 79.5 (C-4), 77.1 (C-5'), 76.9 (C-5 or C-3), 74.8 (C5 or C-3), 73.7 (C-2), 72.5 (C-2'), 70.3 (C-4'), 66.9 (C-17), 62.5 (C-6'), 61.5 (C-6), 56.7 (O*C*H$_3$), 42.8 (C-14), 35.7 (C-3'' or C-6''), 34.0 (C-11), 30.3 (C-3'' or C-6''), 27.8 (C-5''), 25.5 (C-4''), 24.8 (C-16), 14.3 (C-15).

IR (ATR) cm^{-1}: 3342, 2929, 1634, 1542, 1042

ESI/MS$^-$ (*m/z*) (M+Na$^+$); 709.3 HRMS-ESI: cacld for $C_{31}H_{50}N_4O_{13}Na$: 709.3272; Found 709.3271.

4.4 Experimental data - Chapter 3

2-Acetamido-3,4,6-tri-O-acetyl-2-deoxy-α-D-glucopyranosyl chloride (116)[12]

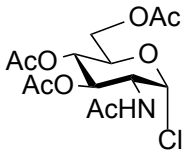

N-Acetylglucosamine (14 g, 63.3 mmol) was added to a flame dried flask and dried over high vacuum for 3 h. To this was added freshly distilled acetyl chloride (45 mL) and stirred for 18 h at room temperature. Chloroform (160 mL) was added to dilute the mixture and it was subsequently lowered to 0 °C. Ice (5 g) was then added to the reaction flask portionwise under stirring. Ice H_2O (200 mL) was added and the flask contents were transferred to a separating funnel. The layers were separated and the organic phase was further quenched with ice H_2O (3 x 200 mL). Cold $NaHCO_3$ (100 mL) was added to the organic portion and effervescence was noted. The organic portion was further washed with cold $NaHCO_3$ (3 x 100 mL). The organics was then dried over Na_2SO_4 and concentrated under reduced pressure. Chromatography (EtOAc, 100 %) afforded the title compound (12.4 g, 54 %) as a white solid.

^{1}H NMR (500 MHz, Chloroform-d) δ 6.18 (d, *J* = 3.8 Hz, 1H, H-1), 5.87 (br s, 1H, N*H*Ac), 5.31 (apt t, *J* = 10.1 Hz, 1H, H-3), 5.20 (apt td, *J* = 9.7, 2.1 Hz, 1H, H-4), 4.56 – 4.50 (m, 1H, H-2), 4.30 – 4.23 (m, 2H, H-5 and H-6a, overlapping peaks), 4.15 – 4.10 (m, 1H, H-6b), 2.09 (s, 3H, $COCH_3$), 2.05 – 2.03 (m, 6H, 2 x $COCH_3$), 1.97 (s, 3H, $COCH_3$).

13C NMR (126 MHz, Chloroform-d) δ 171.5 (C=O), 170.7 (C=O), 170.2 (C=O), 169.2 (C=O), 93.8 (C-1), 71.0 (C-5), 70.2 (C-3), 67.1 (C-4), 61.3 (C-6), 53.6 (C-2), 23.2 (CH_3), 23.2 (CH_3), 20.8 (CH_3), 20.7 (CH_3).

IR (ATR) cm^{-1}: 3241, 1738, 1641, 1541, 1209, 1032

2-Acetamido-3,4,6-tri-O-acetyl-2-deoxy-1-azido-β-D-glucopyranosyl (117)[12]

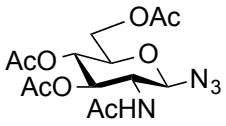

To a solution of compound **116** (5 g, 13.7 mmol) in anhydrous DMF (40 mL) at room temperature was added NaN_3 (1.6 g, 24.6 mmol). The reaction was brought slowly up to reflux under gentle stirring and was heated for 5 h. The mixture was then transferred to ice H_2O (100 mL) in a separating funnel. The quenched mixture was separated and the aqueous phase was back extracted with EtOAc (4 x 100 mL). The combined organics were dried over Na_2SO_4 and concentrated under diminished pressure. The residue was purified by chromatography (EtOAc/Petroleum Ether, 4:1) to yield the title compound (3.4 g, 67 %) as a white solid.

^{1}H NMR (500 MHz, Chloroform-d) δ 5.57 (br s, 1H, N*H*Ac), 5.24 (dd, *J* = 10.6, 9.3 Hz, 1H, H-3), 5.10 (apt t, *J* = 9.7 Hz, 1H, H-4), 4.76 (d, *J* = 9.2 Hz, 1H, H-1), 4.27 (dd, *J* = 12.5, 4.8 Hz, 1H, H-6a), 4.17 (dd, *J* = 12.4, 2.3 Hz, 1H, H-6b), 3.94 – 3.87 (m, 1H, H-2), 3.79 (ddd, *J* = 10.0, 4.8, 2.3 Hz, 1H, H-5), 2.10 (s, 3H, $COCH_3$), 2.04 (apt d, *J* = 3.4 Hz, 6H, 2 x $COCH_3$), 1.98 (s, 3H, $COCH_3$).

^{13}C NMR (126 MHz, Chloroform-d) δ 171.1 (C=O), 170.8 (C=O), 170.5 (C=O), 169.4 (C=O), 88.6 (C-1), 74.2 (C-5), 72.3 (C-3), 68.1 (C-4), 62.0 (C-6), 54.4 (C-2), 23.4 (CH_3), 20.9 (CH_3), 20.8 (CH_3), 20.7 (CH_3).

IR (ATR) cm^{-1}: 3360, 2944, 2104, 1742, 1663, 1518, 1221, 1033

ESI/MS$^-$ (*m/z*) (M+Na$^+$); 395.1 HRMS-ESI: cacld for $C_{14}H_{20}N_4O_8Na$: 395.1179; Found 395.1164.

2-Acetamido-3,4,6-tri-O-acetyl-2-deoxy-1-amine-β-D-glucopyranosyl (118)[12]

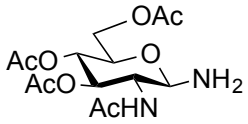

To a solution of compound **117** (6.5 g, 17.5 mmol) in anhydrous degassed EtOAc (120 mL) was added PtO_2 (120 mg, 0.53 mmol). A balloon filled with H_2 was inserted via a needle and rubber septum. The reaction was stirred vigorously for 2 h at room temperature. The reaction mixture was passed through a Celite pad to remove the catalyst. The solvent was removed under diminished pressure and dried over high vacuum to yield the title compound (4.0 g, 66 %) as a grey solid.

^{1}H NMR (500 MHz, Chloroform-d) δ 5.62 (d, *J* = 9.0 Hz, 1H, N*H*Ac), 5.10 – 5.00 (m, 2H, H-3 and H-4, overlapping peaks), 4.21 (dd, *J* = 12.3, 4.9 Hz, 1H, H-6a), 4.13 – 4.09 (m, 2H, H-6b and H-1, overlapping peaks), 4.01 (apt q, *J* = 9.4 Hz, 1H, H-2), 3.63 (ddd, *J* = 9.5, 4.9, 2.4 Hz, 1H, H-5), 2.09 (s, 3H, $COCH_3$), 2.04 (s, 3H, $COCH_3$), 2.02 (s, 3H, $COCH_3$), 1.97 (s, 3H, $COCH_3$).

^{13}C NMR (126 MHz, Chloroform-d) δ 171.7 (C=O), 170.9 (C=O), 170.8 (C=O), 169.4 (C=O), 86.6 (C-1), 73.6 (C-3), 72.9 (C-5), 68.6 (C-4), 62.5 (C-6), 55.1 (C-2), 23.5 (CH_3), 20.9 (CH_3), 20.9 (CH_3), 20.8 (CH_3).

IR (ATR) cm^{-1}: 3401, 3342, 2935, 1749, 1731, 1662, 1534, 1231, 1041

ESI/MS$^-$ (*m/z*) (M+FA-H$^+$); 391.1 HRMS-ESI: cacld for $C_{15}H_{23}N_2O$: 391.1353; Found 391.1367.

2-Acetamido-3,4,6-tri-O-acetyl-2-deoxy-1-amine-β-D-glucopyranoside-1-fluorenylmethyloxycarbonyl-L-asparagine *tert*-butyl ester (119)[12]

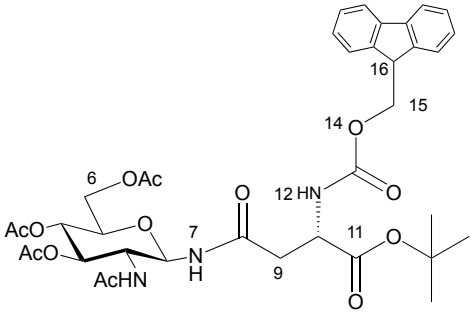

Fmoc aspartic acid with the C-terminus protected (1.2 g, 2.92 mmol) and 2-ethoxy-1-ethoxycarbonyl-1,2-dihydroquinoline (0.722 g, 2.92 mmol) were sequentially added to a solution of compound **118** (1.01 g, 2.92 mmol) in DCM (80 mL). The reaction was stirred for 4.5 h at room temperature and the solvent was removed via reduced pressure to yield a white solid. The solid was suspended in a hot organic mixture (Petroleum Ether/EtOAc, 1:1, 40 mL) and stirred for 5 min. The suspension was filtered and the filter cake was allowed to dry. The filter cake was suspended in chloroform (150 mL) and once again filtered. The mother liquor was concentrated to yield the title compound (1.64 g, 76 %) as a white solid.

^{1}H NMR (500 MHz, Chloroform-d) δ 7.75 (d, *J* = 7.5 Hz, 2H, ArH), 7.60 (d, *J* = 7.5 Hz, 2H, ArH), 7.39 (t, *J* = 7.5 Hz, 2H, ArH), 7.30 (t, *J* = 7.5 Hz, 2H, ArH), 7.18 (d, *J* = 8.2 Hz, 1H, NH, H-7), 6.07 (d, *J* = 8.1 Hz, 1H, N*H*Ac), 5.94 (d, *J* = 8.8 Hz, 1H, NH, H-12), 5.12 (apt t, *J* = 9.6 Hz, 1H, H-4), 5.08 – 5.03 (m, 2H, H-3 and H-1, overlapping peaks), 4.53 – 4.50 (m, 1H, H-10), 4.42 (dd, *J* = 10.5, 7.2 Hz, 1H, H-15a), 4.33 – 4.26 (m, 2H, H-6a and H-15b, overlapping peaks), 4.22 (t, *J* = 7.2 Hz, 1H, H-16), 4.16 – 4.02 (m, 2H, H-2 and H-6b, overlapping peaks), 3.74 (ddd, *J* = 9.9, 4.3, 2.2 Hz, 1H, H-5), 2.84 (dd, *J* = 16.4, 4.7 Hz, 1H, H-9a), 2.70 (dd, *J* = 16.4, 4.4 Hz, 1H, H-9b), 2.07 – 2.03 (m, 9H, 3 x $COCH_3$), 1.95 (s, 3H, $COCH_3$), (s, 9H, *t*-Bu).

^{13}C NMR (126 MHz, Chloroform-d) δ 172.4 (C=O), 172.2 (C=O), 171.2 (C=O), 170.8 (C=O), 170.1 (C=O), 169.4 (C=O), 156.2 (ArC), 144.1 (ArC), 143.9 (ArC), 141.4 (ArC), 127.8 (Ar*C*H), 127.2 (Ar*C*H), 125.3 (Ar*C*H), 120.1 (Ar*C*H), 82.3 (*C*(CH_3)$_3$), 80.5 (C-1), 73.7 (C-5), 73.0 (C-3), 67.7 (C-4), 67.3 (C-15), 61.8 (C-6), 53.6 (C-2), 51.1 (C-10), 47.3 (C-16), 38.1 (C-9), 28.0 (C(*C*H_3)$_3$), 23.2 (CH_3), 20.9 (CH_3), 20.8 (CH_3), 20.7 (CH_3).
IR (ATR) cm^{-1}: 3314, 2980, 1742, 1696, 1660, 1530, 1225, 1041, 737

ESI/MS$^-$ (*m/z*) (M+Na$^+$); 762.3 HRMS-ESI: cacld for $C_{37}H_{45}N_3O_{13}Na$: 762.2850; Found 762.2840.

2-Acetamido-3,4,6-tri-O-acetyl-2-deoxy-1-amine-β-D-glucopyranoside-1-fluorenylmethyloxycarbonyl-L-asparagine (120)[12]

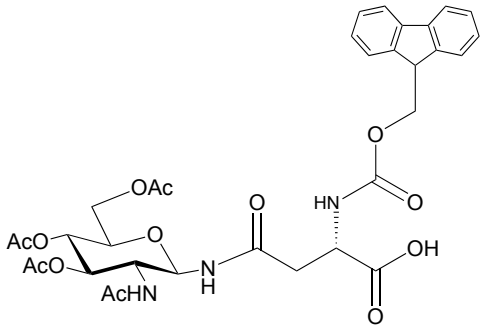

Compound **119** (3.7 g, 5.0 mmol) was dissolved in trifluoroacetic acid (70 mL). The solution was stirred for 3 h at room temperature and then azeotroped with toluene to dryness to yield the title compound (3.24 g, 95 %) as a white solid.

^{1}H NMR (500 MHz, DMSO-d_6) δ 8.58 (d, *J* = 9.3 Hz, 1H, NH, H-7), 7.95 – 7.86 (m, 3H, ArH and N*H*Ac, overlapping peaks), 7.71 (d, *J* = 7.5 Hz, 2H, ArH), 7.51 (d, *J* = 8.5 Hz, 1H, NH, H-12), 7.42 (t, *J* = 7.4 Hz, 2H, ArH), 7.33 (t, *J* = 7.4 Hz, 2H, ArH), 5.18 (apt t, *J* = 9.5 Hz, 1H, H-1), 5.10 (apt t, *J* = 9.8 Hz, 1H, H-3), 4.82 (apt t, *J* = 9.7 Hz, 1H, H-4), 4.42 – 4.36 (m, 1H, H-10), 4.31 – 4.24 (m, 2H, H-15), 4.23 – 4.15 (m, 2H, H-6a and H-16, overlapping peaks), 3.95 (dd, *J* = 12.4, 2.2 Hz, 1H, H-6b), 3.88 (apt q, *J* = 9.8 Hz, 1H, H-2), 3.82 (ddd, *J* = 10.0, 4.2, 2.4 Hz, 1H, H-5), 2.66 (dd, *J* = 16.2, 5.5 Hz, 1H, H-9a), 2.48 (d, *J* = 7.3 Hz, 1H, H-9b, overlapping with DMSO peak), 1.99 (s, 3H, $COCH_3$), 1.96 (s, 3H, $COCH_3$), 1.90 (s, 3H, $COCH_3$) 1.72 (s, 3H, $COCH_3$).

^{13}C NMR (126 MHz, DMSO-d_6) δ 173.4 (C=O), 170.5 (C=O), 170.2 (C=O), 169.9 (C=O), 169.9 (C=O), 169.7 (C=O), 156.3 (ArC), 144.2 (ArC), 141.1 (ArC), 128.1 (Ar*C*H), 127.5 (Ar*C*H), 125.7 (Ar*C*H), 120.6 (Ar*C*H), 78.5 (C-1), 73.8 (C-3), 72.7 (C-5), 68.8 (C-4), 66.2 (C-15), 62.3 (C-6), 52.6 (C-2), 50.4 (C-10), 47.0 (C-16), 37.3 (C-9), 23.0 (CH_3), 21.0 (CH_3), 20.9 (CH_3), 20.8 (CH_3), 20.5 (CH_3).

IR (ATR) cm^{-1}: 3307, 1743, 1697, 1661, 1532, 1224, 1041

ESI/MS$^-$ (*m/z*) (M+H$^+$); 684.2 HRMS-ESI: cacld for $C_{33}H_{38}N_3O_{13}$: 684.2405; Found 684.2405.

4.4.1 General synthesis and purification of somatostatin peptidomimetics

Peptides were synthesised on solid phase through the use of a semi-automatic peptide synthesiser (Activotec P14) using standard Fmoc protocol. The synthesis was carried out on MBHA resin (0.5 mmol / g substitution) along with standard Fmoc amino acids on a 0.1 mmol scale. The resin was pre-swelled for 2 X 10 min in DMF peptide grade (8 mL) solvent for the first coupling. Fmoc deprotection reactions were carried out in 20 % piperidine (2 X 5 minutes). Amino acid coupling reactions were carried out using 4-fold molar excess of incoming amino acid, 3.84 equivalents of coupling reagent HCTU and 3.84 equivalents of 6-Cl-HOBt in addition to 8 equivalents of DIPEA, in DMF (0.06 M based on amount of resin started with). Each subsequent amino acid added was first pre-activated for 5 minutes before adding it to the resin. The modified glyco-amino acid was introduced into the growing peptide chain in the same fashion as the standard amino acids. Reaction times were over the course of 60 minutes followed by an acetylation capping step (15 minutes) using 1 M Ac_2O and 0.4 M DIPEA solution in DMF. The N-terminus was also capped at the end of the synthesis for each peptide using the same conditions as during the synthesis. Peptide cleavage and side chain deprotections were carried out using a cleavage cocktail of TFA : Thioansole : EDT : Anisole (90 : 5 : 3 : 2 v/v/v/v) for 3 h at room temperature. The resin was filtered directly into a falcon tube containing cold diethyl ether where precipitation immediately occurred. The falcon tube was centrifuged (3000 rpm, 15 minutes) and the supernatant was removed. The pellet was re-suspended in fresh cold diethyl ether and once again centrifuged. The supernatant was once again removed and the pellet was dissolved up into an appropriate solvent mixture for HPLC purification.

4.4.1.1Deacetylation of glyco-peptides

Crude peptide pellets from centrifugation were dissolved in methanol (25 mL) and a catalytic amount of sodium methoxide was added until pH 10 was reached, to remove the acetate protecting groups. The reaction mixture was stirred for 30 minutes and acidified to pH 6 using Amberlite H^+ resin. The resin was filtered and the peptides were concentrated under diminished pressure at 30 ˚C.

Crude peptides, both glycosylated and non-glycosylated were purified by preparative reverse phase HPLC using a C8 column YMC Pack (25 x 1 cm. 120 Å, 20μ). Collected fractions were lyophilised giving white fluffy powders in all cases.

Analysis of the purified peptides was performed on Gilson HPLC instrument using Phenomenex (25 x 0.46 cm, 10μ ODS (2)) with a linear gradient of H_2O (0.1 % TFA) and CH_3CN (0.1 % TFA) from 25 to 60 % of CH_3CN in 60 minutes. Characterisation using mass spectrometry (Waters LCT Premier) in conjunction with HPLC analysis at 210 nm confirmed the structures.

Ac-PheTrpLysAspValGlyNH_2 (121)

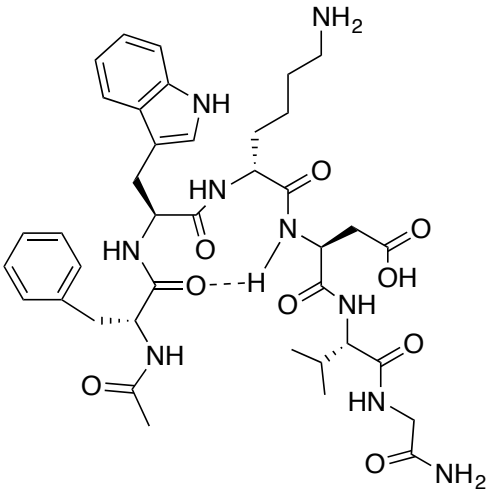

The general method for SPPS and peptide cleavage formed compound **121**.

The crude peptide was purified using preparative HPLC to give the title compound.

ESI/MS^- (*m/z*) calcd 792.40 ($M+H^+$); Found 792.40

Retention Time (min) 19.1

Yield (52 %)

Ac-ValAlaPheTrpLysAspAlaGlyNH_2 (122)

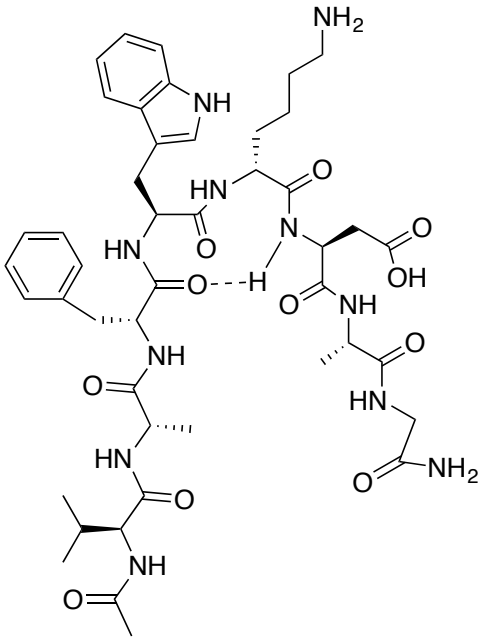

The general method for SPPS and peptide cleavage formed compound **122**.
The crude peptide was purified using preparative HPLC to give the title compound **122**.

ESI/MS^- (*m/z*) calcd 934.48 ($M+H^+$); Found 934.48

Retention Time (min) 20.5

Yield (46 %)

Ac-ValAlaPheTrpLysAsn(2-Acetamido-3,4,6-tri-O-acetyl-2-deoxy-1-amine-β-D-galactopyranosyl)AlaGlyNH_2 (124)

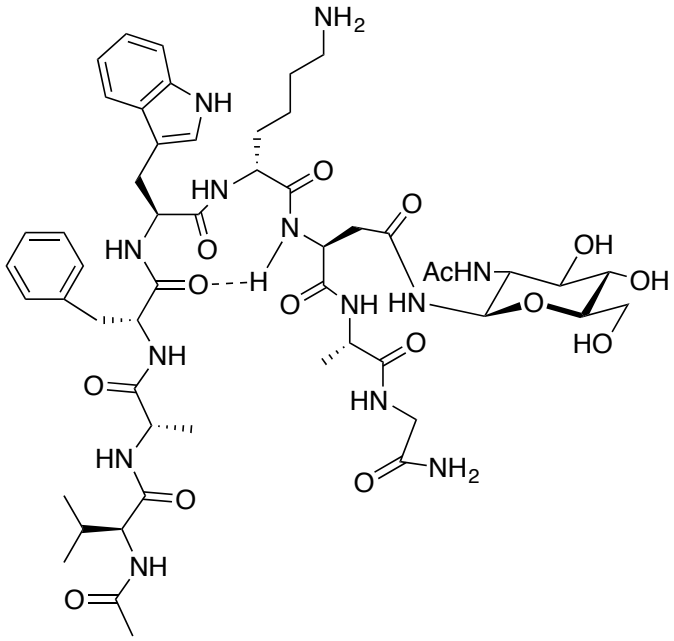

The general method for SPPS and peptide cleavage formed compound **123**.
Crude compound **123** was deacetylated using the general method. The crude peptide was then purified using preparative HPLC to give the title compound **124**.

ESI/MS^- (*m/z*); calcd 1136.57 ($M+H^+$); Found 1136.54

Retention Time (min) 15.1

Yield (41 %)

Ac-ValCysPheTrpLysAspCysGly-NH_2 (125)

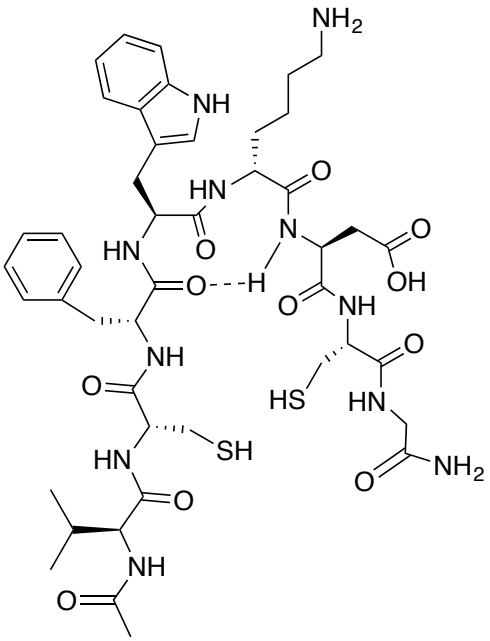

The general method for SPPS and peptide cleavage formed the linear acyclic peptide, compound **125**.

ESI/MS^- (*m/z*) calcd 998.42 ($M+H^+$); Found 998.53

Retention Time (min) 20.7

Ac-ValCysPheTrpLysAspCysGly-NH_2 (126)

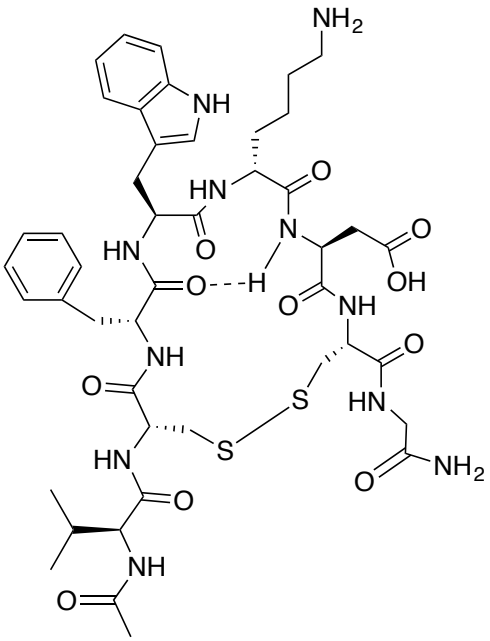

Crude compound **125** (15 mg) was dissolved in a solvent mixture H_2O / AcOH (95:5 v/v, 15 mL). The pH was adjusted to pH 6 with ammonium carbonate. DMSO (1.5 mL) was added and the reaction was stirred for 24 h at room temperature. The crude cyclised peptide was lyophilised and preparative HPLC purification afforded the title compound.

ESI/MS^- (*m/z*); calcd 996.41 ($M+H^+$); Found 996.50

Retention Time (min) 19.3

Yield (45 %)

Ac-ValCysPheTrpLysAsn(2-Acetamido-3,4,6-tri-O-acetyl-2-deoxy-1-amine-β-D-galactopyranosyl) CysGly-NH_2 (129)

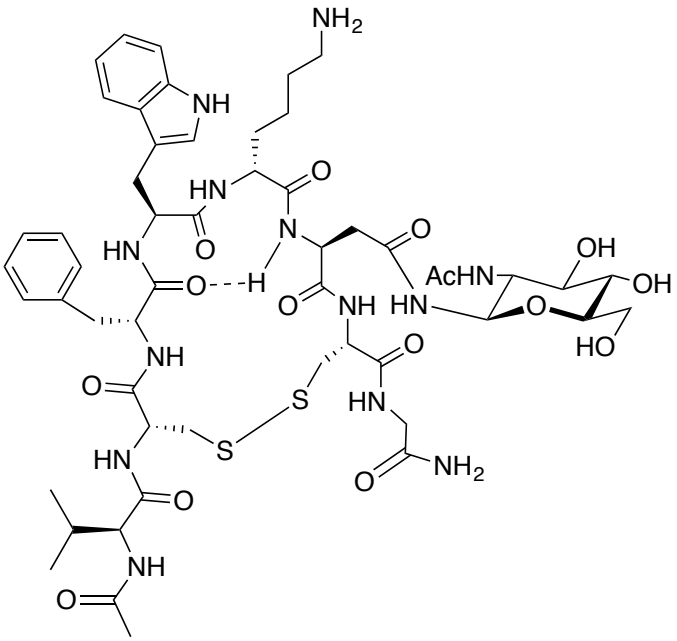

The general method used for SPPS and peptide cleavage formed the protected linear glyco-peptide, compound **127**. Crude **127** was first deacetylated using the general method for deacetylation. However, it was imperative that degassed methanol was used here to avoid the desulfurised impurity. Deprotected compound **128** (10 mg) was dissolved in a solvent mixture H_2O / AcOH (95:5 v/v, 12 mL). The pH was adjusted to pH 6 with ammonium carbonate. DMSO (1 mL) was added and the reaction was stirred for 24 h at room temperature. The crude peptide was lyophilised and preparative HPLC gave the title compound.

ESI/MS^- (*m/z*); calcd 1198.49 ($M+H^+$); Found 1198.48

Retention Time (min) 16.8

Yield (38 %)

4.5 Biological Assay Methods

4.5.1 Cytotoxicity

MTS is a tetrazolium compound, 3-(4,5-dimethylthiazol-2-yl)-5-(3-carboxymethoxyphenyl)-2-(4-sulfophenyl)-2H-tetrazolium that can be reduced by dehydrogenase enzymes within living cells demonstrating cellular metabolic activity and cell viability. Such reduction in the presence of an electron-coupling reagent, phenazine ethosulfate (MPS), results in the production of formazan product that is soluble in tissue culture medium and the absorbance of this formazan product can be measured using spectrophotometry. A549 cells were cultured to confluence in 96-well culture plates using RPMI tissue culture medium with 10 % FCS new-born calf serum and 10 % PSG. An initial cell seeding of 0.1 x 10^5/well yielded a confluent monolayer after 48 hours. Growth medium was replaced with serum-free RPMI 24 hours prior to drug compound treatment. Cells were incubated in humidified 5% CO_2/9 5 % air at 37 °C. Post-treatment, cells were rinsed with PBS and incubated with RPMI 1640 culture medium containing the MTS reagent according to the manufacture's protocol for 45 mins (CellTiter 96® AQueous One Solution Assay, Promega, USA). The absorbance of formazan product in the culture medium was then read using a spectrophotometer at a wavelength of 490nm.

4.5.2 Migration Assay

A549 chemotaxis was performed toward a serum gradient in a modified Boyden chamber consisting of a cell culture insert (6.4 mm diameter, 8-μm pore polyethylene tetraphtalate membrane, [Becton Dickinson]) seated in each well of a 24-well companion plate (Becton Dickinson). A549 cells were grown as subconfluent monolayer cultures then starved for 36 h in serum-free RPMI medium. After detachment and dissociation with 5 mM EDTA, single-cell suspensions were prepared by filtration through a 35 μm mesh cell strainer (Becton Dickinson). Cells were counted and a total of 10 (8) cells suspended in serum-free medium were seeded into the upper chamber of an insert, then positioned in a 24-well plate containing medium with or without 10 % serum. When used, drugs or DMSO (vehicle) were added to the medium at 0.2 % in both chambers. Migration assays were carried out for 12 h in a humidified incubator at 37 °C with 5 % CO2. A549 cells that migrated towards the serum gradient were stained with fluorescent calcein, imaged by fluorescent microscopey and fluorescence intensity was quantified using Simple PCI software (Hamamatsu, Shizuoka, Japan). The migration in response to the test condition was calculated relative to the DMSO vehicle control.

4.5.3 Wound healing assay

Migration of A549 cells was measured using an in vitro wound-healing assay, performed in a 12-well plate (Becton Dickinson). A549 cells were seeded at a density of 5–10 × 104 cells per well, grown to near confluent monolayers in 10 % FCS serum-supplemented RPMI medium, and then starved overnight in a low serum medium (0.5 % FCS). Perpendicular wounds were scratched through the cell monolayer using a sterile 200 μL pipette tip. The cells were then washed twice very gently using PBS, and the scratched areas were photographed at 4X and 20X magnification using microscopy and Simple PCI software (Hamamatsu, Shizuoka, Japan). PBS was removed and replaced with 2 mL of media with or without 2% FCS, and containing drugs or DMSO (vehicle control) at 0.2 % (v⁄v). After 12–24 h in a humidified incubator at 37 °C with 5% CO2, cells were fixed with 3.7 % formaldehyde, permeabilised with ice cold methanol, and stained with a 0.2 % crystal violet solution. Each well was photographed at 4X and 20X magnification and the pictures analyzed with Simple PCI software cell image analysis software. The migration in response to the test condition was calculated as cell coverage of the original cell-free zone and related to DMSO vehicle control.

Bibliography

1. Lo Re, D.; Zhou, Y.; Nobis, M.; Anderson, K. I.; Murphy, P. V., *ChemBioChem* **2014,** *15* (10), 1459-1464.
2. Gaul, C.; Njardarson, J. T.; Shan, D.; Dorn, D. C.; Wu, K.-D.; Tong, W. P.; Huang, X.-Y.; Moore, M. A. S.; Danishefsky, S. J., *Journal of the American Chemical Society* **2004,** *126* (36), 11326-11337.
3. Olpp, T.; Brükner, R., *Synthesis* **2004,** (13), 2135-2152.
4. Ando, K., *The Journal of Organic Chemistry* **1998,** *63* (23), 8411-8416.
5. Lo Re, D.; Zhou, Y.; Mucha, J.; Jones, L. F.; Leahy, L.; Santocanale, C.; Krol, M.; Murphy, P. V., *Chemistry – A European Journal* **2015,** *21* (50), 17989-17989.
6. Ryu, J.-S.; Marks, T. J.; McDonald, F. E., *The Journal of Organic Chemistry* **2004,** *69* (4), 1038-1052.
7. Percec, V.; Leowanawat, P.; Sun, H.-J.; Kulikov, O.; Nusbaum, C. D.; Tran, T. M.; Bertin, A.; Wilson, D. A.; Peterca, M.; Zhang, S.; Kamat, N. P.; Vargo, K.; Moock, D.; Johnston, E. D.; Hammer, D. A.; Pochan, D. J.; Chen, Y.; Chabre, Y. M.; Shiao, T. C.; Bergeron-Brlek, M.; André, S.; Roy, R.; Gabius, H.-J.; Heiney, P. A., *Journal of the American Chemical Society* **2013,** *135* (24), 9055-9077.
8. Allen, J. R.; Allen, J. G.; Zhang, X.-F.; Williams, L. J.; Zatorski, A.; Ragupathi, G.; Livingston, P. O.; Danishefsky, S. J., *Chemistry – A European Journal* **2000,** *6* (8), 1366-1375.
9. Yu, H.; Chokhawala, H.; Karpel, R.; Yu, H.; Wu, B.; Zhang, J.; Zhang, Y.; Jia, Q.; Chen, X., *Journal of the American Chemical Society* **2005,** *127* (50), 17618-17619.
10. Choudhury, Ambar K.; Kitaoka, M.; Hayashi, K., *European Journal of Organic Chemistry* **2003,** *2003* (13), 2462-2470.
11. van Ameijde, J.; Albada, H. B.; Liskamp, R. M. J., *Journal of the Chemical Society, Perkin Transactions 1* **2002,** (8), 1042-1049.
12. Premdjee, B.; Adams, A. L.; Macmillan, D., *Bioorganic & Medicinal Chemistry Letters* **2011,** *21* (17), 4973-4975.